Characterization of Cutting Forces in Milling of Unidirectional and Random Fiber Composites

Shanti Ravali Namburi

A thesis
Submitted in partial fulfilment of the
Requirements for the degree of

Master of Science in Mechanical Engineering

University of Washington
2017

Committee:
Ramulu Mamidala
John Kramlich
Jeffrey Miller

Programme Authorized to Offer Degree:
Mechanical Engineering

University of Washington

Abstract

Characterization of Cutting Forces in
Milling of Unidirectional and Random Fiber Composites

Shanti Ravali Namburi

Chair of the Supervisory Committee:
Professor Ramulu Mamidala
Department of Mechanical Engineering

There is an ever increasing demand for materials with High strength-weight ratio (Specific strength), corrosion resistance in the current aerospace, automotive and consumer industries apart from other technical applications. Among the various materials available with the required superior material properties , Carbon Fiber Reinforced Polymer (CFRP) is one of the most widely used material. It is extremely strong and light in weight with fibers made of carbon. It is a unidirectional composite. Molding is one of the most used method of manufacture. Most processes only produce a near net shape but machining is still required in order to get the final dimensions and shape. However, major challenges are associated with the finish machining by trimming and or drilling of the CFRP material. Some of these are delaminations, fiber pullouts and a short tool life due to the abrasive nature of the fibers and the inhomogeneous nature of the material. Two types of cutting by milling process are undertaken, namely edge trimming and end milling so the forces can be investigated. The effect of cutting parameters namely, Speed , Feed, Depth of cut and angle of cutting on the milling forces has been analyzed using statistical design of experiments (DOE). The cutting has been done in various orientations with respect to the fiber direction in order to see the effect of the orientation on the milling forces. HexMC is

one of the newly emerging composite materials. It has a very high strength value due to its random fiber orientation compared to other unidirectional composites. The same DOE of cutting parameters mentioned above have been used to analyze their effect on the milling forces on this composite. Cutting forces in CFRP found to decrease at high speeds and low feeds and in HexMC found to be influenced by the type of cutting operation.

A. Acknowledgements

First and foremost I would like to thank the three major groups of people without whose involvement, this thesis would not have been completed : My committee, My lab-mates and My family.

I would first like to thank the members of my Committee, not only for their time and extreme patience but also for their wonderful and continuous support and guidance. I am deeply grateful for the intellectual suggestions given by the committee chair Dr. Ramulu Mamidala, Dr. John Kramlich and Dr. Jeffrey Miller. I could not have completed this thesis without the constant, tolerant, meticulous and astute advice of my wonderful adviser, Professor Ramulu. His doors were always open, so whenever I would run into trouble, he would always be there. His perseverance is the reason this work is at a stage it is right now and I couldn't have been luckier to get a more amazing adviser. I cannot express enough gratitude for everything he has done and for his steadfast support throughout the length of my Masters on both professional and personal fronts. I am forever indebted to him. I thank Dr. Jeffrey Miller for teaching me and always being available to give his advice over emails and in person to offer invaluable input. I was fortunate to have the unwavering , relentless support of my lab-mates. I am extremely thankful to Rishi Pahuja and Nishita Anandan for helping me throughout this journey, along with Kapil Gangwar, Neha Kulkarni and Bryan Ferguson for their encouragement in all forms. I thank Anirudh Iyer, who taught me the basics and performed the experiments with me. I thank the Department of Mechanical Engineering at UW, Seattle for its kind help. I have to thank my friends in and out of this department who were a constant wall of support physically and emotionally. I would also like to thank everyone whose names I might have missed as without their input, I could not have done this. Finally I would like to thank my lovely parents Dr. N. Eswara Prasad and N. Swarna Latha and my extended family for believing in me that I could achieve this milestone in life. I cannot express enough love and gratitude to my parents, as they are my backbone and without the strength they give me, I am nothing.

B. Dedication

I dedicate this thesis
With affection
To
Both my wonderful parents.

C. Table of Contents

D. List of Tables

E. List of Figures

Chapter 1 : Introduction and Objective

1.1 Introduction

The mankind has been using composites since ancient times **[1]**. Only the coining of the name composites is new. Before 2000 BC, Flint was one of the first materials used to make cutting tools. Metals were not widely used back then and natural materials that were utilized to make day to day objects were polymers like wood, straw, skins, composites like bricks made of straw and ceramics like stone, and in later stages glass. From 1500 BC, the use of metals and its alloys like Bronze and Iron took over. Metals worked perfectly for numerous applications due to the fact that they could be moulded into any desired shape and had a wide range of both mechanical and material properties that catered to the numerous applications and around 1850's Steel was the most popular material being used. But as time progressed, the need for lighter materials which had high strength and stiffness surfaced. This need necessitated the production of light weight materials called Composites. These composite found their use on various applications like in Automobile, Aerospace, Medical equipment, Prosthetics, Construction, Civil Infrastructure, Electrical appliances, Marine, Consumer appliances and numerous other applications **[2]**. The following Figure 1.1 briefly describes the evolution of engineering materials.

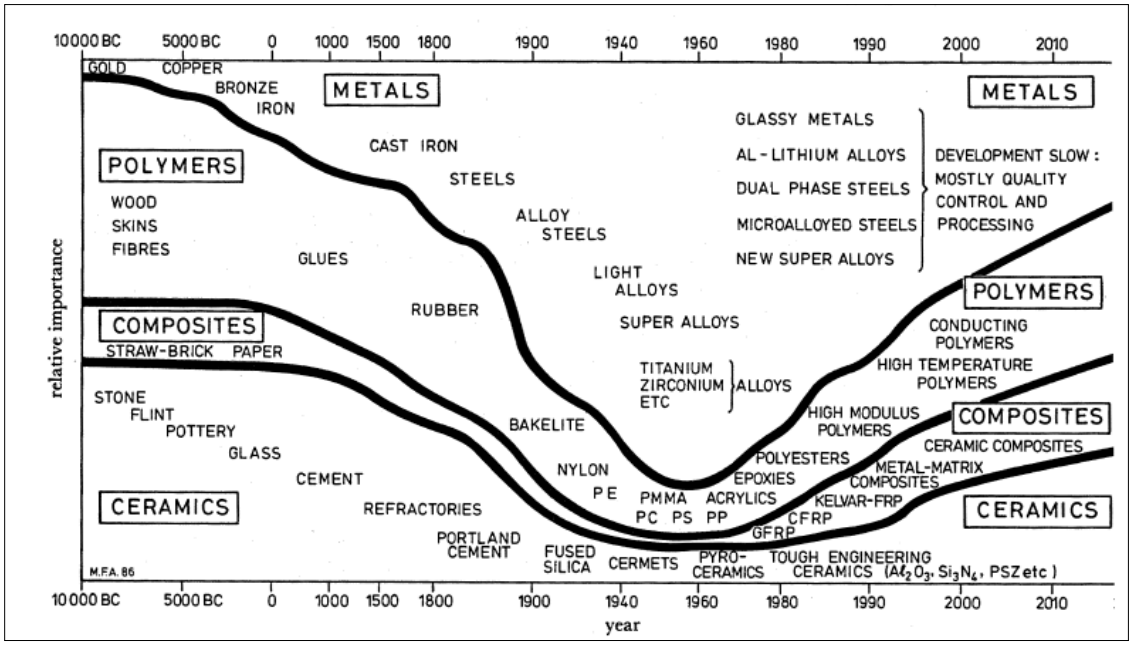

Figure 1.1: The evolution of engineering materials for mechanical and civil engineering [***1***]

The reason that the composite materials are being so widely accepted and used is they are light in weight, high in strength and stiffness, have high flexibility to be designed, can resist corrosion and have high damage tolerance in fatigue **[3,4].** One of the major applications is aircraft components. These properties facilitate their use in aircraft structures which need a light weight, high strength, corrosion resistant material so that the fuel consumption is reduced compared to metal parts and the efficiency is increased in turn. So evidently composites have wide range of uses in modern day world. The following Figure 1.2, shows the percentage of composite used in Boeing 787 and also compares the amount with Boeing 777. The amount has increased from a mere 12% in 777 to 50 % in 787.

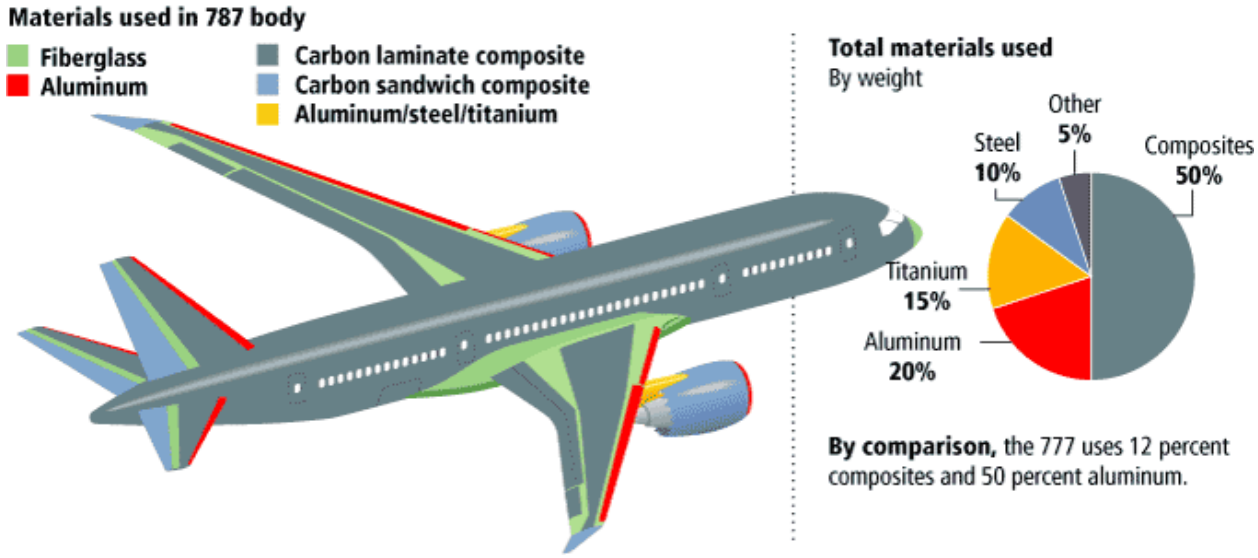

Figure 1.2 : The relative percentage of composites and other materials used in Boeing 787 **[5]**

Composites mainly compose of two or more constituent materials , with different individual properties which when combined produce a material which is completely different and has enhanced properties compared to the parent materials. Most composites mainly have two components , a matrix and a fiber. The matrix material holds and binds the fibers together so that the composite is resistant to damage. The fibers provide strength to the matrix by increasing its stiffness thereby avoiding its failure. The typical materials used for the fibers are Carbon, Glass, silicon carbide and for the matrix are metal, ceramic or plastic **[6].**

Modern composites are mostly artificially made. The most relatable natural composite is the human muscle. The muscles are part of a complex system where the fibers are at different orientations and in different concentrations thus making the whole system very strong and flexible. The bone is a composite in itself which is made of a mineral matrix and has collagen fibers. The muscles and the bones support one another creating a unique efficient structure. Other common examples are wood, clay, fins of a fish, leaves and a few examples of natural fibers are hemp, jute, flax , coir, palm, cotton (Figure 1.3) etc.

Figure 1.3: Examples of natural fibers **[7]**

One of the majorly used composite in recent times is Carbon Fiber Reinforced Polymer (CFRP). Over the years their production costs have reduced drastically due to the new evolving technologies. It has all the majorly desired properties in mechanical and material aspects and hence it is widely used in Aircraft parts such as fuselage, wings etc. Parts made of CFRP's can be moulded to the near net shape and can be machined finally to be used in assembly. There is ample amount of research regarding the machining and use of metals. Relatively there is restricted amount of literature on the Composites. Currently there is a lot of research going on Composites and is a very current research area.

Machining of composites involves some difficulties such as surface/subsurface damages such as delaminations, fiber pull-outs etc ***[8,9]***. Also, the tools used in machining undergo high wear due to the anisotropic and abrasive nature of the material. So to avoid high wear which in turn might cause high cutting forces and thereby higher chances of causing delaminations and other damages, tools with high hardness like PCD (poly crystalline diamond) are used ***[10,11].***

Machining of composites can be done by numerous ways like Drilling, turning, shaping and milling among others. Extensive research has been done on drilling and turning of composites but relatively less research has been done on milling of composites. Milling is one of the majorly used machining process for composites. It is quite a flexible process and can be used to make parts of varying design requirements.

Edge trimming is one of the commonly used machining technique in milling. Though milling is preferred over other machining processes by many, it has a few challenges due to the anisotropic nature of the composite material. A few of these major challenges are fiber pullouts, delamination , high tool wear.

The dust generated from milling the composites has found to be harmful if inhaled as it can cause nasal and skin irritation and could affect the lungs and respiratory system. So further study on machining forces in milling of composites is warranted.

1.2 Objective

Investigation of machining Forces and modelling the process is one of the many ways to better understand the mechanics behind the machining of composites specifically CFRP's and HexMC®. The main aim of this research is to characterize the cutting forces in both the Uni-directional and the random fiber composites and evaluate which process parameters give the optimum specifications. Here, CFRP is a uni-directional composites where all the fibers are aligned in a single fiber direction whereas the HexMC® is a random fiber composite where there is no specific fiber orientation. Experiments will be performed in order to obtain the force data in End milling of the two above mentioned composites by varying the machining parameters of cutting speed, feed and depth of cut and to analyze them in order to better understand the mechanics of cutting. Surface quality was evaluated for specific conditions to see which conditions give a better machined surface.

Chapter 2: Background and Literature survey

2.1 Composite materials - an Introduction

Composites are usually made of two or more materials unlike metals. The idea of creation of composites is that, by combining two materials having distinct properties, we can create a new material which has superior properties compared both the parent materials like flexibility, low weight of a polymer or the strength of a ceramic among many others. The Principle of combined action is the basis of preparation of composites through which better property combinations can be attained by combining two or more unique materials as the mixture would then give "Average" properties. Boeing 777 is 9% composites by weight, whereas the newly developed Boeing 787 is 50% composites by weight. Not only does the use of composite materials reduce the weight of the aircraft, and therefore its fuel consumption, but it also allows new design concepts because composites can be moulded. Moreover, by using composites in the Boeing 787 multiple functions can be integrated into a single system, such as acoustic damping, thermal regulation, and the electrical system **[12].**

Usually composites consist of two basic phases. First one is the matrix which is a continuous phase and the second is the dispersed phase which can be in the form of particulates, fibers or resin. The discontinuous phase is usually harder and stronger than the continuous phase hence is called as the reinforcement or reinforcing material. The purpose of the matrix is to transfer the stress to other phases, to protect the other phases from the harsh environmental conditions and to provide texture, finish, color durability and functionality. Whereas the purpose of the disperse phase is to enhance the properties of the matrix like Young's modulus, creep resistance etc.

Composites can be natural like wood, bones, spider webs, fish fins, wings of a bird, muscle or artificial/man-made (elaborated below). Properties of composites depend on,

- the properties of fiber
- the properties of resin or matrix
- geometry of dispersed phase (particle size, distribution, orientation)
- the ratio of fiber to resin in the composite (Fiber volume fraction)

2.2 Types of Composites/ Classification of Composites

The classification of composites can be done based on various criteria. The flowchart below (Figure 2.1) is a brief summary of the classification.

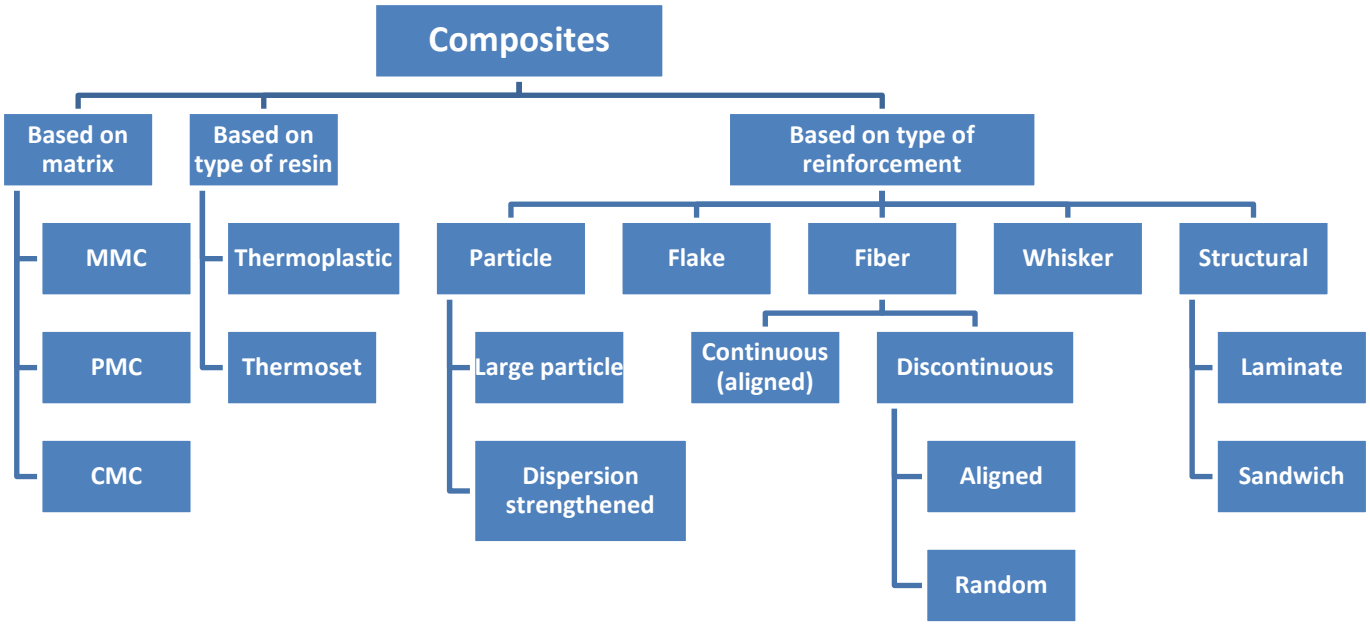

Figure 2.1 : Flowchart depicting the classification of composites

2.2.1 Based on Matrix material :

2.2.1 a) MMC

A MMC or Metal Matrix Composite is made up of at least two phases with at least one being a metal. The other phase could be a ceramic, metal or an organic compound. When a minimum of three phases are present it is called as a hybrid composite. MMC's are made by dispersing a reinforcing material into a continuous metal matrix (**Figures 2.2 , 2.3**). The matrix is usually a lighter metal such as aluminium, magnesium or titanium or cobalt and cobalt- nickel alloy matrices (for high temperature applications), which provides support to the reinforcement. There is change in physical properties like wear resistance, friction coefficient, thermal conductivity etc. The advantages of MMC's are higher temperature capability, Fire resistance, higher transverse stiffness and strength, no moisture absorption, higher electrical and thermal

conductivities. But it also has a few drawbacks such as high cost of some materials, the technology is not fully developed, complex fabrication methods.

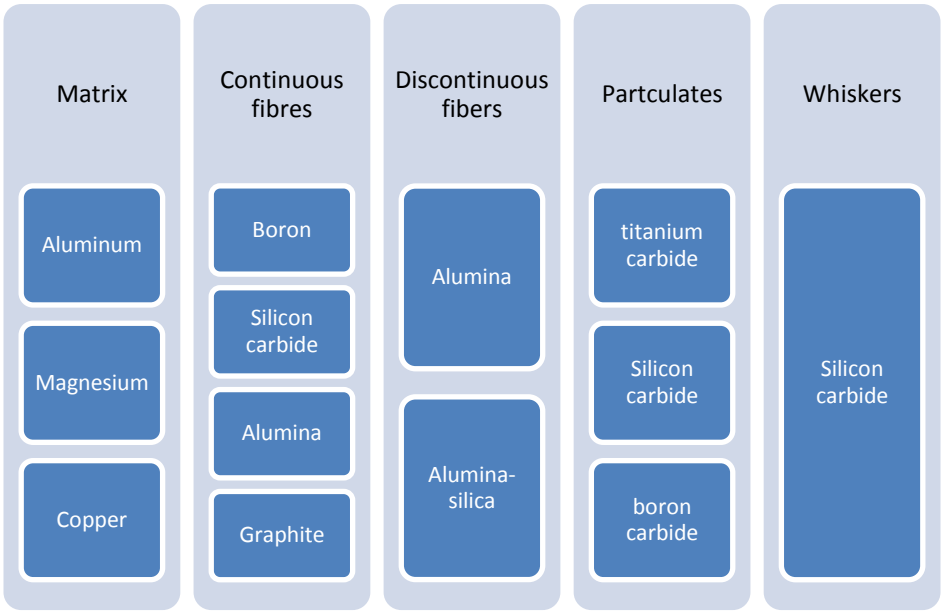

Figure 2.2 : Compositions of various components in major MMC's

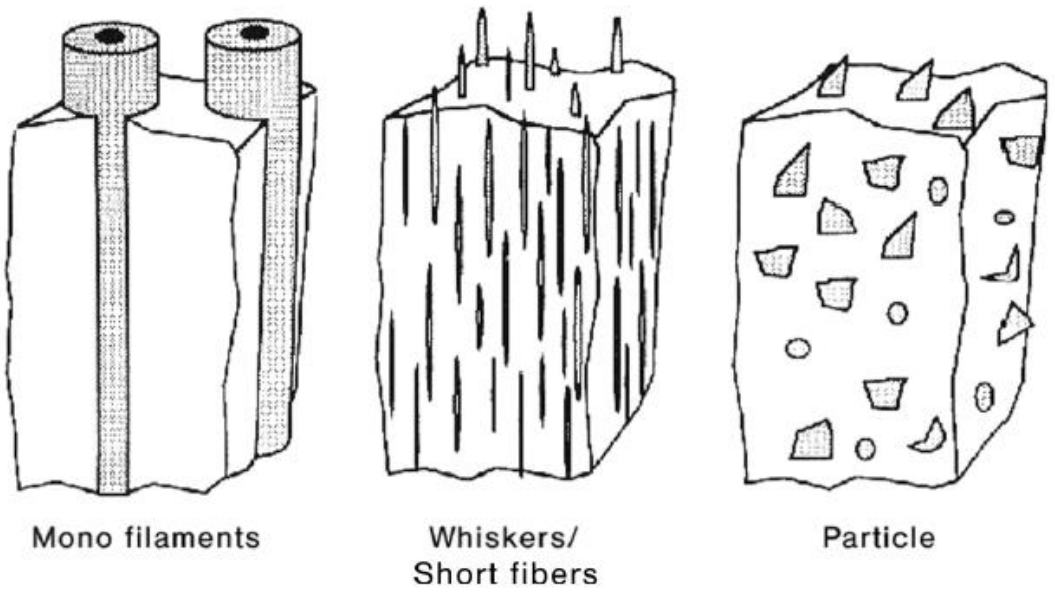

Figure 2.3 : Schematic representation of types of MMC's **[13]**

2.2.1 b) PMC

Polymer matrix composite (PMC) material is the one that uses ductile organic polymer as matrix and brittle fibers as reinforcement. Strength and modulus of fiber are much higher than the matrix (such as resins) material normally (Figure 2.4). So the fibers are the main load-bearing component and for the fibers to bond firmly the matrix material should have good adhesion properties. As a result, in composite materials, the performance of fiber, matrix and the interface between them directly impact on the performance of composite materials. Resin systems such as epoxies and polyesters have limited use for the manufacture of structures on their own, since their mechanical properties are not very high when compared to, for example, most metals. It is when the resin systems are combined with reinforcing fibers such as glass, carbon and aramid, that exceptional properties can be obtained.

The most important fibers in current use are glass, graphite, and aramid. Other organic fibers, such as oriented polyethylene, are also becoming important. PMCs contain about 60 percent reinforcing fiber by volume.

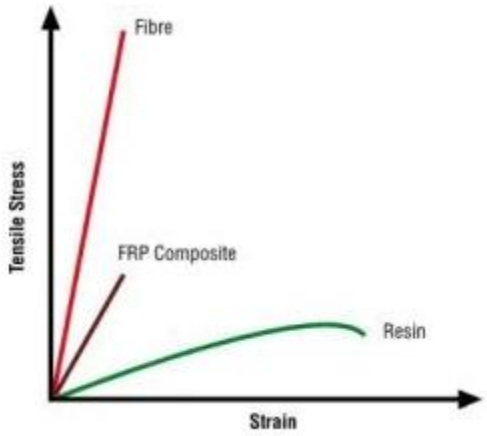

Figure 2.4 : Depiction of Stress vs. strain for composite and its components of resin and fiber

2.2.1 c) CMC

Ceramic matrix composites (CMC's) consist of a ceramic matrix with fibers like silicon carbide which can add refractory properties to the whole composite. The main advantages of CMC's are that they have low density, higher hardness, exceptional thermal and chemical resistance, High melting points, good corrosion resistance, stability at elevated temperatures and high compressive strength. All these properties make CMC's a very suitable option for high temperature(above 1500° C) applications like gas turbine and its components, burners, brake

disks, jet engines, cutting tools, pressure vessels, dies etc (Figure 2.5). General CMC names include combinations of fiber/type of matrix like C/C, C/SiC where C is carbon and SiC is silicon carbide.

Figure 2.5 : Various Applications of CMC materials [49]

Summarizing,

-MMC's have higher modulus of elasticity, ductility and resistance to elevated temperatures than PMC's

- PMC's have high specific strength and specific stiffness

- CMC's were designed to overcome the major disadvantages such as low fracture toughness, brittleness, and limited thermal shock resistance, faced by the traditional ceramics

2.2.2 Based on type of Resin :

2.2.2 a) Thermoplastic

These type of composites are made up of thermoplastic resins like polyester, HDPE, poly-etherimide, polyamide imide, poly-phenylene sulfides etc (see Figure 2.6). They have one or two dimensional molecular structures which have very high melting points of about 260° to 3710 C. During cooling, this softened state at higher temperature can be reversed which would help in

conventional molding techniques. Unlike thermoset resins, thermoplastics can be reused by heating them to their processing temperatures and forming into new desired shapes and this feature saves enormous amounts of time in and is favored in high volume production as in automobile industry. They have relatively weaker temperature strength and chemical stability compared to thermoset resins and higher viscosity which are not suitable for optimum penetration into reinforcement material. Current practices involve use of discontinuous fibers (chopped glass, carbon or graphite) but use of continuous fibers has huge scope in the future.

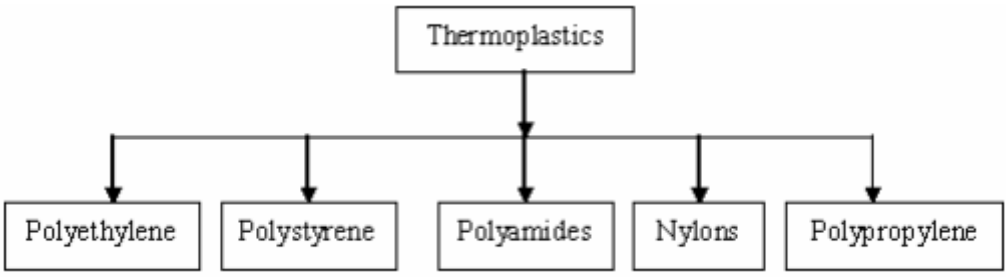

Figure 2.6 : Common examples of Thermoplastics

2.2.2 b) Thermoset

These types of composites are made up of vinyl esters, polyamides, polyesters etc (see Figure 2.7). Though they have low viscosity initially, after curing these have a three dimensional cross linked molecular structure which is bonded well and has high dimensional stability, good resistance to elevated temperatures. They are very flexible in nature as their composition can be altered just by modifying the resin used to get new desired properties if needed. These composites find their use in automobile, naval, aerospace and aeronautical industries. A brief comparison of the thermoplastic and thermoset resins is given in Figure 2.8.

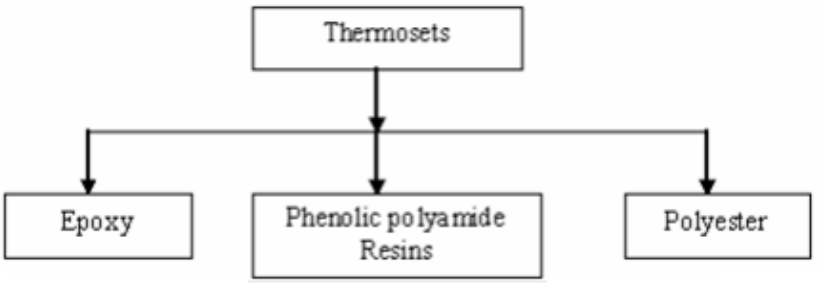

Figure 2.7: Common examples of Thermosets

Resin type	Process temperature	Process time	Use temperature	Solvent resistance	Toughness
Thermoset	Low	High	High	High	Low
Toughened thermoset	↑	↓	↑	↑	↓
Lightly crosslinked thermoplastic	↑	↓	↑	↑	↓
Thermoplastic	High	Low	Low	Low	High

SOURCE: Darrel R. Tenney, NASA Langley Research Center.

Figure 2.8 : Comparison of General characteristics of Thermoset and Thermoplastic matrices **[14]**

2.2.3 Based on type of reinforcement :

2.2.3 a)

i) *Particle/particulate*

The particle/particulate (see Figure 2.9 (a)) are the most widely used type of composites as they have the lowest cost. They can be further classified into two subgroups based on the size of the particles.

- Large particle
- Dispersion strengthened (10-100 nm)

- ***Large particle composites***: These have fillers added to them which improve the properties of the material. The best example is concrete. Concrete has a matrix made of cement and the sand and gravel are added as particulates. An even distribution of similar sized particles is preferred for good reinforcement qualities. A higher particle content in a well bonded composite ensures better mechanical properties as the particles restrain the movement of the matrix.

Other examples include cermets which are made by mixing ceramic particles which are strong and brittle into a soft and ductile metal matrix. The overall effect is a higher toughness. Examples of cermets are cutting tools used for hardened steels made of tungsten carbide or titanium carbide ceramics in Cobalt or Nickel.

- ***Dispersion - strengthened composites***: These have particles which are in the size range of 10-100 nm. The matrix is the load bearing component while the small, hard dispersed particles strengthen the metals and their alloys by obstructing the motion of dislocations thereby limiting plastic deformation.

One of the example is reinforced rubber which uses 20-50 nm carbon particles. It finds its application in automotive tires. Oxides are also often used.

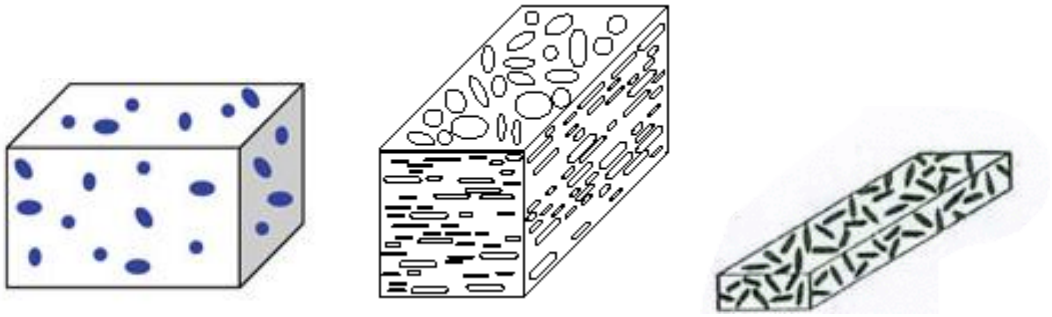

Figure 2.9 : (a)Particulate reinforcement , (b) Flat flakes reinforcement - flake composites, (c) Whisker reinforcements

ii) ***Flake*** :

These are flat, thin pieces/layers/chips broken from a larger piece (Figure 2.9 (b)). They have a two dimensional geometry. They are very good reinforcements as they have equally comparable strength in all directions in the 2D plane. Example of this type is use of aluminium flakes in paints. The flakes get aligned parallel to the coating surface thereby they have a dense packed structure which is a good reinforcement technique.

iii) ***Whisker*** :

They are almost like single crystalline fibers (Figure 2.9 (c)). They are not continuous, but are short in length and have polygonal cross sections.

iv) ***Fiber :***

Fibers are members of material which typically have high aspect ratios i.e., the ratio between a fiber's length to its diameter ratio which is usually around 1000. They are the main reinforcing

component of the composite. They carry the load. These fibers are mainly of two types, namely Continuous and Discontinuous or chopped fibers.

The continuous fibers and long members which are usually aligned in a layer or a laminate form in one or more fiber orientations depending on the application intended (Figure 2.10). On the other hand, the discontinuous fibers are short or chopped and are scattered throughout the matrix till the required thickness is attained. This arrangement can be aligned as in continuous composites or can be random.

This helps these discontinuous composites to be manufactured with ease at relatively lower costs and at a much faster rate compared to the continuous composites.

Some of the common materials used to make these reinforcing fibers are Carbon, glass, wood for applications at room temperatures and materials like silicon carbide for high temperature scenarios.

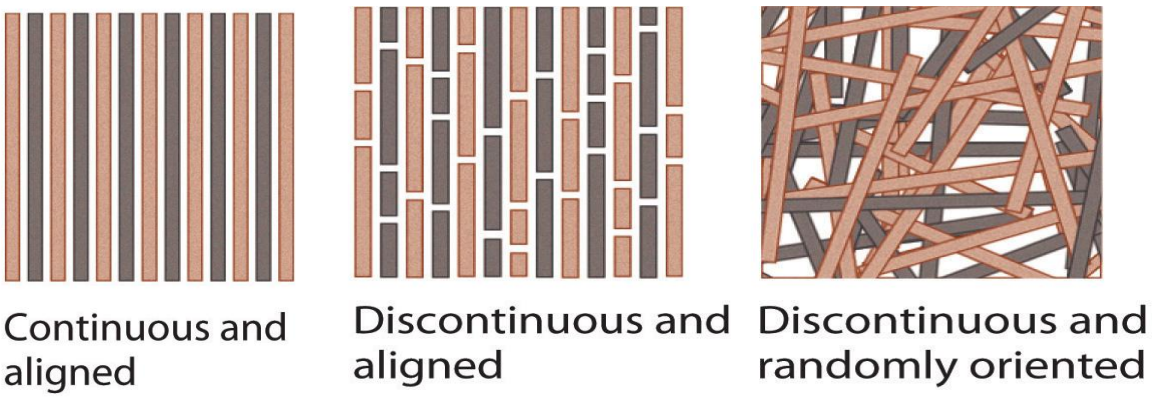

Figure 2.10 : Fiber reinforcements and its types

v) ***Structural :***

These types of composites use not just the composite material but also a homogenous material in various geometrical orientations in order to attain the desired properties. The layup can be mainly in two different ways as below.

Laminar: In Laminar composites, multiple two dimensional sheets of reinforcement of various fiber orientations are stacked and bonded together (Figure 2.11).

The end product has a very high strength as a result of high strength orientations of each panel/sheet in the overall stack. The reinforcement material in these kind of composites can be in many forms such as woven/braided like a fabric, uni-directional fibers or non woven. Common examples are plywood and Ski boards.

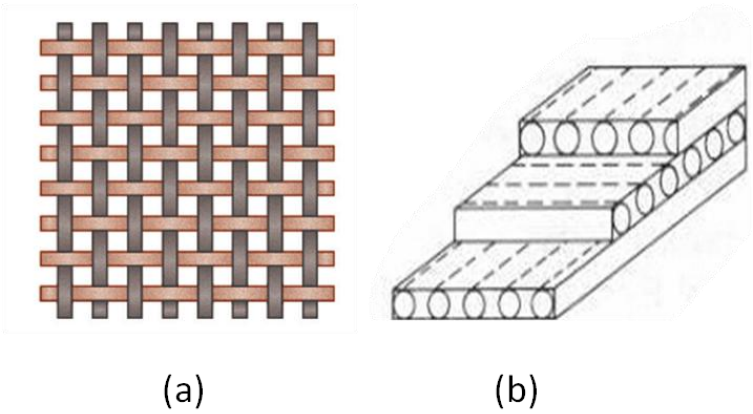

Figure 2.11: Laminar composite examples (a) Fabric , (b) Laminate

Sandwich: In Sandwich composites there are two main sub components namely, the outer "face" material and the inner "core" material (see Figure 2.12). The face material is stiff and has high strength compared to the core material which is lighter in weight and less dense. The properties in the thickness direction are superior in these composites and properties like shear strength. One of the popular pattern is the honeycomb structure which is made up of interlocked hexagonal cells and is covered on top and bottom with strong face sheets. It is used to make rooftops, walls and airplane components.

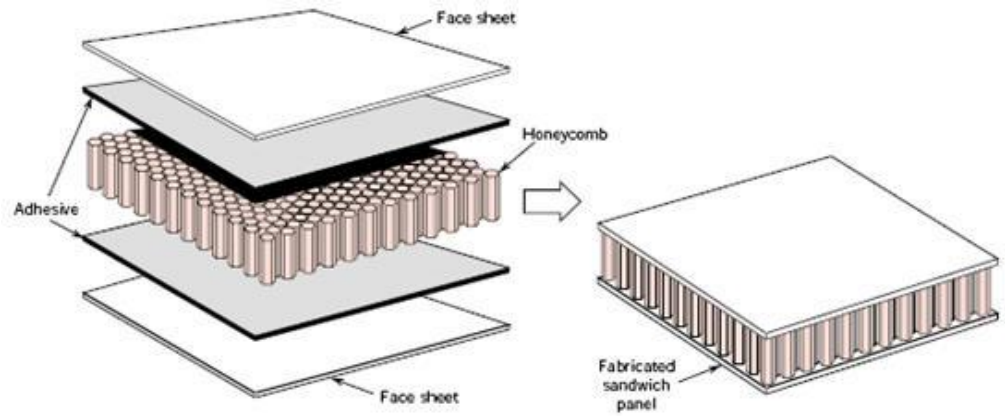

Figure 2.12 : Sandwich structure in a composite; example - Honeycomb pattern **[15]**

2.3 Manufacturing of composites

Manufacture of composites is done by many different methods depending on the type of application they are intended for. Most processes give a near net shape which then need finishing in order to be of the correct dimensional tolerances. The following are some of the popular methods of composite manufacture.

2.3.1 Pultrusion

In this process, the fibers are pulled through resin material and are heated in a die so that the resin can be polymerized and cured. This process creates composites with flexible features such as even cross-section, variable thickness or profiles.

It is a continuous process which is easy to automate and thereby can be very economical. The following Figure 2.13 explains the process in a step by step manner.

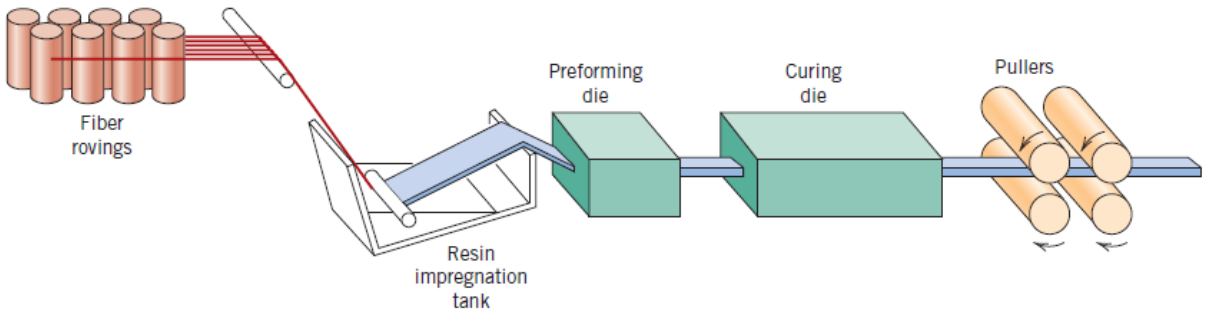

Figure 2.13 : Schematic diagram showing the Pultrusion process **[15]**

2.3.2 Pre-Peg

In this process the, the fibers are impregnated with a resin but unlike pultrusion, the resin is only partially cured. They are delivered to the customers in the form of a tape who then mold and finally cure it completely, to get the final product. It is most preferred for structural applications. The following Figure 2.14 is a schematic of the process.

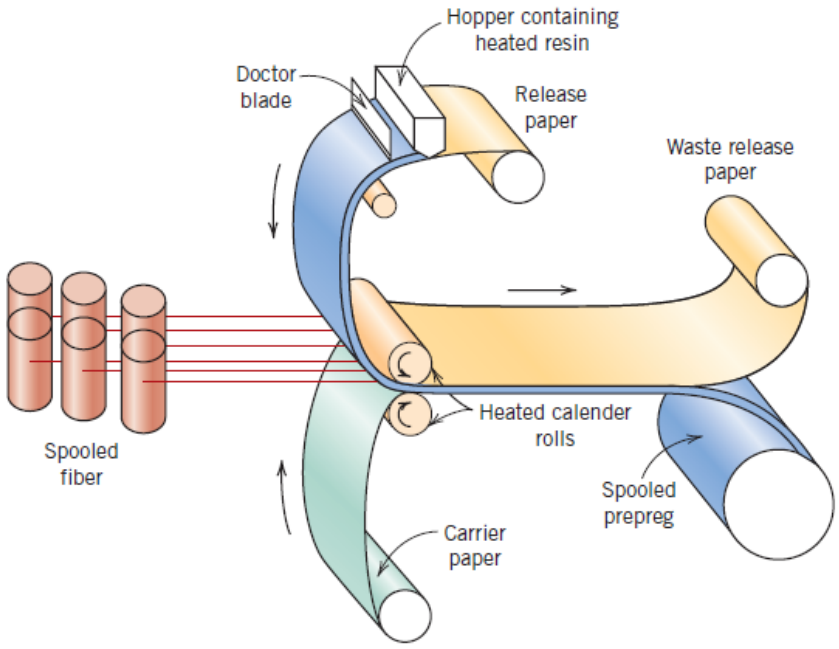

Figure 2.14 : Schematic diagram illustrating the production of prepeg tape using a thermoset polymer **[15]**

2.3.3 Filament winding

In this process, continuous fibers either individually or in tows/groups are run through a resin material and are then rolled around an automated mandrel to create a hollow shape which is usually cylindrical (see Figure 2.15). After the desired thickness is reached in terms of number of layers is reached, they are cured to get the product. Depending on which mechanical properties are needed, the fibers can be wound in various ways like helical, circumferential or polar.

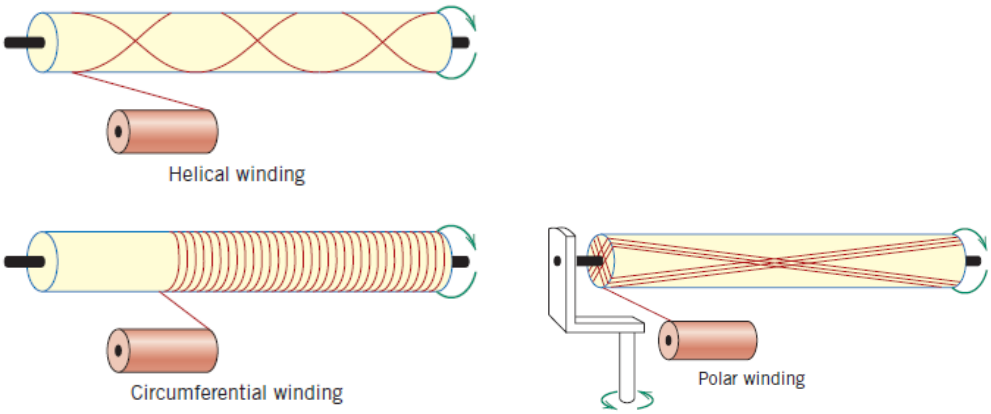

Figure 2.15 : Schematic representations of helical, circumferential and polar filament winding techniques **[15]**

2.3.4 Hand layup process

This process is manual and is not automated. In this process, the mold and the resin are prepared. Then the fibers are placed in the mold and after the resin is added, the pre layup process is completed and the whole thing is cured and de-molded and finishing is done to get the final product (Figure 2.16).

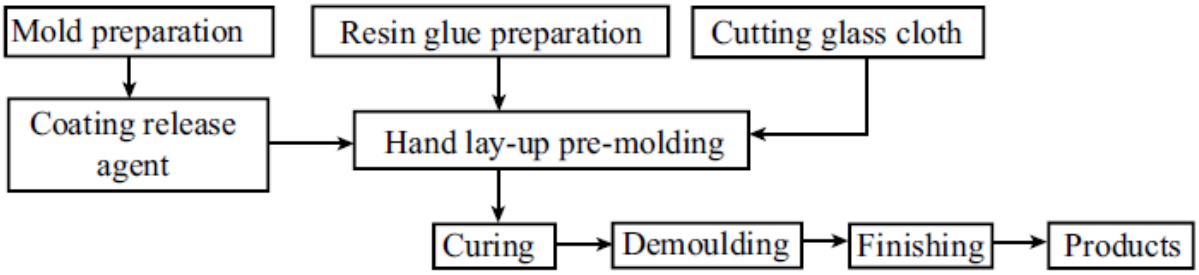

Figure 2.16 : Technique flow chart of FRP by hand layup **[16]**

There are many other composite production methods, such as molding (autoclave, vacuum bag, pressure bag, resin transfer etc), spray layup process, lanxide process, tufting among others (see **Table [2-1]**) **[17]**.

Table [2-1] : Various composite production techniques with examples **[14]**

Technique	Characteristics	Examples
Sheet molding	Fast, flexible, 1-2" fiber	SMC automotive body panels
Injection molding	Fast, high volume very short fibers, thermoplastics	Gears, fan blades
Resin transfer molding	Fast, complex parts, good control of fiber orientation	Automotive structural panels
Prepreg tape lay-up	Slow, laborious, reliable, expensive (speed improved by automation)	Aerospace structures
Pultrusion	Continuous, constant cross-section parts	I-beams, columns
Filament winding	Moderate speed, complex geometries, hollow parts	Aircraft fuselage, pipes, drive shafts
Thermal forming (future)	Reinforced thermoplastic matrices; fast, easy repair, joining	All of above

SOURCE: Office of Technology Assessment, 1988.

2.4 Characteristics of composites

The characteristics of composites are summarised in **Table [2-2]**. Two most important characteristics, namely the specific strength and specific stiffness are shown in Figure 2.17.

Table [2-2]: Specific strength and specific modulus of some common used materials and fiber composites **[16]**

Materials	Density (g/cm^3)	Tensile strength (GPa)	Elastic modulus (10^2GPa)	Specific strength (10^6cm)	Specific modulus (10^8cm)
Steel	7.8	1.03	2.1	1.3	2.7
Aluminum alloy	2.8	0.47	0.75	1.7	2.6
Titanium alloy	4.5	0.96	1.14	2.1	2.5
Glass fiber composite materials	2.0	1.06	0.4	5.3	2.0
Carbon fiber II/epoxy composite materials	1.45	1.50	1.4	10.3	9.7
Carbon fiber I/epoxy composite materials	1.6	1.07	2.4	6.7	15
Organic fiber/epoxy composites	1.4	1.40	0.8	1.0	5.7
Boron fiber/epoxy composites	2.1	1.38	2.1	6.6	10
Boron fiber/aluminum matrix composites	2.65	1.0	2.0	3.8	7.5

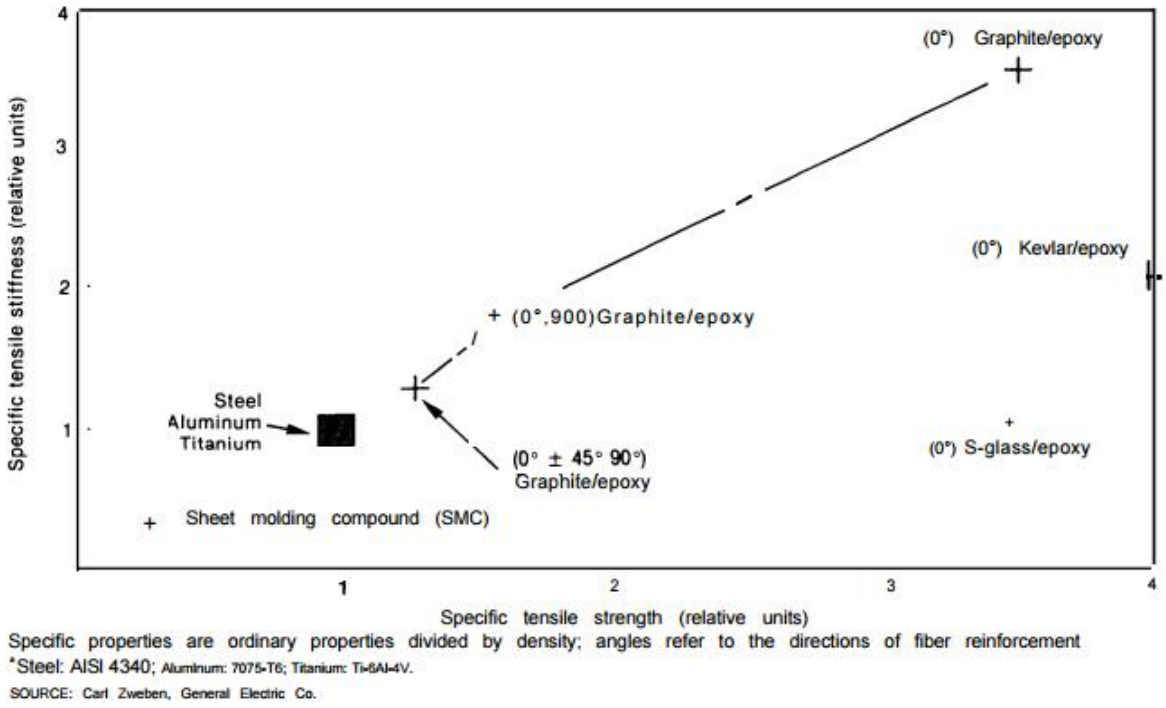

Specific properties are ordinary properties divided by density; angles refer to the directions of fiber reinforcement
*Steel: AISI 4340; Aluminum: 7075-T6; Titanium: Ti-6Al-4V.
SOURCE: Carl Zweben, General Electric Co.

Figure 2.17 : Comparison of the specific strength and stiffness of various composites and metals **[14]**

2.5 Advantages and Disadvantages

2.5.1 Advantages

Some of the major advantages of using composites are,

- High specific strength (ratio of strength and density), high specific modulus (ratio of modulus and density), high stiffness
- Good fatigue resistance and damage tolerance
- Good damping characteristics
- high flexibility in design (size and shape) due to their anisotropic nature
- Light in weight
- Good surface properties like corrosion resistance, tailored surface finish
- Thermal properties like low thermal conductivity, low coefficient of thermal expansion help them to be used in high temperature applications
- Electric properties such as high dielectric strength, non magnetic
- Cost wise, they are economical because they can be mass produced, part-wise consolidated, low production time, long durability

2.5.2 Disadvantages

Some of the disadvantages associated with composites are,

- High cost of raw materials and production/fabrication
- They are relatively more brittle than wrought metals so can be easily damaged
- Properties in the transverse direction may be weak
- Matrix does not have high strength so it has low toughness and can degrade when exposed to environment
- Disposal and reuse are difficult
- Difficult to attach numerous parts together

- Repair technology is still in early stages of development and is not easy as the materials require a temperature controlled (cold) transport which gives them limited shelf life, curing whether hot or cold takes time and in some cases special tooling might be required, and analyzing is difficult

2.6 Applications of composites

Composites are being widely used in the present day world due to their various properties like light weight, design flexibility, high stiffness among many others. Initially the glass fiber composites were used but when it was realized that they have high mass and low modulus, the focus shifted to lightweight carbon fiber composites which could sustain high loads while not having high mass. Later on advanced composite materials like polyamides were created and used [**16**]. Aircraft industry is one of the leading users of composite materials. The use of composites in commercial aircrafts has been steadily increasing. Boeing 777 released in 1995 had composites up to 10% of its total structural weight and Airbus A380 released in 2007 used 20% composites in structural weight. Boeing 787 and Airbus A350 XWB are projected to use 50% and 52% respectively [18]. Aircraft industry isn't the only one using composites in large volumes but they are being used in automobile industry, space applications, marine applications etc **[**18-20**].**

Some of the major applications are:

- High temperature areas like gas turbine components(turbine blades, combustion chambers), brake disks, brake system components, components for burners, flame holders and hot gas ducts, heat shield systems(under thermal shock and heavy vibration conditions)
- Electrical mouldings
- Automobile parts in body of cars, bicycles etc
- Marine applications like shafts, hulls and spars (for racing boats)
- Electronic circuit boards, communication antennae
- Sealants and gaskets
- Safety equipment like ballistic protection, air bags in cars etc

- In railway coach components
- Carbide drills made of cobalt matrix which is tough with tungsten carbide particles inside
- Laminates in decorative purposes

2.7 Machining of Composites

The behaviour of a composite material during machining depends on diverse fibre and matrix properties, the fibre orientation and the relative volume of the matrix and the fibres **[18,21,22].** During machining of composite laminates the tool encounters the matrix and fibre materials alternately with varying responses to machining by both of these materials. The chip formation in orthogonal cutting can be due to fracture or shear or a combination of both dependent on the fibre orientation and tool geometry. Since the fibres are abrasive, tooling materials resistant to abrasive wear such as Polycrystalline Diamond (PCD) and Carbide Cutters are widely used in composites machining. The majority of machining operations of CFRP's are either edge machining/trimming and/or drilling of holes in laminates. Though production of composites can be done to near net shape, additional finishing operations are needed to achieve the specified dimensional tolerances to get the final product.

As most CFRP's are near net manufactured, trimming generally is considered a low material removal process compared to the total volume of the material. The largest influence on the machinability of any CFRP laminate is the type of fibre reinforcement used and its mechanical properties. The mechanical properties of high tensile strength, high modulus of elasticity, high yield strength and thermal properties of the fibre reinforcement have a great effect on the machinability of the laminate. To truly understand the mechanics of trimming of CFRP laminates, the cutting mechanism involved with these processes need to be studied. One of the earliest works on the study of cutting mechanisms was carried out by Koplev **[22].** He conducted a series of cutting tests on CFRP composite material to study the chip formation process and the machined surface on unidirectional material. His unique methodology of capturing the small chips using the 'macrochip method' is still in use by today's experimental investigators. This method uses the application of a rubber adhesive to the workpiece surface to collect the small chips, which are then transferred to a double-sided adhesive tape for observation and analysis. His experiments showed that the resultant surface quality of the machined surface was dependent

on the fibre orientation, the smoothest surface obtained when the cutting direction was parallel to the fibre orientation. Perpendicular to fibre machining usually resulted in an increase in resultant surface roughness. His conclusions on chip formation were that chips were formed by brittle fracture of both the fibres and the matrix. The chip formation varies if the machining is perpendicular to the fibres or parallel to the fibres. During perpendicular to fibre machining, the tool exerts a compressive force with its front surface on the material causing the composite to fracture and creating a chip. Similarly on during parallel to the fibre machining process, a compressive force is exerted causing chips to be created but it is accompanied by cracking on the front of the tool tip which helps in initiation of the next chip creation process. Koplev also analyzed the relationship between cutting forces and the chip formation process and tool geometries. He concluded that the principal cutting force was proportional to the depth of cut and varied with the rake angle increasing with its increase. His work is considered as one of the founding bodies of work in the study of mechanics of orthogonal machining of CFRP composite materials. in addition to the chip formation the researchers concluded that during machining three different types of chips are created **[22-28] :**

- Powder like chips – produced by fracture
- Ribbon like chips – unbroken segments, produced by fracture with fibre breakage
- Large brush like chips – produced by delamination at the end of a cut

Their study also linked surface roughness to high cutting speeds and lower feed rates, an affect they attributed to heat build-up as a result of poor thermal conductivity. Bhatnagar et al. **[24]** in their studies observed that the in-plane shear strength of a composite material influenced its machinability. Using the Iosipescu shear test they calculated the shear strength and plotted the variation of in-plane shear strength with the fibre angle. They studied the two process variables, machining direction and Fibre orientation. The machining direction being expressed as the angle between the cutting velocity vector and the fibre orientation in a plane perpendicular to the cutting edge of the tool. The fibre orientation is the angle measured counter-clockwise from the datum of the machined surface. For fibre orientation less than 90°, they found that the fibres break in tension and chips are produced ahead of the cutting edge of the tool by shearing the matrix in a plane along the fibre orientation. Their study also showed the cutting forces to be higher for fibre orientations less than 90°. For Fibre angles greater than 90°, they showed that the fibres experience compression and bending are broken by shearing. They used Merchant's model

to create a predictive model for cutting forces by substituting the fibre angle instead of the shear plane angle. They also noted that the friction condition on the rake face of the tool changes depending on the fibre orientations. This indicates that the tool wear not only depends on the direction of cutting but also on the individual fibre orientations. Chip formation in orthogonal edge trimming of graphite/epoxy composite was studied by Arola, Ramulu & Wang **[25].** They found that the characteristics of chip formation were primarily dependent on Fibre orientation with only secondary effects from tool geometry and operating conditions. An increase in the rake angle of the tool was found to localize the extent of fracture from the tool nose, resulting in smaller discontinuous chips, giving better machined surface quality. They observed three different cutting mechanisms during edge trimming of the unidirectional graphite/epoxy laminate. In 0^o fibre orientations, chip formation mechanisms included failure along the fibre-matrix interface through cantilever bending and fracture perpendicular to the fibre direction. In positive fibre orientations up to 75^o chip formation involved compressive loading induced shear at the tool nose. In the 90^o and negative fibre orientations chip formation and material removal in trimming comprised out-of-plane shear with severe compressive loading induced intra-laminar deformation. Chip formation during orthogonal edge trimming of unidirectional graphite/epoxy composite is shown in Figure 2.18 from Wang, Ramulu & Arola **[26-28]**

However, in Industry, Drilling and Milling are two of the most popular machining methods adopted to carry out the most of the structural fabrications and finishing process. . Relatively, more research has been done on the drilling of composites compared to the milling of composites. The research herein will primarily focus on milling of Carbon fiber Reinforced Composites (CFRP) and HexMC ®materials. Milling of composites is discussed in detail in the following section.

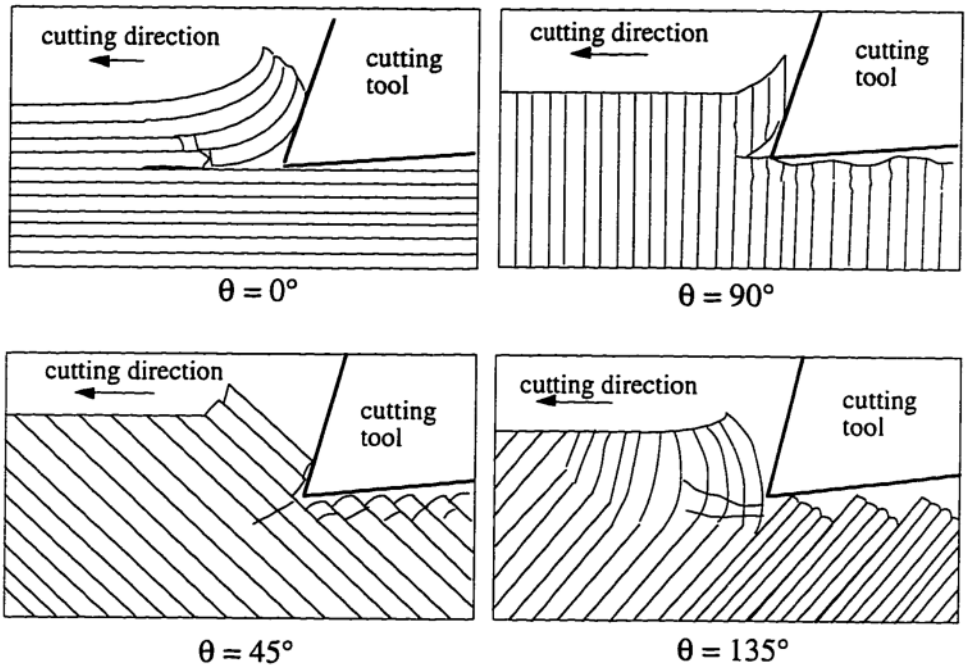

Figure 2.18 : Chip Formation in Orthogonal Trimming of Unidirectional Graphite/Epoxy Laminate, Wang, Ramulu & Arola [26]

A variety of machining methods can be used to machine composites **[2-3,27,29]** . Uhlmann et al **[30]** compared different methods like milling, water jet cutting, CO_2 jet cutting and grinding of CFRP's. They found out that by using higher pressure and higher feed rates, water jet cutting can achieve good work piece surface quality and that CO_2 and belt grinding processes show good potential to be a high productive process with high quality of machined surfaces. Slamani et al **[31]** studied the effects of machining parameters on cutting forces during a high speed robotic trimming of CFRP's. They found that the feed rate is one of the main influencing parameter on cutting force components. The robot configuration was added as an independent variable in a new extended model whose prediction capacity was increase significantly from the model used before in their research. So it was realized that this models allowed the robotic trimming process to have better control of the robot deflection, and an overall increase in machining quality because of less tool wear and by avoiding delamination. There are quite a few papers on review of various kinds of machining processes for Composite materials in the literature **[32,33]** that state and compare the traditional methods with the latest technologically advanced procedures. These give us a good idea on the evolution of machining methods over the years.

2.8 Milling of composites

Extensive research has been done on machining of composites **[22-29]**. There are a few models in literature **[23,34,35]** which explain the cutting mechanism behind milling of composites. This research mainly focuses on comparing the cutting mechanism of a uni-directional composite and a random fiber composite.

2.8.1 Fundamentals of Milling

Milling is a type of machining process which uses rotary cutters to remove material from a work piece. A small amount of material is removed in each rotation as each tooth cuts into the material. It can be used to perform a variety of operations and can easily be called as one of the most popular and commonly used process in the current industry and machine shops. It is different from the other machining operations in such a way that the cutting is not continuous but is repetitive in regular intervals as the cutting teeth engage and disengage with the work piece material. In today's modern CNC machines, three -axis (XYZ) movement is possible along with high speeds of spindle rotation and a wide range of feeds. Typically both the cutting tool and the work piece can be moved which facilitates the cutting of many surfaces with different orientations. There are mainly two types of milling which are End milling (face milling) and edge trimming (peripheral milling) as shown in the Figure 2.19 below.

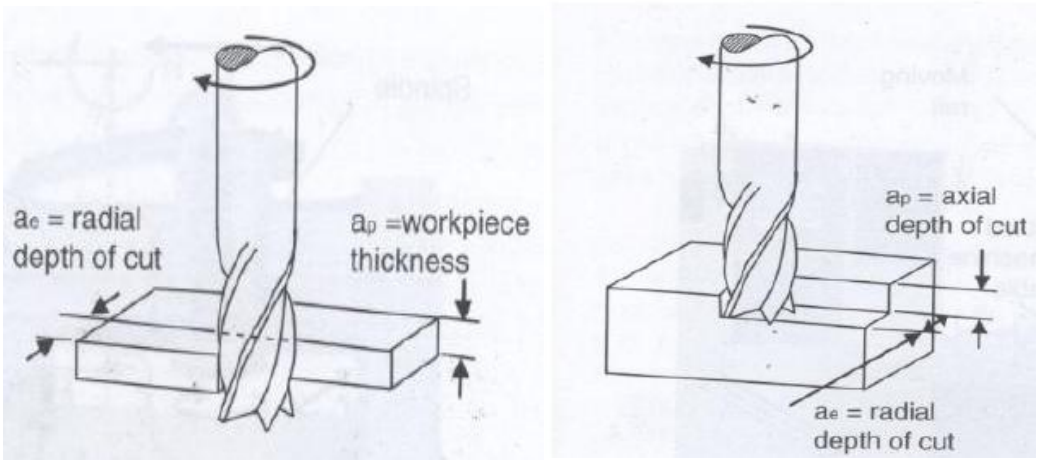

(a) (b)

Figure 2.19 : Types of Milling, a) Edge trimming , (b) End milling

- ***Edge trimming*** : In this type of milling the cutting tool axis is parallel to the surface of the work piece to be cut and the work piece is engaged in the cutter's radial direction. The cutting is carried out by the end or the edges on the periphery of the tool. It is usually done in horizontal (spindle) milling machines but can also be done on vertical (spindle) milling machines.

In edge trimming the tool diameter is usually small and the entire thickness of the work piece is covered due to the axial engagement of the tool. There are various variations to edge trimming like slab milling, slotting, side milling, Straddle milling and Form milling as shown in Figure 2.20 below.

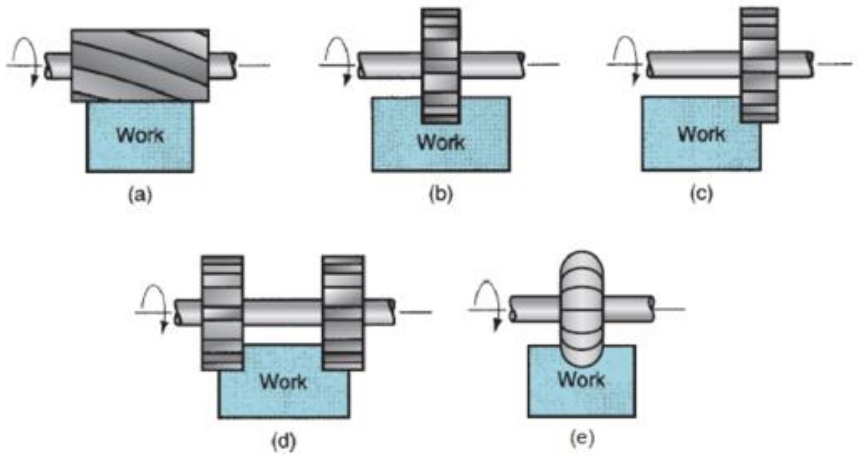

Figure 2.20 : Types of edge trimming - a) Slab milling, b) Slotting, c) Side milling, d) Straddle milling, e) Form cutting **[50]**

- ***End milling*** : In this case of milling the engagement in the axial direction might be less than the work piece thickness and thereby creates a slot. Vertical milling machine is mostly used but horizontal milling machine is used for face milling. The number of flutes chosen in an end mill are determined by various factors such as work piece material and its dimensions along with the milling conditions like spindle power etc. The following Figure 2.21 compares different number of flutes and their characteristic features.

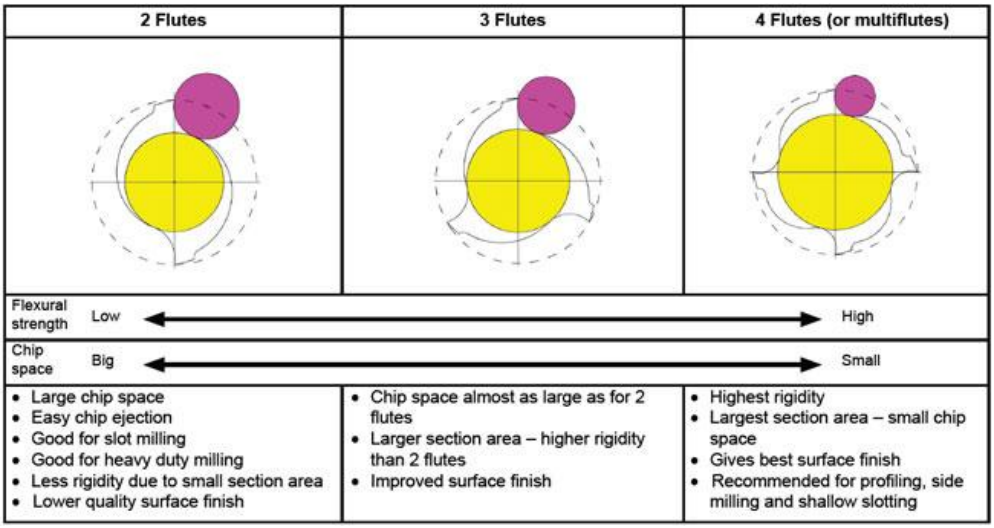

Figure 2.21 : End mill - Characteristic comparison of different number of flutes **[51]**

The spindle holds the cutting tool and the work piece is held on the machine table. Depending on how the cutter rotation and the work piece feed direction interact, there are two types of milling, Conventional (Up) Milling and Climb (down) milling as shown in Figure 2.22. In conventional milling, the cutter rotates in the opposite direction of the feed whereas during climb milling, the cutter rotates in the same direction as the feed. Backlash (see Figure 2.23), which is the play between the lead screw and the nut in the machine table, plays an important role in deciding between these two types of milling. Typically conventional milling was preferred as it eliminated backlash but most modern machines compensate for it or have eliminators which then made climb milling a more popular approach.

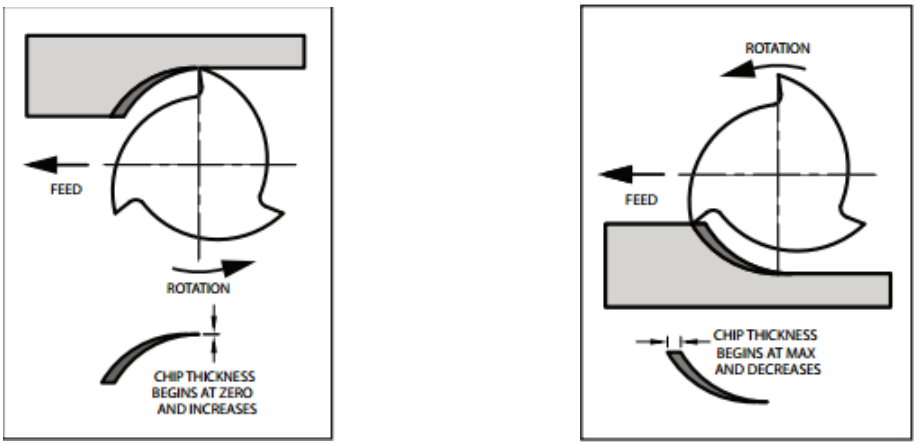

(a) (b)

Figure 2.22 : a) Conventional Milling, b) Climb milling **[52]**

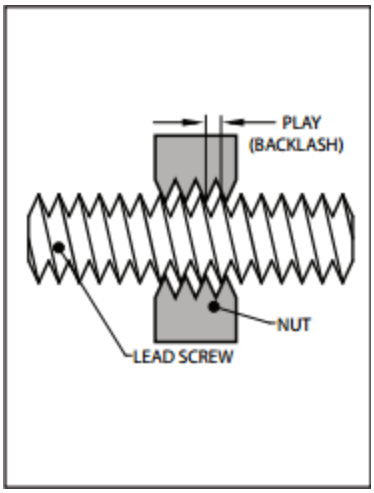

Figure 2.23 : Figure depicting backlash in milling process **[30]**

Conventional Milling (Up milling)

- The chip thickness starts from zero and increases gradually
- The engaging forces are low and cause the work piece to lift up
- Extensive fixtures are needed to compensate for the lift
- Heat is diffused better and work hardening is produced
- Chips are carried upwards by the teeth and they fall in front of the cutter causing an uneven surface and re-cutting of chips.

Climb Milling (Down milling)

- the chip thickness starts from maximum and gradually decreases
- The engaging forces are high and tend to push the work piece against the holding surface
- Less elaborate/complex fixtures are needed here
- More heat is generated here but is likely to get transferred to the chip
- Chips fall behind the cutter and are removed so there is lesser chance of re-cutting
- Down milling creates a cleaner shear plane which causes lesser rubbing of the tool thereby increasing the life of the tool
- Higher rake angles may also be used here due to the downward push of the work piece

Climb milling is generally the best way to machine parts today since it reduces the load from the cutting edge, leaves a better surface finish, and improves tool life. During conventional milling, the cutter tends to dig into the work piece and may cause the part to be cut out of tolerance. Even though climb milling is the preferred way to machine parts, there are times when conventional milling is the recommended choice. Backlash, which is typically found in older and manual machines, is a huge concern with climb milling.

If the machine does not counteract backlash, conventional milling should be implemented. Conventional milling is also suggested for use on casting or forgings or when the part is case hardened since the cut begins under the surface of the material **[32**].

2.8.2 Process parameters in Milling and cutting conditions

Milling is one of the popular methods to machine FRP's. There are many variables involved in any machining process that influence the overall cutting. There are input variables which are independent and dependent variables. Some of the independent input variables are, material of the work piece, machining process used, material of the cutting tool, parameters of cutting such as depth of cuts in axial and radial directions, spindle speed and feed rate, and geometry of the work piece. And then there are dependent variables. Various selection criteria are used to narrow down a particular process intended for use based on machinability **[36].**

Some of the common and popularly chosen parameters to quantify machinability are **[36]**:

- Cutting speed for a target tool life
- Power required
- Volume of material removed
- Tool life
- Tool forces
- Surface finish
- Temperature

The machinability of FRP's in milling is mainly characterized by tool wear, surface roughness and delamination **[37-40].** Ucar and Wang **[37]** performed end milling on CFRC and found out cutting conditions that satisfied their criteria of machinability in terms of cutting speed and feed rate.

2.8.3 Milling Force models

Most CFRP parts are produced near net shape but need further machining operations to give them their final shape. Milling is one of the popular methods to do this. To fully understand the behavior of the material under the influence of various cutting parameters and to optimize the whole process, we need to study the models which predict the cutting forces and other output variables like surface roughness or tool wear. These models vary a little for Uni-directional (UD) composites and multi-directional (MD) composites.

2.8.3.1 Uni -directional composites

-Karpat et al **[34]** created a force model which predicted the cutting forces during milling of UD CFRP laminates. They used two different fiber oriented UD laminates and measured the forces using a rotating type dynamometer. The following equations was developed to represent the forces in x and y directions as a function of chip thickness (h), feed (f), tool rotation angle (φ), axial depth of cut (a_p), and fiber cutting angle (β).

Fiber cutting angle β is given by,

$$\beta_{\emptyset,0} = \emptyset + \theta \quad if\ \beta \geq 180 \quad then\ \beta = mod(\beta, 180)$$

Based on different fiber cutting angles (β), various chip formation mechanisms are identified as follows,

a) β = 0 ; α = Positive

Bending stress » fibers are peeled off of the matrix;

α = Negative or Zero

Due to buckling of fibers » Small chips

b) β = 45° ; α = Positive

Due to compressive stresses » fibers are crushed » shear failure of fiber matrix interface » generation of cracks above and below cutting plane

c) β = 90°

Due to high inter-laminar shear stresses » Chips fracture along fiber matrix interface (similar to 45°)

d) β = 135°

Due to bending and inter-laminar failure » fibers are fractured and hence are peeled off surface

Cutting forces in x-y direction for tool with helix angle (γ) = 0 and rake angle (α) = 0,

$$\begin{bmatrix} F_x \\ F_y \end{bmatrix} = a_p \sum_{j=0}^{s-1} g_j \left(h_j \begin{bmatrix} -\cos\emptyset & \sin\emptyset \\ \sin\emptyset & -\cos\emptyset \end{bmatrix} \begin{bmatrix} K_{tc}(\beta) \\ K_{rc}(\beta) \end{bmatrix} + \begin{bmatrix} -\cos\emptyset & \sin\emptyset \\ \sin\emptyset & -\cos\emptyset \end{bmatrix} \begin{bmatrix} K_{te}(\beta) \\ K_{re}(\beta) \end{bmatrix} \right) h_j$$
$$= f \sin(\emptyset_j)$$

where,

'g' is a Control function to define if the tool is in cut or not and ' $\varphi_j(t)$' gives the instantaneous location of the tooth and are represented by,

$$\emptyset_j = \emptyset_0 - j\frac{2\pi}{s} \qquad j = 0,1,\ldots\ldots,s$$

$$g_j(\emptyset_j) = \begin{Bmatrix} 1 & \emptyset_s \le \emptyset_j \le \emptyset_e \ \ and \ \ h_j > 0 \\ 0 & elsewhere \end{Bmatrix}$$

A sinusoidal function is considered to compensate for the tool's eccentricity and to account for this, h is modified as follows,

$$h_j = f \sin(\emptyset_j) + \begin{bmatrix} \sin(\emptyset_j + \varphi) & \cos(\emptyset_j + \varphi) \end{bmatrix} \begin{bmatrix} e_0 \sin(\emptyset_0 + \varphi) \\ e_0 \cos(\emptyset_0 + \varphi) \end{bmatrix}$$

When helix angle is to be changed other than to zero, the cutting force models have to be modified.

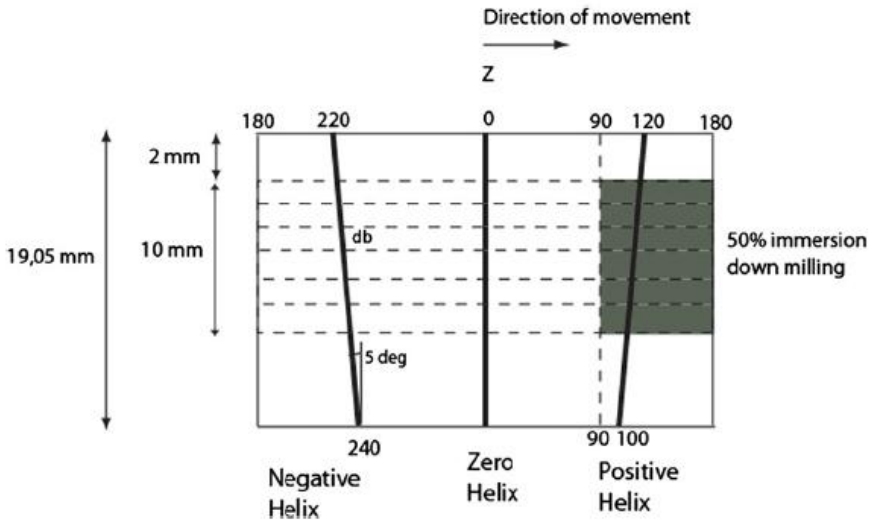

Figure 2.24 : Unrolled periphery of the variable helix milling cutter in [34]

z = 0 represents bottom surface of cutter.

Due to helix angles, cutting edges enter and leave the cut with a delay. dφ gives the incremental cutter rotation angle. The following equation gives us the number of steps in the force simulation model so that angles for each axial slice match dφ.

$$number\ of\ steps = \frac{360D}{2db\tan(\gamma)}$$

Bottom clearance = 2 mm ; Axial depth of cut = 10 mm;

Following equation gives us the matrix which calculates the delay based on the calculation of entry and exit angles for 0,+ve and -ve helix teeth as a function of bottom clearance and axial depth of cut.

$$delay = \lambda = \begin{bmatrix} 0 & 118 & 222 \\ \dots & \dots & \dots \\ 0 & 109 & 230 \end{bmatrix}$$

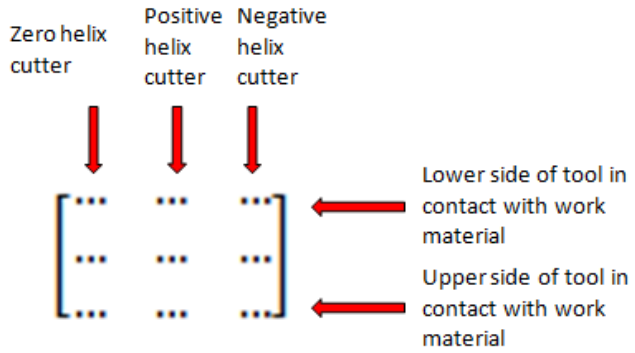

Figure 2.25 : Matrix used to calculate the delay

In each simulation step (dφ) is updated and for each slice 'db' , the forces are calculated and summed up in axial direction.

The fiber cutting angle keeps changing in slotting operation and is represented by the following matrix,

$$Fiber\ Cut\ Direction = \begin{bmatrix} 0(180)\ldots & \ldots 45\ldots & \ldots 90\ldots & \ldots 135\ldots & \ldots 0(180) \\ 45\ldots & \ldots 90\ldots & \ldots 135\ldots & \ldots 0(180)\ldots & \ldots 45 \\ 90\ldots & \ldots 135\ldots & \ldots 0(180)\ldots & \ldots 45\ldots & \ldots 90 \\ 135\ldots & \ldots 0(180)\ldots & \ldots 45\ldots & .90\ldots & \ldots 135 \end{bmatrix}$$

Three representative location at 45°,90° and 135° are chosen to see variation of cutting force coefficients.

At each location, 4 different fiber cutting angles can be obtained based on FD.

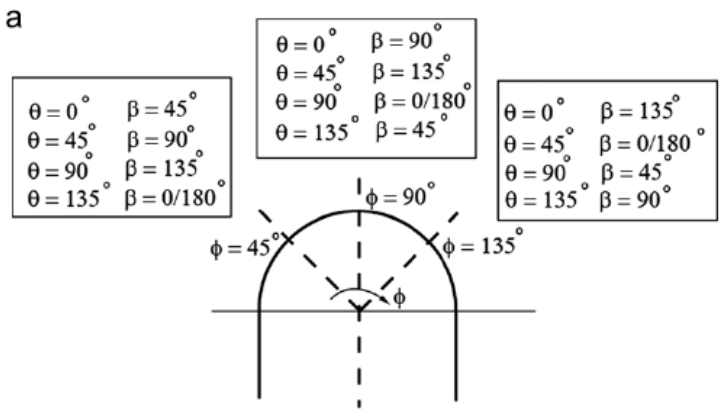

Figure 2.26 : Fiber cutting angles based on fiber direction

The average cutting force coefficients in tangential and radial directions can be determined by considering diagonal elements given in above matrix.

A least squares optimization algorithm is used to represent cutting force coefficients in sine function form as in following equations,

$$K_{tc} = 830 + 410\ \sin\left(2\beta_{\emptyset,0} + \ 215\right) \quad \left(\frac{N}{mm^2}\right)$$

$$K_{rc} = 3000 + 1810\ \sin\left(2\beta_{\emptyset,0} + \ 175\right) \quad \left(\frac{N}{mm^2}\right)$$

Rubbing forces are included in the above equation of K_{rc} . To remove them, values calculated during entry (tool rotation angle φ= 0 ° - 25°) and exit (tool rotation angle φ= 145 ° - 180°) are REMOVED.

$$K_{rc} = 2200 + 1400\ \sin\left(2\beta_{\emptyset,0} + \ 175\right) \quad \left(\frac{N}{mm^2}\right)$$

Further, Karpat and co-workers also found that the sine function could represent the relationship between force coefficients and cutting angle well. The maximum radial cutting force coefficient occurred at 140° and tangential coefficient at 120°. The machining forces were lower for the 45°/135° laminate compared to the 0°/90° laminate and a 45° cutting angle was found to improve surface quality. See Appendix M for the background basic equations.

2.8.3.2 Multi -directional composites

Karpat et al **[34,35]** modeled milling of multi-directional CFRP material along with UD CFRP **[34]**. The equations used are similar to equations 1-4 with slight modifications. They found good agreement between modeled predicted data and measured data. Baohai et al **[41]** predicted cutting forces in circular end milling. Predicting forces in circular milling is complex compared to the linear milling process as the cutting angle is continuously changing. The instantaneous parameters are taken into consideration and the forces are calculated by integrating the values from small differential elements of cutting flute. The final -cutting force coefficients in tangential, radial and axial directions are found from functions in terms of the radial depth of cut. This model was found to agree well as the simulation results were similar to the measured

results. Kalla et al **[42]** predicted cutting forces in helical end milling of CFRP material with the help of a mechanistic force model. The elemental forces were first resolved into components and then summed up as total forces acting on each tooth. The cutting force coefficients in this model are imported from an ANN database and from previous literature. They observed that this model had higher accuracy in prediction in UD composites compared to MD composites. Sorrentino and Turchetta **[39]** calculated the tangential and radial cutting forces in end milling of CFRP as a function of Fx, Fy and angular position of cutter(θ) with the following equation.

$$F_T = F_y cos\theta - F_x sin\theta \; and \; F_R = F_x cos\theta + F_y sin\theta$$

They also performed regression analysis as a function of the three main parameters of feed speed, depth of cut and chip thickness to find out the values of the cutting force components F_T and F_R.

Chapter 3: Experimental Procedure and Methodology

3.1 Introduction

The machining process used in this research, concentrates mainly on end milling and edge trimming of composites. Three main process parameters have been chosen from literature**[41]**, namely Cutting speed, feed of the work piece and the depth of cut. Along with these three parameters, the effects of fiber orientation have also been studied by performing the experiments on two different types of materials with varying fiber directions. The experimental conditions have been chosen by performing DOE using the Design Expert software. Surface roughness measurements and SEM micrographs have been taken for selective experiments to analyze the surface properties after machining.

3.2 Materials and Tests performed

Two main types of materials were used in this research mainly different based on their fiber orientation. The first material used is a unidirectional Carbon Fiber Reinforced Composite (CFRP). It is a carbon epoxy laminate, cured in the autoclave and pre-peg manufactured from unidirectional tape without fiberglass face sheets which uses Toray T800H high strength, intermediate modulus yarn and toughened epoxy resin 3900-2 **[27].** The second material used is a random fiber HexMC ® composite manufactured by Hexcel company. It is made from long carbon fibers and low resin content which makes it suitable for high volume and complex shaped part production. It's specific tensile modulus is 29 and density is 1.55 g/cm^3 **[38]** . The following **Table [3-1]** gives a detailed description of the materials used and their properties. A diamond cutter was used to cut the materials into smaller pieces suitable for experimentation. Three main types of experiments were performed, Edge trimming, Semi circular slot test and an octagonal slot test. Figure 3.1 shows the two materials used.

Figure 3.1 : Materials used, Left - UD CFRP, Right - Random fiber HexMC

Table [3-1]: Materials Used, their properties and Type of Experiments performed

S.No.	Test Type	Mfg.	Length (in)	Width (in)	Thickness (in)	Type	No. of Plies	Layup
1.	Uni Directional CFRP - Edge trim	Toray	48	48	0.25	Uni	67	[100% / 0% / 0%], $[0]_{67}$
2.	Semi-circular Slot test	Toray	48	48	0.75	Uni	100	[100% / 0% / 0%], $[0]_{100}$
3.	Octagonal Slot test	Toray	48	48	0.25	Uni	67	[100% / 0% / 0%], $[0]_{67}$
4.	HexMC® - Edge trim	Hexcel	35	35	0.5	Random	-	Random

Sample Preparation :

Figure 3.2 is a schematic showing the sample preparation.

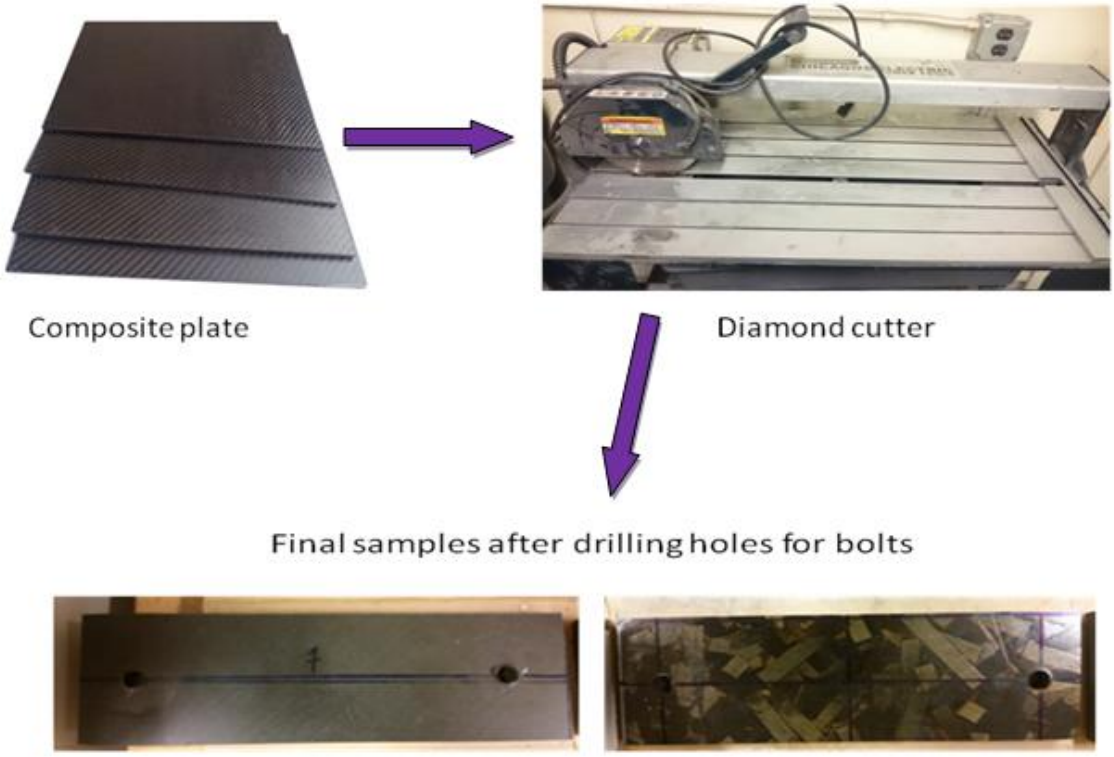

Figure 3.2 : Schematic to represent sample preparation

3.3 Experimental Setup

A HAAS TM1P CNC milling machine (Figure 3.3 below) was used to machine in this research. The specifications of this machine are given in the **Table [3-2]** below. The machining was done without the use of any coolant or liquid, in a dry condition as these experiments were also used to take in data related to dust **[40]**. To contain the dust within a small area, a plexiglass containment box was used into which vacuum pipes were fitted into for continuous absorption of dust and further analysis. An aluminium fixture designed by Jeffrey Miller **[27]** has been used for securing all the work pieces. To collect the instantaneous force data, a Kistler 9123C dynamometer has been used. Further detailed description of this dynamometer will be given in **section 3.4** .

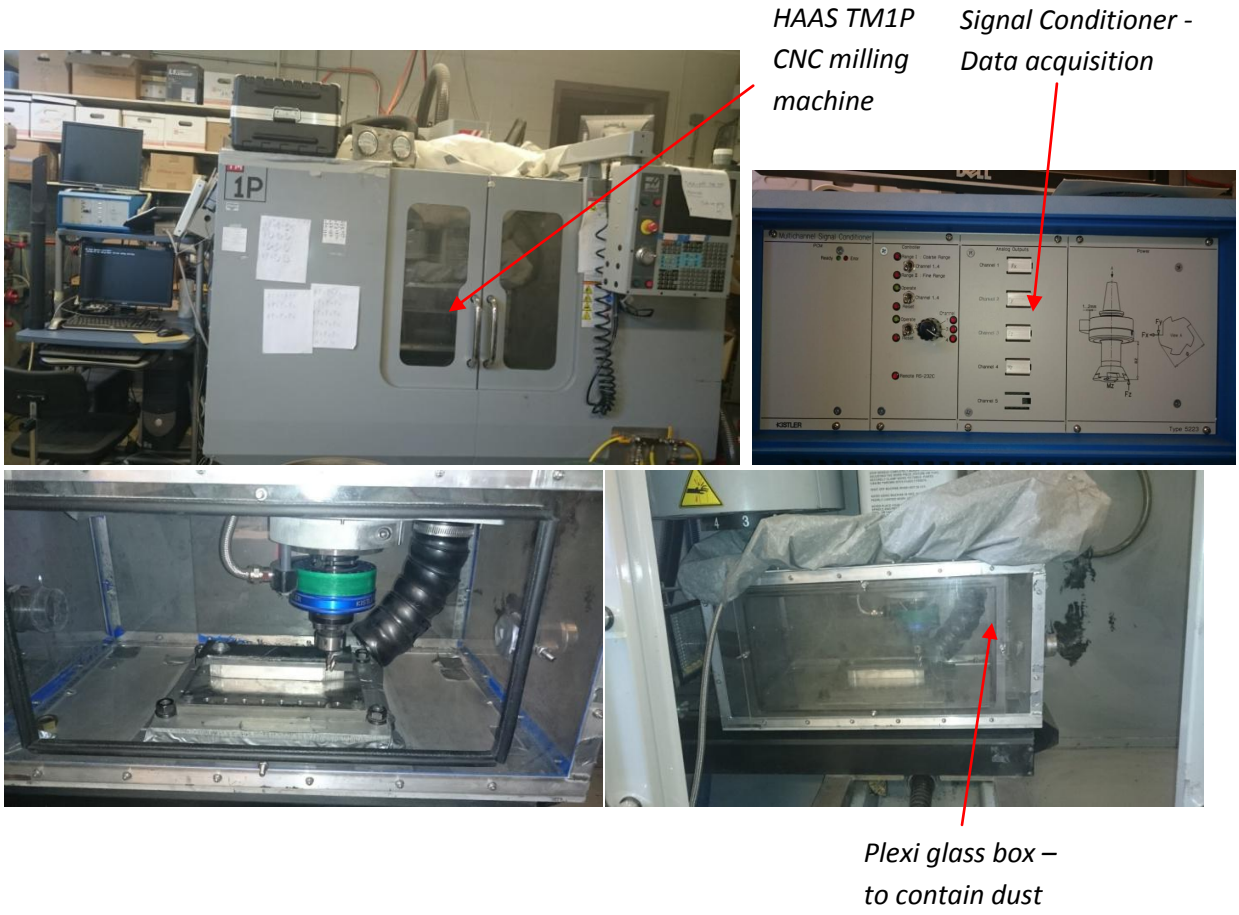

Figure 3.3 : (Top) *HAAS TM 1P milling machine and Plexiglass box (bottom)*

Table [3-2]: HAAS TM1P CNC milling machine specifications **[40]**

Item	Value	Units
Maximum spindle speed	6000	rpm
Maximum spindle torque	45 Nm @ 1200 rpm	Nm
Maximum spindle rating	5.6	kW
Spindle cooling type	Air cooling	-
Maximum travel in X direction	762	mm
Maximum travel in Y direction	305	mm
Maximum travel in Z direction	406	mm
Maximum cutting feed rate	10.2	m/min
Maximum thrust force	8896	N
Spindle taper	Taper 40 (BT 40)	-
Maximum tool diameter	89	mm
Accuracy	0.01	mm
Repeatability	0.005	mm
Acceleration (HAAS)	1,600,000	encoder counts/sec^2
Encoder counts/inch	138,718	encoder counts/inch

3.4 Equipment Used

3.4 a) Dynamometer

The dynamometer is a tool used to measure the force and torque. It can be stationary or a rotating type. Figure 3.4 is a representation of major types of dynamometers which are most commonly used. Each of the above types has its own advantages, which are summarized in the following **Table [3-3].**

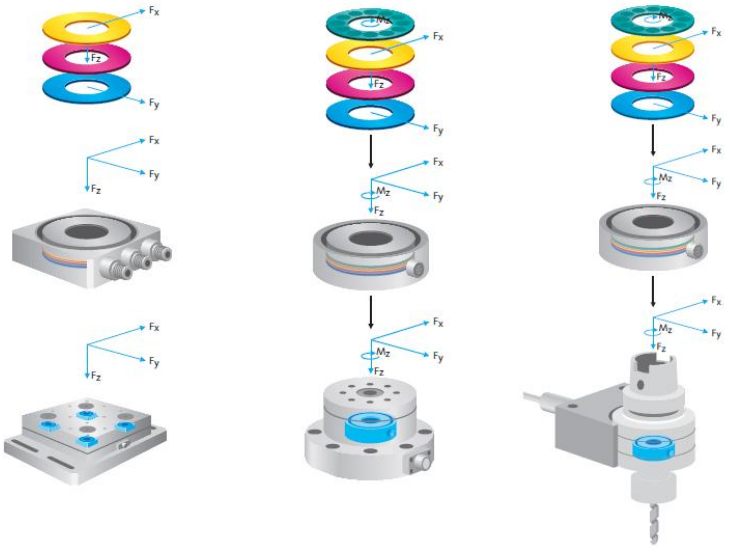

Figure 3.4 : *a) Stationary 3 component dynamometer (left) , b) Stationary 4 component dynamometer(middle), c) Rotating type dynamometer (right)* ***[43]***

Table [3-3]: Advantages of Dynamometers [43]

Stationary Dynamometers	***Rotating Dynamometers***
• Very versatile • Very robust • Coordinate system is non - rotating	• Mz, the torque is measured directly • The measurement is done close to the tool • If the mass of the work piece is changed, there isn't any influence on the dynamics

The dynamometer used in this research for collecting force and torque data is a Kistler 9123C (Figure 3.5) rotating 4 component type dynamometer. The cutting forces are measured at the rotating edge.

The measurements that can be taken with this are Forces in X,Y and Z (F_X,F_Y,F_Z) directions along with moment in Z direction on a rotating tool. The forces in tangential (F_t) and radial (F_r) direction are calculated. The dynamometer consists of a four component sensor fitted under high preload between a base plate and top plate. A zero point identification (Type 5221B2) is available as an option which allows to correlate the force signals with the tool edge.

The applications of this type of dynamometer include investigations of wear and cutting processes near the tool edge during milling and drilling. The acting force vector on one-edged tools can directly be measured. This dynamometer is especially suitable for high speed fine machining **[41].** Kistler Dynoware DAQ software is used for data acquisition and processing where the input is taken through a PCI DAQ card. This type of rotating dynamometers can measure the cutting forces instantaneously independent of the size of the work piece unlike fixed dynamometers.

Figure 3.5 : Kistler 9123C rotating dynamometer

3.4 b) Data acquisition system

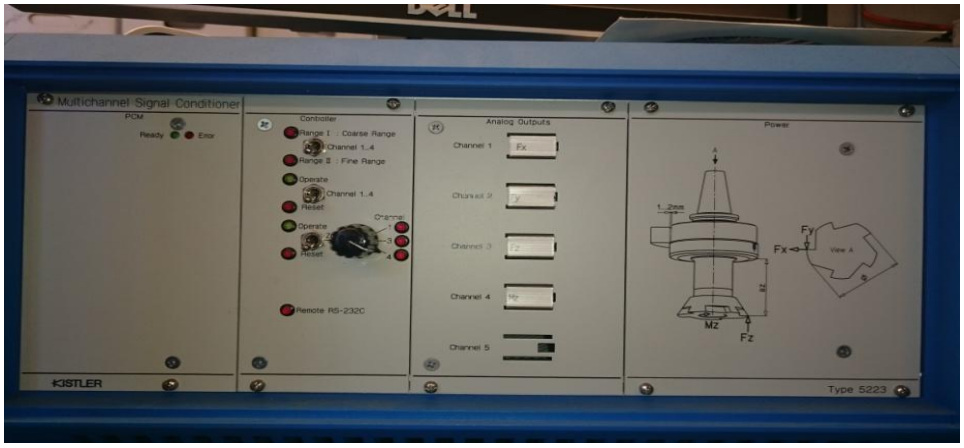

Figure 3.6 : Kistler Multichannel signal conditioner

The output from the dynamometer which gives us the values of forces and torque are processed by the signal conditioner (Figure 3.6) and sent to the computer for display. There are multiple channels which can be set to take in different forces.

The analog outputs are set to measure Fx, Fy,Fz and Mz on Channels 1,2,3 and 4 respectively. There are two ranges, the fine and the coarse range which can be set according to our needs. The fine range has been chosen for this research work. Figure [3-7] shows a schematic of how the data acquisition process works **[48]**.

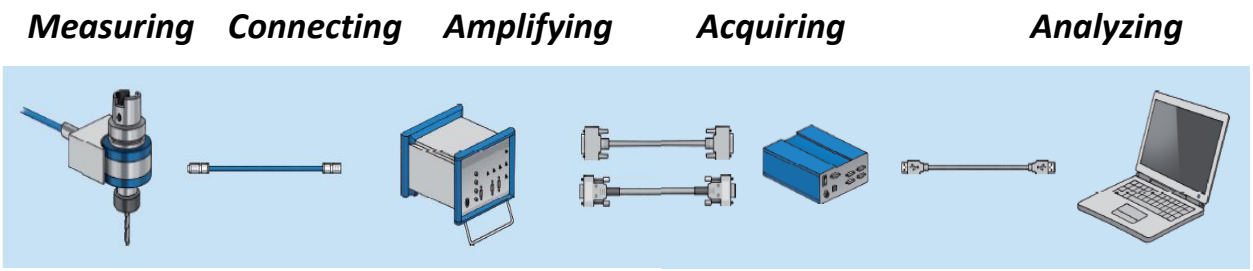

Figure 3.7 : Signal acquisition process from start to end

3.5 Tool Used

All the milling experiments in this research have been carried with one type of cutting tool. The tool used was a 4 flute, 0.5 in (12.7mm) diameter carbide end mill with a ~ 30° helix angle with no coating. Figure 3.8 is a representation of it.

A total of 6 tools were used, 5 for cutting CFRP and 1 to cut HexMC. The tools were changed periodically depending on the extent of cutting done. **Tables [3-4]** and **[3-5]** give additional specifications of the tool.

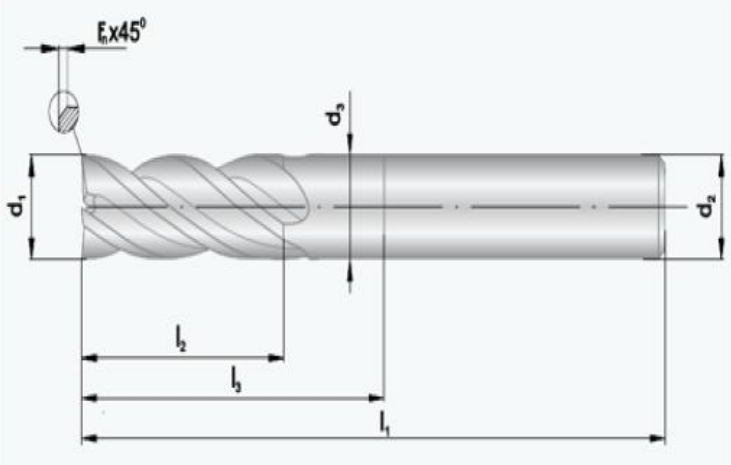

Figure 3.8 : Flat nose end mill [47]

Table [3-4]: Cutting tool specifications [45]

Item	Value
No. of flutes (geometry)	4-flute helix
Helix angle	~ 30°
Chamfer of edge	Fn x45° - 0.13"
Diameter of flute	0.48"
Diameter of shank	0.5"
Maximum depth of cut	l_2 = 2.2"
Overall length of tool	l_1 = 4"
Material	Micro grain solid carbide
Coating	-
Manufacture	Niagara Cutters

Table [3-5]: Cutting tools used

Tool Name	*Tool S.No.*	*Tool Specifications*	*Used for (Experiments)*
A	S1216152/1	NIAGARA .500", C2 CARBIDE USA, S1216152/1, LEAD = 2.7207; B1-2144-4150; 4 FL SE CC ; 0.5 * 0.5 * 1 * 3 CARBIDE	CFRP Edge Trimming Exp's : 1-6
C	S14700615/1	NIAGARA .500, CARBIDE USA, S14700615/1, LEAD = 2.7207; B121444150; CARB 1/2*1/2*1*3 4F 17018109 S147700615/1 121 / 407	CFRP Edge Trimming Exp's : 12-16
D	S1200127/1	NIAGARA .500", CARBIDE USA, S1200127/1, LEAD = 2.7207; B1-2144-4150; 4 FL SE CC ; 0.5 * 0.5 * 1 * 3 CARBIDE	CFRP Edge Trimming Exp's : 7-11
E	S1216152/1	NIAGARA .500", C2 CARBIDE USA, S1216152/1, LEAD = 2.7207; B1-2144-4150; 4 FL SE CC ; 0.5 * 0.5 * 1 * 3 CARBIDE	CFRP Edge Trimming Exp's : 17-24
F	S1306658/1	NIAGARA .500", C2 CARBIDE USA, S1306658/1, LEAD = 2.7207; B1-2144-4150; 4 FL SE CC ; 0.5 * 0.5 * 1 * 3 CARBIDE	CFRP Circular test Exp's : C1 - C5
G	S1200127/1	NIAGARA .500", CARBIDE USA, S1200127/1, LEAD = 2.7207; B1-2144-4150; 4 FL SE CC ; 0.5 * 0.5 * 1 * 3; CARBIDE	HexMC Edge Trimming

3.6 Surface Roughness Measurements

Surface roughness measurements were made using a Mahr Marsurf GD 25 contour machine (Figure 3.9). A probe (Figure 3.10) is attached to the machine which measure the surface profiles and gives output of various roughness values such as Ra, Rz and Rt etc. An additional automated moving base made by one of the students in the MSTL lab was used to move the table with precision in required small amounts with the help of a program as per needed.

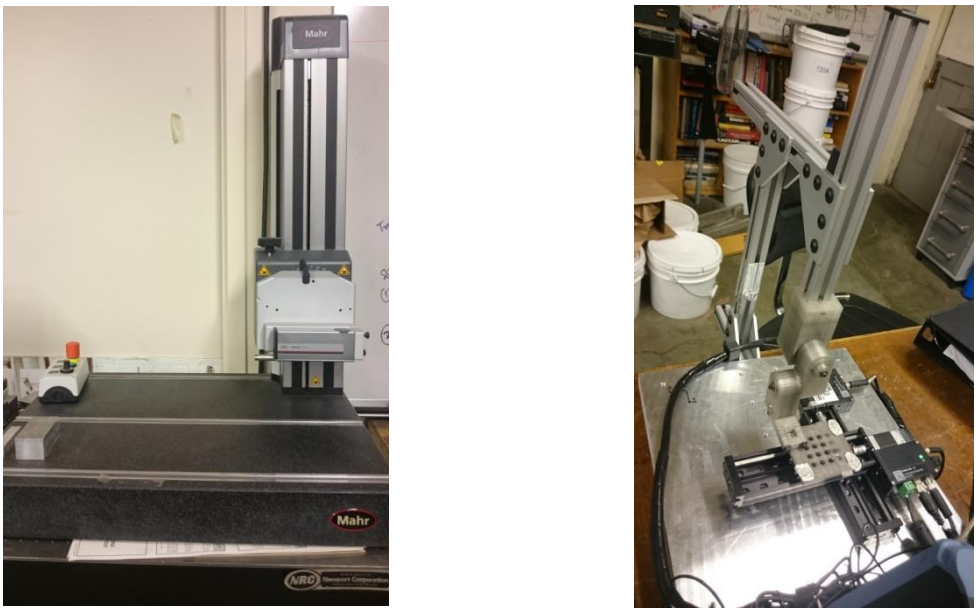

Figure 3.9 : Mahr Marsurf Surface roughness machine (left) and automated moving base (right)

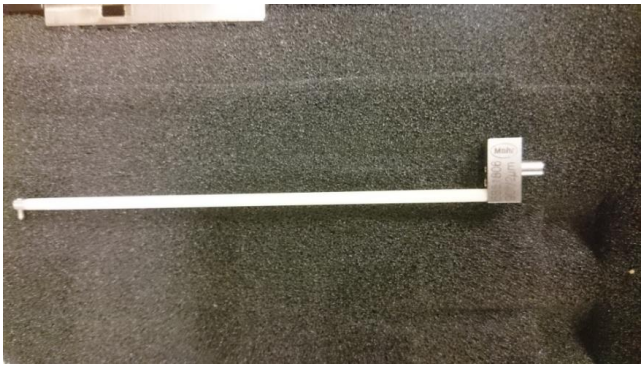

Figure 3.10 : Typical Surface roughness measurement Probe

3.7 Design of Experiments (DOE) and Test Matrix

3.7.1 End Milling/ Edge trimming

Edge trimming or more commonly known as end milling was performed on both the composites. Multiple passes were cut on the work piece with a constant radial depth of cut of 0.762 mm (0.03"). Each pass is 177.8 mm (7") long and alternated between climb and conventional milling in each pass due to the feed direction relative to direction of the cutting tool rotation. Figure 3.11 is a schematic to show how the edge trimming was performed.

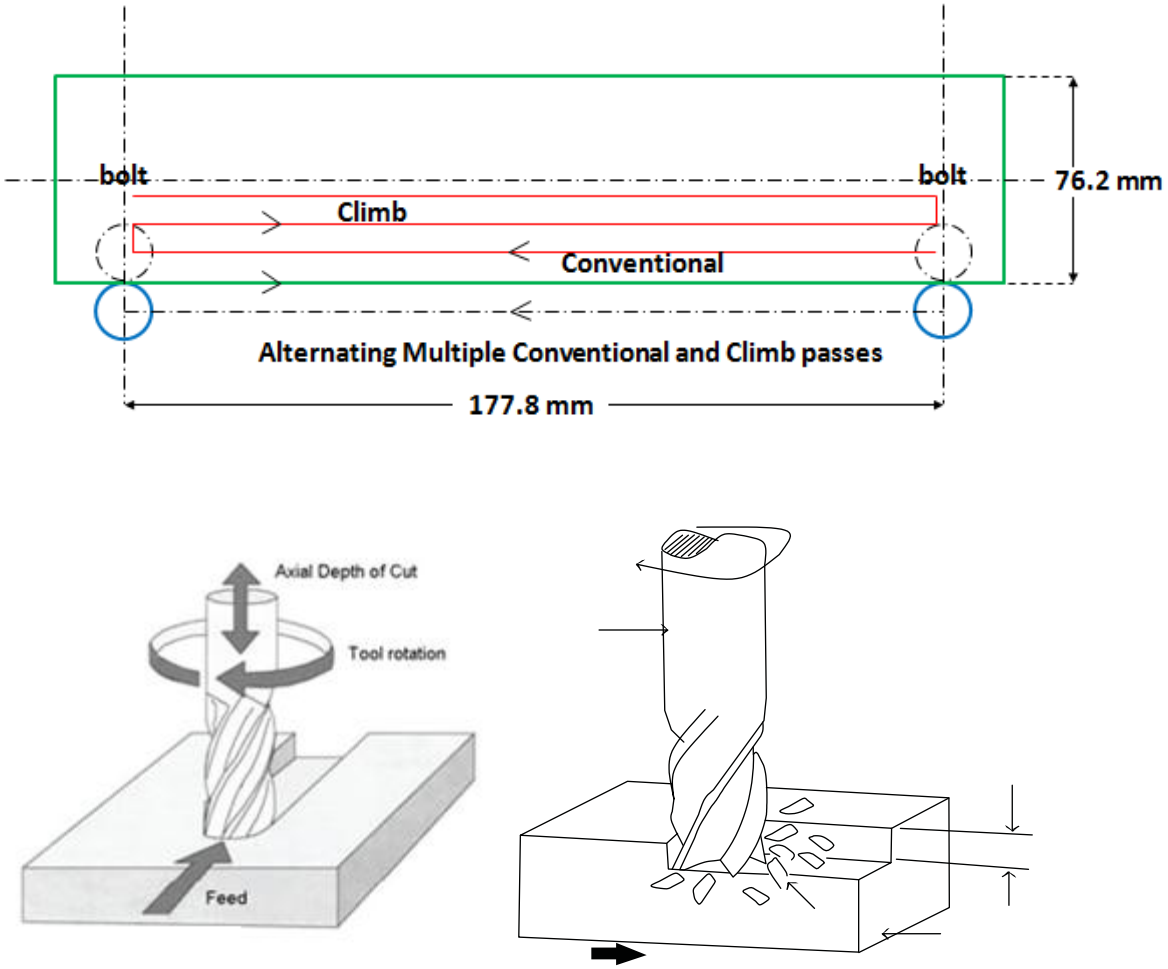

Figure 3.11 : Top - Schematic to show edge trimming of Composites
Bottom - (left) Slot cutting schematic ; (right) Schematic of edge trimming

The number of alternating passes depend on the feed rate parameter. Since they are three different values, the number of passes differed too. **Table [3-6]** gives these values.

Table [3-6]: Number of passes in end milling based on Feed value

S.No.	Feed rate (mm/min)	No. of Passes
1	635	10
2	381	6
3	127	3

3.7.1 a) DOE for CFRP- Edge Trim: The effective way to mill composites depends on the parameters and their values chosen for the machining. The three major parameters chosen in this work are Spindle speed, Feed and Depth of Cut (DOC). These were chosen based on previously seen literature and general experience.

Three levels of each of these parameters were taken and then statistical analysis was done in the Stat Ease software, an ANOVA tool to get the optimum set of experiments with the given machining parameters which give us a fair idea by choosing the set of experiments which give us a trend and cover the maximum possible range by mathematics of probability and uncertainty to make inferences about a given data set.

The three levels chosen for each parameter for Edge trimming of CFRP are,

- Speed - 1000 rpm, 3000 rpm, 6000 rpm
- Feed - 127 mm/min , 381 mm/min, 635 mm/min
- DOC (axial) - 2.54 mm, 3.81 mm, 6.35 mm

The matrix obtained from the Stat Ease software for the edge trimming of CFRP is given in **Table [3-7]**. Figure 3.12 shows the UD CFRP after machining.

Table [3-7]: Statistical Design matrix for edge trimming of CFRP composite

Run	FACTOR 1 A : SPEED (RPM)	FACTOR 2 B : FEED (MMPM)	FACTOR 3 C : DOC (MM)
1	6000	635	6.35
2	6000	635	3.81
3	3000	635	3.81
4	6000	635	2.54
5	3000	635	2.54
6	1000	635	2.54
7	1000	635	6.35
8	1000	635	3.81
9	6000	381	6.35
10	6000	381	3.81
11	6000	381	2.54
12	3000	381	6.35
13	3000	381	3.81
14	3000	381	2.54
15	1000	381	2.54
16	1000	381	6.35
17	6000	127	3.81
18	3000	127	3.81
19	1000	127	3.81
20	1000	127	2.54
21	3000	127	2.54
22	6000	127	6.35
23	3000	127	6.35
24	1000	127	6.35

Figure 3.12 : Uni Directional CFRP work piece after Edge trimming , Top view (top), Side view (bottom)

3.7.1 b) DOE for HexMC - Edge Trim

The machining parameters chosen for Edge trimming of HexMC composite material are similar to those chosen for CFRP. They are Spindle Speed, Feed and Depth of Cut (DOC). The material available was limited, so only two levels were chosen for each machining parameter. The levels chosen were the minimum and maximum to give us the trend with respect to the extreme behaviour.

The two levels chosen for each parameter for Edge trimming of HexMC are,

- Speed - 1000 rpm, 6000 rpm
- Feed - 127 mm/min , 635 mm/min
- DOC (axial) - 2.54 mm, 6.35 mm

The matrix obtained from the Stat Ease software for the edge trimming of CFRP is given in **Table [3-8].** Figure 3.13 shows the HexMC composite work piece after machining.

Table [3-8]: Statistical Design matrix for edge trimming of HexMC composite

Run	FACTOR 1 A : SPEED (RPM)	FACTOR 2 B : FEED (MMPM)	FACTOR 3 C : DOC (MM)
1	6000	635	6.35
2	6000	127	6.35
3	6000	635	2.54
4	6000	127	2.54
5	1000	127	6.35
6	1000	635	6.35
7	1000	635	2.54
8	1000	127	2.54

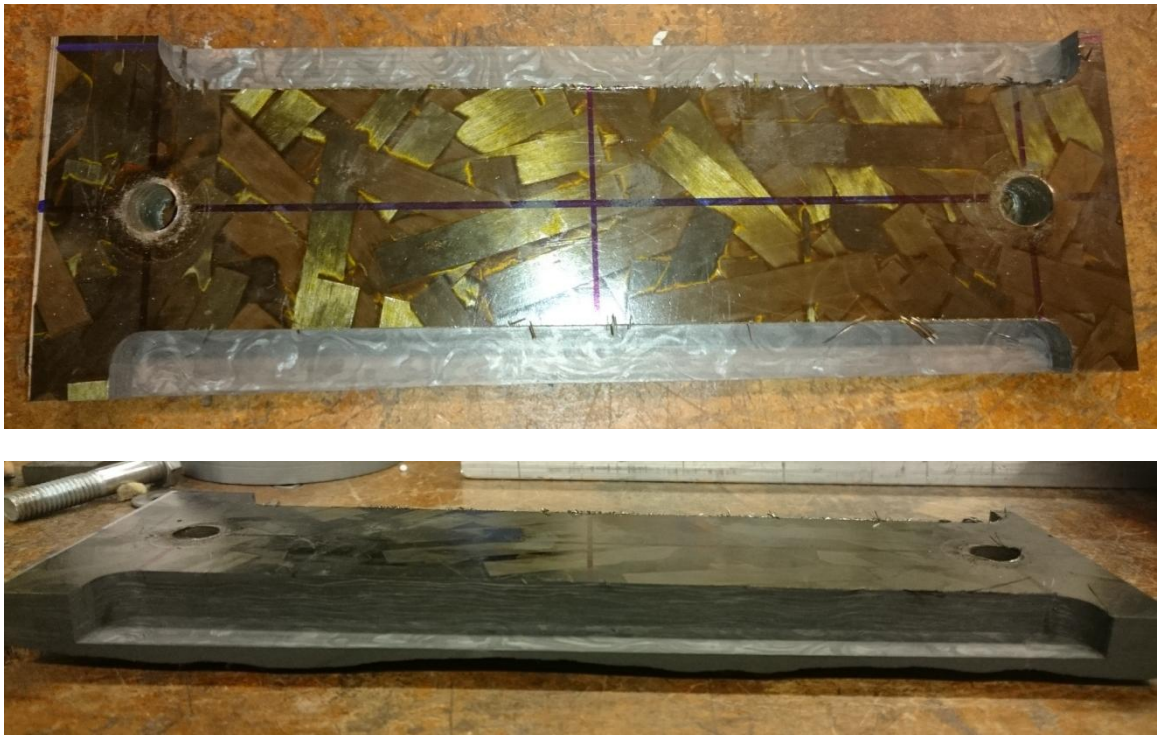

Figure 3.13 : Random fiber HexMC work piece after Edge trimming , Top view (top), Side view (bottom)

3.7.2 Circular Slot testing - CFRP composite

A slot milling test was performed on the Uni directional CFRP composite to see the effects of the fiber direction on the machining based on continuously changing cutting angles. The work piece was 25.4 mm (1 inch) thick and the its other dimensions were around 215 mm x 115 mm. The CNC program used is mentioned in Appendix A. Figure 3.14 shows a schematic of the slot test performed. Figure 3.15 shows the Continuously changing angles in a Circular slot test, Figure 3.16 shows the octagonal work Piece after the Circular slot test - before and after dust cleanup, Figure 3.17 shows a Close up of the Circular Slot test which has extensive fiber failure. The machining parameters are mentioned in **Table [3-9].**

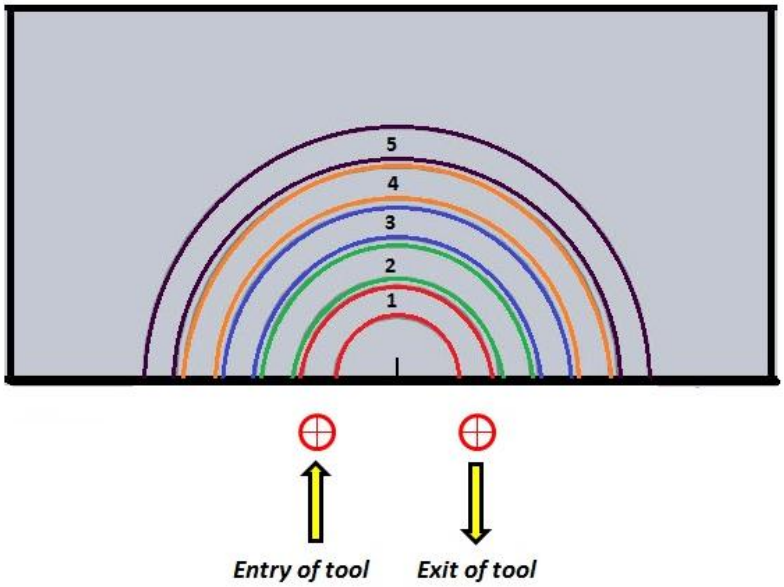

Figure 3.14 : Schematic to show Circular slot test on UD CFRP

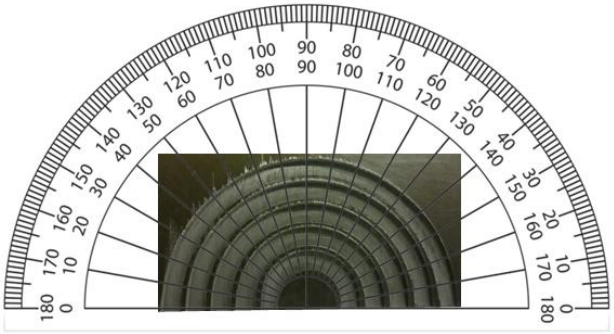

Figure 3.15 : Continuously changing angles in a Circular slot test

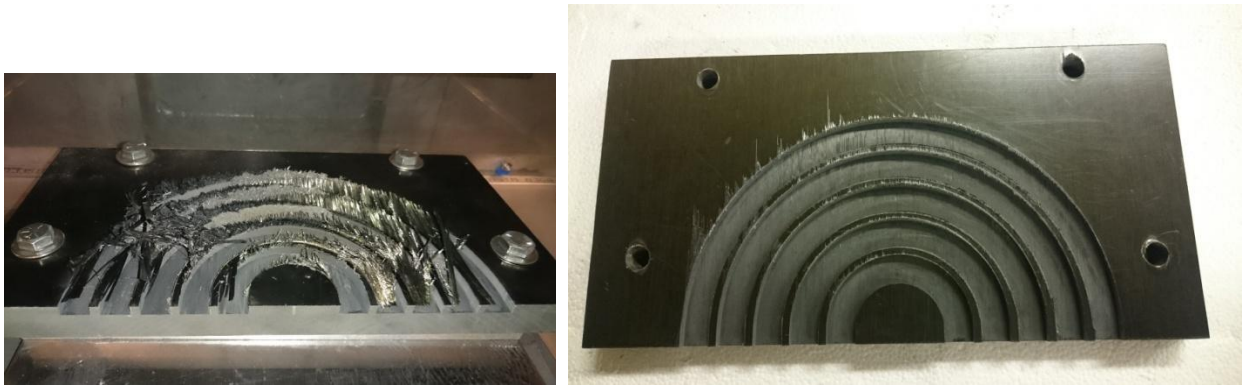

Figure 3.16 : Work Piece after the Circular slot test - before and after dust cleanup (left to right)

Table [3-9]: Circular Slot test - Machining parameters

Slot No.	Slot Diameter (mm)	Speed (rpm)	Feed (mm/min)	DOC (mm)
1	50.8	1000	127	5.08
2	82.55	6000	254	5.08
3	114.3	6000	381	5.08
4	146.05	3000	508	5.08
5	177.8	3000	635	5.08

Figure 3.17 : Close up of Circular Slot test - Fiber failure

3.7.3 Octagonal Slot testing - CFRP composite

An Octagonal slot milling test was performed on the Uni directional CFRP composite to see the effects of the fiber direction on the machining based on different cutting angles. The work piece was 25.4 mm (1 inch) thick and the its other dimensions were around 175 mm x 115 mm. **Figure 3.18** shows a schematic of the slot test.

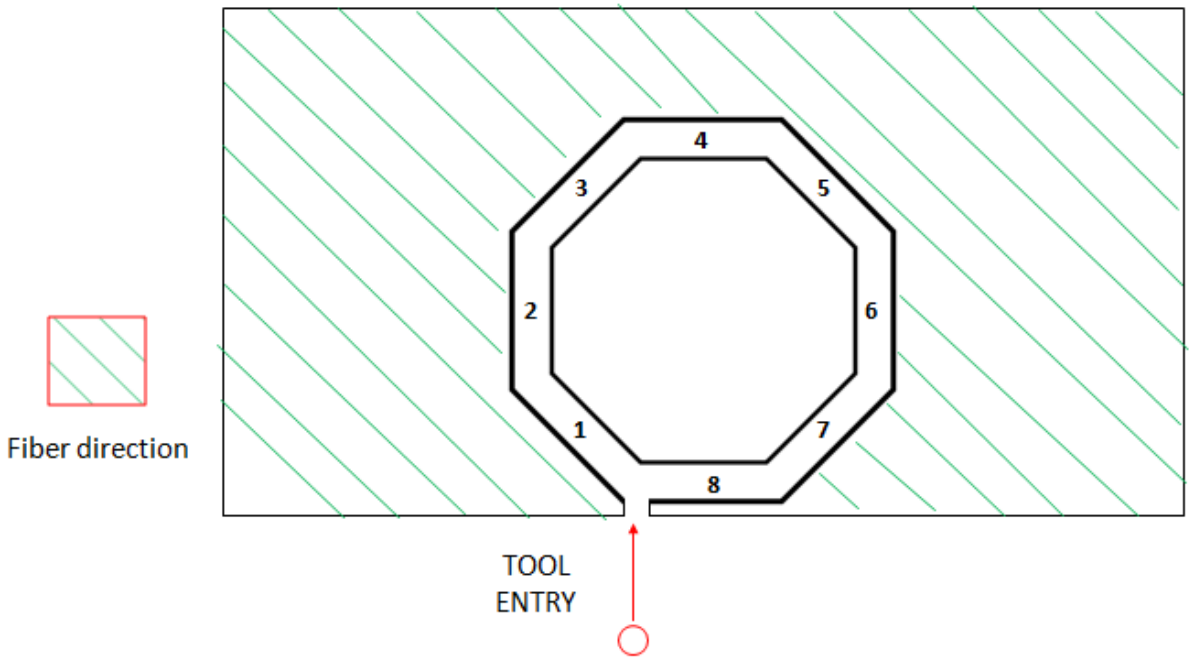

Figure 3.18 : Schematic to show Circular slot test on UD CFRP

This test was performed to see how the angle affects the cutting quality and fiber failure. It is known that the fiber delaminations are usually higher at ± 45° **[26]** . The CNC program used is in Appendix A. **Table [3-10]** shows the cutting conditions for this octagonal slot test. Figure 3.19 shows the slot after the slot milling is done. The cutting tool used is similar to previous experiments, a 12.7 mm (0.5 inch) 4 flute flat nose carbide end mill with 30° helix angle. The relative angle/position of each cut with respect to the Fiber Direction (FD) of UD CFRP Octagonal slot test is depicted in Figure 3.20 **.**

Table [3-10]: Octagonal Slot test - Machining parameters

Slot No.	Slot Length (mm)	Speed (rpm)	Feed (mm/min)	DOC (mm)	Relative angle wrt Fiber direction (Degrees)
1	35.96	1000	25.4	5.08	0°
2	38.1	1000	25.4	5.08	45°
3	35.96	1000	25.4	5.08	90°
4	50.8	1000	25.4	5.08	135°
5	35.96	1000	25.4	5.08	180°
6	38.1	1000	25.4	5.08	225°
7	35.96	1000	25.4	5.08	270°
8	50.8	1000	25.4	5.08	315°

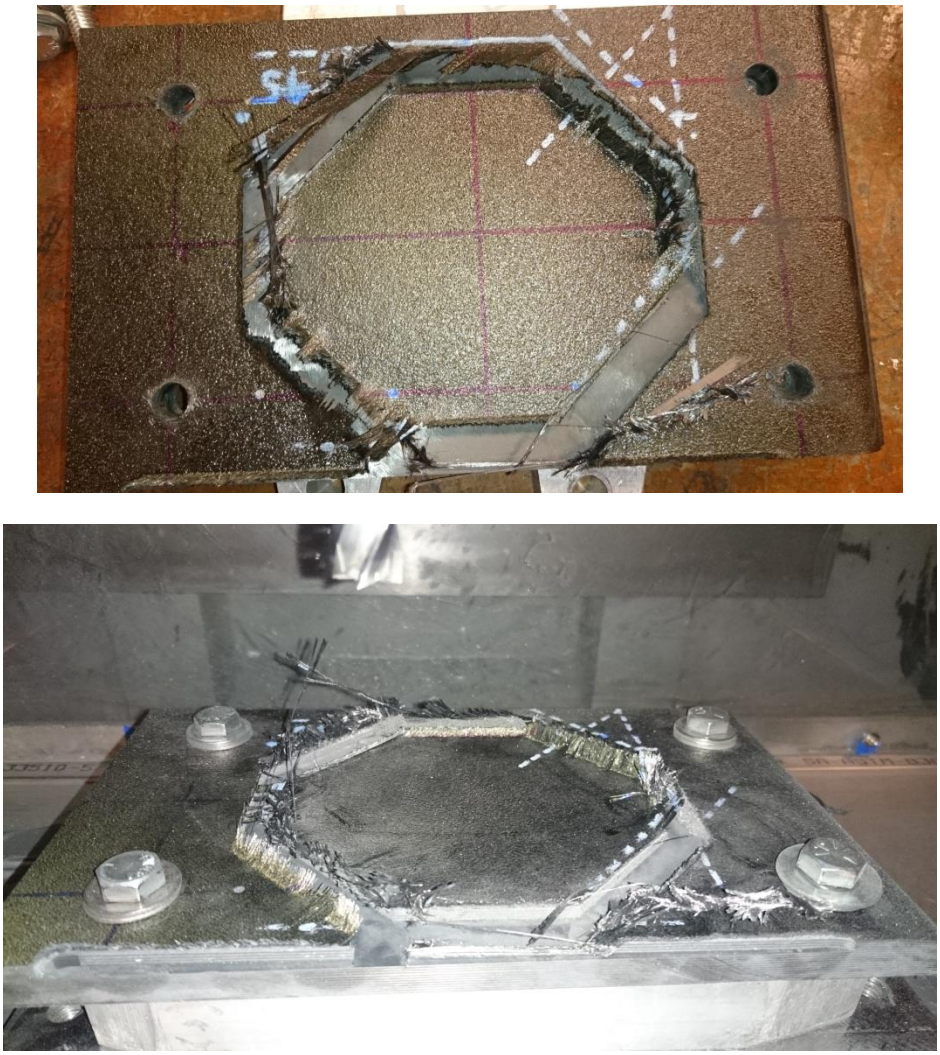

Figure 3.19 : Work Piece after the Octagonal slot test - Top view (top) , Side view (bottom)

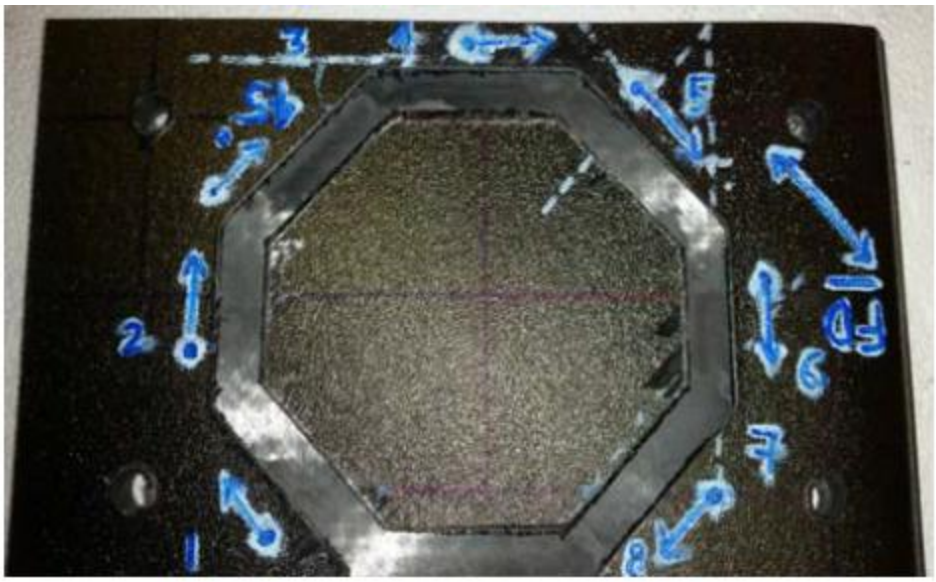

Figure 3.20 : Relative angle/position of each cut with respect to the Fiber Direction (FD) of UD CFRP - Octagonal slot test

Chapter 4: Results

Linear edge trimming or end milling, Circular slot test and Octagonal test were done on Uni directional CFRP composite and HexMC random fiber composite. Three machining parameters chosen were Speed, Feed and DOC. Multiple responses or analog outputs were extracted from the Dynoware software. All the responses / outputs obtained are given in **Table [4-1]**. A raw data file (.dwg) from a dynoware software, takes in the data from the signal conditioner and analyses and plots the data in the computer. A typical raw data graph of the responses looks like Figure 4.1 .

Table [4-1] : Responses from Dynoware software

Fx	Force in X direction	Measured	Channel 1
Fy	Force in Y direction	Measured	Channel 2
Fz	Force in Z direction	Measured	Channel 3
Mz	Torque in Z direction	Measured	Channel 4
Ft	Tangential force	Calculated	$Ft = \frac{Mz}{r}$, where r = radius of cutting tool
Fr	Radial force	Calculated	$Fr = \sqrt{Fx^2 + Fy^2 - Ft^2}$

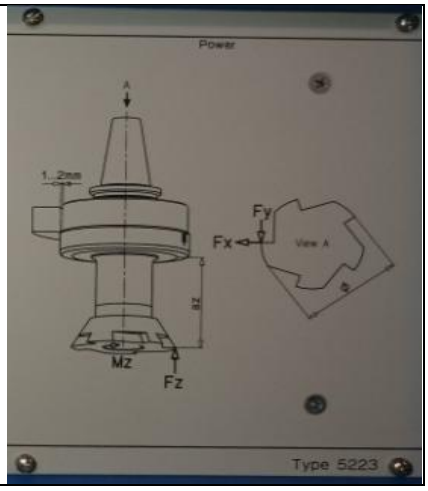

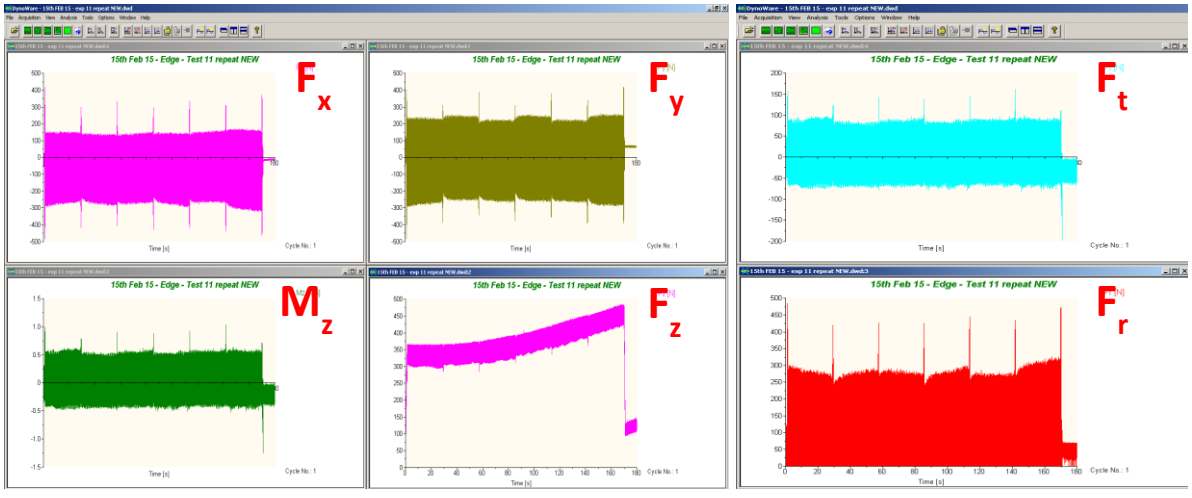

Figure 4.1 : An example of Raw data graphs of responses in edge trimming
(All units in [N])

The rotating dynamometer used in this research has a sensor which detects every rotation taken by it. This is set to be measured and displayed in Channel 6 , it's called Zero Count. Figure 4.2 shows how a grey spike for every rotation detected and 1 rotation is taken to be between two spikes. We used a 4 flute tool – so there are 4 spikes in each cutter rotation.

There are hills and valleys within each cutter rotation as each flute removes some material and this process of removal of material causes a sudden drop in force which causes the dip in force and then the next flute comes into contact with the material again and there is an increase in force and then dips again and the cycle continues.

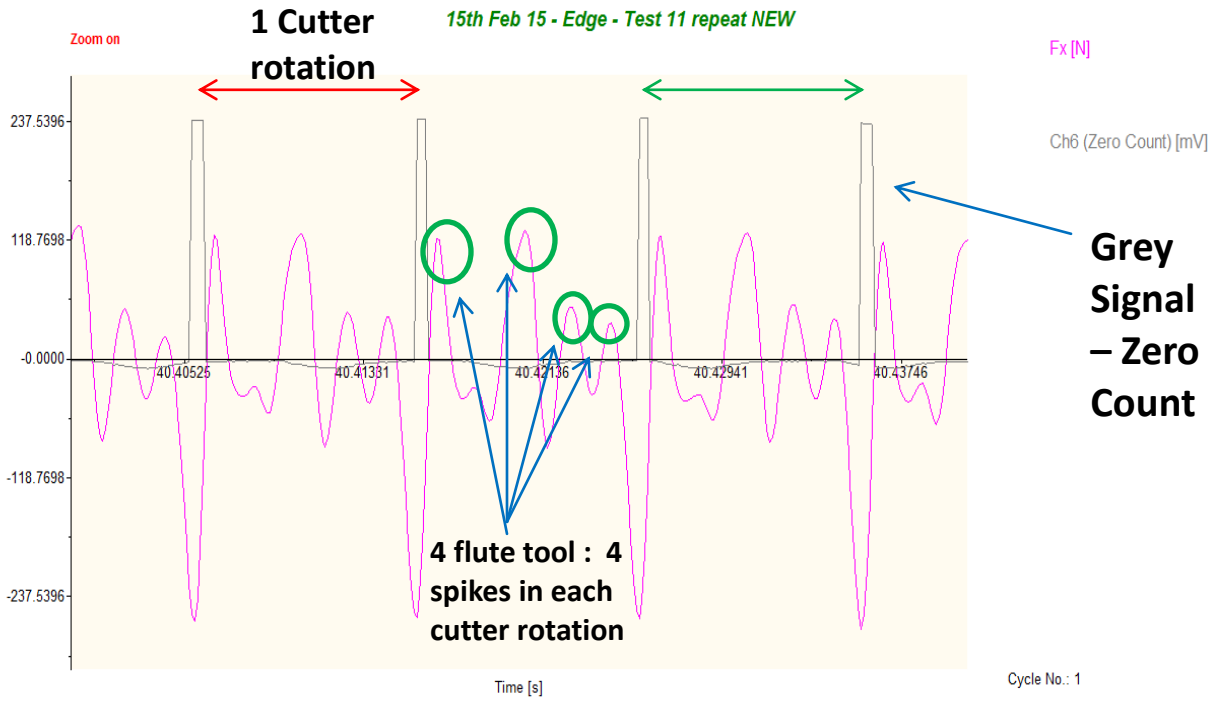

Figure 4.2: Zero Count in Dynoware

From the raw data of forces and torque which are the responses as outputs, we had to extract the values in each scenario. The value of " ***average of maximum force*** " was found out using a MATLAB code [Appendix B], which used the concept of finding the maximum of the 4 spikes in each cutter rotation and then averaging out these maximum values to get the desired results. Figure 4.3 illustrates this mechanism.

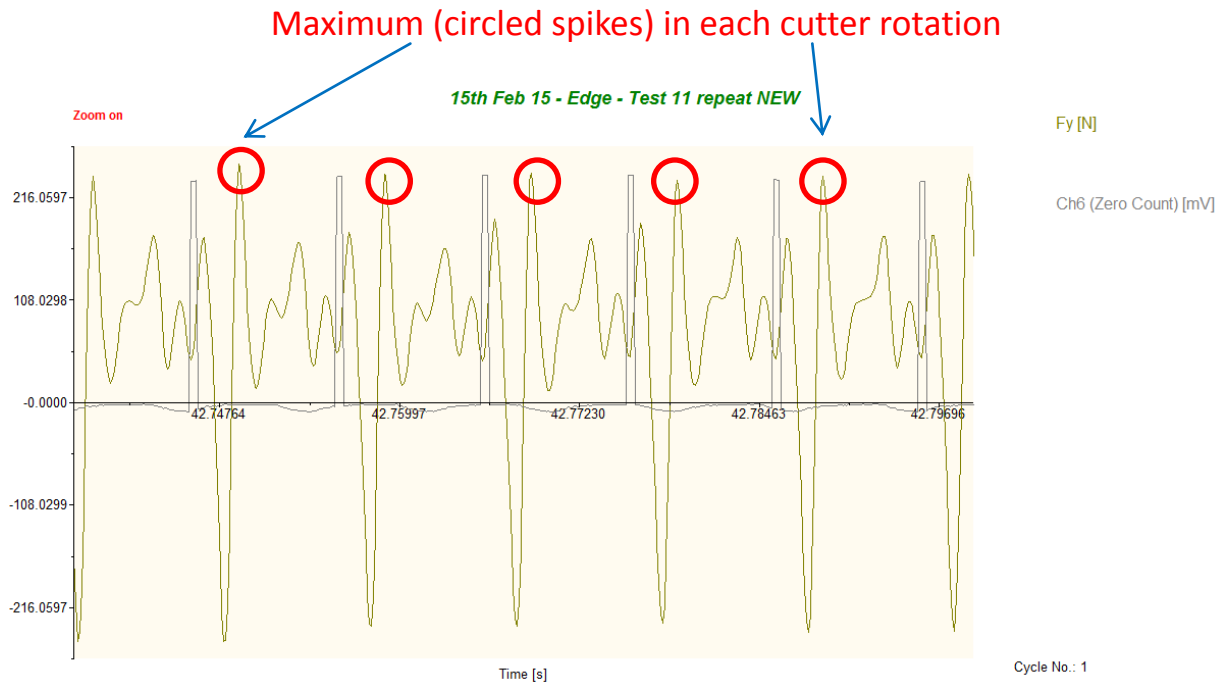

Figure 4.3 : Logic behind calculating - " Avg of Max Forces "

Conventional vs. Climb : Identification for Edge trimming

In each experiment, multiple passes were cut alternating between Conventional and Climb type of milling. Figure 4.4 shows the schematic of how to differentiate a Climb cut form a Conventional cut in general. The climb and conventional cuts which are specific to this research are represented in Figure 4.5.

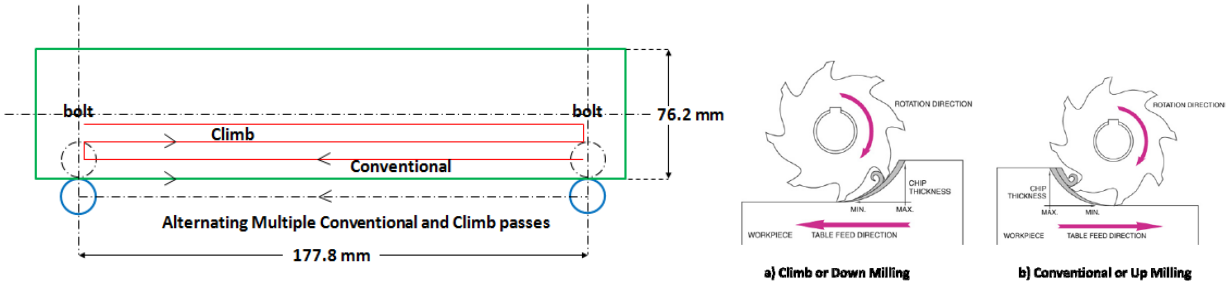

Figure 4.4 : Example to show which cut is Climb and which is Conventional

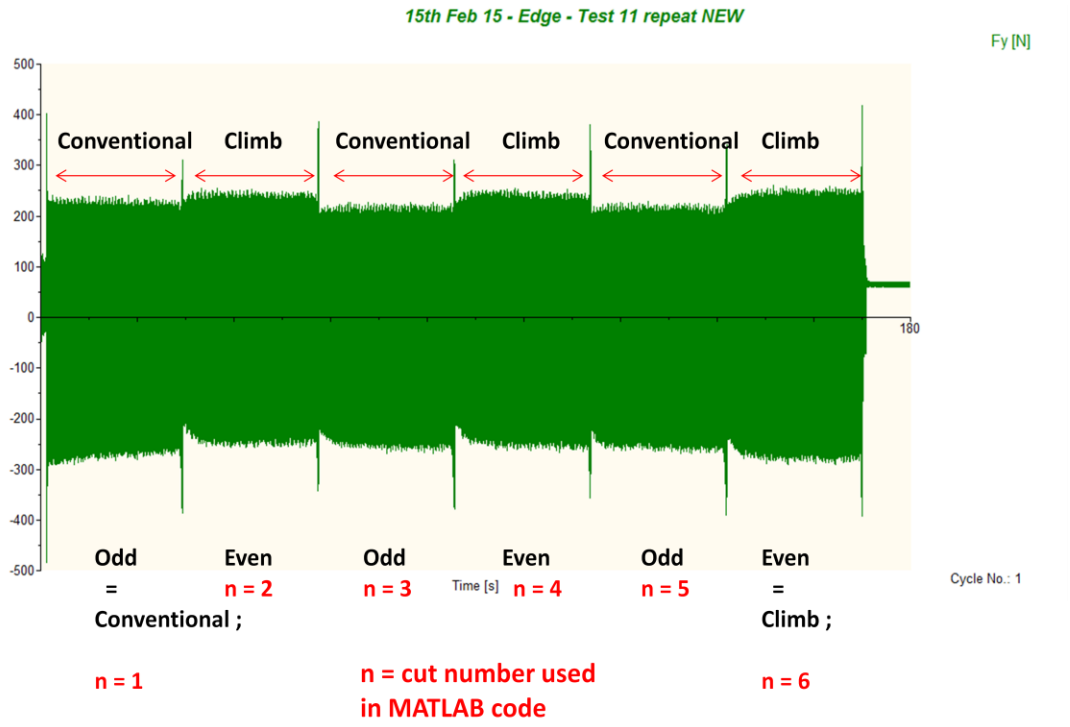

Figure 4.5 : Climb vs. Conventional in each experiment

To get the values of the forces, [Appendix B]

- ***Cut number 3 i.e., n = 3 was chosen for Odd = Conventional cuts***
- ***Cut number 2 i.e., n = 2 was chosen for Even = Climb cuts***

There are spikes (red circles), as shown in Figure 4.6 . These are caused when the cut is shifting from the Conventional to Climb and so forth throughout each experiment . They help us in differentiating easily when the cut has ended and started.

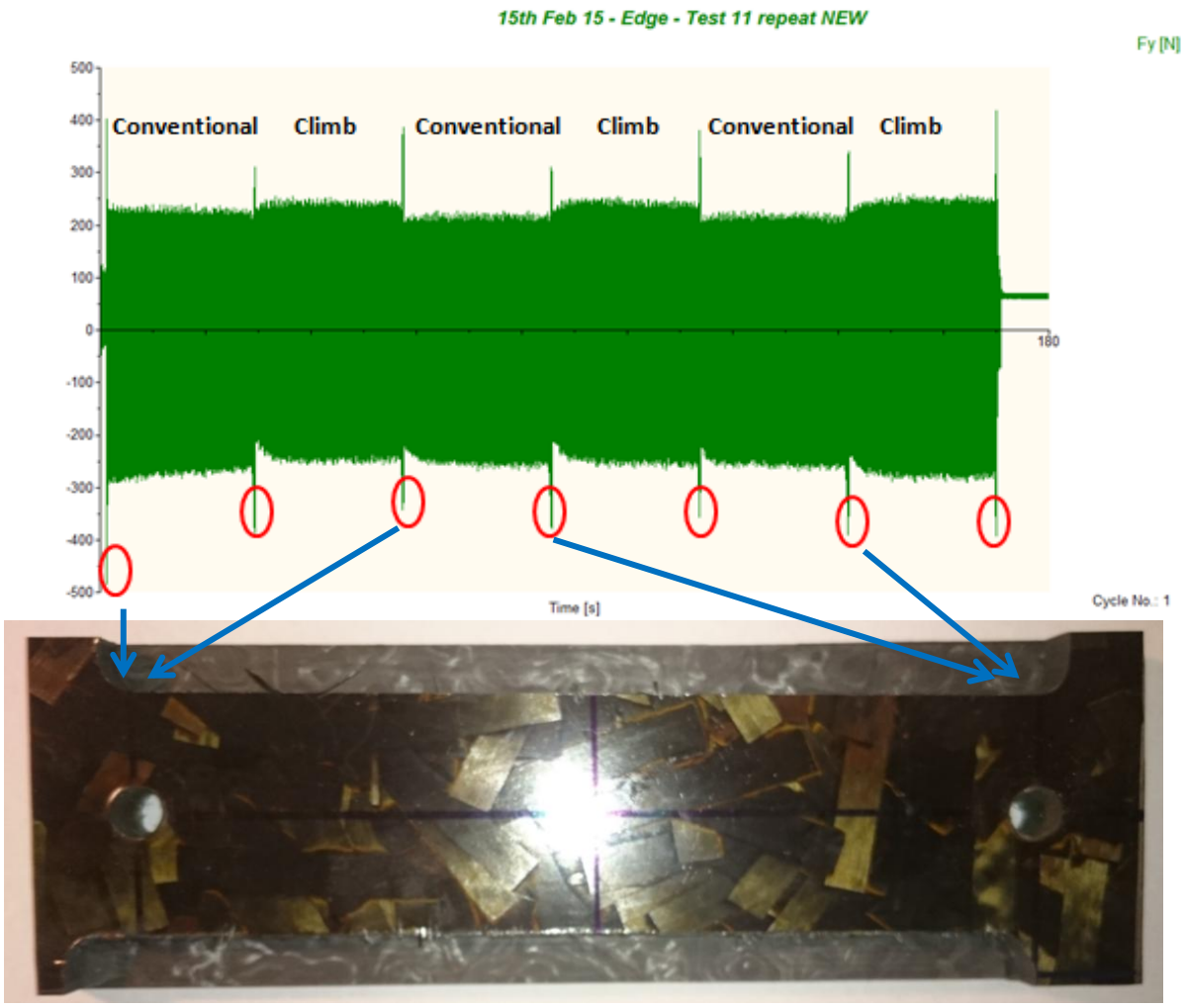

Figure 4.6 : Reason for Spikes between major cuts

Drift Compensation in Fz :

Drift is when the data signal doesn't align with the Zero Force line as seen in Fz and some other forces in a few cases, but it drifts upward. This drift (Figure 4.7) needs to be compensated and the acceptable value for it as obtained from Dynoware is it can be upto 0.2 Nm/min. If the drift exceeds this value, it should be compensated for by rotating the signal to get aligned with the zero line. To do this, the best way to run the CNC program is in such a way that the cutter rotates in the air for a few seconds before and after each cut. This zero shift data (in the air data) can help in signal compensation for drift and Shift. Shift is when the signal as a whole is above or below the zero line and isn't aligned properly (Figure 4.8).

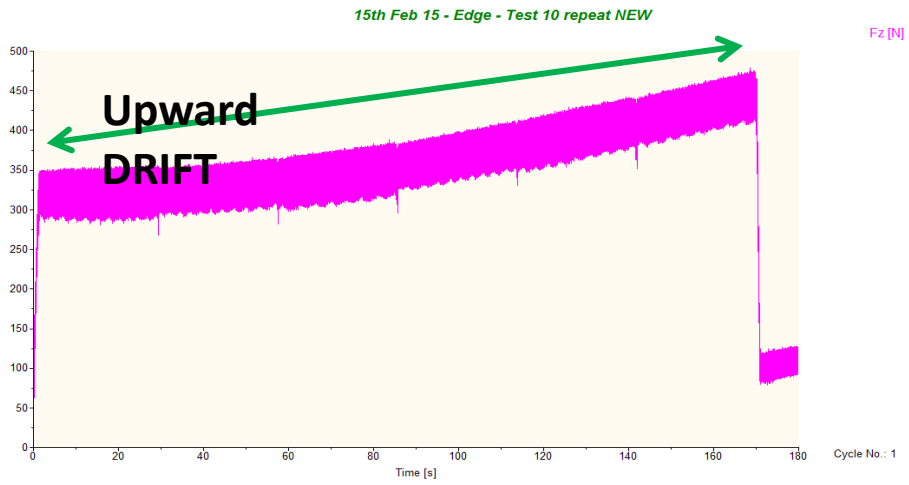

Figure 4.7: Demonstration of DRIFT

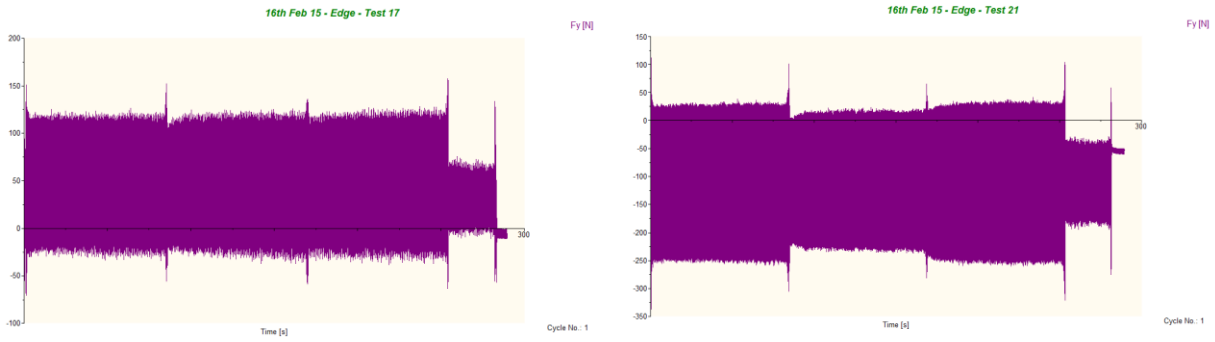

Figure 4.8: Demonstration of SHIFT

4.1 CFRP Edge trimming results

The values obtained from the MATLAB codes and checked with raw data graphs for the Edge trimming of Uni directional CFRP in Climb Milling cut for all 24 experiments are displayed in **Table [4-2].** The values are the average of the maximum values of each response.

Table [4-2]: Climb (Even) CFRP Edge Trimming Results

Climb (Even) CFRP Edge Trimming								
Exp No.	**Speed (rpm)**	**Feed (mm/min)**	**DOC (mm)**	**Fx (N)**	**Fy (N)**	**Fz (N)**	**Ft (N)**	**Fr (N)**
1	6000	635	6.35	147.0557	296.2237	352.9007	33.47906	330.1072
2	6000	635	3.81	124.3528	196.48	364.3681	69.7257	260.3185
3	3000	635	3.81	142.6883	225.9399	110.3443	81.08723	288.1932
4	6000	635	2.54	132.9077	153.2047	351.8228	68.50684	236.0783
5	3000	635	2.54	75.98222	69.59672	101.1752	37.01456	91.44643
6	1000	635	2.54	107.9102	128.8896	16.58417	91.97703	45.88853
7	1000	635	6.35	166.2718	220.3663	13.17831	155.9619	75.89456
8	1000	635	3.81	133.8486	150.1785	14.69146	154.1934	229.3373
9	6000	381	6.35	70.47931	124.6208	352.3794	55.3981	243.5754
10	6000	381	3.81	108.6469	164.497	342.0669	61.51088	254.8276
11	6000	381	2.54	124.5871	231.661	355.4408	58.6007	229.949
12	3000	381	6.35	63.70763	116.9892	0.616674	40.9948	139.4685
13	3000	381	3.81	75.36931	179.8706	105.8219	38.10018	184.4947
14	3000	381	2.54	64.58246	75.9303	96.24969	40.06289	148.6741
15	1000	381	2.54	138.9012	235.9876	18.30895	100.7486	148.0343
16	1000	381	6.35	271.9911	357.581	46.73847	149.4524	237.1923
17	6000	127	3.81	39.77207	106.4616	348.2369	22.52094	94.84424
18	3000	127	3.81	109.3032	120.6139	91.9742	22.49764	133.5392
19	1000	127	3.81	177.5098	211.8711	4.453244	57.99336	120.7981
20	1000	127	2.54	150.5485	167.1413	5.674638	48.91275	60.22712
21	3000	127	2.54	105.5187	9.282591	81.73019	27.39969	227.1718
22	6000	127	6.35	180.6007	182.986	332.2785	43.64885	194.9746
23	3000	127	6.35	151.2013	261.8044	62.12269	45.75911	262.6991
24	1000	127	6.35	415.8302	431.2792	8.582838	113.2083	459.9976

The values obtained from the MATLAB codes and checked with raw data graphs for the Edge trimming of Uni directional CFRP in Conventional milling cut for all 24 experiments are displayed in **Table [4-3].**

Table [4-3]: Conventional (Odd) CFRP Edge Trimming Results

Conventional (Odd) CFRP Edge Trimming								
Exp No.	**Speed (rpm)**	**Feed (mm/min)**	**DOC (mm)**	**Fx (N)**	**Fy (N)**	**Fz (N)**	**Ft (N)**	**Fr (N)**
1	6000	635	6.35	143.1149657	275.8503	364.7114	33.36993	311.1462
2	6000	635	3.81	101.5559251	174.2728	368.1563	70.623	239.687
3	3000	635	3.81	153.2877402	224.1279	112.6527	75.46583	316.3304
4	6000	635	2.54	104.6265993	136.8084	356.0724	71.9315	210.8921
5	3000	635	2.54	59.06374515	110.5862	113.7669	35.6466	119.7625
6	1000	635	2.54	94.42651504	126.0127	22.12614	80.73293	140
7	1000	635	6.35	172.9833239	235.1539	18.32296	152.8115	225
8	1000	635	3.81	143.6453902	143.8556	20.28835	154.641	218.4237
9	6000	381	6.35	79.92945992	115.9064	363.429	57.94921	258.9037
10	6000	381	3.81	112.8018956	137.521	350.0182	65.67046	262.9074
11	6000	381	2.54	125.3632514	203.2971	363.8001	64.58286	230.9507
12	3000	381	6.35	74.85130077	124.6906	6.703777	34.27733	166.013
13	3000	381	3.81	96.40978285	209.843	111.3645	43.47756	212.6087
14	3000	381	2.54	70.76549456	98.6738	100.2196	42.63078	152.265
15	1000	381	2.54	139.5168102	220.7682	23.96494	98.85523	260
16	1000	381	6.35	278.0023945	346.8159	48.36253	147.822	320
17	6000	127	3.81	44.10432505	109.1953	357.9492	25.8273	97.64605
18	3000	127	3.81	136.3261143	141.4977	108.1768	30.9997	152.2137
19	1000	127	3.81	177.4816121	204.8916	7.973164	61.44043	215
20	1000	127	2.54	142.0233758	157.246	6.540984	51.1524	175
21	3000	127	2.54	120.9973979	22.99295	85.52739	33.15409	247.9018
22	6000	127	6.35	177.6106938	182.3015	354.4235	47.74905	194.4933
23	3000	127	6.35	161.9910388	267.6451	77.55997	46.26357	267.8589
24	1000	127	6.35	386.1639253	396.624	20.56	102.1051	424.7395

4.2 HexMC Edge trimming results

The values obtained from the MATLAB codes and checked with raw data graphs for the Edge trimming of Random Fiber HexMC in Climb Milling cut for all 8 experiments are displayed in **Table [4-4].** The values are the average of the maximum values of each response.

Table [4-4]: Climb (Even) HexMC Edge Trimming Results

Climb (Even) HexMC Edge Trimming								
Exp No.	**Speed (rpm)**	**Feed (mm/min)**	**DOC (mm)**	**Fx (N)**	**Fy (N)**	**Fz (N)**	**Ft (N)**	**Fr (N)**
1	6000	635	6.35	133.2376	364.2612	373.23637	70.154	366.63047
2	6000	127	6.35	220.748	350.7327	28.679959	75.548463	380.30959
3	6000	635	2.54	200.4337	105.7998	392.96902	69.497331	400.933151
4	6000	127	2.54	162.3139	260.1835	25.484417	55.1144513	257.617251
5	1000	127	6.35	351.0996	451.1789	25.3152836	86.54677	459.32525
6	1000	635	6.35	454.3612	494.6293	93.10847	183.60054	496.472899
7	1000	635	2.54	249.8575	357.024	7.9711415	90.848156	380.52993
8	1000	127	2.54	387.6653	502.3149	19.3138315	124.37951	499.54867

The values obtained from the MATLAB codes and checked with raw data graphs for the Edge trimming of Random Fiber HexMC in Conventional Milling cut for all 8 experiments are displayed in **Table [4-5].**

Table [4-5]: Conventional (Odd) HexMC Edge Trimming Results

Conventional (Odd) HexMC Edge Trimming								
Exp No.	**Speed (rpm)**	**Feed (mm/min)**	**DOC (mm)**	**Fx (N)**	**Fy (N)**	**Fz (N)**	**Ft (N)**	**Fr (N)**
1	6000	635	6.35	119.73684	373.11918	392.11682	60.385502	362.50328
2	6000	127	6.35	220.4424	351.31099	30.069604	55.415462	340.35353
3	6000	635	2.54	187.60634	100.31868	435.22236	67.162829	399.590897
4	6000	127	2.54	172.65266	285.55477	26.629158	59.419908	262.775458
5	1000	127	6.35	341.62139	430.39882	15.747067	96.80027	428.78717
6	1000	635	6.35	483.50717	502.8593	99.342005	205.56577	501.794256
7	1000	635	2.54	310.36221	399.993	4.9071033	124.91106	389.1026
8	1000	127	2.54	367.23959	495.02711	22.432769	107.56642	494.15034

4.3 CFRP Circular Slot results

The Circular slot test was performed to see the effect of continuously changing cutting angles with respect to the Fiber direction as the Composite is Uni directional. To see this effect the forces were plotted with respect to the Angle which ranges from 0° to 180° as it is a semi-circular slot. The forces in each circular cut plotted with respect to the cutting angle are shown in Figures 4.9 to 4.13 . **Table [4-6]** mentions the machining parameters used to cut the circular slot test.

Table [4-6] : Circular Slot test - Machining parameters

Slot No.	Slot Diameter (mm)	Speed (rpm)	Feed (mm/min)	DOC (mm)
C1	50.8	1000	127	5.08
C2	82.55	6000	254	5.08
C3	114.3	6000	381	5.08
C4	146.05	3000	508	5.08
C5	177.8	3000	635	5.08

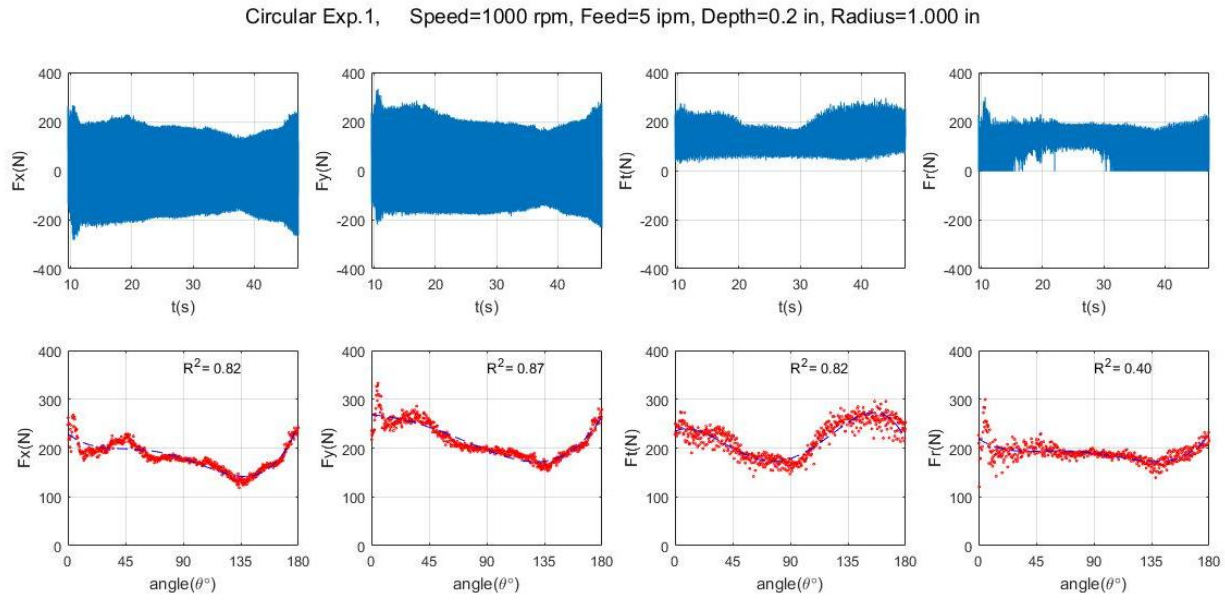

Figure 4.9 : Circular Slot C1 Force vs. Angle Plot

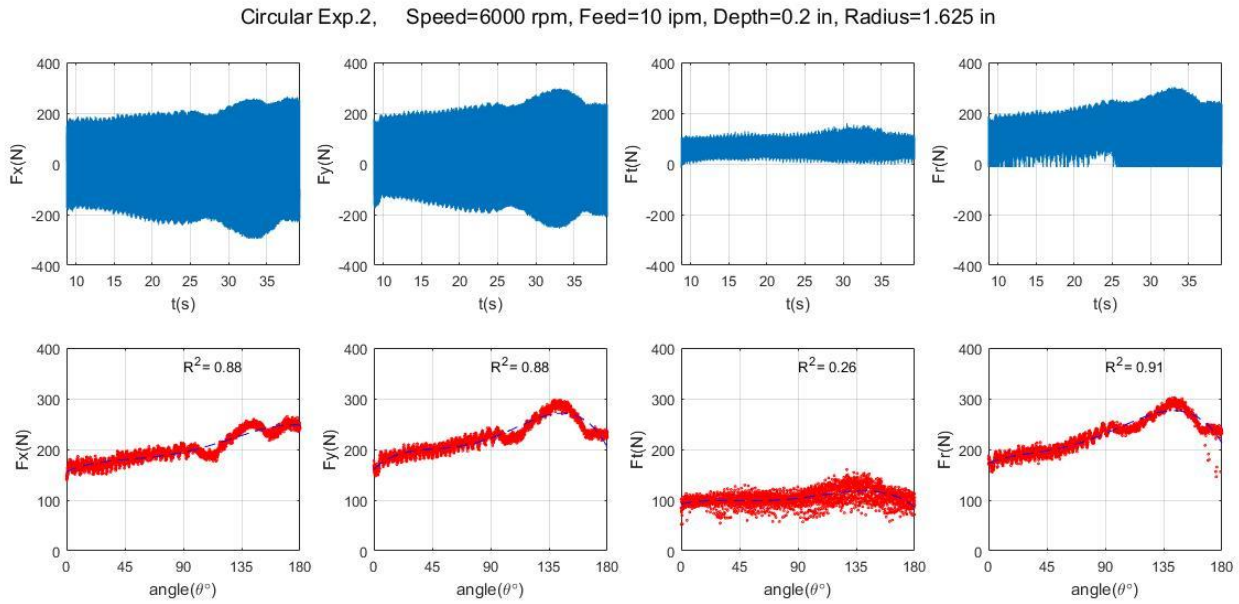

Figure 4.10 : Circular Slot C2 Force vs. Angle Plot

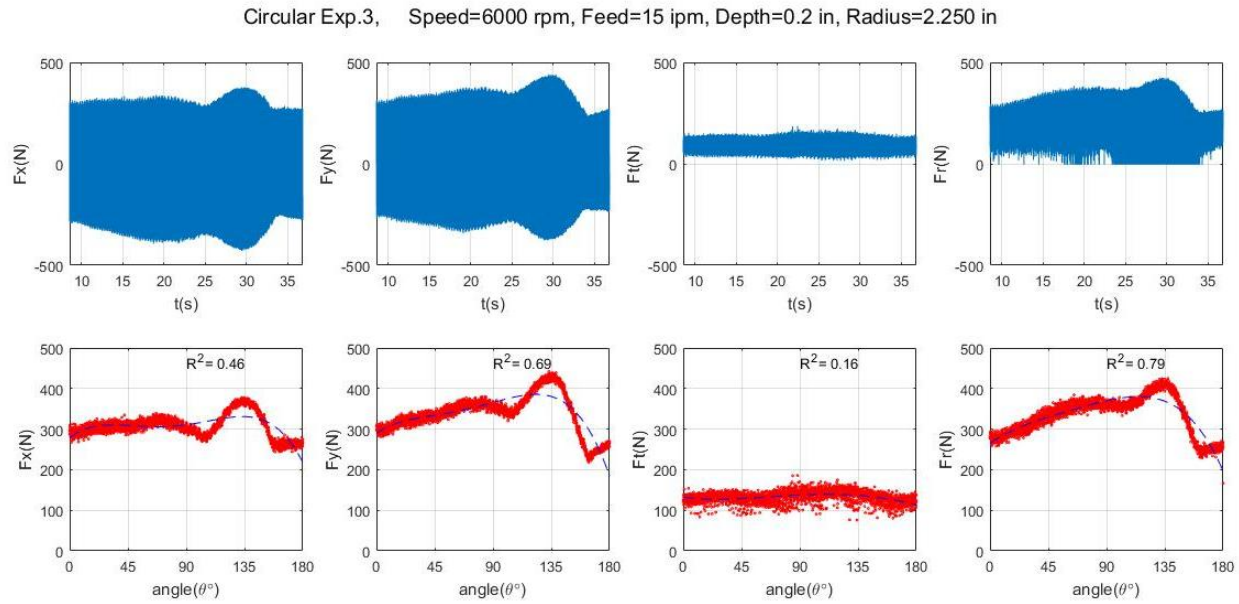

Figure 4.11 : Circular Slot C3 Force vs. Angle Plot

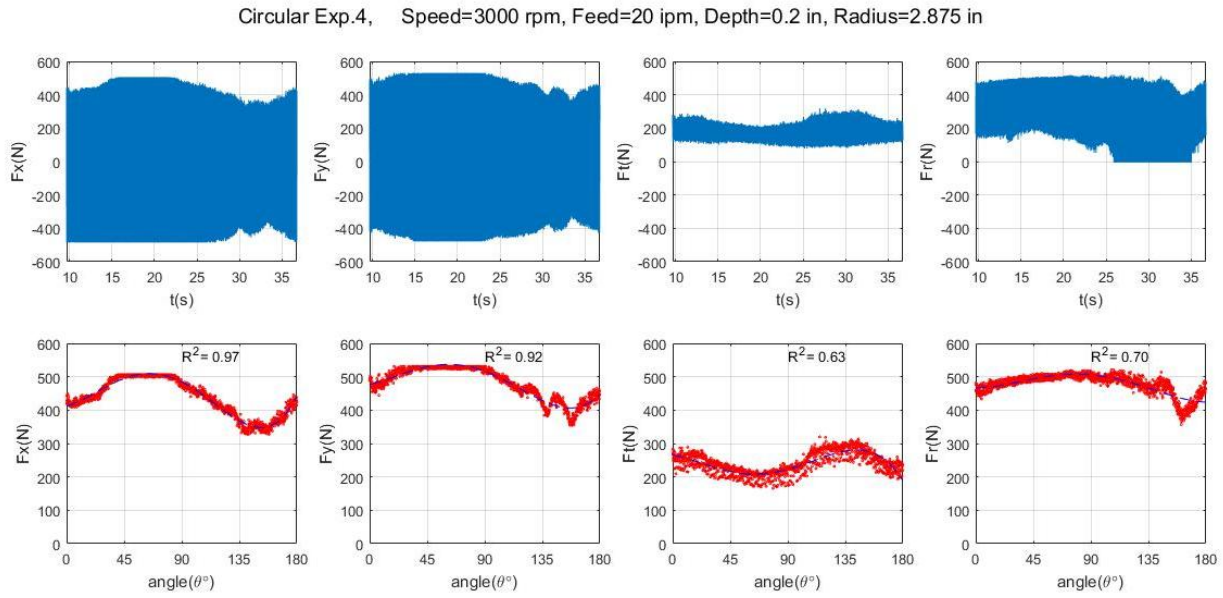

Figure 4.12 : Circular Slot C4 Force vs. Angle Plot

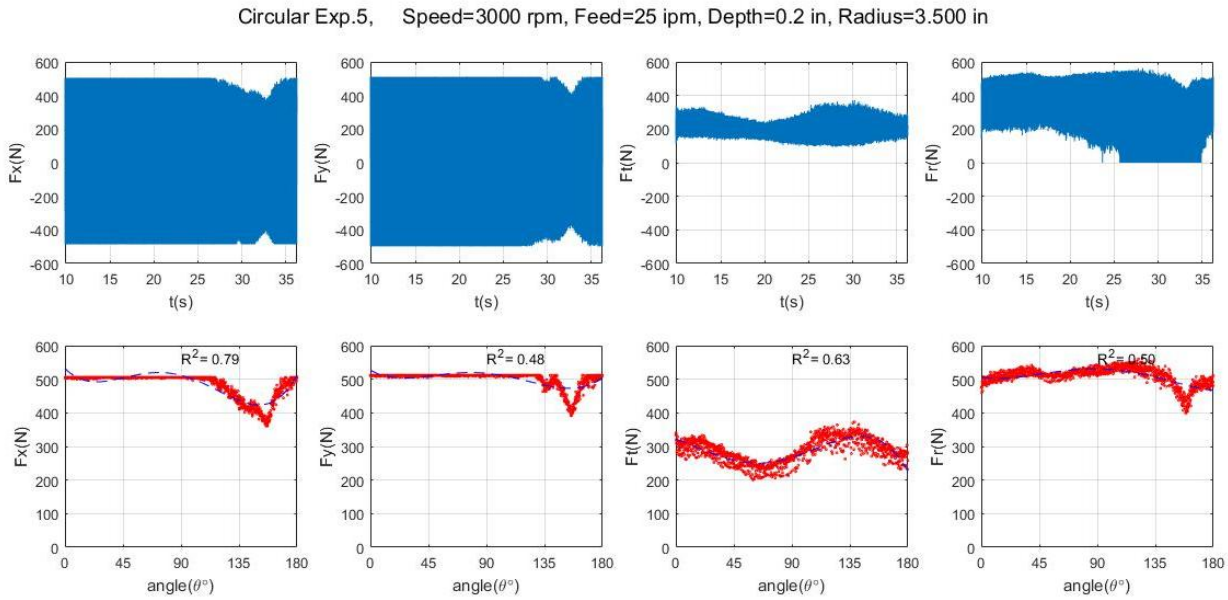

Figure 4.13 : Circular Slot C5 Force vs. Angle Plot

4.4 CFRP Octagonal Slot results

The Octagonal slot test was performed to see the effect of changing angle with respect to fiber direction similar to Circular slot test. But here, the angle is not continuously changing unlike circular test. And this test also helps us to corroborate the validity of test results in both cases. Figure 4.14 is a schematic of the Octagonal slot test with the relative angles to fiber direction. The forces Fx and Fy per tooth with respect to angle are plotted in Figure 4.15 and similarly forces Ft and Fr per tooth with respect to angle are plotted in Figure 4.16 . The force results from the octagonaltest are tabulated in **Table [4-7].**

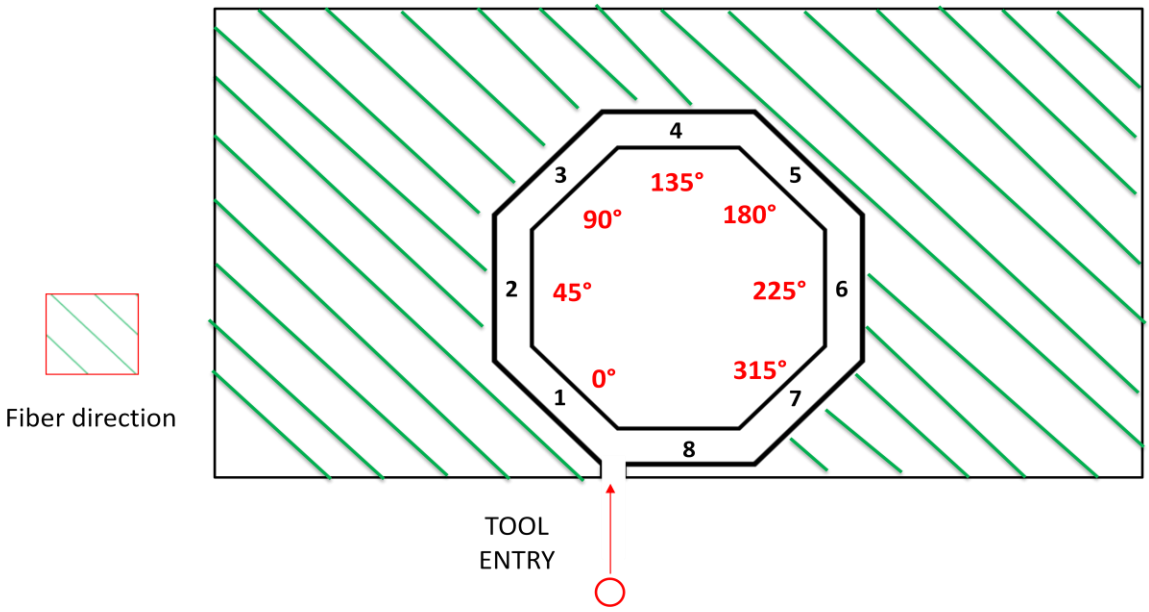

Figure 4.14 : Octagonal slot test - each cut with relative angle to Fiber Direction (FD)

Table [4-7] : Octagonal Slot test - Results

Cut No.	Angle	Fx (N)	Fy (N)	Fz (N)	Mz (Nm)	Ft (N)	Fr (N)
1	0°	83.35263	80.27639	38.94395	2.141657	84.31723	64.44682
2	45°	79.87404	76.35205	35.08587	2.027153	79.80917	62.57598
3	90°	76.61709	72.13233	31.34275	1.882457	74.11248	62.07701
4	135°	74.38532	72.14909	28.43734	1.818201	71.5827	62.123
5	180°	70.82166	68.19582	27.2973	1.850264	72.84504	60.51175
6	225°	78.20923	74.4342	25.48446	1.941947	76.45462	64.63538
7	270°	86.14329	82.90981	25.62144	2.100892	82.71229	63.4588
8	315°	86.08289	84.30368	16.93087	1.97953	77.93427	74.77963

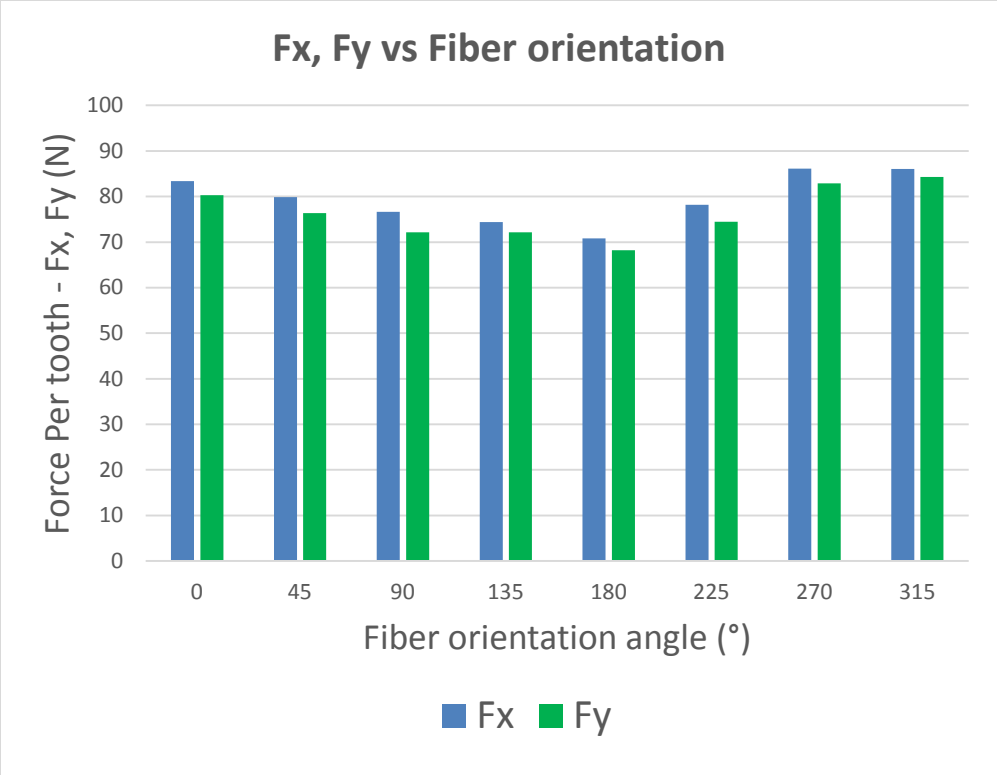

Figure 4.15 : Octagonal slot test - Fx and Fy per tooth wrt FD angle

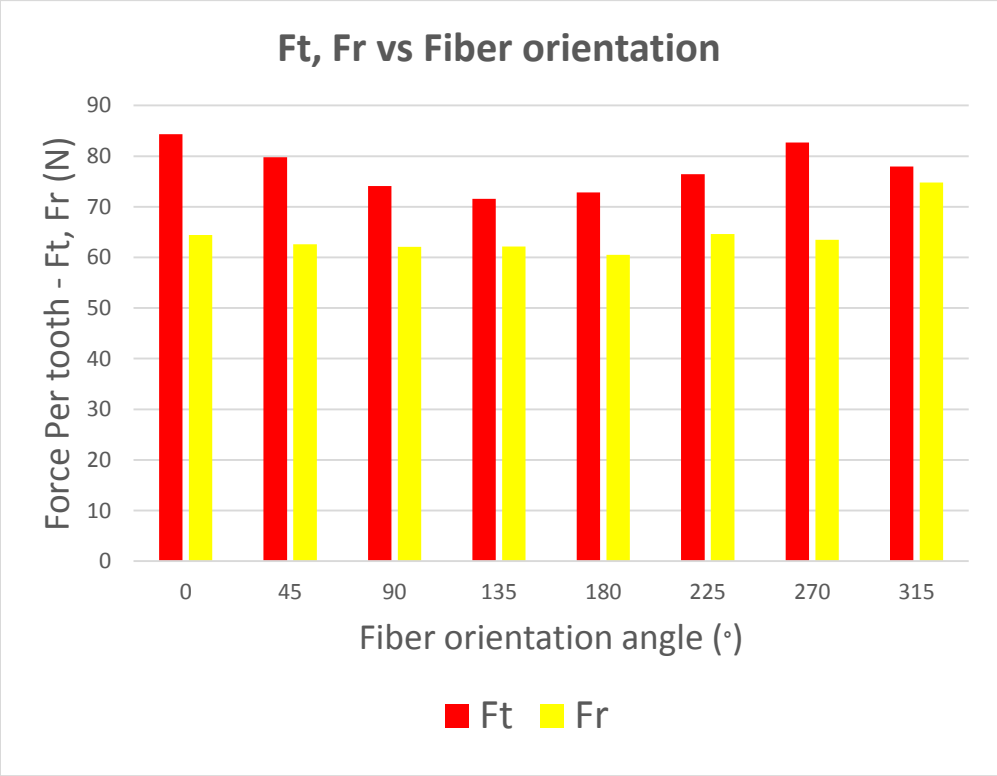

Figure 4.16 : Octagonal slot test - Ft and Fr per tooth wrt FD angle

4.5 Surface Roughness results - HexMC

To measure the surface roughness, additional tests were performed on HexMC composite. Four levels of Feed and 3 levels of Speed were chosen to machine the work piece.

The levels are,

- Feed - 2.12 mm/s , 5 mm/s , 10 mm/s , 15 mm/s
- Speed - 1000 rpm, 3000 rpm , 6000 rpm

In total 10 experiments were performed with the following cutting conditions mentioned in **Table [4-8]** and whose results are tabulated in **Table [4-9].** These conditions are schematically represented in Figure 4.17.

Table [4-8]: HexMC Surface roughness tests - Machining conditions

Exp No.	Speed (rpm)	Feed (mm/sec)	DOC (mm)
1a	6000	15	20.32
1b	6000	10	20.32
1c	6000	5	20.32
1d	3000	15	20.32
1e	3000	10	20.32
2a	3000	5	20.32
2b	1000	15	20.32
2c	1000	10	20.32
2d	1000	5	20.32
2e	1000	2.12	20.32

The surface roughness machine along with the attached automated moving base is shown in Figure 4.18.

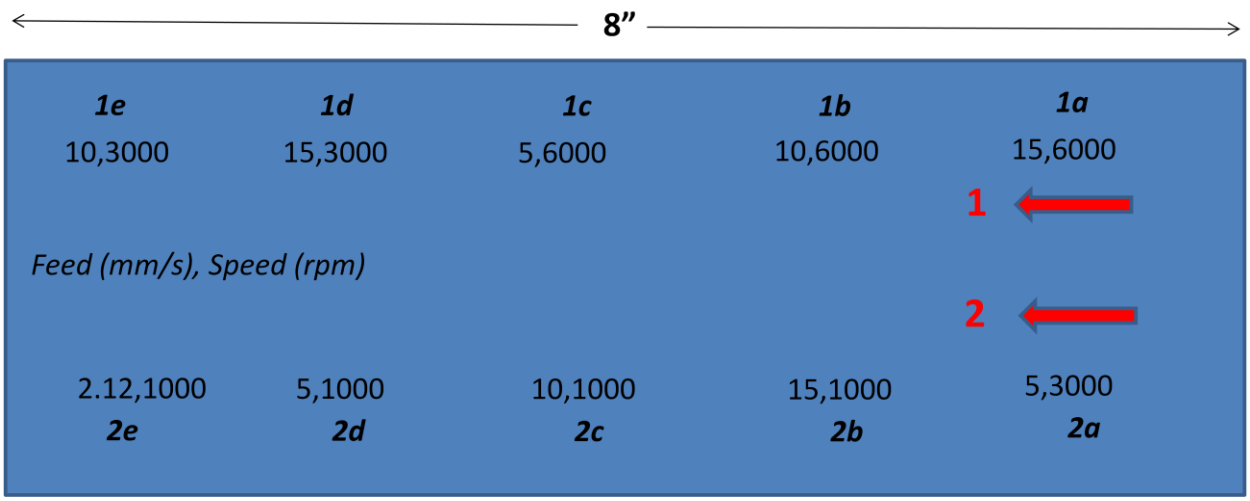

Figure 4.17 : Schematic showing HexMC Surface roughness tests with Machining conditions

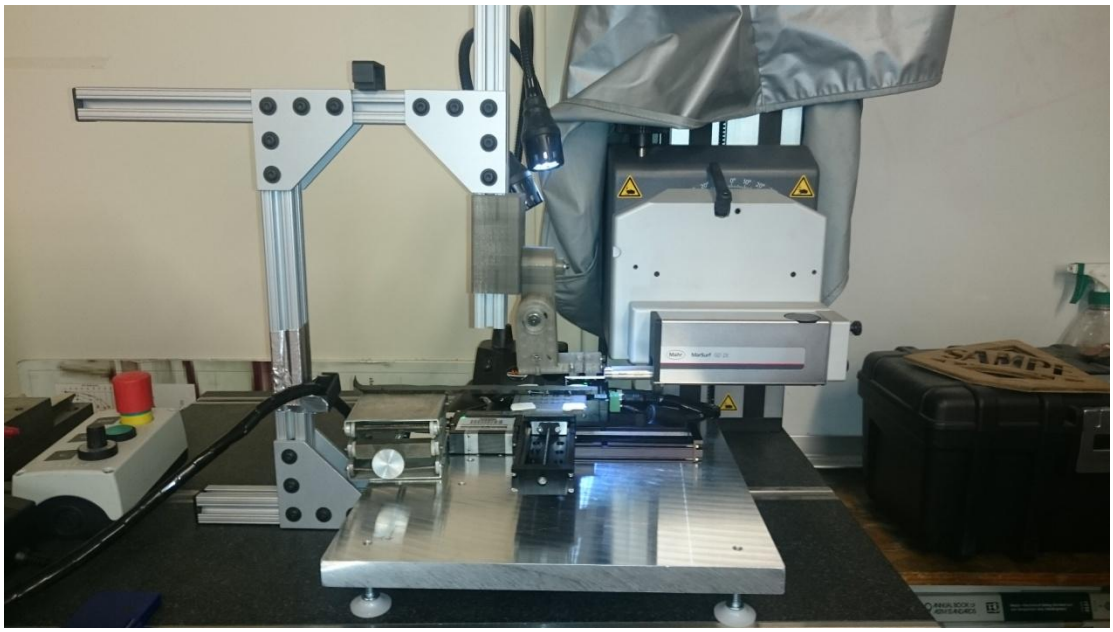

Figure 4.18 : Surface roughness testing machine with automated moving base mounted

The HexMC composite after machining was cut so that the machined surfaces Figure 4.19 could be measured for surface roughness.

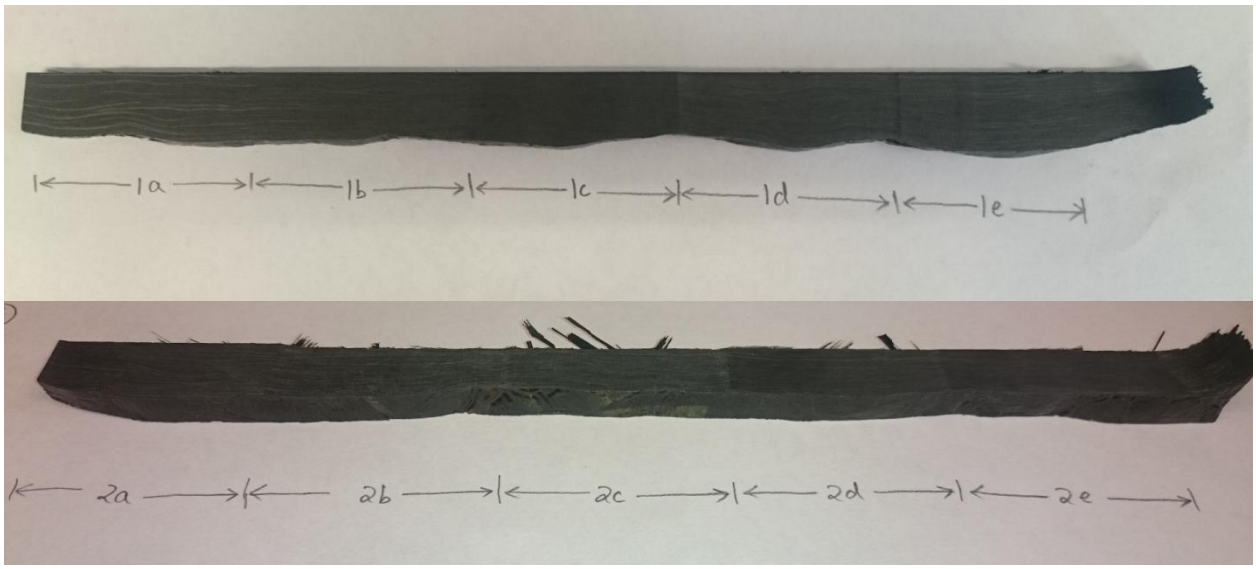

Figure 4.19 : HexMC composite work piece after machining for Surface roughness tests

Table [4-9]: HexMC Surface roughness tests - Results

Exp	Traverse Feed (mm/s)	Speed (rpm)	Ra (µm)	Rq (µm)	Rz (µm)	Rt (µm)	Rsk	Rku	h (from top) (mm)
1a	15	6000	5.1816	7.3856	34.8069	58.5906	-1.4315	6.7352	2
	15	6000	2.5306	3.5093	15.8998	24.6045	-0.9846	5.8728	4
	15	6000	2.689	3.204	13.3917	16.2313	0.1148	2.1714	6
	15	6000	2.503	3.4722	17.9032	37.297	0.6143	8.3523	8
1b	10	6000	2.4202	3.1628	15.071	19.419	-0.2588	3.2979	2
	10	6000	1.949	2.4332	10.8125	12.3197	0.0825	2.5118	4
	10	6000	2.1055	2.5441	11.1801	14.2458	-0.0837	2.5679	6
	10	6000	2.484	3.1454	14.9722	21.5935	-0.4458	3.4736	8
1c	5	6000	1.1071	1.4192	6.7397	9.2554	0.3774	3.4778	2
	5	6000	2.0212	2.6344	13.5892	18.308	-0.1154	3.6163	4
	5	6000	1.2519	1.578	7.9174	10.7492	0.2534	3.0149	6
	5	6000	1.8432	2.2993	10.1494	13.4684	0.2409	2.668	8
1d	15	3000	4.3255	5.4626	22.3839	44.6579	-0.4212	4.9242	2
	15	3000	3.4455	4.0996	16.8624	23.0688	-0.3022	2.5525	4
	15	3000	3.2908	4.1216	18.4327	27.318	0.022	3.2609	6
	15	3000	2.3011	2.9219	13.7467	22.4059	-0.6533	4.0091	8
1e	10	3000	4.4114	18.3475	21.9327	8.7773	2.3883	0.361	2
	10	3000	4.4878	17.0937	20.9632	8.625	2.0012	0.3389	4
	10	3000	2.2807	2.7903	13.3456	14.4655	-0.0315	2.5367	6
	10	3000	2.7354	3.4673	15.8903	23.9464	-0.4209	3.8038	8
2a	5	3000	1.4597	1.8883	9.2826	13.1261	-0.1384	3.4295	2
	5	3000	2.4255	3.4686	16.1547	30.5203	-1.5987	9.7655	4
	5	3000	2.6546	3.5346	16.1456	22.3107	-0.7669	3.9672	6
	5	3000	2.4097	3.266	15.7459	23.7378	-0.8614	4.8807	8
2b	15	1000	1.7198	2.4521	11.4231	18.234	-1.4527	7.2027	2
	15	1000	1.4469	1.7926	7.9803	10.2033	-0.3791	2.6354	4
	15	1000	1.8902	2.6351	12.2868	22.0543	-1.161	7.7643	6
	15	1000	3.4258	5.027	23.966	35.9863	-1.7537	8.3668	8
2c	10	1000	1.134	1.5058	7.9821	12.6192	-0.9007	5.543	2
	10	1000	3.0009	4.3785	18.5841	29.1782	-1.3658	6.2761	4
	10	1000	1.8859	2.4586	13.2329	16.6461	-0.8434	4.3744	6
	10	1000	2.5402	3.2879	15.1515	19.3352	-0.6875	3.9791	8
2d	5	1000	1.1074	1.5898	7.6832	13.4551	-1.4673	8.2716	2
	5	1000	1.4296	1.7316	8.9945	11.851	-0.2326	2.7398	4
	5	1000	1.0462	1.3871	8.2706	14.8208	-0.6553	5.725	6
	5	1000	0.9826	1.2758	7.2587	9.5897	-0.4389	4.2668	8
2e	2.12	1000	1.3175	1.7335	9.256	12.3739	-0.7639	3.922	2
	2.12	1000	0.9838	1.2949	7.9578	11.1326	-0.6494	4.6036	4
	2.12	1000	1.1323	1.5877	7.8194	12.9821	-0.888	6.0267	6
	2.12	1000	0.9624	1.2693	8.0708	10.5776	-0.021	4.2045	8

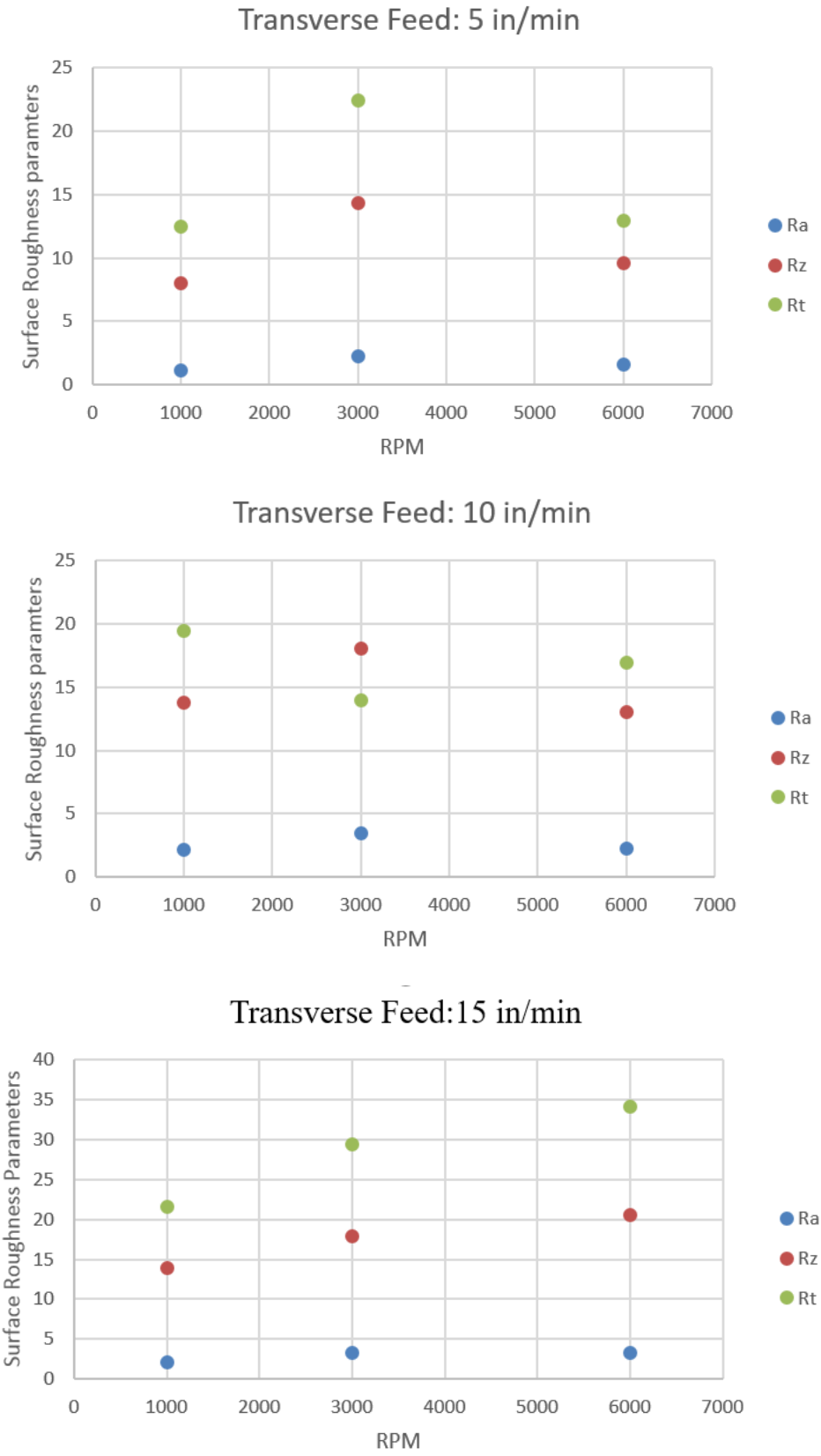

Figure 4.20 : Surface roughness results with varying feed values

Figure 4.20 shows the Ra, Rz, Rt values plotted at three different levels of feed with respect to speed. At low feed value, all three Rt, Rz and Ra values are following a increasing and then a decreasing pattern as the speed increases. At medium feed, both Ra and Rz follow the same pattern as before in low feed as speed increases, but Rt follows an inverted pattern where it decreases first and then increases. At high feed value, all three roughness values follow an almost linear increasing pattern as the speed increases.

Chapter 5: Discussion and Analysis

After performing the experiments and extracting the data, analysis of the data is essential to understand the behavior of the material under the set cutting conditions. One of the popular methods which is used in this research to do this is Design of Experiments or more commonly referred to as DOE. It is a method which is used to deduce how different factors influence a process and thereby affect the output such as the Force responses. It can be highly effective to manage process parameters which are given to it as inputs so that the outputs obtained are optimum.

The Design Expert software from Stat Ease is used in this research to analyze the results mentioned before in Chapter 4. The main sections that are going to be analyzed via this software are,

- CFRP Edge trim results

  - Climb (Even) milling

  - Conventional (Odd) milling

- HexMC Edge trim results

  - Climb (Even) milling

  - Conventional (Odd) milling

Numerous models were compared in order to finalize the best possible model for every data set. The models that were finally chosen for each Force response/output are mentioned in **Tables [5-1], [5-4], [5-7] and [5-10].** These models sometimes require us to ignore some data sets that are out of a boundary. The experiments which were ignored , were removed as they were out of bounds of a parameter whose calculation is shown below or sometimes by trial and error.

Parameter used to ignore some data sets:

It is known that usually the following relation holds true as it is the relation used to calculate Fr in Dynoware**.**

$$Fx^2 + Fy^2 = Ft^2 + Fr^2$$

because, $Fr = \sqrt{Fx^2 + Fy^2 - Ft^2}$

where $Ft = \frac{Mz}{r}$, $where\ r = cutter\ tool\ radius$

And the term active Force is calculated by, $Fa = \sqrt{Fx^2 + Fy^2} = \sqrt{Ft^2 + Fr^2}$

From the results obtained, the value of $\frac{\sqrt{Fx^2+Fy^2}}{\sqrt{Ft^2+Fr^2}}$ was calculated. Ideally it should be around 1. So the experiments which were higher than and around 1.5 or lower than and around 0.5 were ignored.

The general trend observed for the milling forces is that the ***forces are low for High speeds and Low feeds***. The analyses done in subsequent sections are to see if this trend is followed or not and why is the behavior of the material in a particular way.

Each analysis required inputs and outputs. The inputs are called " *Factors* " and the outputs are taken as " *Responses* ". Since we already have the data for the Average of Maximum Forces i.e., Fx, Fy, Fz, Ft and Fr for each milling scenario for both the materials, a method called the *Response surface* was chosen and then the option *Historical Data* was chosen to give the values into the software. For historical data and response surface analyses, backward approach is considered to be the most robust option as it gives all the model terms a chance to be included in the model.

Alpha out refers to the ext criteria for removing terms in the model.

After entering the statistical design matrix into the software, we choose a model which fits the data better than the others and then ANOVA is performed. From ANOVA the basic and major inferences we take are the interaction effects of factors/inputs and the behavior of the model and R^2 values among others.

The model gives us predicted values and these are calculated with a formula given in each response's ANOVA. These formulae have been tabulated in each section. This helps us to know as to which terms are contributing and which are not and by how much.

5.1 Analysis of CFRP Edge trims

5.1.1 CFRP - Climb (Even) - Edge trim

Table [5-1] gives us the models used to get the ANOVA output from Stat Ease Software for CFRP Climb milling edge trims. The models that were finally chosen for each Force response/output are mentioned in **Table [5-1]** and the statistical design matrix in **Table [5-2].** Details are given in Appendix I.

Table 5-1 : CFRP - Climb (Even) - Edge Trim ANOVA

CFRP - Climb (Even) - Edge Trim ANOVA				
Experiment(s) Ignored	**Force**	**Model Used**		
		Process Order	**Selection**	**Alpha Out**
6,16,19,20	Fx	Cubic	Backward	0.05
6,16,19,20	Fy	Cubic	Backward	0.1
6,16,19,20	Fz	Quadratic	Backward	0.1
6,16,19,20	Ft	Quadratic	Backward	0.1
6,16,19,20	Fr	Cubic	Backward	0.05

Statistical Matrix :

Table 5-2 : Statistical matrix used For ANOVA of CFRP Climb (Even) - Edge Trim

Run	Factor 1 A:Speed rpm	Factor 2 B : Feed mm/min	Factor 3 C : DOC mm	Response 1 Fx N	Response 2 Fy N	Response 3 Fz N	Response 4 Ft N	Response 5 Fr N
1	6000	635	6.35	143.115	275.8503	364.7114	33.36993	311.1462
2	6000	635	3.81	101.5559	174.2728	368.1563	70.623	239.687
3	3000	635	3.81	153.2877	224.1279	112.6527	75.46583	316.3304
4	6000	635	2.54	104.6266	136.8084	356.0724	71.9315	210.8921
5	3000	635	2.54	59.06375	110.5862	113.7669	35.6466	119.7625
6	1000	635	2.54	94.42652	126.0127	22.12614	80.73293	140
7	1000	635	6.35	172.9833	235.1539	18.32296	152.8115	225
8	1000	635	3.81	143.6454	143.8556	20.28835	154.641	218.4237
9	6000	381	6.35	79.92946	115.9064	363.429	57.94921	258.9037
10	6000	381	3.81	112.8019	137.521	350.0182	65.67046	262.9074
11	6000	381	2.54	125.3633	203.2971	363.8001	64.58286	230.9507
12	3000	381	6.35	74.8513	124.6906	6.703777	34.27733	166.013
13	3000	381	3.81	96.40978	209.843	111.3645	43.47756	212.6087
14	3000	381	2.54	70.76549	98.6738	100.2196	42.63078	152.265
15	1000	381	2.54	139.5168	220.7682	23.96494	98.85523	260
16	1000	381	6.35	278.0024	346.8159	48.36253	147.822	320
17	6000	127	3.81	44.10433	109.1953	357.9492	25.8273	97.64605
18	3000	127	3.81	136.3261	141.4977	108.1768	30.9997	152.2137
19	1000	127	3.81	177.4816	204.8916	7.973164	61.44043	215
20	1000	127	2.54	142.0234	157.246	6.540984	51.1524	175
21	3000	127	2.54	120.9974	22.99295	85.52739	33.15409	247.9018
22	6000	127	6.35	177.6107	182.3015	354.4235	47.74905	194.4933
23	3000	127	6.35	161.991	267.6451	77.55997	46.26357	267.8589
24	1000	127	6.35	386.1639	396.624	20.56	102.1051	424.7395

Formulae from ANOVA :

Table 5-3 : Formulae from ANOVA of CFRP Climb (Even) - Edge Trim

	Force	Formula
CFRP - Climb (Even)	Fx	*Fx = 511.091 + -0.264178 * Speed + -0.811455 * Feed + 62.6966 * DOC + 0.000592868 * Speed * Feed + -0.331276 * Feed * DOC + 2.46841e-005 * Speed^2 + 0.000254741 * Feed^2 + -3.64656e-008 * Speed^2 * Feed + -3.06937e-007 * Speed * Feed^2 + 0.000394733 * Feed^2 * DOC*
	Fy	Fy = 688.976 + -0.567693 * Speed + 0.587117 * Feed + 46.5394 * DOC + 0.00086403 * Speed * Feed + 0.054463 * Speed * DOC + -0.727699 * Feed * DOC + 6.56662e-005 * Speed^2 + -0.00222853 * Feed^2 + -6.74273e-008 * Speed^2 * Feed + -7.47015e-006 * Speed^2 * DOC + -3.44241e-007 * Speed * Feed^2 + 0.000990311 * Feed^2 * DOC
	Fz	Fz = -36.4149 + 0.0575097 * Speed + 13.2618 * DOC + -0.0176222 * Speed * DOC + 1.40543e-006 * Speed^2 + 2.51052e-006 * Speed^2 * DOC
	Ft	Ft = 124.944 + -0.0640784 * Speed + 0.0609507 * Feed + 9.30673 * DOC + -0.00200161 * Speed * DOC + 8.27937e-006 * Speed^2
	Fr	Fr = 922.16 + 0.00132701 * Speed + -1.99878 * Feed + -370.353 * DOC + -9.90762e-005 * Speed * Feed + -0.0206571 * Speed * DOC + 1.03791 * Feed * DOC + 7.62361e-006 * Speed^2 + 51.4481 * DOC^2 + 4.60416e-005 * Speed * Feed * DOC + -0.136235 * Feed * DOC^2

3D Surface Plot to show interaction effects :

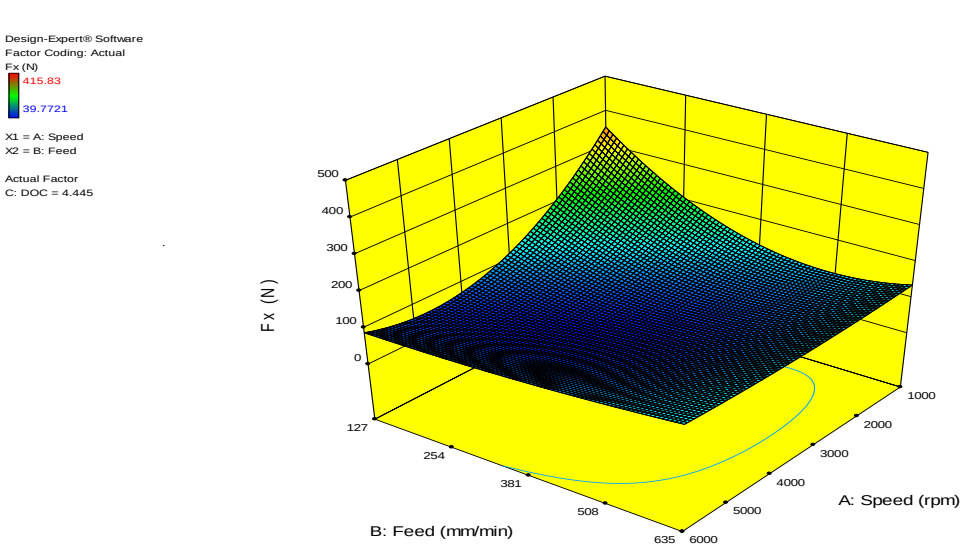

Figure 5.1 : 3D surface Plot - Fx - CFRP Climb (Even) Edge trim

Figure 5.1 shows us the interaction effects of the two of the factors Speed and Feed with the Force response Fx. We can see that at higher speed, the force Fx is almost constant with change in feed. But at lower speed, the force is highest at the lowest feed.

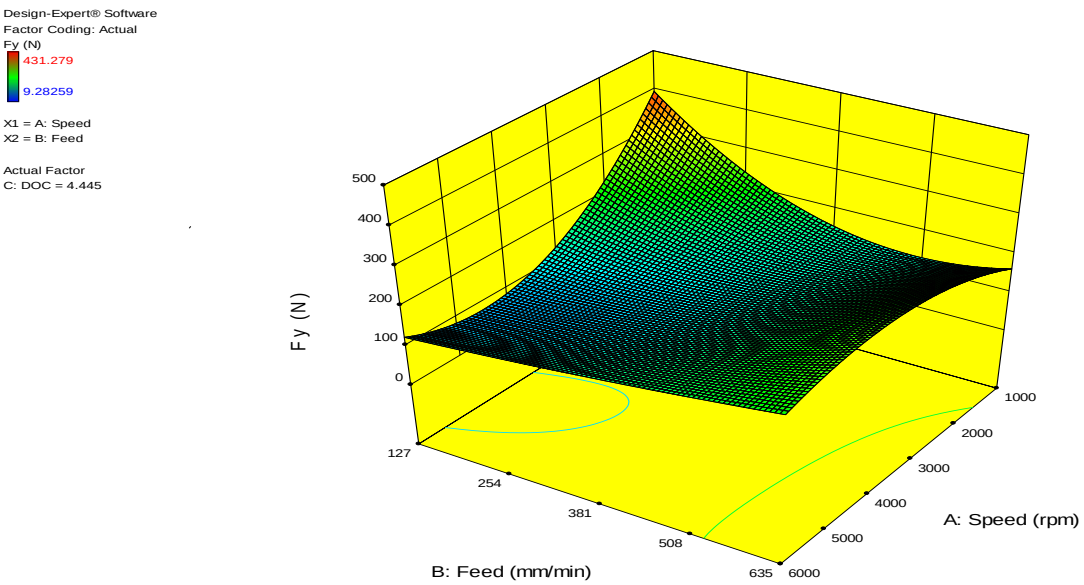

Figure 5.2 : 3D surface Plot - Fy - CFRP Climb (Even) Edge trim

For the Force Fy (Figure 5.2) in Climb cutting, the highest force is at lowest speed and lowest feed and the lower forces are at low feeds and high speeds.

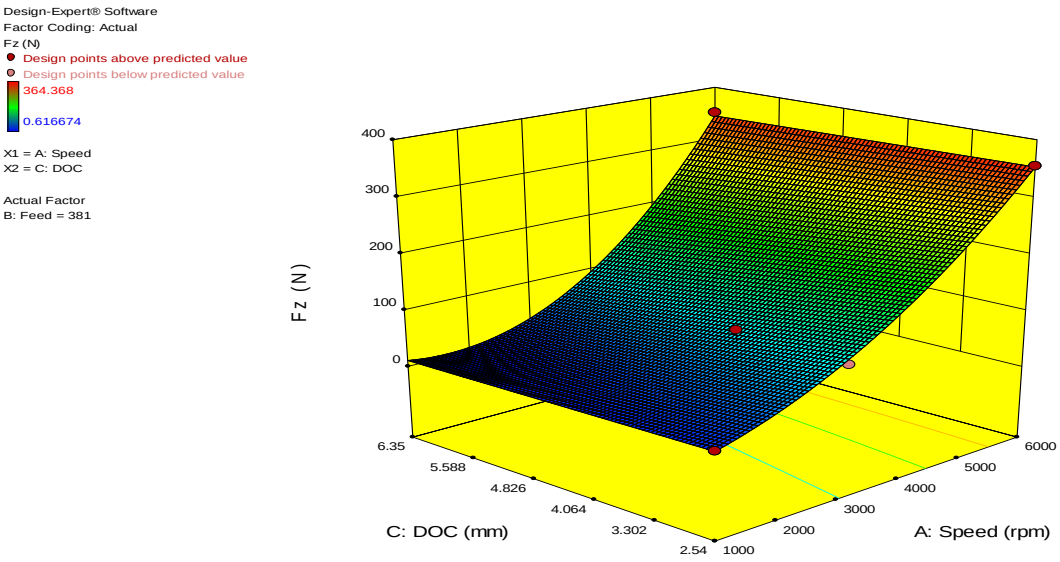

Figure 5.3 : 3D surface Plot - Fz - CFRP Climb (Even) Edge trim

For the Force Fz (Figure 5.3) in Climb cutting, the model which fit the data best, had interaction effects of Speed and Depth of cut (DOC) influencing the force. High speeds have the highest force for all DOC's.

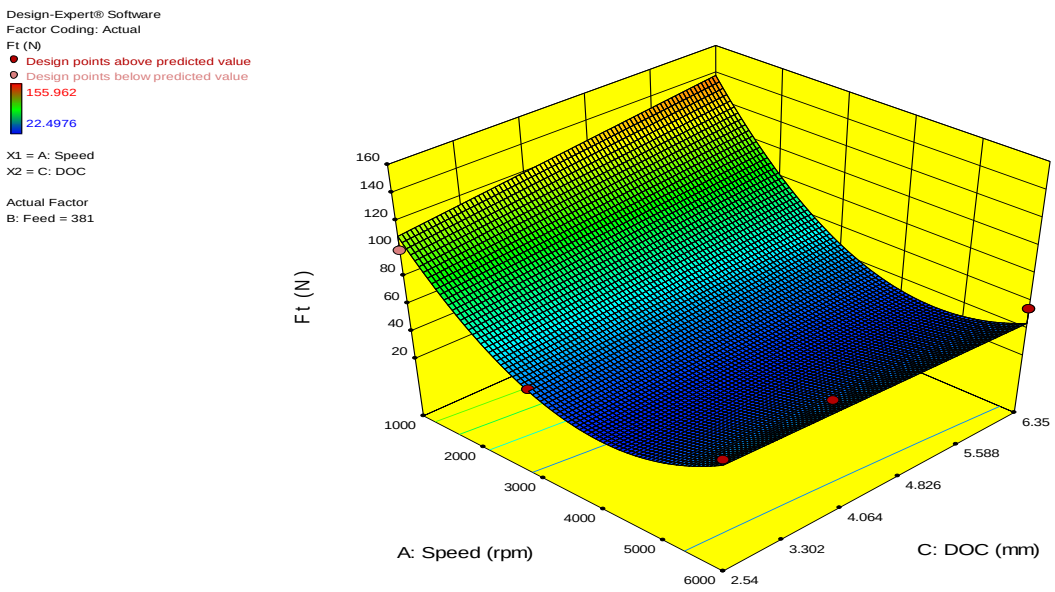

Figure 5.4 : 3D surface Plot - Ft - CFRP Climb (Even) Edge trim

For force Ft, the interaction between Speed and DOC (Figure 5.4), show that the optimum conditions to get the lowest forces are at high speeds and low DOC.

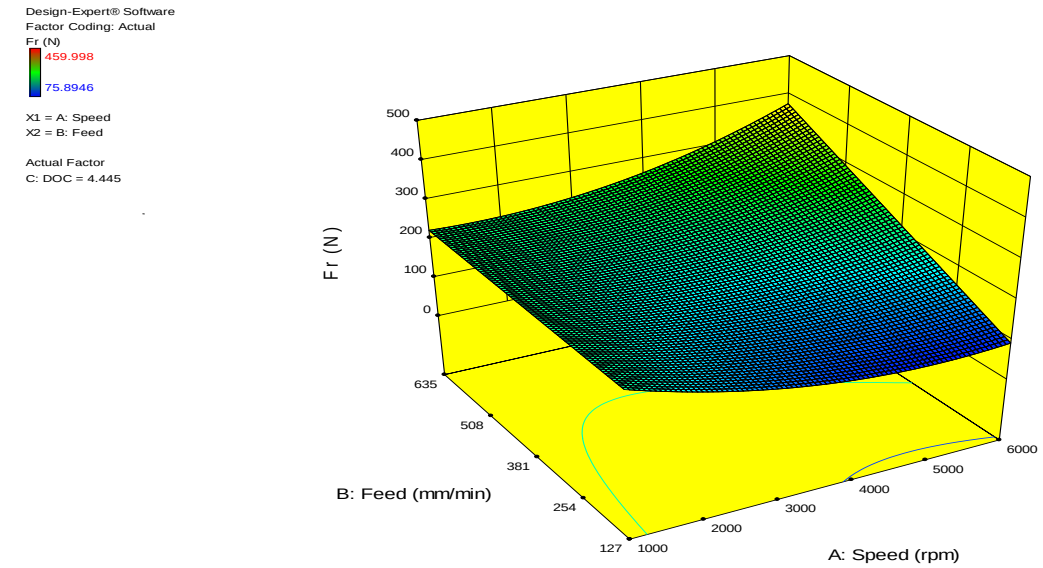

Figure 5.5 : 3D surface Plot - Fr - CFRP Climb (Even) Edge trim

Figure 5.5 shows us the interaction effects of Speed and Feed with the Force response Fx. We can see that at higher speed, the force Fr is increasing with an increase in feed value. But at lower speed, the force is almost constant with varying feeds.

Summary of 3D graphs of CFRP Climb cuts :

Table 5-4 : Summarization of 3D interactions - CFRP Climb cuts

3D interactions - CFRP Climb cuts						
Force	**Trend**	**Speed**	**Feed**	**DOC**	**Force value (N)**	**Comments**
Fx	Low forces @	↑	↓	-	90	**Figure 5.1** shows us the interaction effects of the two of the factors Speed and Feed with the Force response Fx. We can see that at higher speed, the force Fx is almost constant with change in feed. But at lower speed, the force is highest at the lowest feed.
	High forces @	↓	↓	-	350	
Fy	Low forces @	↑	↓	-	110	For the Force Fy (**Figure 5.2**) in Climb cutting, the highest force is at lowest speed and lowest feed and the lower forces are at low feeds and high speeds.
	High forces @	↓	↓	-	390	
Fz	Low forces @	↓	-	**All DOC**	10	For the Force Fz (**Figure 5.3**) in Climb cutting, the model which fit the data best, had interaction effects of Speed and Depth of cut (DOC) influencing the force. High speeds have the highest force for all DOC's.
	High forces @	↑	-	**All DOC**	350	
Ft	Low forces @	**Mid**	-	↓	25	For force Ft, the interaction between Speed and DOC (**Figure 5.4**), show that the optimum conditions to get the lowest forces are at high speeds and low DOC.
	High forces @	↓	-	↑	135	
Fr	Low forces @	↑	↓	-	80	**Figure 5.5** shows us the interaction effects of Speed and Feed with the Force response Fx. We can see that at higher speed, the force Fr is increasing with an increase in feed value. But at lower speed, the force is almost constant with varying feeds.
	High forces @	↑	↑	-	380	

5.1.2 CFRP - Conventional (Odd) - Edge trim

Table 5-5 gives us the models used to get the ANOVA output from Stat Ease Software for CFRP Conventional milling edge trims. The models that were finally chosen for each Force response/output are mentioned in **Table [5-5]** and the statistical design matrix in **Table [5-6].** Also see Appendix **J.**

Table 5-5 : CFRP – Conventional (Odd) - Edge Trim ANOVA

CFRP – Conventional (Odd) - Edge Trim ANOVA				
Experiment(s) Ignored	**Force**	**Model Used**		
		Process Order	**Selection**	**Alpha Out**
16,18,22,24	Fx	Cubic	Backward	0.05
16,18,22,24	Fy	Cubic	Backward	0.15
16,18,22,24	Fz	Cubic	Backward	0.15
16,18,22,24	Ft	Cubic	Backward	0.15
16,18,22,24	Fr	Quadratic	Backward	0.15

Statistical Matrix :

Table 5-6 : Statistical matrix used For ANOVA of CFRP – Conventional (Odd) - Edge Trim

Run	Factor 1 A:Speed rpm	Factor 2 B : Feed mm/min	Factor 3 C : DOC mm	Response 1 Fx N	Response 2 Fy N	Response 3 Fz N	Response 4 Ft N	Response 5 Fr N
1	6000	635	6.35	143.115	275.8503	364.7114	33.36993	311.1462
2	6000	635	3.81	101.5559	174.2728	368.1563	70.623	239.687
3	3000	635	3.81	153.2877	224.1279	112.6527	75.46583	316.3304
4	6000	635	2.54	104.6266	136.8084	356.0724	71.9315	210.8921
5	3000	635	2.54	59.06375	110.5862	113.7669	35.6466	119.7625
6	1000	635	2.54	94.42652	126.0127	22.12614	80.73293	140
7	1000	635	6.35	172.9833	235.1539	18.32296	152.8115	225
8	1000	635	3.81	143.6454	143.8556	20.28835	154.641	218.4237
9	6000	381	6.35	79.92946	115.9064	363.429	57.94921	258.9037
10	6000	381	3.81	112.8019	137.521	350.0182	65.67046	262.9074
11	6000	381	2.54	125.3633	203.2971	363.8001	64.58286	230.9507
12	3000	381	6.35	74.8513	124.6906	6.703777	34.27733	166.013
13	3000	381	3.81	96.40978	209.843	111.3645	43.47756	212.6087
14	3000	381	2.54	70.76549	98.6738	100.2196	42.63078	152.265
15	1000	381	2.54	139.5168	220.7682	23.96494	98.85523	260
16	1000	381	6.35	278.0024	346.8159	48.36253	147.822	320
17	6000	127	3.81	44.10433	109.1953	357.9492	25.8273	97.64605
18	3000	127	3.81	136.3261	141.4977	108.1768	30.9997	152.2137
19	1000	127	3.81	177.4816	204.8916	7.973164	61.44043	215
20	1000	127	2.54	142.0234	157.246	6.540984	51.1524	175
21	3000	127	2.54	120.9974	22.99295	85.52739	33.15409	247.9018
22	6000	127	6.35	177.6107	182.3015	354.4235	47.74905	194.4933
23	3000	127	6.35	161.991	267.6451	77.55997	46.26357	267.8589
24	1000	127	6.35	386.1639	396.624	20.56	102.1051	424.7395

Formulae from ANOVA :

Table 5-7 : Formulae from ANOVA of CFRP Conventional (Odd) - Edge Trim

	Force	Formula
CFRP - Conventional (Odd)	Fx	*Fx = 124.705 + -0.0489645 * Speed + 0.206829 * Feed + 45.8363 * DOC + 0.000221629 * Speed * Feed + -0.297946 * Feed * DOC + -0.000481235 * Feed^2 + -2.3765e-007 * Speed * Feed^2 + 0.000401325 * Feed^2 * DOC*
	Fy	Fy = 15.3267 + -0.26756 * Speed + 2.504 * Feed + 83.2867 * DOC + 0.000286183 * Speed * Feed + 0.0342615 * Speed * DOC + -0.740432 * Feed * DOC + 3.41569e-005 * Speed^2 + -0.00369419 * Feed^2 + -3.46856e-008 * Speed^2 * Feed + -4.65582e-006 * Speed^2 * DOC + 0.000960132 * Feed^2 * DOC
	Fz	Fz = -86.7531 + -0.0604277 * Speed + 0.709601 * Feed + 66.9843 * DOC + 0.000192065 * Speed * Feed + 0.0196251 * Speed * DOC + -0.350249 * Feed * DOC + 6.99467e-006 * Speed^2 + -0.00092262 * Feed^2 + -10.5545 * DOC^2 + -2.96631e-005 * Speed * Feed * DOC + -1.12207e-007 * Speed * Feed^2 + 0.000393269 * Feed^2 * DOC + 0.0156797 * Feed * DOC^2
	Ft	Ft = 71.1606 + -0.0130881 * Speed + -0.000949021 * Feed + -6.69459 * DOC + -9.30215e-007 * Speed * Feed + -0.00965593 * Speed * DOC + 0.185704 * Feed * DOC + 2.52158e-006 * Speed^2 + -0.000628867 * Feed^2 + -0.159189 * DOC^2 + -2.15946e-005 * Speed * Feed * DOC + 8.90823e-009 * Speed^2 * Feed + 0.00201329 * Speed * DOC^2 + 0.000139935 * Feed^2 * DOC + -0.0253884 * Feed * DOC^2
	Fr	Fr = 206.614 + -0.0205548 * Speed + -0.131147 * Feed + 14.2259 * DOC + 5.38482e-005 * Speed * Feed

3D Surface Plots to show interaction effects :

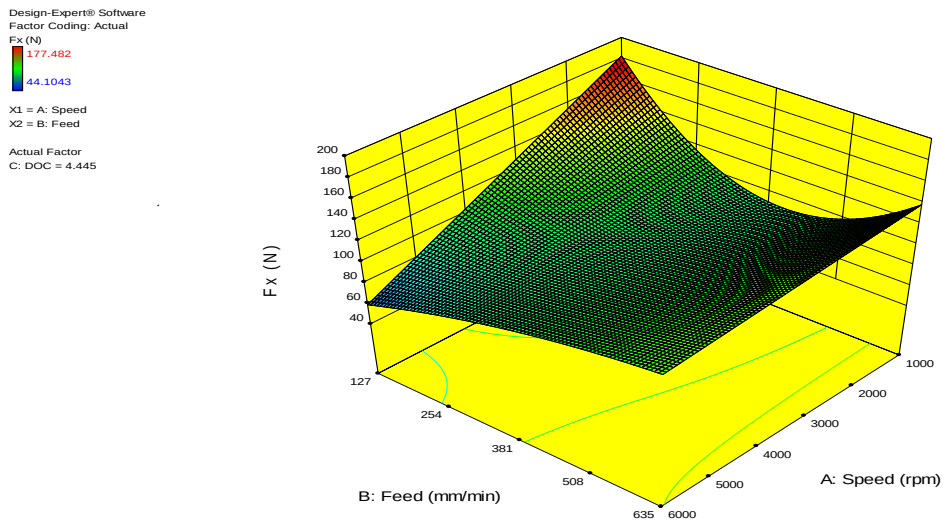

Figure 5.6 : 3D surface Plot - Fx - CFRP Conventional (Odd) Edge trim

For Conventional milling, the force Fx (Figure 5.6) is lowest at high speed and low feed. At low speeds the force is lowest at mid feed value.

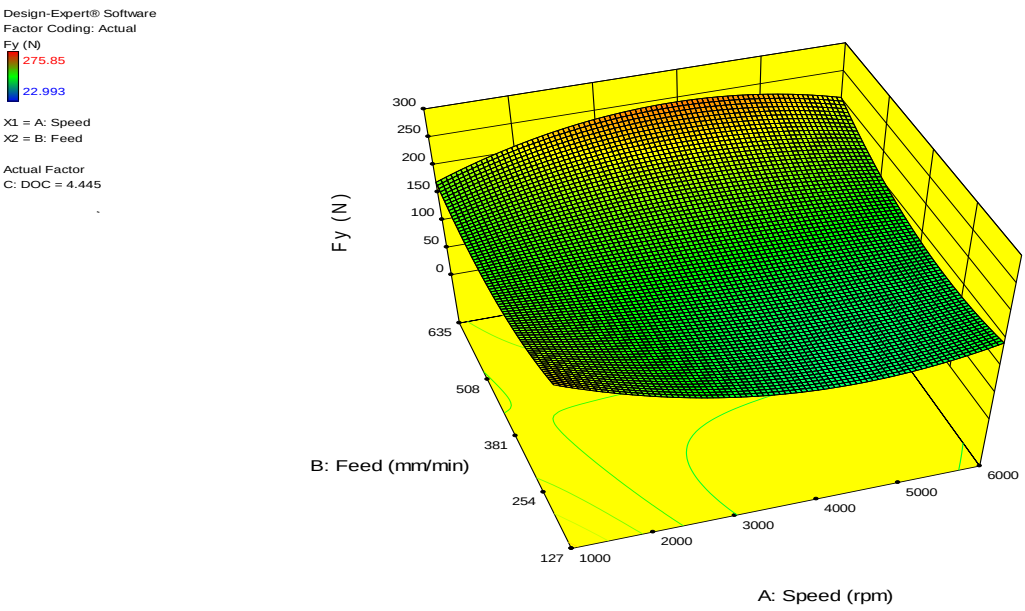

Figure 5.7 : 3D surface Plot - Fy - CFRP Conventional (Odd) Edge trim

For force Fy in Conventional milling (Figure 5.7), the highest value of force is found to be at high feed and mid speed for the range. And lowest at higher speeds and lower feeds.

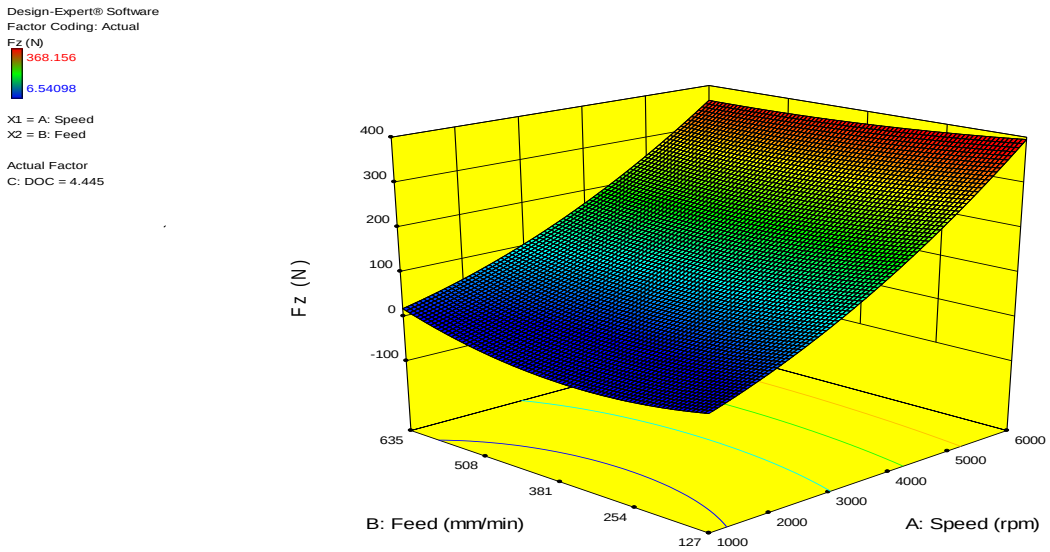

Figure 5.8 : 3D surface Plot - Fz - CFRP Conventional (Odd) Edge trim

Similar to Climb cut, The Fz in Conventional cut (Figure 5.8) is highest at higher speeds and lower at lower speeds. And at any feed, the force is increasing with an increase in speed.

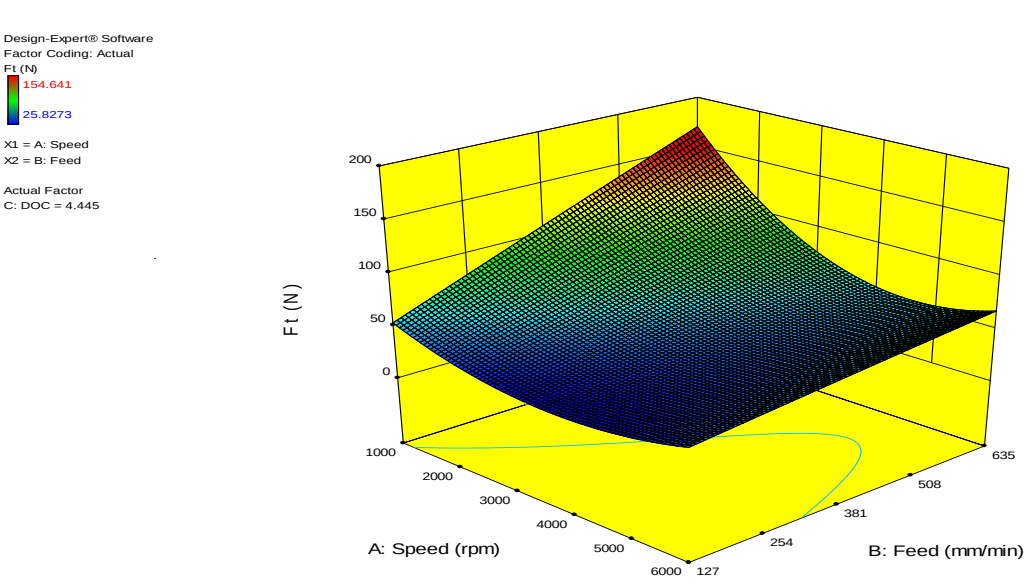

Figure 5.9 : 3D surface Plot - Ft - CFRP Conventional (Odd) Edge trim

The tangential force Ft in Conventional milling (Figure 5.9), shows an increasing force trend with an increasing feed at a given speed and the force is highest at high feed and low speed.

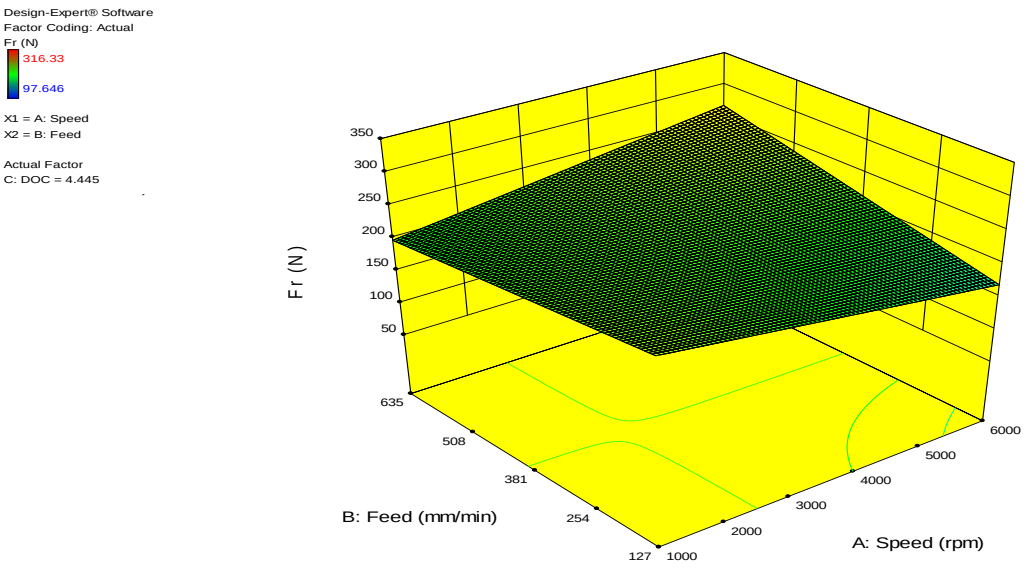

Figure 5.10 : 3D surface Plot - Fr - CFRP Conventional (Odd) Edge trim

Figure 5.10 shows us that in conventional milling, the radial force Fr is lower at high speed and low feed and highest when both factors speed and feed are at their highest values.

Summary of 3D graphs of CFRP Conventional cuts :

Table 5-8 : Summarization of 3D interactions - CFRP Conventional cuts

3D interactions - CFRP Conventional cuts						
Force	**Trend**	**Speed**	**Feed**	**DOC**	**Force value (N)**	**Comments**
Fx	Low forces @	↑	↓	-	50	For Conventional milling, the force Fx (**Figure 5.6**) is lowest at high speed and low feed. At low speeds the force is lowest at mid feed value.
	High forces @	↓	↓	-	180	
Fy	Low forces @	↑	↓	-	90	For force Fy in Conventional milling (**Figure 5.7**), the highest value of force is found to be at high feed and mid speed for the range. And lowest at higher speeds and lower feeds.
	High forces @	**Mid**	↑	-	240	
Fz	Low forces @	↓	↓	-	10	Similar to Climb cut, The Fz in Conventional cut (**Figure 5.8**) is highest at higher speeds and lower at lower speeds. And at any feed, the force is increasing with an increase in speed.
	High forces @	↑	↓	-	390	
Ft	Low forces @	↑	↓	-	30	The tangential force Ft in Conventional milling (**Figure 5.9**), shows an increasing force trend with an increasing feed at a given speed and the force is highest at high feed and low speed.
	High forces @	↓	↑	-	170	
Fr	Low forces @	↑	↓	-	160	**Figure 5.10** shows us that in conventional milling, the radial force Fr is lower at high speed and low feed and highest when both factors speed and feed are at their highest values.
	High forces @	↑	↑	-	265	

5.2 Analysis of HexMC Edge trims

5.1.1 HexMC - Climb (Even) - Edge trim

Table 5-9 gives us the models used to get the ANOVA output from Stat Ease Software for HexMC Climb milling edge trims. Also see Appendix K.

Table 5-9 : HexMC - Climb (Even) - Edge Trim ANOVA

HexMC - Climb (Even) - Edge Trim ANOVA				
Experiment(s) Ignored	**Force**	**Model Used**		
		Process Order	**Selection**	**Alpha Out**
3,6	Fx	Quadratic	Backward	0.1
3,6	Fy	Quadratic	Backward	0.1
3,6	Fz	Quadratic	Backward	0.1
3,6	Ft	Quadratic	Backward	0.1
3	Fr	Quadratic	Backward	0.1

Statistical Matrix :

Table 5-10 : Statistical matrix used For ANOVA of HexMC Climb (Even) - Edge Trim

Run	Factor 1 A:Speed rpm	Factor 2 B : Feed mm/min	Factor 3 C : DOC mm	Response 1 Fx N	Response 2 Fy N	Response 3 Fz N	Response 4 Ft N	Response 5 Fr N
1	6000	635	6.35	133.2376	364.2612	373.23637	70.154	366.63047
2	6000	127	6.35	220.748	350.7327	28.679959	75.548463	380.30959
3	6000	635	2.54	200.4337	105.7998	392.96902	69.497331	400.933151
4	6000	127	2.54	162.3139	260.1835	25.484417	55.1144513	257.617251
5	1000	127	6.35	351.0996	451.1789	25.3152836	86.54677	459.32525
6	1000	635	6.35	454.3612	494.6293	93.10847	183.60054	496.472899
7	1000	635	2.54	249.8575	357.024	7.9711415	90.848156	380.52993
8	1000	127	2.54	387.6653	502.3149	19.3138315	124.37951	499.54867

Formulae from ANOVA :

Table 5-11 : Formulae from ANOVA of HexMC Climb (Even) - Edge Trim

	Force	Formula
HexMC Climb (Even)	Fx	*Fx = 412.893 + -0.0314882 * Speed + -0.175018 * Feed*
	Fy	Fy = 549.862 + -0.0431841 * Speed + -0.305961 * Feed + 7.02858e-005 * Speed * Feed
	Fz	Fz = 42.9718 + -0.0170714 * Speed + -0.170163 * Feed + 0.000141928 * Speed * Feed
	Ft	Ft = 107.322 + -0.0067305 * Speed
	Fr	Fr = 483.793 + -0.0248234 * Speed

3D Surface Plot to show interaction effects :

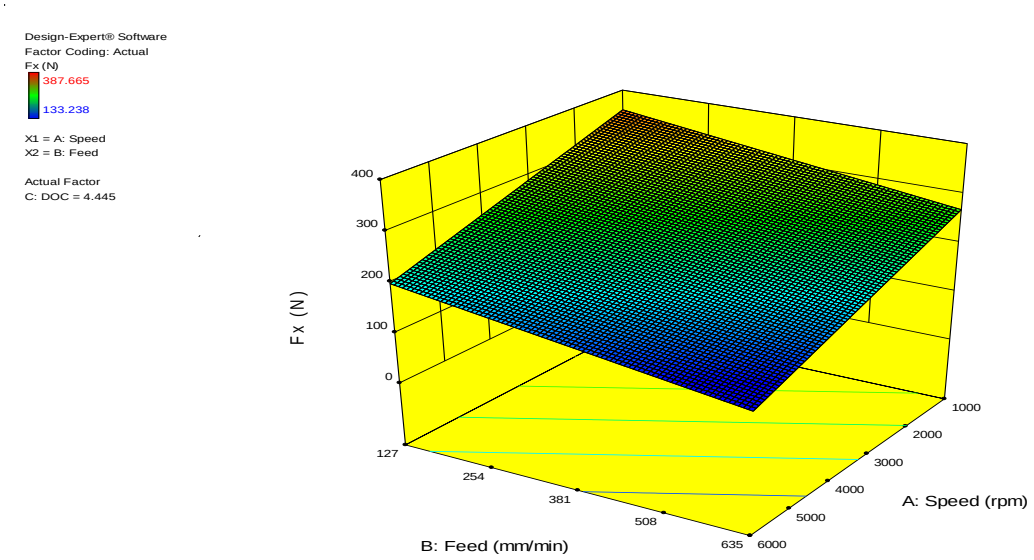

Figure 5.11 : 3D surface Plot - Fx - HexMC - Climb (Even) Edge trim

From figure 5.11, the force Fx for Climb cutting in HexMC shows that it is lowest at high speeds and high feed and highest at low feed and low speed.

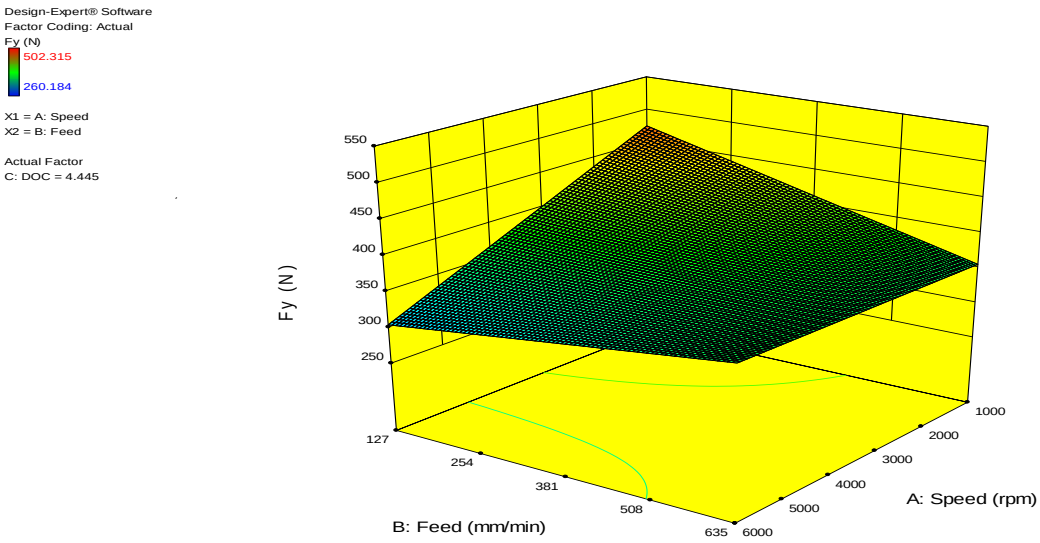

Figure 5.12 : 3D surface Plot - Fy - HexMC - Climb (Even) Edge trim

The force Fy in climb cutting of HexMC is shown in figure 5.12, interacting with the factors speed and feed, and similar for Fx, the forces are highest at low speeds and feeds and lower high speed and low feed.

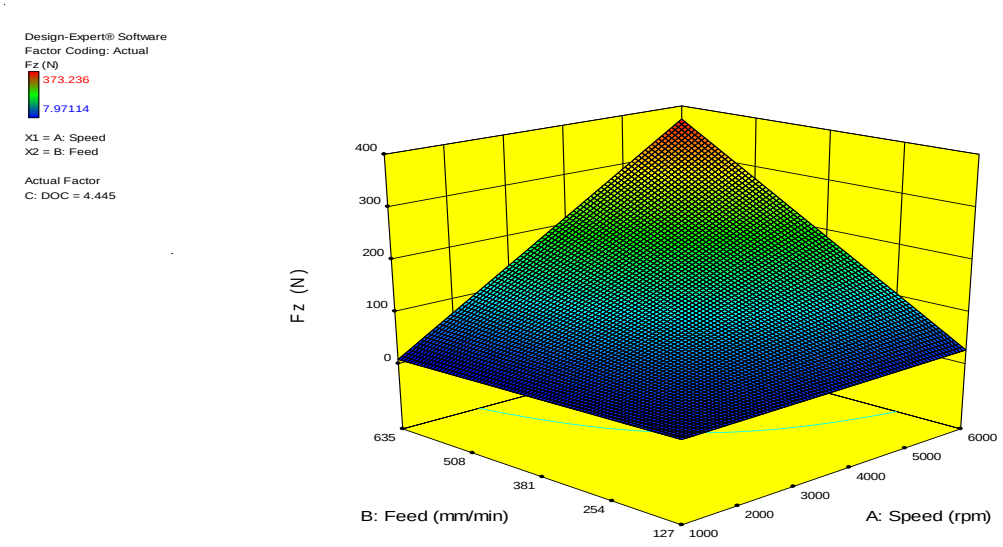

Figure 5.13 : 3D surface Plot - Fz - HexMC - Climb (Even) Edge trim

The force in Z direction Fz, has a drastic increase in its value as speed and feed increase and is lowest at low speed and feed values as shown in figure 5.13.

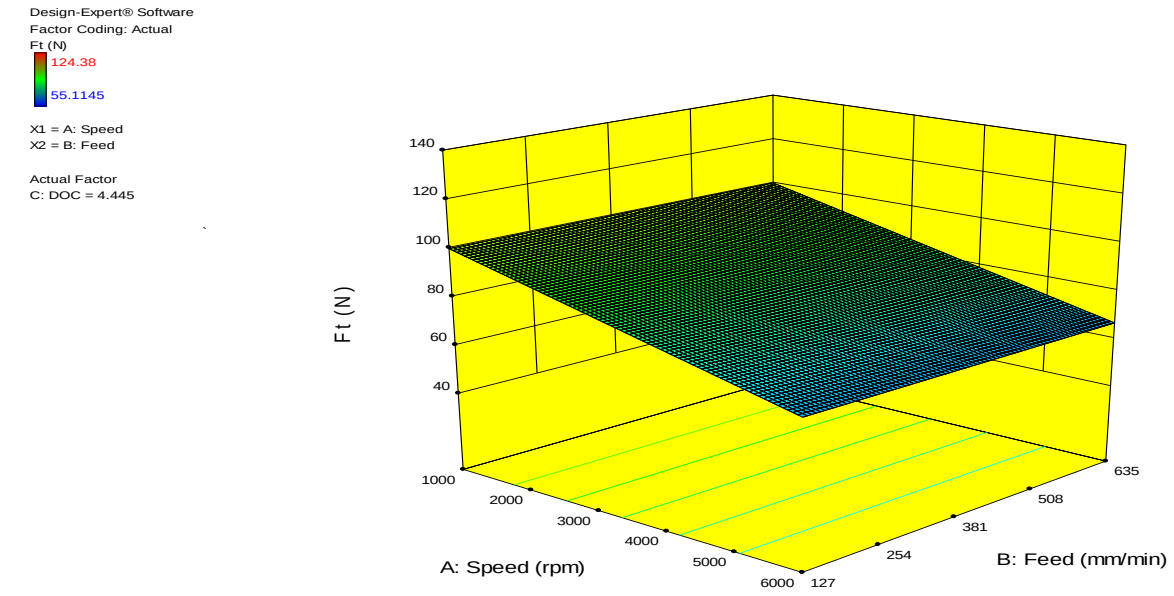

Figure 5.14 : 3D surface Plot - Ft - HexMC - Climb (Even) Edge trim

The tangential force in Climb cut (figure 5.14), Ft is seen to remain constant at any given speed with changing feeds but is higher when the speed is low.

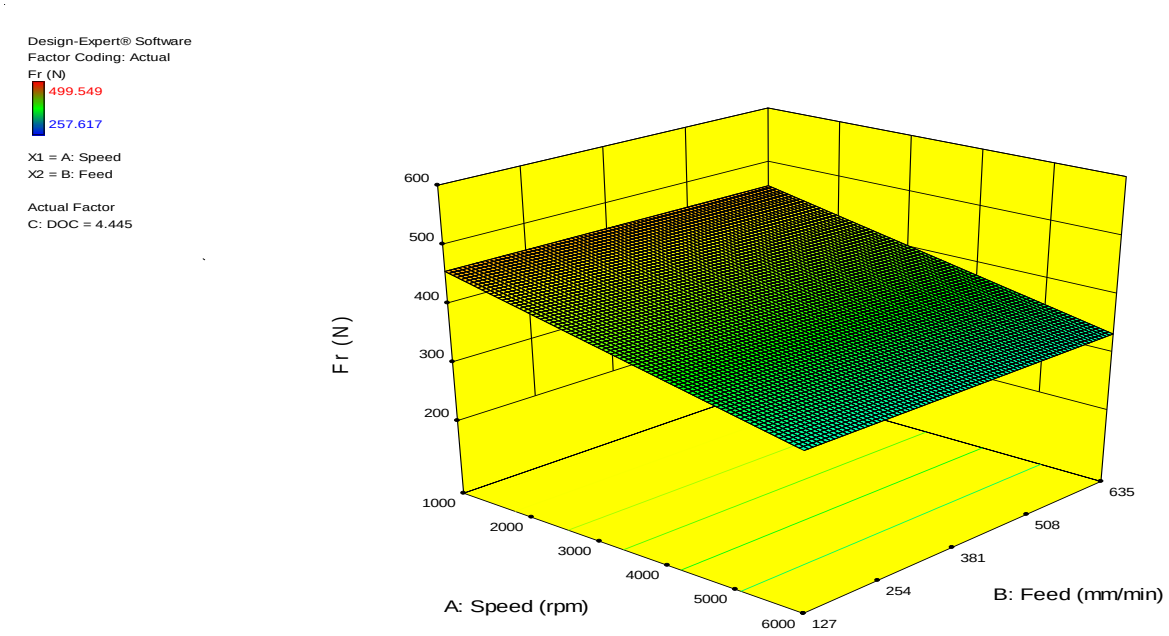

Figure 5.15 : 3D surface Plot - Fr - HexMC - Climb (Even) Edge trim

Force Fr in climb cutting Figure 5.15 follows a similar pattern as Ft in HexMC, where the force is higher at low speeds and feed is appearing to remain constant with varying speed. The magnitude of the highest force in Fr is almost four times higher than Ft's highest force value.

Table 5-12 : Summarization of 3D interactions - HexMC Climb cuts

3D interactions - HexMC Climb cuts						
Force	**Trend**	**Speed**	**Feed**	**DOC**	**Force value (N)**	**Comments**
Fx	Low forces @	↑	↓	-	120	From **figure 5.11**, the force Fx for Climb cutting in HexMC shows that it is lowest at high speeds and high feed and highest at low feed and low speed.
	High forces @	↓	↓	-	350	
Fy	Low forces @	↑	↓	-	300	The force Fy in climb cutting of HexMC is shown in **figure 5.12**, interacting with the factors speed and feed, and similar for Fx, the forces are highest at low speeds and feeds and lower high speed and low feed.
	High forces @	↓	↓	-	475	
Fz	Low forces @	↑	↓	-	10	The force in Z direction Fz, has a drastic increase in its value as speed and feed increase and is lowest at low speed and feed values as shown in **figure 5.13**.
	High forces @	↑	↑	-	380	
Ft	Low forces @	↑	↓	-	60	The tangential force in Climb cut (**figure 5.14**), Ft is seen to remain constant at any given speed with changing feeds but is higher when the speed is low.
	High forces @	↓	**All**	-	100	
Fr	Low forces @	↑	↓	-	260	Force Fr in climb cutting follows a similar pattern as Ft in HexMC, where the force is higher at low speeds and feed is appearing to remain constant with varying speed. The magnitude of the highest force in Fr is almost four times higher than Ft's highest force value.
	High forces @	↓	**All**	-	450	

5.1.2 HexMC - Conventional (Odd) - Edge trim

Table 5-13 gives us the models used to get the ANOVA output from Stat Ease Software for HexMC Conventional milling edge trims. Also see Appendix L.

Table 5-13 : HexMC – Conventional (Odd) - Edge Trim ANOVA

HexMC – Conventional (Odd) - Edge Trim ANOVA				
Experiment(s) Ignored	**Force**	**Model Used**		
		Process Order	**Selection**	**Alpha Out**
3,6	Fx	Quadratic	Backward	0.1
6	Fy	2FI	Manual	- (Terms taken A,B,C,BC)
6	Fz	Cubic	Backward	0.15
6	Ft	Quadratic	Backward	0.1
6	Fr	Cubic	Backward	0.15

Statistical Matrix :

Table 5-14 : Statistical matrix used For ANOVA of HexMC – Conventional (Odd) - Edge

Run	Factor 1 A : Speed rpm	Factor 2 B : Feed mm/min	Factor 3 C : DOC mm	Response 1 Fx N	Response 2 Fy N	Response 3 Fz N	Response 4 Ft N	Response 5 Fr N
1	6000	25	0.25	119.73684	373.11918	392.11682	60.385502	362.50328
2	6000	5	0.25	220.4424	351.31099	30.069604	55.415462	340.35353
3	6000	25	0.1	187.60634	100.31868	435.22236	67.162829	399.590897
4	6000	5	0.1	172.65266	285.55477	26.629158	59.419908	262.775458
5	1000	5	0.25	341.62139	430.39882	15.747067	96.80027	428.78717
6	1000	25	0.25	483.50717	502.8593	99.342005	205.56577	501.794256
7	1000	25	0.1	310.36221	399.993	4.9071033	124.91106	389.1026
8	1000	5	0.1	367.23959	495.02711	22.432769	107.56642	494.15034

Formulae from ANOVA :

Table 5-15 : Formulae from ANOVA of HexMC Conventional (Odd) - Edge Trim

	Force	Formula
HexMC Conventional (Odd)	Fx	*Fx = 408.757 + -0.0337594 * Speed + -0.118975 * Feed*
	Fy	Fy = 598.943 + -0.0392156 * Speed + -0.565146 * Feed + -14.3164 * DOC + 0.113893 * Feed * DOC
	Fz	Fz = 37.0186 + -0.0192009 * Speed + -0.140846 * Feed + 2.29609 * DOC + 0.00016577 * Speed * Feed + -0.0214329 * Feed * DOC
	Ft	Ft = 114.093 + -0.00831414 * Speed + 0.0427015 * Feed + -1.88521 * DOC + -5.03146e-006 * Speed * Feed
	Fr	Fr = 519.134 + -0.0395733 * Speed + -0.202236 * Feed + 5.9783e-005 * Speed * Feed

3D Surface Plot to show interaction effects :

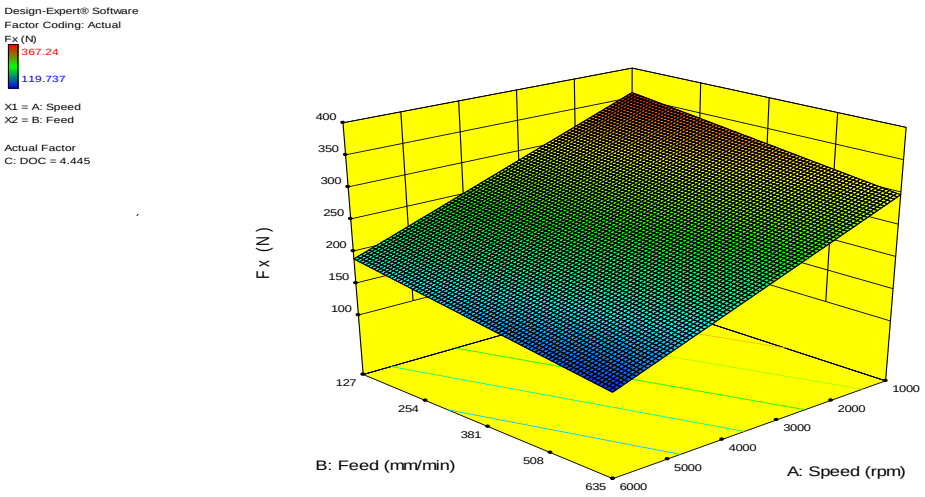

Figure 5.16 : 3D surface Plot - Fx - HexMC - Conventional (Odd) Edge trim

The force in X direction Fx in Conventional milling of HexMC, is highest at low speed and low feed as seen in figure 5.16. The lowest value of force is at high speed and high feed.

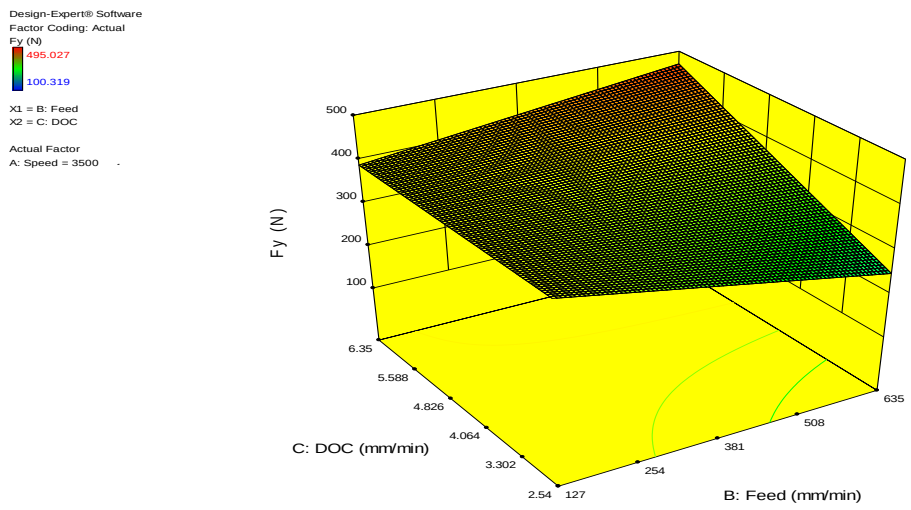

Figure 5.17 : 3D surface Plot - Fy - HexMC - Conventional (Odd) Edge trim

The Fy force is highest at higher DOC and highest feed. Figure 5.17 also shows that the force is lowest at highest feed and lowest DOC.

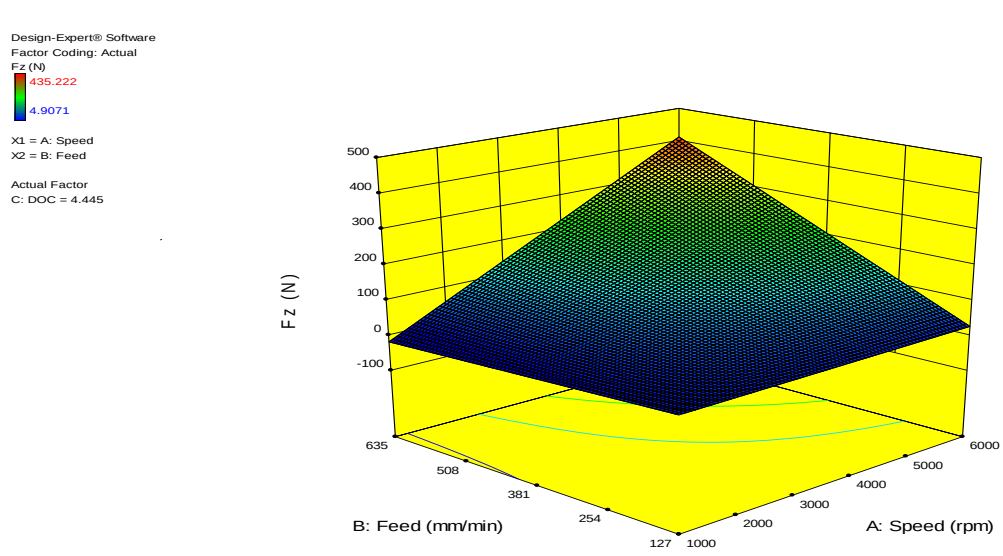

Figure 5.18 : 3D surface Plot - Fz - HexMC - Conventional (Odd) Edge trim

Fz as seen in figure 5.18 is very high at high speed and high feed and lower at low speed and low feed.

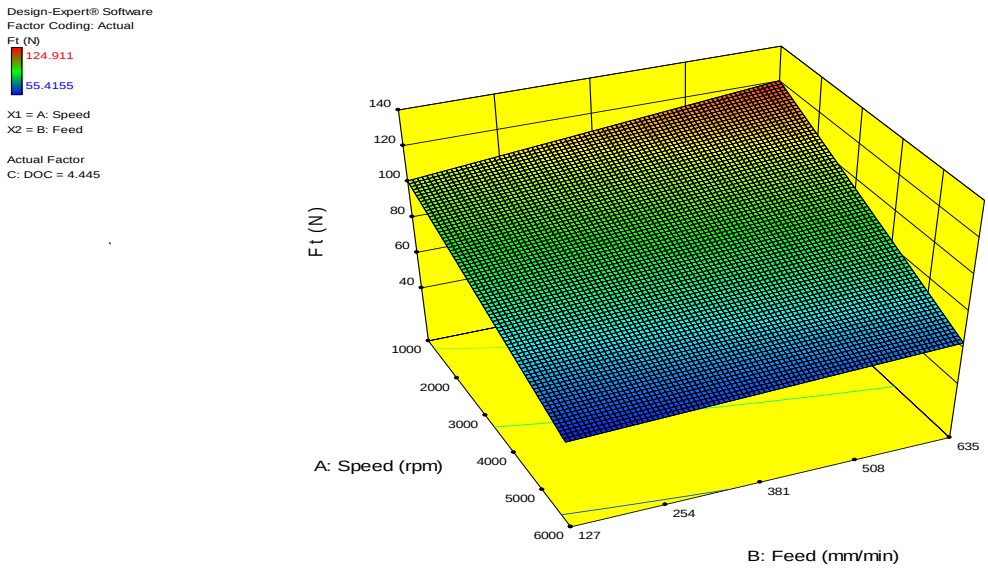

Figure 5.19 : 3D surface Plot - Ft - HexMC - Conventional (Odd) Edge trim

The tangential force Ft in conventional HexMC cut increases with a decrease in the speed and is highest at the highest feed and lowest speed figure 5.19.

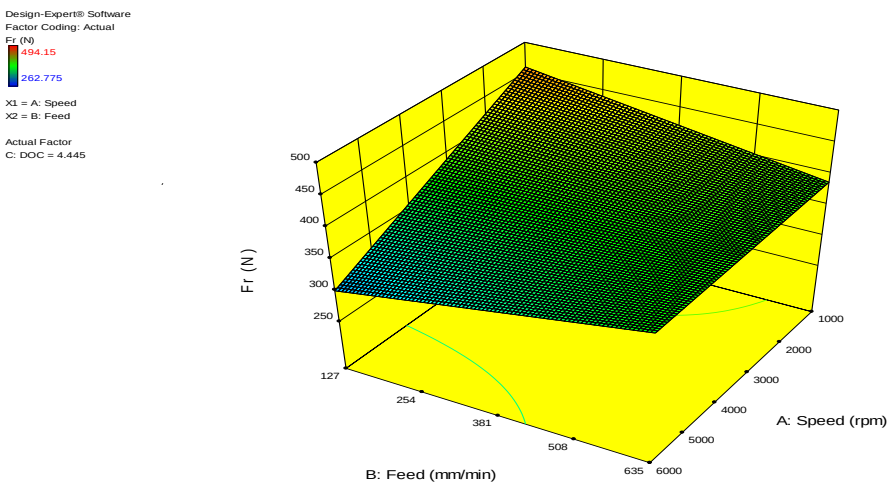

Figure 5.20 : 3D surface Plot - Fr - HexMC - Conventional (Odd) Edge trim

Force Fr is highest at low speed and feed but is lowest at high speed and low feed in conventional cut of HexMC as seen in figure 5.20 .

Summary of 3D graphs of HexMC Conventional cuts

Table 5-16 : Summarization of 3D interactions - HexMC Conventional cuts

3D interactions - HexMC Conventional cuts						
Force	**Trend**	**Speed**	**Feed**	**DOC**	**Force value (N)**	**Comments**
Fx	Low forces @	↑	↑	-	110	The force in X direction Fx in Conventional milling of HexMC, is highest at low speed and low feed as seen in **figure 5.16**. The lowest value of force is at high speed and high feed.
	High forces @	↓	↓	-	360	
Fy	Low forces @	-	↑	↓	210	The Fy force is highest at higher DOC and highest feed. **Figure 5.17** also shows that the force is lowest at highest feed and lowest DOC.
	High forces @	-	↑	↑	480	
Fz	Low forces @	↑	↓	-	10	Fz as seen in **figure 5.18** is very high at high speed and high feed and lower at low speed and low feed.
	High forces @	↑	↑	-	410	
Ft	Low forces @	↑	↑	-	60	The tangential force Ft in conventional HexMC cut increases with a decrease in the speed and is highest at the highest feed and lowest speed.
	High forces @	↓	↑	-	120	
Fr	Low forces @	↑	↓	-	300	Force Fr is highest at low speed and feed but is lowest at high speed and low feed in conventional cut of HexMC as seen in **figure 5.20**
	High forces @	↓	↓	-	460	

5.3 Inferences from Edge trim results of CFRP and HexMC

Comparison of Raw data for CFRP and HexMC :

To understand how the data behaves, it is essential to compare the raw data. This is done with the help of the raw Dynoware graphs which are acquired during the end milling tests. Two different sets of experiments are compared, one at low speed and the other at high speed.

Low Speed :

- *CFRP – exp 6 – 1000 rpm, 635 mmpm, 2.54 mm*
- *HexMC – exp 7 - 1000 rpm, 635 mmpm, 2.54 mm*

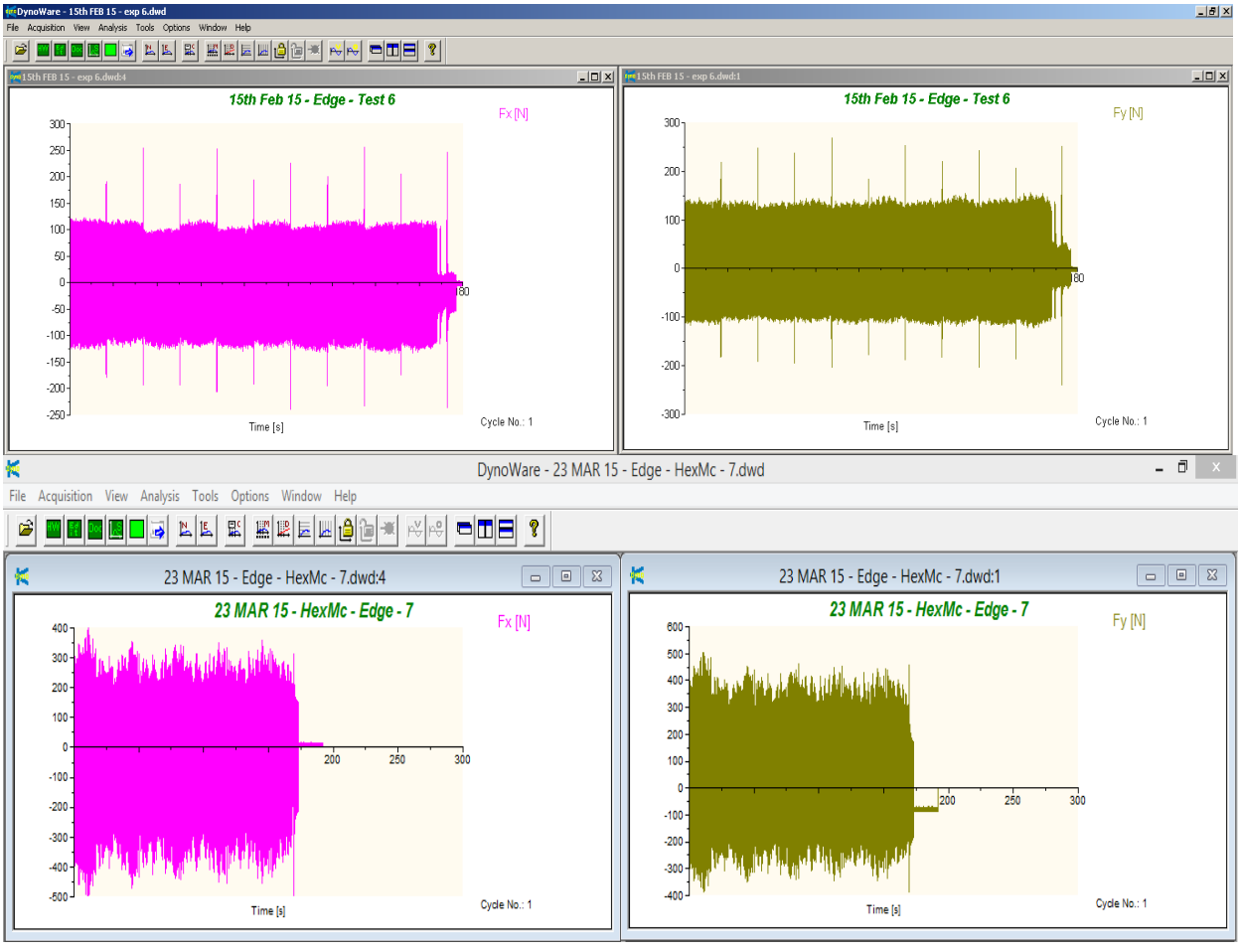

Figure 5.21 : Raw data comparison - CFRP and HexMC at Low speed

High Speed :

- *CFRP – exp 4 – 6000 rpm, 635 mmpm, 2.54 mm*
- *HexMC – exp 3 - 6000 rpm, 635 mmpm, 2.54 mm*

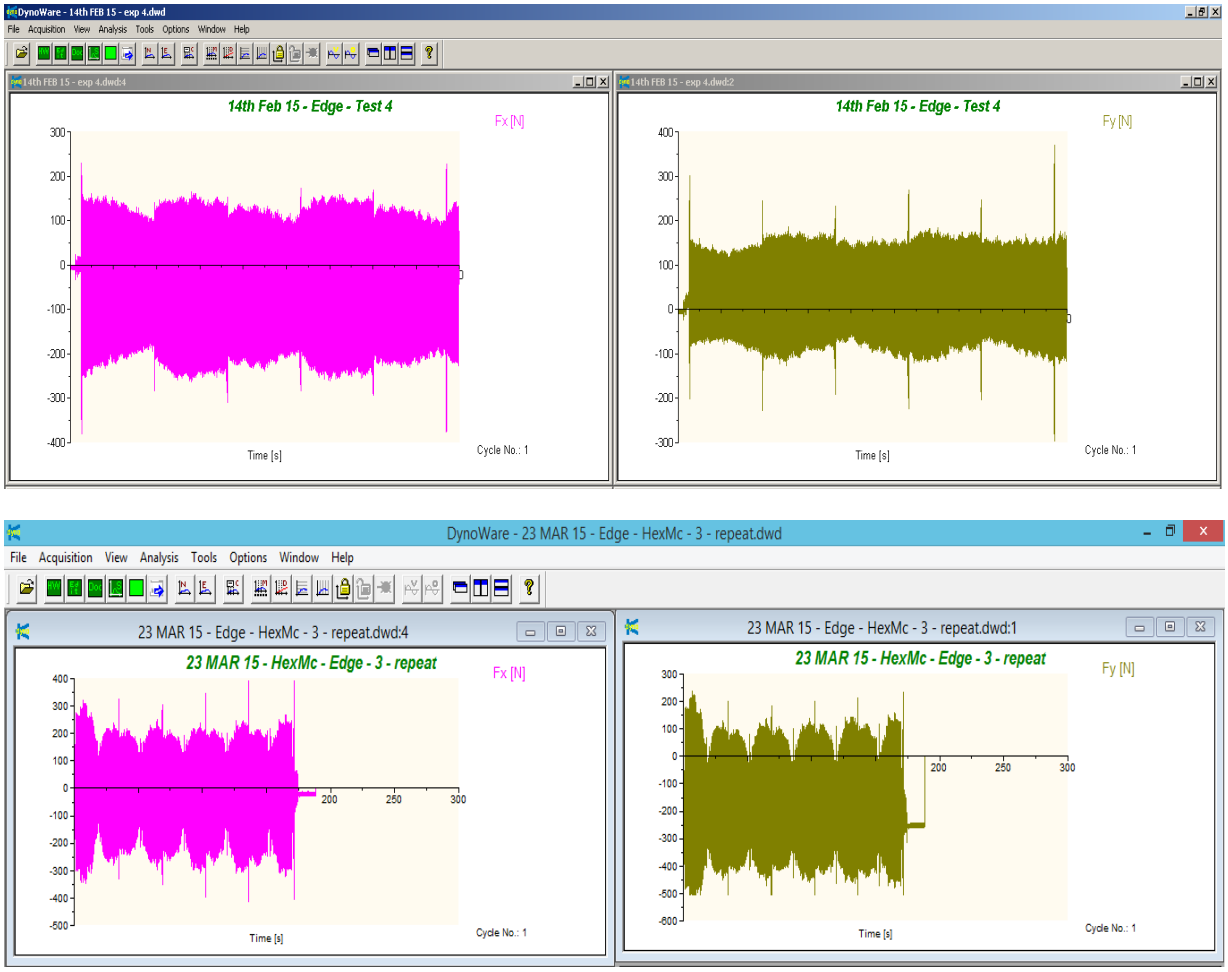

Figure 5.22 : Raw data comparison - CFRP and HexMC at High speed

Comparison of Fx and Channel 6 data for CFRP and HexMC :

CFRP – Exp 6 – Fx and Ch 6 data – Conventional (Odd)

HexMC – Exp 7 – Fx and Ch 6 data – Conventional

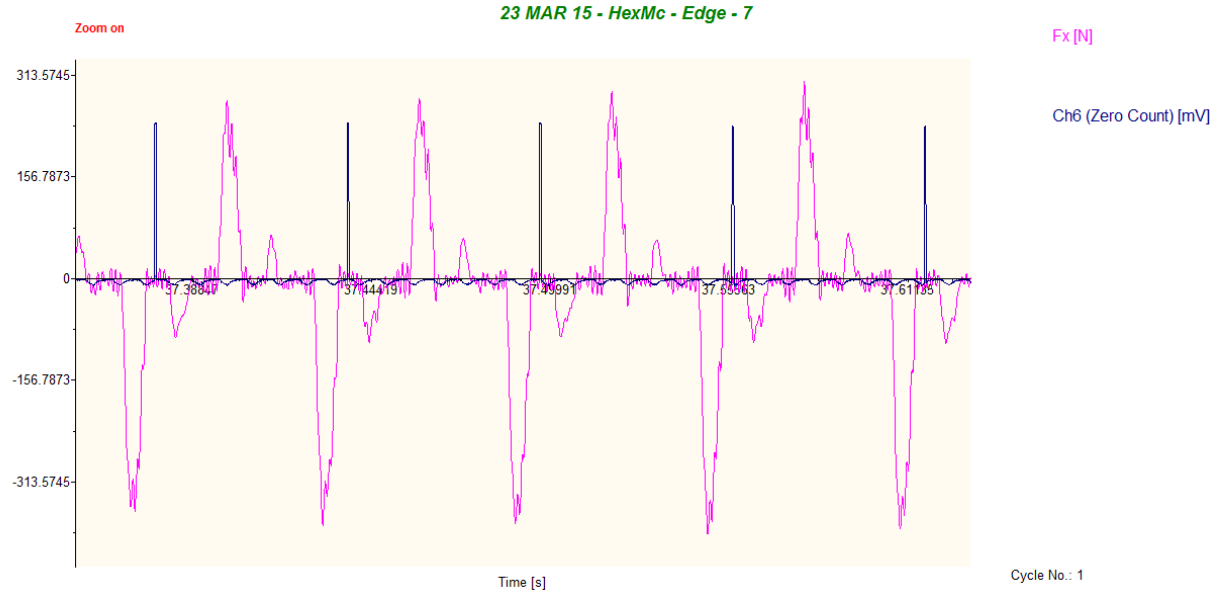

Figure 5.23 : Force and Channel 6 comparison for CFRP and HexMC - Conventional (Odd)

CFRP – Exp 6 – Fx and Ch 6 data – Climb (Even)

HexMC – Exp 6 – Fx and Ch 6 data – Climb (Even)

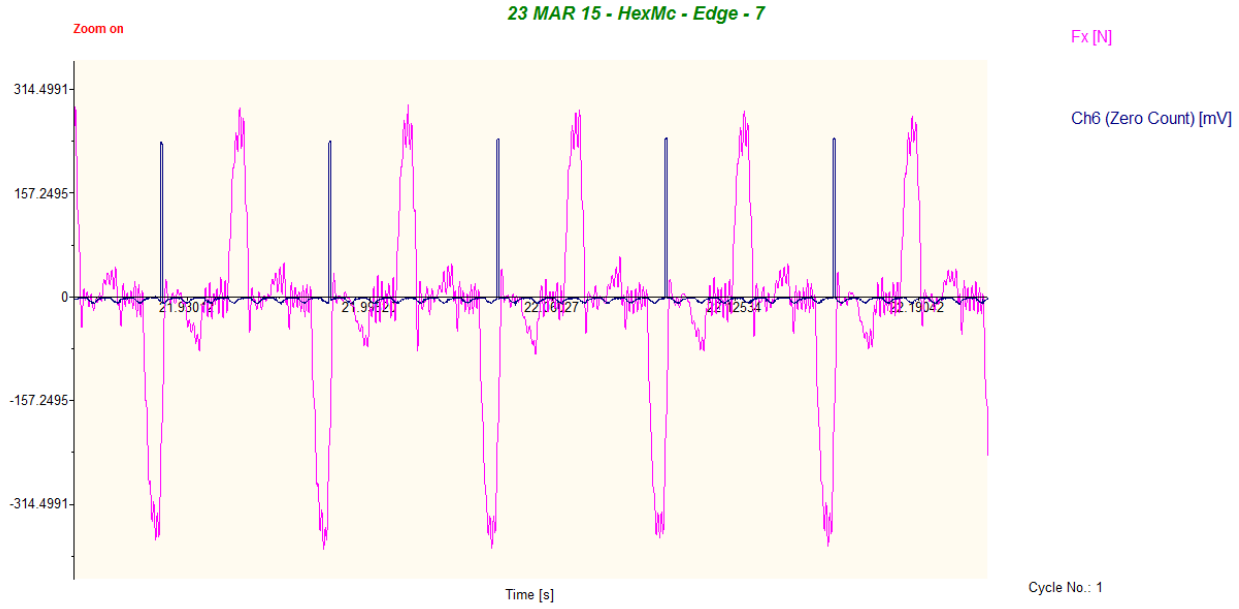

Figure 5.24 : Force and Channel 6 comparison for CFRP and HexMC - Climb (Even)

The tables 5-17 and 5-18 below, show us the comparison of the force behaviours in CFRP and HexMC materials in Climb and Conventional milling.

Table 5-17 : Force behaviour CFRP - Climb vs. Conventional

		CFRP - Climb				CFRP - Conventional			
Force	**Trend**	**Speed**	**Feed**	**DOC**	**Force value (N)**	**Speed**	**Feed**	**DOC**	**Force value (N)**
Fx	Low forces @	↑	↓	-	90	↑	↓	-	50
	High forces @	↓	↓	-	350	↓	↓	-	180
Fy	Low forces @	↑	↓	-	110	↑	↓	-	90
	High forces @	↓	↓	-	390	**Mid**	↑	-	240
Fz	Low forces @	↓	-	**All**	10	↓	↓	-	10
	High forces @	↑	-	**All**	350	↑	↓	-	390
Ft	Low forces @	**Mid**	-	↓	25	↑	↓	-	30
	High forces @	↓	-	↑	135	↓	↑	-	170
Fr	Low forces @	↑	↓	-	80	↑	↓	-	160
	High forces @	↑	↑	-	380	↑	↑	-	265

As it can be seen for Table 5-18, the forces in CFRP for Climb and Conventional, follow almost the same pattern except at a few places. It is seen that overall , the theory that high speeds and low feeds give low forces holds true and is in conjunction with the results seen in this study for CFRP which is a Uni directional material.

Table 5-18 : Force behaviour HexMC - Climb vs. Conventional

		HexMC - Climb				HexMC - Conventional			
Force	**Trend**	**Speed**	**Feed**	**DOC**	**Force value (N)**	**Speed**	**Feed**	**DOC**	**Force Value (N)**
Fx	Low forces @	↑	↓	-	120	↑	↑	-	110
	High forces @	↓	↓	-	350	↓	↓	-	360
Fy	Low forces @	↑	↓	-	300	-	↑	↓	210
	High forces @	↓	↓	-	475	-	↑	↑	480
Fz	Low forces @	↑	↓	-	10	↑	↓	-	10
	High forces @	↑	↑	-	380	↑	↑	-	410
Ft	Low forces @	↑	↓	-	60	↑	↑	-	60
	High forces @	↓	**All**	-	100	↓	↑	-	120
Fr	Low forces @	↑	↓	-	260	↑	↓	-	300
	High forces @	↓	**All**	-	450	↓	↓	-	460

From Table 5-19 which compares the force trends in HexMC material for Climb and Conventional milling cuts, overall it is seen that high speeds and low feeds in Climb cuts and High speeds and high feeds for Conventional cuts are preferable to obtain lower cutting forces except in a few places. This trend could be attributed due to the random fiber orientation of the HexMC material.

It can also be seen that the force values in Climb and Conventional for HexMC are very close and differ only by a very small percentage.

5.4 Analysis of CFRP - Circular Slot test

The circular slot tests along with the parameters was previously mentioned in Section 4.3. The Figures 4.9 to 4.13 show the trend of the forces with respect to the angle.

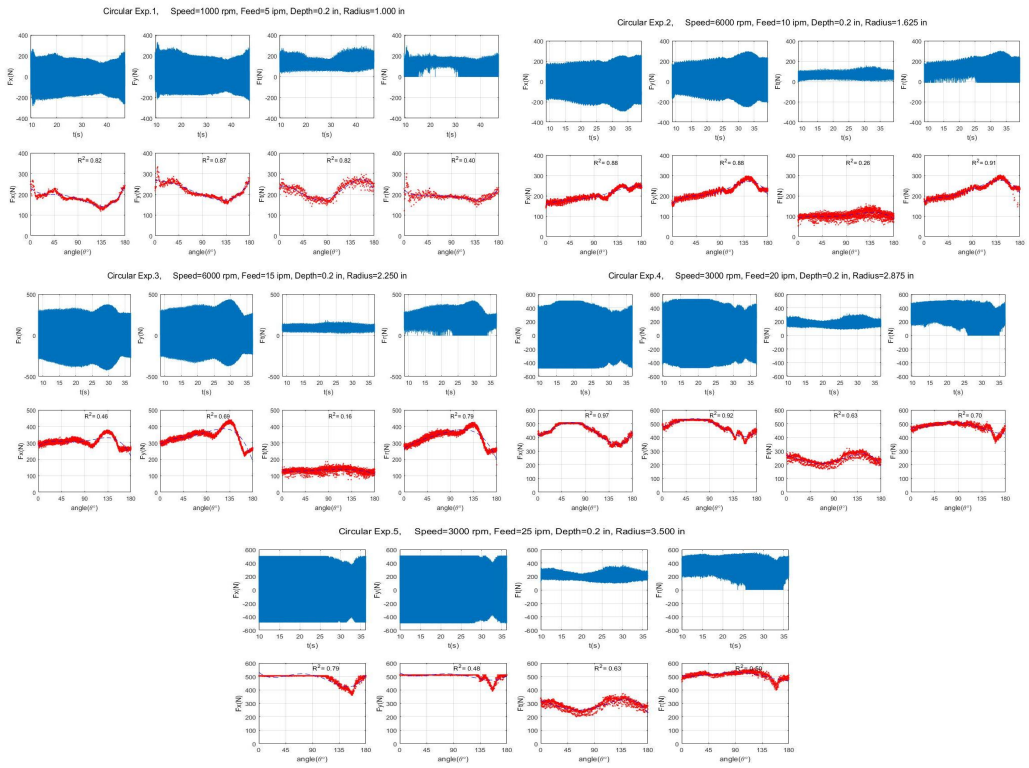

Figure 5.25 : Compilation of Circular slot Force vs. Angle plots

From figure 5.25, we can see that the forces have a dip at the angle 135° most of the time. The delamination is highest at this angle, so the forces drop as the fibers are removed from the laminate which causes this dip in the plots.

5.5 Analysis of CFRP - Octagonal Slot test

The Octagonal slot test results were mentioned in Section 4.4.

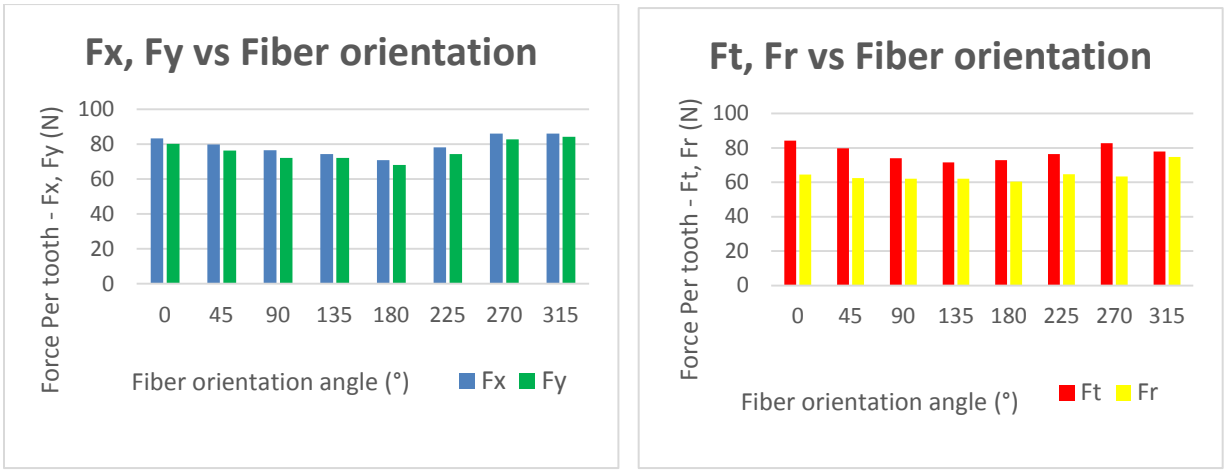

Figure 5.26 : Compilation of Octagonal slot Force/tooth vs. Angle plots

Based on Figure 5.26 above, we can see that the forces are follow a decreasing pattern till 135° - 180° and then slowly increase till the end. This force trend corroborates with the trend observed in circular slot tests that the forces are lower in this range of angles.

5.6 Inferences from Circular and Octagonal CFRP Slot tests

With two different types of tests being carried on CFRP material, one is the Circular slot and the other is an Octagonal slot test, the effect of the cutting angle on the cutting forces was observed. From both these tests it is observed that the forces are lowest at -45° angle which is in agreement with literature **[32, 34].**

5.7 SEM (Scanning Electron Microscope) Images

SEM imaging was done on the HexMC composite from the tests done for surface roughness. From the SEM micrographs (Figure 5.27) , fiber pullouts and edge delaminations were found to be more pronounced in HexMC composite in comparison to UDL materials.

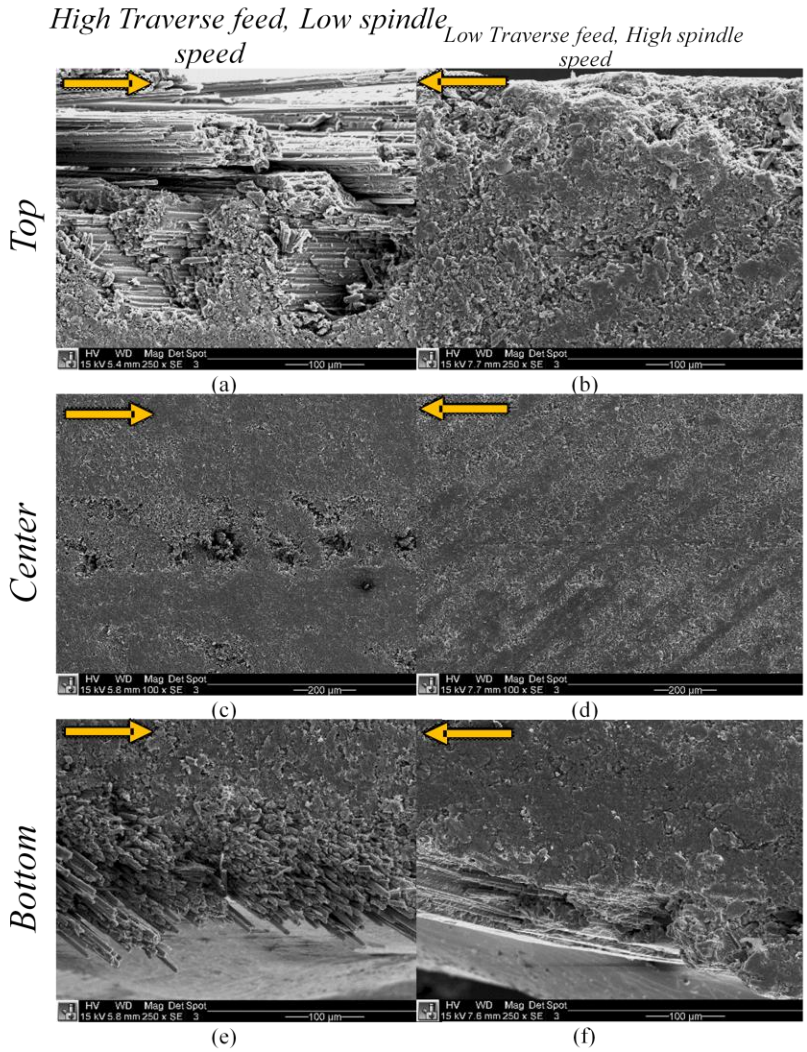

Figure 5.27 : SEM Images - Microstructural Characteristics - Conventional (Odd) - HexMC roughness data

From Figure 5.27**,** it was observed that,

(a),(b) - High degree of type I and type II delamination was observed at the top surface where the uncut fibers from the surface plies protrude.

-300µm bunch pull out → 1/3 rd

(c),(d) - Matrix smearing and thermal degradation

- Visible damage at only 135° fiber plies

(e),(f) - Severe delamination and pullouts at the bottom

Chapter 6 : Conclusions

Based on experimental investigation of i) edge trimming tests on a Uni directional material CFRP and a random fiber composite HexMC materials, ii) Circular slot tests and Octagonal slot tests on CFRP material, the following conclusions were drawn:

- For CFRP climb and conventional cutting, majority of the forces followed the trend where the forces were low at high speeds and low feeds
- For HexMC,
  - High speeds and low feeds were preferable to get lower cutting forces for climb milling cuts
  - Whereas, High speeds and high feeds showed low force values in conventional milling cuts
- In Circular and Orthogonal slot tests on CFRP material, it showed that the damage was highest in -45° direction and due to this fiber pullouts. Unlike the orthogonal cutting, uncut fibers were clearly showed the interaction angle effects and the fibers were displaced from the laminate material.

- *6.1 Future Work :*

The dynamometer (rotating type) used in this investigation was drifting frequently. So this rotating tool dynamometer must be calibrated carefully and the cutting edge alignment is crucial in cutting force notation and compensation of any drifting in the force signals.

Additional experiments must be performed with varying machining parameters in a different range than what was performed to see the cutting force effects and developed model validity . Different materials with various fiber orientations and material type, can be used to assess and corroborate the results. Also, the tools used can be changed to see the effect of their changed geometry on the forces.

References

1. *MF Ashby, Technology of 1990s: Advanced materials and predictive design. Phil. Trans. R. Soc. Lond. A. 1987; Vol. 322, pp. 393-407*
2. *Dandekar, C. R., and Shin, Y. C., 2012, "Modeling of Machining of Composite Materials: A Review," Int J. Mach. Tools Manuf., 57, pp. 102–121*
3. *Teti R (2002) Machining of Composite Materials. Annals of the CIRP 51(2):611– 634*
4. *Dransfield K, Baillie C, Mai Y-W (1994) Improving the Delamination Resistance of CFRP by Stitching – A Review. Composites Science and Technology 50(3):305–317*
5. *Boeing 787 - FROM THE GROUND UP, AERO magazine, article QTR_04, 06*
6. *W. D. (Rik) Brouwer, Natural Fibre Composites in Structural Components: Alternative Applications for Sisal, (http://www.fao.org/docrep/004/y1873e/y1873e0a.htm - accessed on 3/17/2016)*
7. *Natural composite materials , (http://hellomaterialsblog.com/2012/06/11/a-design-boost-for-natural-fibre-composites/ - accessed on 12/2/16)*
8. *Davim JP, Reis P (2005) Damage and accessed on 3/17/2016Dimensional Precision on Milling Carbon Fiber-Reinforced Plastics Using Design Experiments. Journal of Materials Pro-cessing Technology 160(2):160–167*
9. *Hintze W, Hartmann D, Schutte C (2011) Occurrence and Propagation of De-lamination During the Machining of Carbon Fiber Reinforced Plastics (CFRPs) – An Experimental Study. Composites Science and Technology 71(15):1719–1726*
10. *Karpat Y, Polat N (2013) Mechanistic Force Modelling for Milling of Carbon Fiber Reinforced Polymers with Double Helix Tools. Annals of the CIRP 62(1):95–9*
11. *Sreejith PS, Krishnamurthy R, Malhotra SK, Narayanasamy K (2000) Evaluation of PCD Tool Performance During Machining of Carbon/Phenolic Ablative Composites. Journal of Materials Processing Technology 104(1–2):53–5*
12. *Contemporary materials , (http://2012books.lardbucket.org/books/principles-of-general-chemistry-v1.0/s16-09-contemporary-materials.html - accessed on 11/28/2016)*
13. *T. W. Clyne, P. J. Withers, An Introduction to Metal Matrix Composites, Cambridge University Press, Cambridge (1993)*
14. *Polymer matrix composites, (https://www.princeton.edu/~ota/disk2/1988/8801/880106.PDF - accessed on 11/28/2016)*
15. *Callister, Material science and Engineering, 7th Edition*
16. *Wang et al, Polymer matrix composites and technology, Woodhead publishing, (https://www.elsevier.com/__data/assets/pdf_file/0011/87176/Polymer-Matrix-Composites-and-Technology_Intro_Excerpt.pdf- accessed on 11/28/2016)*
17. *Composite material, fabrication methods, Wikipedia. (https://en.wikipedia.org/wiki/Composite_material#Fabrication_methods accessed on 3/19/16)*

18. *Miller, J.L., Investigation of Machinability and Dust Emissions in Edge Trimming of Laminated Carbon Fiber Composites, in Department of Mechanical Engineering. 2014, University of Washington: Seattle*
19. *B.J. Ash, R.W. Siegel, and L.S. Schadler. 2004. Glass-transition temperature behavior of alumina/PMMA nanocomposites. J. Polymer Science Part B: Polymer Physics (42):4371-4383*
20. *B.J. Ash, A. Eitan, and L.S. Schadler. 2004. Polymer nanocomposites with particle and carbon nanotube fillers. In Dekker Encyclopedia of Nanoscience and Nanotechnology, 1st ed., J.A. Schwarz, C.I. Contescu, and K. Putyera, eds. New York: Marcel Dekker, pp. 2917-2930*
21. *Komanduri, R. Machining Fiber Reinforced Plastics, Mechanical Engineering, 115(4), 58-64, 1993.*
22. *Koplev, A., Lystrup, A. & Vorm, T. Cutting Process, Chips and Cutting Forces in Machining CFRP, Composites, 14(4), 371–376, 1983*
23. *Hocheng, H., Puw, H. & Huang, Y. Preliminary Study on Milling of Unidirectional Carbon-Fibre Reinforced Plastics. Composites Mfg, 4(2), 103–10;*
24. *Bhatnagar, N., Ramakrishnan, N., Naik, H. & Komanduri, R. On the Machining of Fiber-Reinforced Plastic (FRP) Composite Laminates. Int. Journal of Machine Tools & Manufacture, 35(5), 701– 716, 1995.*
25. *Arola, D, Ramulu, M. & Wang, D. Chip Formation in Orthogonal Trimming of Unidirectional Graphite/Epoxy Composite, Composites Part A, 27A, 121-133, 1996*
26. *Wang. D, Ramulu, M. & Arola, D. "Orthogonal Cutting Mechanisms of Graphite/Epoxy Composite. Part I: Unidirectional Laminate", International Journal of Machine Tools & Manufacture. Vol. 35, No. 12, 1623-1638, 1995*
27. *Jahangir, S., Ramulu, M. & Koshy, P. Machining of Ceramics and Composites, Marcel Dekker Inc., 1999.*
28. *Wang,D.H., Ramulu, M., ., Arola, D., ., "Orthogonal Cutting Mechanisms of Graphite/Epoxy Laminate. Part 2: Multidirectional Laminate.", International Journal of Machine Tools and Manufacturing, Vol. 35, No. 12, (1995), pp. 1639-1648.*
29. *S .Gordon, M. T .Hillery, A review of the cutting composite materials, Proceedings of the Institution of Mechanical Engineers Part L : Journal of Materials: Design and Applications, 217(2003)35–45*
30. *E. Uhlmann, F. Sammler, S. Richarz, F. Heitmuller, M. Bilz, Machining of Carbon Fibre Reinforced Plastics, Procedia CIRP 24,19 – 24, 2014, New Production Technologies in Aerospace Industry - 5th Machining Innovations Conference (MIC 2014)*
31. *Mohamed Slamani , Sébastien Gauthier, Jean-François Chatelain, A study of the combined effects of machining parameters on cutting force components during high speed robotic trimming of CFRPs, Measurement 59, 268–283, 2015*
32. *J.Y. Sheikh-Ahmad, Machining of Polymer Composites,Springer,2009*
33. *S. Abrate, D. Walton, Machining of composite materials, Part1 : traditional- methods, Composites Manufacturing 3(2)(1992)75–83*

34. *Yigit Karpat , Onur Bahtiyar , Burak Deger , Mechanistic force modeling for milling of unidirectional carbon fiber reinforced polymer laminates International Journal of Machine Tools and Manufacture 56, 2012, 79 -93*
35. *Yigit Karpat, Onur Bahtiyar, Burak Deger, Milling Force Modelling of Multidirectional Carbon Fiber Reinforced Polymer Laminates, Procedia CIRP 1, 460 – 465, 2012, 5th CIRP Conference on High Performance Cutting 2012*
36. *Creese, Robert C., "Introduction to Manufacturing Processes and Materials.", Marcel Dekker, Inc., New York, 1999*
37. *M. Ucar, Y. Wang, End-milling machinability of a carbon fiber reinforced laminated composite, Journal of advanced materials, Volume 37, No. 4, pg 46-52, October 2005*
38. *Oliver Pecat, Rüdiger Rentsch, Ekkard Brinksmeier, "Influence of milling process parameters on the surface integrity of CFRP", Procedia CIRP 1, 466 – 470, 2012*
39. *Luca Sorrentino and Sandro Turchetta, "Cutting Forces in Milling of Carbon Fibre Reinforced Plastics", International Journal of Manufacturing Engineering, Volume 2014, Nov 2014, Article ID 439634*
40. *L. Sorrentino & S. Turchetta, Milling of Carbon fiber reinforced plastics : Analysis of cutting forces and surface roughness, 18th International conference on composite materials, 2015*
41. *Wu Baohai , Yan Xue , Luo Ming , Gao Ge , Cutting force prediction for circular end milling process, Chinese Journal of Aeronautics, 26(4): 1057–1063, April 2013*
42. *Devi Kalla, Jamal Sheikh-Ahmad, Janet Twomey, " Prediction of cutting forces in helical end milling fiber reinforced polymers", International Journal of Machine Tools & Manufacture 50, 882–891, 2010*
43. *V. Madhavan, G. Lipczynski, B. Lane, E. Whitenton , Fiber orientation angle effects in machining of unidirectional CFRP laminated composites, Journal of Manufacturing Processes 20, 431–442, 2015*
44. *Qinglong An , Weiwei Ming, Xiaojiang Cai and Ming Chen, Effects of tool parameters on cutting force in orthogonal machining of T700/LT03A unidirectional carbon fiber reinforced polymer laminates, Journal of Reinforced Plastics and Composites Vol. 34(7) 591–602, 2015*
45. *Anirudh Krishnan Iyer, Characterization of Composite Dust generated during Milling of Uni-Directional and Random fiber composites, Department of Mechanical Engineering, University of Washington, Seattle*
46. *Kistler, Instruction Manual: Rotating Cutting Force Dynamometer 9123C, 9123C_002-042e09.10, Kistler Instrumente, AG, Switzerland*
47. *Picture acquired from - Kalpakjian, S., Manufacturing Processes for Engineering Materials. Addison Wesley Longman, 1997*
48. *Cutting force measurement, Kistler brochure*
49. *Article " Future is hot for ceramic matrix composites in engines", SAE International, 2009 (http://articles.sae.org/6112/) , accessed on 11/28/16*

50. *Figure procured from - (http://teknikmesinmanufaktur.blogspot.com/2015/01/macam-pengefraisan.html - accessed on 11/28/2016)*
51. *Figure procured from - (http://www.nestools.com/technical-information-milling.php - accessed on 11/28/2016)*
52. *Figure procured from - (http://www.harveytool.com/secure/Content/Documents/Tech_ConventionalMillingVsClimbMilling.pdf - accessed on 11/28/2016)*
53. *R.P.H. Faassen , N. van de Wouw , J.A.J. Oosterling , H. Nijmeijer, "Prediction of regenerative chatter by modelling and analysis of high-speed milling", International Journal of Machine Tools & Manufacture, Vol 43, pg 1437-1446, 2003*

Appendix - A - CNC Programs

Program 1 : Edge trimming for 25 in/min feed

O12363 (25 in/min edge trim for 3 minutes dust collection time)
T1 H01 G43
G91 (incremental)
M03 S6000 (spindle on CW)
G01 F25. Y0.03 (feed 25 .03 in Y)
G01 F25. X-7.0 (climb cut in X)
G01 F25. Y0.03 (feed into part .03)
G01 F25. X7.0 (Conventional cut in X)
G01 F25. Y0.03 (feed 25 .03 in Y)
G01 F25. X-7.0 (climb cut in X)
G01 F25. Y0.03 (feed into part .03)
G01 F25. X7.0 (Conventional cut in X)
G01 F25. Y0.03 (feed 25 .03 in Y)
G01 F25. X-7.0 (climb cut in X)
G01 F25. Y0.03 (feed 25 .03 in Y)
G01 F25. X7.0 (climb cut in X)
G01 F25. Y0.03 (feed into part .03)
G01 F25. X-7.0 (Conventional cut in X)
G01 F25. Y0.03 (feed 25 .03 in Y)
G01 F25. X7.0 (climb cut in X)
G01 F25. Y0.03 (feed into part .03)
G01 F25. X-7.0 (Conventional cut in X)
G01 F25. Y0.03 (feed 25 .03 in Y)
G01 F25. X7.0 (climb cut in X)
G01 F25. Y0.03 (feed into part .03)
G01 F25. X7.0 (Conventional cut in X)
M30 (end of program)

Program 2 : Edge trimming for 15 in/min feed

```
O12365 (15 in/min edge trim for 3 minutes dust collection time)
T1 H01 G43
G91 (incremental)
M03 S6000 (spindle on CW)
G01 F15. Y0.03 (feed 25 .03 in Y)
G01 F15. X-7.0 (climb cut in X)
G01 F15. Y0.03 (feed into part .03)
G01 F15. X7.0 (Conventional cut in X)
G01 F15. Y0.03 (feed 25 .03 in Y)
G01 F15. X-7.0 (climb cut in X)
G01 F15. Y0.03 (feed into part .03)
G01 F15. X7.0 (Conventional cut in X)
G01 F15. Y0.03 (feed 25 .03 in Y)
G01 F15. X-7.0 (climb cut in X)
G01 F15. Y0.03 (feed 25 .03 in Y)
G01 F15. X7.0 (climb cut in X)
M30 (end of program)
```

Program 3 : Edge trimming for 5 in/min feed

```
O12367 (5 in/min edge trim for 3 minutes dust collection time)
T1 H01 G43
G91 (incremental)
M03 S6000 (spindle on CW)
G01 F5. Y0.03 (feed 25 .03 in Y)
G01 F5. X-7.0 (climb cut in X)
G01 F5. Y0.03 (feed into part .03)
G01 F5. X7.0 (Conventional cut in X)
G01 F5. Y0.03 (feed 25 .03 in Y)
G01 F5. X-7.0 (climb cut in X)
G01 F5. X7.0 (No CUT RETURN PASS in X)
M30 (end of program)
```

Program 4 : Octagonal cut

```
O12369 (OCTAGON CUT)
T1 H01 G43
G91 (incremental)
M03 S1000 (spindle on CW)
G01 F1. Y0.4 (lead into the part)
G01 F1. X-1.414 Y1.414 (point a to b)
G01 F1. Y1.5 (point b to c)
G01 F1. X1.414 Y1.414 (POINT C TO D)
G01 F1. X2.0 (POINT D TO E)
G01 F1. X1.414 Y-1.414 (POINT E TO F)
G01 F1. Y-1.5 (POINT F TO G)
G01 F1. X-1.414 Y-1.414 (POINT G TO H)
G01 F1. X-2.0 (POINT H TO A)
M30 (end of program)
```

Program 5 : Circular cut

```
012355 (HALF SLOT MILLING ALL CUTS)  ;
T1 H01 G43 ;
G91 ;
;
;
M03 S1000 ;
G01 F25. X-1. ;
G01 F5. Y1. ;
G02 X2. Y0. I1. J0. F5. ;
G01 F5. Y-1. ;
G01 F25. X-1. ;
;
;
M03 S6000 ;
G01 F25. X-1.625 ;
G01 F10. Y1. ;
G02 X3.25 Y0.  I1.625 J0.  F10. ;
```

```
G01 F10. Y-1. ;
G01 F25. X-1.625 ;
;
;
;
M03 S6000 ;
G01 F25. X-2.25 ;
G01 F15. Y1. ;
G02 X4.5 Y0. I2.25 J0. F15. ;
G01 F15. Y-1. ;
G01 F25. X-2.25 ;
;
;
;
M03 S3000 ;
G01 F25. X-2.875 ;
G01 F20. Y1. ;
G02 X5.75  Y0.  I2.875  J0. F20.  ;
G01 F20. Y-1. ;
G01 F25. X-2.875 ;
;
;
;
M03 S3000 ;
G01 F25.  X-3.5;
G01 F25.  Y1. ;
G02 X7.  Y0.  I3.5  J0.  F25. ;
G01 F25.  Y-1. ;
G01 F25.  X-3.5 ;
M30 ;
```

Program 6 : HexMC cut for Roughness and SEM

```
012375;
T1 H01 G43 ;
G91  (incremental) ;
( ?) ;
M03 S6000 (spindle CW) ;
G01 F35.4   Y-0.64 ;
G01 F35.4   Z-0.8 ;
G01 F35.4   X1.6   Y0.64 ;
G01 F35.4   Z0.8 ;
( ?) ;
G01 F23.6   Z-0.8 ;
(G01 F23.6   X1-0.6?)  ;
G00 O00001 F23.6 Z0.8 ;
( ?) ;

G01 F11.8   Z-0.8 ;
 (G01 F11.8   X1- .6?)  ;
G00 O00001 F11.8  Z0.8 ;
( ?) ;
M05 (Spindle Stop) ;
M03 S3000 (SPINDLE CW) ;
G01 F35.4 Z-0.8 ;
G01 F35.4 X-1.6 ;
G00 O00001 F35.4 Z0.8 ;
( ?) ;
G01 F23.6 Z-0.8 ;
G01 F23.6 X-2.5 ;
G01 F35.4 Z0.8 ;
( ?) ;
G01 F23.6 Z-0.8 ;
(G01 F23.6 X1-0.6?) ;
G00 O00001 F23.6 Z0.8 ;
( ?) ;
G01 F11.8 Z-0.8 ;
(G01 F11.8 X1- .6?) ;
```

```
G00 O00001 F11.8 Z0.8 ;
( ?) ;
M05 (Spindle stop) ;
M03 S3000 (SPINDLE CW) ;
G01 F35.4 Z-0.8 ;
G01 F35.4 X-1.6 ;
G00 O00001 F35.4 Z0.8 ;
( ?) ;
G01 F23.6 Z-0.8 ;
G01 F23.6 X-2.5 ;
G00 O00001 F23.6 Z0.8 ;
( ?) ;
M05 ;
M30 ( PROGRAM END) ;
```

Appendix - B - Matlab codes to calculate Average of Maximum Force values

Fx - End milling cutting CFRP :

```
clear all;
close all;
clc;

%loading the data file
%addpath('U:\Research\Rishi - matlab codes');
no=2; %cut number as in 3 is for odd and 2 is for even

for i=1:24 %Experiment number
i %Displaying experiment number
clear o p t Fy ch6 pks ch6_1 locs pks1 locs1 pks2 locs2 pks3 locs3 i1 i2 ii1 ii2 zeroshift txmax Fxmax Fxmax1
Fmax
name=sprintf('e%d',i); %creating the name of the data file to be fetched
load(name,'-mat'); %fetching the data file ".mat files"

t=eval(sprintf('e%d(:,1)',i)); %time
Fx=eval(sprintf('e%d(:,2)',i));%Fx data
ch6=eval(sprintf('e%d(:,7)',i));%channel 6 data



% hold all;
% plot(t,Fx); %Plotting time and Fx
% plot(t,ch6,'r');figure();%Plotting time and channel 6
% grid on



%Specifying data
dat=xlsread('doe','A3:D26'); %reading the doe file
for k=1:size(dat,1)
if dat(k,1)==i
   m=k; %m is the corresponding row number
end
end

res=1.25e-4; %time between two data points
rpm= dat(m,2);
feed= dat(m,3);
gap=(60/rpm); %time gap for each cutter rotation in seconds
loc=7; %length of cut in inches



% Finding the peaks in ch6 for zeroshift
ch6_1 = ch6(1:2/res);
[pks,locs]=findpeaks(ch6_1,'MinPeakDistance',gap/res-10,'MinPeakHeight',100);
```

```
% hold all;
% plot(t(1:2/res),ch6_1,'r');
% plot(t(locs), ch6_1(locs), 'ob');
% figure();


%Zero Shift
i1=1; %starting index of initial zero shift data
i2=locs(1)-gap/res; %end index of initial zero shift data
width=floor( (i2-i1)/(gap/res) );%number of cutter rotations in zero shift data
i3= i1 + width*(gap/res);
zeroshift=mean(Fx(i1:i3));

if i2<gap/res   %this is different for other variables
   i2=1;
   zeroshift=0;
end

if i==5 %signal at i5 is an exception
   zeroshift=mean(Fx(i1:i1+gap/res));
end

zshift(i,1)=zeroshift; %saving the zeroshift values for each experiment number
Fx=Fx-zshift(i,1); %shifting data


% Selecting the cut to be analyzed
cut_gap=60*loc/feed; % Time range for conventional/climb
number=no;
% [pks1,locs1]=findpeaks(Fx,'MinPeakDistance',cut_gap/res);


%Exceptions
if i==1
   clear locs1
   locs1=floor([1.5449/res;18.3941;35.2441;52.1526]/res);
elseif i==2
    clear locs1
    locs1=floor([2.7147;19.6040;36.4637;53.2926]/res);
elseif i==3
    clear locs1
    locs1=floor([0.1904;16.9057;33.9296;50.7453]/res);
elseif i==4
    clear locs1
    locs1=floor([2.6860;19.5651;36.4053;53.3038]/res);
elseif i==5
   clear locs1
   locs1=[3458;138665;274083;405971;544275;679029;814784;948270;1084817;1218462;1347004;1400680];
elseif i==6
    clear locs1
    locs1=floor([0.1053;16.7636;33.6694;50.4913]/res);
elseif i==7
    clear locs1
    locs1=floor([0.0307;16.8235;33.6592;50.5484]/res);
```

```
elseif i==8
    clear locs1
    locs1=floor([0.0889;16.7952;33.7600;50.5882]/res);
elseif i==9
    clear locs1
    locs1=floor([1.3251;29.3896;57.5434;85.6722]/res);
elseif i==10
    clear locs1
    locs1=floor([1.3331;29.4365;57.5217;85.6599]/res);
elseif i==11
    clear locs1
    locs1=floor([1.2929;29.3416;57.4533;85.5897]/res);
elseif i==12
    clear locs1
    locs1=floor([4.3952;28.3551;56.5543;84.6536]/res);
elseif i==13
    clear locs1
    locs1=floor([0.2673;28.2436;56.3902;84.4621]/res);
elseif i==14
    clear locs1
    locs1=floor([.4692;28.5049;56.5897;84.7432]/res);
elseif i==15
    clear locs1
    locs1=floor([0.3298;28.1000;56.1739;84.1380]/res);
elseif i==16
    clear locs1
    locs1=floor([0.0588;28.2178;56.2039;84.4105]/res);
elseif i==17
    clear locs1
    locs1=floor([1.2894;85.4449;170.1539;254.0603]/res);
elseif i==18
    clear locs1
    locs1=floor([0.2563;84.4302;168.8952;253.0856]/res);
elseif i==19
   clear locs1
   locs1=[2282;675483;1351973;2028192;2253409];
elseif i==20
    clear locs1
    locs1=floor([0.3000;84.4066;168.3448;252.8018]/res);
elseif i==21
    clear locs1
    locs1=floor([0.3478;84.4420;168.6854;253.0972]/res);
elseif i==22
   clear locs1
   locs1=[11280;687626;1360950;2036408;2263023];
elseif i==23
   clear locs1
   locs1=[2282;675483;1351973;2028192;2253409];
elseif i==24
   clear locs1
   locs1=[2181;675157;1353993;2026011];
end
ii1=locs1(number)+1/res; %starting index number of the data to be analyzed
ii2=locs1(number+1)-1/res;%Ending index number of the data to be analyzed

%finding peaks in the selected cut/ data
```

```
[pks2,locs2]=findpeaks(ch6(ii1:ii2),'MinPeakDistance',gap/res-10,'MinPeakHeight',100);

% hold all;
% plot(t(ii1:ii2),ch6(ii1:ii2),'r',t(locs2+ii1-1),ch6(locs2+ii1-1),'ob');figure();

%selecting maximum value in each cutter rotation
locs3=locs2+ii1-1;
for o=2:length(locs3)
   [Fxmax1 p]=max(Fx(locs3(o-1):locs3(o))); %finding maximum force in each cutter rotation
   Fxmax(o-1)=Fxmax1;
   index(o-1)=locs3(o-1)+p;
   txmax(o-1)=t(index(o-1));
end
%
% hold all
% grid on
% plot(txmax,Fxmax);
% legend(name); figure();


FXavg(i,1)=mean(Fxmax)
% FXmax(i,1)=Fmax
end

FF(:,1)=FXavg(:,1);
% FF(:,2)=FXmax(:,1);
```

Fy - End milling cutting CFRP :

```
clear all;
close all;
clc;

%loading the data file
% addpath('U:\Research\Rishi - matlab codes');
no=2;
for i=1:24
 i
clear t Fy ch6 pks ch6_1 locs pks1 locs1 pks2 locs2 i1 i2 ii1 ii2 zeroshift tymax Fymax Fymax1 Fmax
name=sprintf('e%d',i);
load(name,'-mat');

t=eval(sprintf('e%d(:,1)',i));
Fy=eval(sprintf('e%d(:,3)',i));
ch6=eval(sprintf('e%d(:,7)',i));
%
% hold all;
% plot(t,Fy);
% plot(t,ch6,'r');figure();
% grid on


%Specifying data
dat=xlsread('doe','A3:D26');
for k=1:size(dat,1)
if dat(k,1)==i
   m=k;
end
end
res=1.25e-4;
rpm= dat(m,2);
feed= dat(m,3);
gap=(60/rpm); %time gap for each cutter rotation
loc=7; %length of cut in inches

% Finding the peaks in ch6
ch6_1 = ch6(1:2/res);
[pks,locs]=findpeaks(ch6_1,'MinPeakDistance',gap/res-10,'MinPeakHeight',100);
% hold all;
% plot(t(1:2/res),ch6_1,'r');
% plot(t(locs), ch6_1(locs), 'ob');
% figure();



%Zero Shift
i1=1; %starting index of initial zero shift data
i2=locs(1)-gap/res; %end index of initial zero shift data
width=floor( (i2-i1)/(gap/res) );%number of cutter rotations in zero shift data
i3= i1 + width*(gap/res);
zeroshift=mean(Fy(i1:i3));
```

```
if i2<gap/res   %this is different for other variables
    i2=1;
    zeroshift=0;
end
zshift(i,1)=zeroshift;
Fy=Fy-zshift(i,1);

if i==5 %signal at i5 is an exception
    zeroshift=mean(Fy(i1:i1+gap/res));
end

% Selecting the cut to be analyzed
cut_gap=60*loc/feed; %time range for conventional/climb
number=no;
% [pks1,locs1]=findpeaks(Fy,'MinPeakDistance',cut_gap/res);


%Exceptions
if i==1
    clear locs1
    locs1=floor([1.5449/res;18.3941;35.2441;52.1526]/res);
elseif i==2
     clear locs1
     locs1=floor([2.7147;19.6040;36.4637;53.2926]/res);
elseif i==3
     clear locs1
     locs1=floor([0.1904;16.9057;33.9296;50.7453]/res);
elseif i==4
     clear locs1
     locs1=floor([2.6860;19.5651;36.4053;53.3038]/res);
elseif i==5
    clear locs1
    locs1=[3458;138665;274083;405971;544275;679029;814784;948270;1084817;1218462;1347004;1400680];
elseif i==6
     clear locs1
     locs1=floor([0.1053;16.7636;33.6694;50.4913]/res);
elseif i==7
     clear locs1
     locs1=floor([0.0307;16.8235;33.6592;50.5484]/res);
elseif i==8
     clear locs1
     locs1=floor([0.0889;16.7952;33.7600;50.5882]/res);
elseif i==9
     clear locs1
     locs1=floor([1.3251;29.3896;57.5434;85.6722]/res);
elseif i==10
     clear locs1
     locs1=floor([1.3331;29.4365;57.5217;85.6599]/res);
elseif i==11
     clear locs1
     locs1=floor([1.2929;29.3416;57.4533;85.5897]/res);
elseif i==12
     clear locs1
```

```
    locs1=floor([4.3952;28.3551;56.5543;84.6536]/res);
elseif i==13
    clear locs1
    locs1=floor([0.2673;28.2436;56.3902;84.4621]/res);
elseif i==14
    clear locs1
    locs1=floor([.4692;28.5049;56.5897;84.7432]/res);
elseif i==15
    clear locs1
    locs1=floor([0.3298;28.1000;56.1739;84.1380]/res);
elseif i==16
    clear locs1
    locs1=floor([0.0588;28.2178;56.2039;84.4105]/res);
elseif i==17
    clear locs1
    locs1=floor([1.2894;85.4449;170.1539;254.0603]/res);
elseif i==18
    clear locs1
    locs1=floor([0.2563;84.4302;168.8952;253.0856]/res);
elseif i==19
   clear locs1
   locs1=[2282;675483;1351973;2028192;2253409];
elseif i==20
    clear locs1
    locs1=floor([0.3000;84.4066;168.3448;252.8018]/res);
elseif i==21
    clear locs1
    locs1=floor([0.3478;84.4420;168.6854;253.0972]/res);
elseif i==22
   clear locs1
   locs1=[11280;687626;1360950;2036408;2263023];
elseif i==23
   clear locs1
   locs1=[2282;675483;1351973;2028192;2253409];
elseif i==24
   clear locs1
   locs1=[2181;675157;1353993;2026011];
end



ii1=locs1(number) + 1/res;
ii2=locs1(number+1) - 1/res;

[pks2,locs2]=findpeaks(ch6(ii1:ii2),'MinPeakDistance',gap/res-10,'MinPeakHeight',100);
% plot(t(ii1:ii2),ch6(ii1:ii2),'r',t(locs2+ii1-1),ch6(locs2+ii1-1),'ob');figure();

%selecting maximum value in the identified range
Fmax=max(Fy(ii1:ii2));


locs3=locs2+ii1-1;
for o=2:length(locs3)
   [Fymax1 p]=max(Fy(locs3(o-1):locs3(o)));
```

```
    Fymax(o-1)=Fymax1;
    index(o-1)=locs3(o-1)+p;
    tymax(o-1)=t(index(o-1));
end
hold all
grid on
plot(tymax,Fymax);
legend(name);figure();

FYavg(i,1)=mean(Fymax)
% FYmax(i,1)=Fmax
end

FF(:,1)=FYavg(:,1);
% FF(:,2)=FYmax(:,1);
```

Fz - End milling cutting CFRP :

```
clear all;
close all;
clc;

%loading the data file
addpath('U:\Research\Rishi - matlab codes');
no=2;

for i=1:24
i
clear o p t Fz ch6 pks ch6_1 locs pks1 locs1 pks2 locs2 pks3 locs3 i1 i2 ii1 ii2 zeroshift tzmax Fzmax Fzmax1 Fmax
a1 a2
name=sprintf('e%d',i);
load(name,'-mat');

t=eval(sprintf('e%d(:,1)',i));
Fz=eval(sprintf('e%d(:,4)',i));
ch6=eval(sprintf('e%d(:,7)',i));


% hold all;
% plot(t,Fz);
% plot(t,ch6,'r');figure();
% grid on


%Specifying data
dat=xlsread('doe','A3:D26');
for k=1:size(dat,1)
if dat(k,1)==i
   m=k;
end
end
res=1.25e-4;
rpm= dat(m,2);
feed= dat(m,3);
gap=(60/rpm); %time gap for each cutter rotation
loc=7; %length of cut in inches

% Finding the peaks in ch6
ch6_1 = ch6(1:2/res);
[pks,locs]=findpeaks(ch6_1,'MinPeakDistance',gap/res-10,'MinPeakHeight',100);
% hold all;
% plot(t(1:2/res),ch6_1,'r');
% plot(t(locs), ch6_1(locs), 'ob');
% figure();


%Zero Shift
i1=1; %starting index of initial data
i2=locs(1)-10; %end index of initial data
```

```
zeroshift=mean(Fz(i1:i2));
zshift(i,1)=zeroshift;
% plot(t(i1:i2),Fz(i1:i2))
Fz=Fz-zeroshift;
% hold all
% plot(t,Fz,'b')

a1=polyfit(t(10/res:length(Fz)),Fz(10/res:length(Fz)),1);
% y=a1(2) + t*a1(1);
% plot(t,y,'r');
% plot(t,y-t*a1(1),'g');figure();

if i==5 %signal at i5 is an exception
   zeroshift=mean(Fz(i1:i1+gap/res));
end

Fz=Fz-a1(1)*t;
% plot(t,Fz,'r'); figure();


% Selecting the cut to be analyzed
cut_gap=60*loc/feed; % Time range for conventional/climb
number=no;
% [pks1,locs1]=findpeaks(-Fz,'MinPeakDistance',cut_gap/res);


%Exceptions
if i==1
   clear locs1
   locs1=floor([1.5449/res;18.3941;35.2441;52.1526]/res);
elseif i==2
    clear locs1
    locs1=floor([2.7147;19.6040;36.4637;53.2926]/res);
elseif i==3
    clear locs1
    locs1=floor([0.1904;16.9057;33.9296;50.7453]/res);
elseif i==4
    clear locs1
    locs1=floor([2.6860;19.5651;36.4053;53.3038]/res);
elseif i==5
   clear locs1
   locs1=[3458;138665;274083;405971;544275;679029;814784;948270;1084817;1218462;1347004;1400680];
elseif i==6
    clear locs1
    locs1=floor([0.1053;16.7636;33.6694;50.4913]/res);
elseif i==7
    clear locs1
    locs1=floor([0.0307;16.8235;33.6592;50.5484]/res);
elseif i==8
    clear locs1
    locs1=floor([0.0889;16.7952;33.7600;50.5882]/res);
elseif i==9
    clear locs1
    locs1=floor([1.3251;29.3896;57.5434;85.6722]/res);
```

```
elseif i==10
    clear locs1
    locs1=floor([1.3331;29.4365;57.5217;85.6599]/res);
elseif i==11
    clear locs1
    locs1=floor([1.2929;29.3416;57.4533;85.5897]/res);
elseif i==12
    clear locs1
    locs1=floor([4.3952;28.3551;56.5543;84.6536]/res);
elseif i==13
    clear locs1
    locs1=floor([0.2673;28.2436;56.3902;84.4621]/res);
elseif i==14
    clear locs1
    locs1=floor([.4692;28.5049;56.5897;84.7432]/res);
elseif i==15
    clear locs1
    locs1=floor([0.3298;28.1000;56.1739;84.1380]/res);
elseif i==16
    clear locs1
    locs1=floor([0.0588;28.2178;56.2039;84.4105]/res);
elseif i==17
    clear locs1
    locs1=floor([1.2894;85.4449;170.1539;254.0603]/res);
elseif i==18
    clear locs1
    locs1=floor([0.2563;84.4302;168.8952;253.0856]/res);
elseif i==19
   clear locs1
   locs1=[2282;675483;1351973;2028192;2253409];
elseif i==20
    clear locs1
    locs1=floor([0.3000;84.4066;168.3448;252.8018]/res);
elseif i==21
    clear locs1
    locs1=floor([0.3478;84.4420;168.6854;253.0972]/res);
elseif i==22
   clear locs1
   locs1=[11280;687626;1360950;2036408;2263023];
elseif i==23
   clear locs1
   locs1=[2282;675483;1351973;2028192;2253409];
elseif i==24
   clear locs1
   locs1=[2181;675157;1353993;2026011];
end



ii1=locs1(number)+1/res;
ii2=locs1(number+1)-1/res;

[pks2,locs2]=findpeaks(ch6(ii1:ii2),'MinPeakDistance',gap/res-10,'MinPeakHeight',100);
hold all;
% plot(t(ii1:ii2),ch6(ii1:ii2),'r',t(locs2+ii1-1),ch6(locs2+ii1-1),'ob');figure();
```

```
%selecting maximum value in the identified range
Fmax=max(Fz(ii1:ii2));

%selecting maximum value in each cutter rotation
locs3=locs2+ii1-1;
for o=2:length(locs3)
   [Fzmax1 p]=max(Fz(locs3(o-1):locs3(o)));
   Fzmax(o-1)=Fzmax1;
   index(o-1)=locs3(o-1)+p;
   tzmax(o-1)=t(index(o-1));
end

% hold all
% grid on
% plot(tzmax,Fzmax);
% legend(name);figure();

FZavg(i,1)=mean(Fzmax)
% FZmax(i,1)=Fmax
end

FF(:,1)=FZavg(:,1);
% FF(:,2)=FZmax(:,1);
```

Ft - End milling cutting CFRP :

```
clear all
clearvars;
close all
clc;

%loading the data file
% addpath('U:\Research\Rishi - matlab codes');
no=2;

for i=1:24
i
clear o p t Ft ch6 pks ch6_1 locs pks1 locs1 pks2 locs2 pks3 locs3 i1 i2 ii1 ii2 zeroshift zshift ttmax Ftmax Ftmax1
Fmax
name=sprintf('e%d',i);
load(name,'-mat');

t=eval(sprintf('e%d(:,1)',i));
Ft=eval(sprintf('e%d(:,8)',i));
ch6=eval(sprintf('e%d(:,7)',i));

% hold all;
% plot(t,Ft);
% plot(t,ch6,'r');figure();
% grid on


%Specifying data
dat=xlsread('doe','A3:D26');
for k=1:size(dat,1)
if dat(k,1)==i
   m=k;
end
end
res=1.25e-4;
rpm= dat(m,2);
feed= dat(m,3);
gap=(60/rpm); %time gap for each cutter rotation
loc=7; %length of cut in inches

% Finding the peaks in ch6
ch6_1 = ch6(1:2/res);
[pks,locs]=findpeaks(ch6_1,'MinPeakDistance',gap/res-10,'MinPeakHeight',100);

% hold all;
% plot(t(1:2/res),ch6_1,'r');
% plot(t(locs), ch6_1(locs), 'ob');
% figure();



%Zero Shift
```

```
i1=1; %starting index of initial zero shift data
i2=locs(1)-gap/res; %end index of initial zero shift data
width=floor( (i2-i1)/(gap/res) );%number of cutter rotations in zero shift data
i3= i1 + width*(gap/res);
zeroshift=mean(Ft(i1:i3));

if i2<gap/res   %this is different for other variables
   i2=1;
   zeroshift=0;
end

if i==5 %signal at i5 is an exception
   zeroshift=mean(Ft(i1:i1+gap/res));
end

zshift(i,1)=zeroshift;
Ft=Ft-zshift(i,1);



% Selecting the cut to be analyzed
cut_gap=60*loc/feed; % Time range for conventional/climb
number=no;
% [pks1,locs1]=findpeaks(Ft,'MinPeakDistance',cut_gap/res);

%Exceptions
if i==1
   clear locs1
   locs1=floor([1.5449/res;18.3941;35.2441;52.1526]/res);
elseif i==2
    clear locs1
    locs1=floor([2.7147;19.6040;36.4637;53.2926]/res);
elseif i==3
    clear locs1
    locs1=floor([0.1904;16.9057;33.9296;50.7453]/res);
elseif i==4
    clear locs1
    locs1=floor([2.6860;19.5651;36.4053;53.3038]/res);
elseif i==5
   clear locs1
   locs1=[3458;138665;274083;405971;544275;679029;814784;948270;1084817;1218462;1347004;1400680];
elseif i==6
    clear locs1
    locs1=floor([0.1053;16.7636;33.6694;50.4913]/res);
elseif i==7
    clear locs1
    locs1=floor([0.0307;16.8235;33.6592;50.5484]/res);
elseif i==8
    clear locs1
    locs1=floor([0.0889;16.7952;33.7600;50.5882]/res);
elseif i==9
    clear locs1
    locs1=floor([1.3251;29.3896;57.5434;85.6722]/res);
elseif i==10
    clear locs1
    locs1=floor([1.3331;29.4365;57.5217;85.6599]/res);
```

```
elseif i==11
    clear locs1
    locs1=floor([1.2929;29.3416;57.4533;85.5897]/res);
elseif i==12
    clear locs1
    locs1=floor([4.3952;28.3551;56.5543;84.6536]/res);
elseif i==13
    clear locs1
    locs1=floor([0.2673;28.2436;56.3902;84.4621]/res);
elseif i==14
    clear locs1
    locs1=floor([.4692;28.5049;56.5897;84.7432]/res);
elseif i==15
    clear locs1
    locs1=floor([0.3298;28.1000;56.1739;84.1380]/res);
elseif i==16
    clear locs1
    locs1=floor([0.0588;28.2178;56.2039;84.4105]/res);
elseif i==17
    clear locs1
    locs1=floor([1.2894;85.4449;170.1539;254.0603]/res);
elseif i==18
    clear locs1
    locs1=floor([0.2563;84.4302;168.8952;253.0856]/res);
elseif i==19
   clear locs1
   locs1=[2282;675483;1351973;2028192;2253409];
elseif i==20
    clear locs1
    locs1=floor([0.3000;84.4066;168.3448;252.8018]/res);
elseif i==21
    clear locs1
    locs1=floor([0.3478;84.4420;168.6854;253.0972]/res);
elseif i==22
   clear locs1
   locs1=[11280;687626;1360950;2036408;2263023];
elseif i==23
   clear locs1
   locs1=[2282;675483;1351973;2028192;2253409];
elseif i==24
   clear locs1
   locs1=[2181;675157;1353993;2026011];
end


ii1=locs1(number)+1.5/res;
ii2=locs1(number+1)-1.5/res;


[pks2,locs2]=findpeaks(ch6(ii1:ii2),'MinPeakDistance',gap/res-10,'MinPeakHeight',100);
hold all;
% plot(t(ii1:ii2),ch6(ii1:ii2),'r',t(locs2+ii1-1),ch6(locs2+ii1-1),'ob');figure();

%selecting maximum value in the identified range
Fmax=max(Ft(ii1:ii2));
```

```
%selecting maximum value in each cutter rotation
locs3=locs2+ii1-1;
for o=2:length(locs3)
   [Ftmax1 p]=max(Ft(locs3(o-1):locs3(o)));
   Ftmax(o-1)=Ftmax1;
   index(o-1)=locs3(o-1)+p;
   ttmax(o-1)=t(index(o-1));
end

% hold all
% grid on
% plot(ttmax,Ftmax);
% legend(name);

FTavg(i,1)=mean(Ftmax)
% FTmax(i,1)=Fmax
end


FF(:,1)=FTavg(:,1);
% FF(:,2)=FTmax(:,1);
```

Fr - End milling cutting CFRP :

```
clear all;
close all;
clc;

%loading the data file
% addpath('U:\Research\Rishi - matlab codes');
no=2;

for i=1:5
i
clear o p t Fr ch6 pks ch6_1 locs pks1 locs1 pks2 locs2 pks3 locs3 i1 i2 ii1 ii2 zeroshift zshift trmax Frmax Frmax1
Fmax
name=sprintf('e%d',i);
load(name,'-mat');

t=eval(sprintf('e%d(:,1)',i));
Fr=eval(sprintf('e%d(:,9)',i));
ch6=eval(sprintf('e%d(:,7)',i));

% hold all;
% plot(t,Fr);
% plot(t,ch6,'r');figure();
% grid on


%Specifying data
dat=xlsread('doe','A3:D26');
for k=1:size(dat,1)
if dat(k,1)==i
   m=k;
end
end
res=1.25e-4;
rpm= dat(m,2);
feed= dat(m,3);
gap=(60/rpm); %time gap for each cutter rotation
loc=7; %length of cut in inches

% Finding the peaks in ch6
ch6_1 = ch6(1:2/res);
[pks,locs]=findpeaks(ch6_1,'MinPeakDistance',gap/res-10,'MinPeakHeight',100);

% hold all;
% plot(t(1:2/res),ch6_1,'r');
% plot(t(locs), ch6_1(locs), 'ob');
% figure();

%Zero Shift
i1=1; %starting index of initial zero shift data
i2=locs(1)-gap/res; %end index of initial zero shift data
width=floor( (i2-i1)/(gap/res) );%number of cutter rotations in zero shift data
i3= i1 + width*(gap/res);
```

```
zeroshift=mean(Fr(i1:i3));

if i2<gap/res  %this is different for other variables
   i2=1;
   zeroshift=0;
end
zeroshift=mean(Fr(i1:i2));
zshift(i,1)=zeroshift;
Fr=Fr-zshift(i,1);

if i==5 %signal at i5 is an exception
   zeroshift=mean(Fr(i1:i1+gap/res));
end

% Selecting the cut to be analyzed
cut_gap=60*loc/feed; % Time range for conventional/climb
number=no;
% [pks1,locs1]=findpeaks(Fr,'MinPeakDistance',cut_gap/res);

%Exceptions
if i==1
   clear locs1
   locs1=floor([1.5449/res;18.3941;35.2441;52.1526]/res);
elseif i==2
    clear locs1
    locs1=floor([2.7147;19.6040;36.4637;53.2926]/res);
elseif i==3
    clear locs1
    locs1=floor([0.1904;16.9057;33.9296;50.7453]/res);
elseif i==4
    clear locs1
    locs1=floor([2.6860;19.5651;36.4053;53.3038]/res);
elseif i==5
   clear locs1
   locs1=[3458;138665;274083;405971;544275;679029;814784;948270;1084817;1218462;1347004;1400680];
elseif i==6
    clear locs1
    locs1=floor([0.1053;16.7636;33.6694;50.4913]/res);
elseif i==7
    clear locs1
    locs1=floor([0.0307;16.8235;33.6592;50.5484]/res);
elseif i==8
    clear locs1
    locs1=floor([0.0889;16.7952;33.7600;50.5882]/res);
elseif i==9
    clear locs1
    locs1=floor([1.3251;29.3896;57.5434;85.6722]/res);
elseif i==10
    clear locs1
    locs1=floor([1.3331;29.4365;57.5217;85.6599]/res);
elseif i==11
    clear locs1
    locs1=floor([1.2929;29.3416;57.4533;85.5897]/res);
elseif i==12
    clear locs1
```

```
    locs1=floor([4.3952;28.3551;56.5543;84.6536]/res);
elseif i==13
    clear locs1
    locs1=floor([0.2673;28.2436;56.3902;84.4621]/res);
elseif i==14
    clear locs1
    locs1=floor([.4692;28.5049;56.5897;84.7432]/res);
elseif i==15
    clear locs1
    locs1=floor([0.3298;28.1000;56.1739;84.1380]/res);
elseif i==16
    clear locs1
    locs1=floor([0.0588;28.2178;56.2039;84.4105]/res);
elseif i==17
    clear locs1
    locs1=floor([1.2894;85.4449;170.1539;254.0603]/res);
elseif i==18
    clear locs1
    locs1=floor([0.2563;84.4302;168.8952;253.0856]/res);
elseif i==19
   clear locs1
   locs1=[2282;675483;1351973;2028192;2253409];
elseif i==20
    clear locs1
    locs1=floor([0.3000;84.4066;168.3448;252.8018]/res);
elseif i==21
    clear locs1
    locs1=floor([0.3478;84.4420;168.6854;253.0972]/res);
elseif i==22
   clear locs1
   locs1=[11280;687626;1360950;2036408;2263023];
elseif i==23
   clear locs1
   locs1=[2282;675483;1351973;2028192;2253409];
elseif i==24
   clear locs1
   locs1=[2181;675157;1353993;2026011];
end



ii1=locs1(number)+1/res;
ii2=locs1(number+1)-1/res;

[pks2,locs2]=findpeaks(ch6(ii1:ii2),'MinPeakDistance',gap/res-10,'MinPeakHeight',100);
hold all;
% plot(t(ii1:ii2),ch6(ii1:ii2),'r',t(locs2+ii1-1),ch6(locs2+ii1-1),'ob');figure();

%selecting maximum value in the identified range
Fmax=max(Fr(ii1:ii2));

%selecting maximum value in each cutter rotation
locs3=locs2+ii1-1;
for o=2:length(locs3)
   [Frmax1 p]=max(Fr(locs3(o-1):locs3(o)));
```

```
    Frmax(o-1)=Frmax1;
    index(o-1)=locs3(o-1)+p;
    trmax(o-1)=t(index(o-1));
end

% hold all
% grid on
% plot(trmax,Frmax);
% legend(name);figure();

FRavg(i,1)=mean(Frmax)
% FRmax(i,1)=Fmax
end


FF(:,1)=FRavg(:,1);
% FF(:,2)=FRmax(:,1);
```

Fx - End milling cutting HexMC :

```
clear all;
close all;
clc;

%loading the data file
%addpath('U:\Research\Rishi - matlab codes');
no=2; %cut number

for i=1:8 %Experiment number
i %Displaying experiment number
clear o p t Fy ch6 pks ch6_1 locs pks1 locs1 pks2 locs2 pks3 locs3 i1 i2 ii1 ii2 zeroshift txmax Fxmax Fxmax1
Fmax
name=sprintf('MAR 15 - Edge - HexMc - %d',i); %creating the name of the data file to be fetched
load(name,'-mat'); %fetching the data file ".mat files"
%data1=eval(sprintf('MAR 15 - Edge - HexMc - %d',i));
% t=data1(:,1); %time
% Fx=data1(:,2);%Fx data
% ch6=data1(:,7);%channel 6 data
% hold all;
% plot(t,Fx); %Plotting time and Fx
% plot(t,ch6,'r');figure();%Plotting time and channel 6
% grid on
%Specifying data
dat=xlsread('doe_hexmc.xlsx'); %reading the doe file
t=time;
for k=1:size(dat,1)
if dat(k,1)==i
   m=k; %m is the corresponding row number
end
end

res=1.25e-4; %time between two data points
rpm= dat(m,2);
feed= dat(m,3);
gap=(60/rpm); %time gap for each cutter rotation in seconds
loc=7; %length of cut in inches


% Finding the peaks in ch6 for zeroshift
ch6_1 = ch6(1:2/res);
[pks,locs]=findpeaks(ch6_1,'MinPeakDistance',gap/res-10,'MinPeakHeight',100);
if i==5
   ch6_1=ch6(1:10/res);
   [pks,locs]=findpeaks(ch6_1,'MinPeakDistance',gap/res-100,'MinPeakHeight',100);
   plot(t,ch6)
end

% hold all;
% plot(t(1:2/res),ch6_1,'r');
% plot(t(locs), ch6_1(locs), 'ob');
% figure();
```

```
%Zero Shift
i1=1; %starting index of initial zero shift data
i2=locs(1)-gap/res; %end index of initial zero shift data
width=floor( (i2-i1)/(gap/res) );%number of cutter rotations in zero shift data
i3= i1 + width*(gap/res);
zeroshift=mean(Fx(i1:i3));

if i2<gap/res   %this is different for other variables
   i2=1;
   zeroshift=0;
end

% if i==5 %signal at i5 is an exception
%     zeroshift=mean(Fx(i1:i1+gap/res));
% end

zshift(i,1)=zeroshift; %saving the zeroshift values for each experiment number
Fx=Fx-zshift(i,1); %shifting data


% Selecting the cut to be analyzed
cut_gap=60*loc/feed; % Time range for conventional/climb
number=no;
% [pks1,locs1]=findpeaks(Fx,'MinPeakDistance',cut_gap/res);


%Exceptions
if i==1
   clear locs1

locs1=floor([1.259703;18.158992;35.009734;51.90765;68.768376;85.616124;102.438288;119.344815;136.147011;
153.113815;169.715587
]/res);
elseif i==2
    clear locs1
    locs1=floor([0.253838;84.632597;168.540621;252.873955]/res);
elseif i==3
    clear locs1

locs1=floor([1.352303;18.241857;35.042805;51.899913;68.860726;85.648696;102.530368;119.357794;136.259453
;153.096718;169.837764]/res);
elseif i==4
    clear locs1
    locs1=floor([0.363534;84.226382;168.543117;252.692999]/res);
elseif i==5
   clear locs1
   locs1=floor(([9.9244498;94.217022;178.448646;262.491951])/res);
elseif i==6
    clear locs1

locs1=floor([0.011856;16.860726;33.726195;50.559341;67.455759;84.287158;101.184575;118.079246;134.925621
;151.807188;168.403345]/res);
elseif i==7
```

```
    clear locs1

locs1=floor([0.0463;16.702359;33.540122;50.434793;67.273056;84.162112;101.00287;117.890428;134.736553;15
1.618245;167.976164]/res);
elseif i==8
    clear locs1
    locs1=floor([0.025708;83.450768;167.801572;251.843754]/res);
end
% elseif i==9
%     clear locs1
%     locs1=floor([1.3251;29.3896;57.5434;85.6722]/res);
% elseif i==10
%     clear locs1
%     locs1=floor([1.3331;29.4365;57.5217;85.6599]/res);
% elseif i==11
%     clear locs1
%     locs1=floor([1.2929;29.3416;57.4533;85.5897]/res);
% elseif i==12
%     clear locs1
%     locs1=floor([4.3952;28.3551;56.5543;84.6536]/res);
% elseif i==13
%     clear locs1
%     locs1=floor([0.2673;28.2436;56.3902;84.4621]/res);
% elseif i==14
%     clear locs1
%     locs1=floor([.4692;28.5049;56.5897;84.7432]/res);
% elseif i==15
%     clear locs1
%     locs1=floor([0.3298;28.1000;56.1739;84.1380]/res);
% elseif i==16
%     clear locs1
%     locs1=floor([0.0588;28.2178;56.2039;84.4105]/res);
% elseif i==17
%     clear locs1
%     locs1=floor([1.2894;85.4449;170.1539;254.0603]/res);
% elseif i==18
%     clear locs1
%     locs1=floor([0.2563;84.4302;168.8952;253.0856]/res);
% elseif i==19
%    clear locs1
%    locs1=[2282;675483;1351973;2028192;2253409];
% elseif i==20
%     clear locs1
%     locs1=floor([0.3000;84.4066;168.3448;252.8018]/res);
% elseif i==21
%     clear locs1
%     locs1=floor([0.3478;84.4420;168.6854;253.0972]/res);
% elseif i==22
%    clear locs1
%    locs1=[11280;687626;1360950;2036408;2263023];
% elseif i==23
%    clear locs1
%    locs1=[2282;675483;1351973;2028192;2253409];
% elseif i==24
%    clear locs1
%    locs1=[2181;675157;1353993;2026011];
```

```
% end
%

ii1=locs1(number)+1/res; %starting index number of the data to be analyzed
ii2=locs1(number+1)-1/res;%Ending index number of the data to be analyzed

%finding peaks in the selected cut/ data
[pks2,locs2]=findpeaks(ch6(ii1:ii2),'MinPeakDistance',gap/res-10,'MinPeakHeight',100);
if i==5
   [pks2,locs2]=findpeaks(ch6(ii1:ii2),'MinPeakDistance',gap/res-100,'MinPeakHeight',100);
end
% hold all;
% plot(t(ii1:ii2),ch6(ii1:ii2),'r',t(locs2+ii1-1),ch6(locs2+ii1-1),'ob');figure();

%selecting maximum value in each cutter rotation
locs3=locs2+ii1-1;

for o=2:length(locs3)
   [Fxmax1 p]=max(Fx(locs3(o-1):locs3(o))); %finding maximum force in each cutter rotation
   Fxmax(o-1)=Fxmax1;
   index(o-1)=locs3(o-1)+p;
   txmax(o-1)=t(floor(index(o-1)));
end
%
% hold all
% grid on
% plot(txmax,Fxmax);
% legend(name); figure();
dat1=xlsread('zshift.xlsx');

FXavg(i,1)=mean(Fxmax)
Fx_actual(i,1)=FXavg(i,1)-dat1(i,1);
% FXmax(i,1)=Fmax

end

FF(:,1)=FX_actual(:,1);
% FF(:,2)=FXmax(:,1);
save Force_Fx.dat FF -ASCII
```

Fy - End milling cutting HexMC :

```
clear all;
close all;
clc;

%loading the data file
% addpath('U:\Research\Rishi - matlab codes');
no=2;
for i=1:8
 i
clear t Fy ch6 pks ch6_1 locs pks1 locs1 pks2 locs2 i1 i2 ii1 ii2 zeroshift tymax Fymax Fymax1 Fmax
name=sprintf('MAR 15 - Edge - HexMc - %d',i); %creating the name of the data file to be fetched
load(name,'-mat'); %fetching the data file ".mat files"
dat=xlsread('doe_hexmc.xlsx'); %reading the doe file
t=time;

%
% hold all;
% plot(t,Fy);
% plot(t,ch6,'r');figure();
% grid on


%Specifying data
for k=1:size(dat,1)
if dat(k,1)==i
   m=k;
end
end
res=1.25e-4;
rpm= dat(m,2);
feed= dat(m,3);
gap=(60/rpm); %time gap for each cutter rotation
loc=7; %length of cut in inches

% Finding the peaks in ch6
ch6_1 = ch6(1:2/res);
[pks,locs]=findpeaks(ch6_1,'MinPeakDistance',gap/res-10,'MinPeakHeight',100);
if i==5
   ch6_1=ch6(1:10/res);
   [pks,locs]=findpeaks(ch6_1,'MinPeakDistance',gap/res-100,'MinPeakHeight',100);
   plot(t,ch6)
end
% hold all;
% plot(t(1:2/res),ch6_1,'r');
% plot(t(locs), ch6_1(locs), 'ob');
% figure();



%Zero Shift
i1=1; %starting index of initial zero shift data
i2=locs(1)-gap/res; %end index of initial zero shift data
```

```
width=floor( (i2-i1)/(gap/res) );%number of cutter rotations in zero shift data
i3= i1 + width*(gap/res);
zeroshift=mean(Fy(i1:i3));


if i2<gap/res   %this is different for other variables
   i2=1;
   zeroshift=0;
end
zshift(i,1)=zeroshift;
Fy=Fy-zshift(i,1);
% if i==5 %signal at i5 is an exception
%     zeroshift=mean(Fy(i1:i1+gap/res));
% end

% Selecting the cut to be analyzed
cut_gap=60*loc/feed; %time range for conventional/climb
number=no;
% [pks1,locs1]=findpeaks(Fy,'MinPeakDistance',cut_gap/res);


%Exceptions
if i==1
   clear locs1

locs1=floor([1.259703;18.158992;35.009734;51.90765;68.768376;85.616124;102.438288;119.344815;136.147011;
153.113815;169.715587
]/res);
elseif i==2
    clear locs1
    locs1=floor([0.253838;84.632597;168.540621;252.873955]/res);
elseif i==3
    clear locs1

locs1=floor([1.352303;18.241857;35.042805;51.899913;68.860726;85.648696;102.530368;119.357794;136.259453
;153.096718;169.837764]/res);
elseif i==4
    clear locs1
    locs1=floor([0.363534;84.226382;168.543117;252.692999]/res);
elseif i==5
   clear locs1
   locs1=floor(([9.9244498;94.217022;178.448646;262.491951])/res);
elseif i==6
    clear locs1

locs1=floor([0.011856;16.860726;33.726195;50.559341;67.455759;84.287158;101.184575;118.079246;134.925621
;151.807188;168.403345]/res);
elseif i==7
    clear locs1

locs1=floor([0.0463;16.702359;33.540122;50.434793;67.273056;84.162112;101.00287;117.890428;134.736553;15
1.618245;167.976164]/res);
elseif i==8
    clear locs1
    locs1=floor([0.025708;83.450768;167.801572;251.843754]/res);
```

```
% elseif i==9
%      clear locs1
%      locs1=floor([1.3251;29.3896;57.5434;85.6722]/res);
% elseif i==10
%      clear locs1
%      locs1=floor([1.3331;29.4365;57.5217;85.6599]/res);
% elseif i==11
%      clear locs1
%      locs1=floor([1.2929;29.3416;57.4533;85.5897]/res);
% elseif i==12
%      clear locs1
%      locs1=floor([4.3952;28.3551;56.5543;84.6536]/res);
% elseif i==13
%      clear locs1
%      locs1=floor([0.2673;28.2436;56.3902;84.4621]/res);
% elseif i==14
%      clear locs1
%      locs1=floor([.4692;28.5049;56.5897;84.7432]/res);
% elseif i==15
%      clear locs1
%      locs1=floor([0.3298;28.1000;56.1739;84.1380]/res);
% elseif i==16
%      clear locs1
%      locs1=floor([0.0588;28.2178;56.2039;84.4105]/res);
% elseif i==17
%      clear locs1
%      locs1=floor([1.2894;85.4449;170.1539;254.0603]/res);
% elseif i==18
%      clear locs1
%      locs1=floor([0.2563;84.4302;168.8952;253.0856]/res);
% elseif i==19
%     clear locs1
%     locs1=[2282;675483;1351973;2028192;2253409];
% elseif i==20
%      clear locs1
%      locs1=floor([0.3000;84.4066;168.3448;252.8018]/res);
% elseif i==21
%      clear locs1
%      locs1=floor([0.3478;84.4420;168.6854;253.0972]/res);
% elseif i==22
%     clear locs1
%     locs1=[11280;687626;1360950;2036408;2263023];
% elseif i==23
%     clear locs1
%     locs1=[2282;675483;1351973;2028192;2253409];
% elseif i==24
%     clear locs1
%     locs1=[2181;675157;1353993;2026011];
end



ii1=locs1(number) + 1/res;
ii2=locs1(number+1) - 1/res;
```

```
[pks2,locs2]=findpeaks(ch6(ii1:ii2),'MinPeakDistance',gap/res-10,'MinPeakHeight',100);
if i==5
   [pks2,locs2]=findpeaks(ch6(ii1:ii2),'MinPeakDistance',gap/res-100,'MinPeakHeight',100);
end
% plot(t(ii1:ii2),ch6(ii1:ii2),'r',t(locs2+ii1-1),ch6(locs2+ii1-1),'ob');figure();

%selecting maximum value in the identified range
Fmax=max(Fy(ii1:ii2));


locs3=locs2+ii1-1;
for o=2:length(locs3)
   [Fymax1 p]=max(Fy(locs3(o-1):locs3(o)));
   Fymax(o-1)=Fymax1;
   index(o-1)=locs3(o-1)+p;
   tymax(o-1)=t(floor(index(o-1)));
end
hold all
grid on
plot(tymax,Fymax);
legend(name);figure();
dat1=xlsread('zshift.xlsx');

FYavg(i,1)=mean(Fymax)

Fy_actual(i,1)=FYavg(i,1)-dat1(i,2);
% FYmax(i,1)=Fmax
end

FF(:,1)=Fy_actual(:,1);
% FF(:,2)=FYmax(:,1);
save Force_Fy.dat FF -ASCII
```

Fz - End milling cutting HexMC :

```
clear all;
close all;
clc;

%loading the data file
addpath('C:\Users\Nishita\Desktop\Shanti\HEXMC TXT');
no=2;

for i=1:8
i
clear o p t Fz ch6 pks ch6_1 locs pks1 locs1 pks2 locs2 pks3 locs3 i1 i2 ii1 ii2 zeroshift tzmax Fzmax Fzmax1 Fmax
a1 a2
name=sprintf('MAR 15 - Edge - HexMc - %d',i); %creating the name of the data file to be fetched
load(name,'-mat'); %fetching the data file ".mat files"

% hold all;
% plot(t,Fz);
% plot(t,ch6,'r');figure();
% grid on


%Specifying data
dat=xlsread('doe_hexmc.xlsx'); %reading the doe file
t=time;
for k=1:size(dat,1)
if dat(k,1)==i
   m=k;
end
end
res=1.25e-4;
rpm= dat(m,2);
feed= dat(m,3);
gap=(60/rpm); %time gap for each cutter rotation
loc=7; %length of cut in inches

% Finding the peaks in ch6
ch6_1 = ch6(1:2/res);
[pks,locs]=findpeaks(ch6_1,'MinPeakDistance',gap/res-10,'MinPeakHeight',100);
if i==5
   ch6_1=ch6(1:10/res);
   [pks,locs]=findpeaks(ch6_1,'MinPeakDistance',gap/res-100,'MinPeakHeight',100);
   %plot(t,ch6)
end
% hold all;
% plot(t(1:2/res),ch6_1,'r');
% plot(t(locs), ch6_1(locs), 'ob');
% figure();


%Zero Shift
i1=1; %starting index of initial data
i2=locs(1)-10; %end index of initial data
```

```
zeroshift=mean(Fz(i1:i2));
zshift(i,1)=zeroshift;
% plot(t(i1:i2),Fz(i1:i2))
Fz=Fz-zeroshift;
% hold all
% plot(t,Fz,'b')

a1=polyfit(t(10/res:length(Fz)),Fz(10/res:length(Fz)),1);
% y=a1(2) + t*a1(1);
% plot(t,y,'r');
% plot(t,y-t*a1(1),'g');figure();

% if i==5 %signal at i5 is an exception
%     zeroshift=mean(Fz(i1:i1+gap/res));
% end

Fz=Fz-a1(1)*t;
% plot(t,Fz,'r'); figure();


% Selecting the cut to be analyzed
cut_gap=60*loc/feed; % Time range for conventional/climb
number=no;
% [pks1,locs1]=findpeaks(-Fz,'MinPeakDistance',cut_gap/res);


%Exceptions
if i==1
   clear locs1

locs1=floor([1.259703;18.158992;35.009734;51.90765;68.768376;85.616124;102.438288;119.344815;136.147011;
153.113815;169.715587
]/res);
elseif i==2
    clear locs1
    locs1=floor([0.253838;84.632597;168.540621;252.873955]/res);
elseif i==3
    clear locs1

locs1=floor([1.352303;18.241857;35.042805;51.899913;68.860726;85.648696;102.530368;119.357794;136.259453
;153.096718;169.837764]/res);
elseif i==4
    clear locs1
    locs1=floor([0.363534;84.226382;168.543117;252.692999]/res);
elseif i==5
   clear locs1
   locs1=floor(([9.9244498;94.217022;178.448646;262.491951])/res);
elseif i==6
    clear locs1

locs1=floor([0.011856;16.860726;33.726195;50.559341;67.455759;84.287158;101.184575;118.079246;134.925621
;151.807188;168.403345]/res);
elseif i==7
    clear locs1
```

```
locs1=floor([0.0463;16.702359;33.540122;50.434793;67.273056;84.162112;101.00287;117.890428;134.736553;15
1.618245;167.976164]/res);
elseif i==8
    clear locs1
    locs1=floor([0.025708;83.450768;167.801572;251.843754]/res);
end



ii1=locs1(number)+1/res;
ii2=locs1(number+1)-1/res;

[pks2,locs2]=findpeaks(ch6(ii1:ii2),'MinPeakDistance',gap/res-10,'MinPeakHeight',100);
if i==5
   [pks2,locs2]=findpeaks(ch6(ii1:ii2),'MinPeakDistance',gap/res-100,'MinPeakHeight',100);
end
hold all;
% plot(t(ii1:ii2),ch6(ii1:ii2),'r',t(locs2+ii1-1),ch6(locs2+ii1-1),'ob');figure();

%selecting maximum value in the identified range
Fmax=max(Fz(ii1:ii2));

%selecting maximum value in each cutter rotation
locs3=locs2+ii1-1;
for o=2:length(locs3)
   [Fzmax1 p]=max(Fz(locs3(o-1):locs3(o)));
   Fzmax(o-1)=Fzmax1;
   index(o-1)=locs3(o-1)+p;
   tzmax(o-1)=t(index(o-1));
end

% hold all
% grid on
% plot(tzmax,Fzmax);
% legend(name);figure();
%plot(t,Fz)
dat1=xlsread('zshift.xlsx');

FZavg(i,1)=mean(Fzmax)
Fz_actual(i,1)=FZavg(i,1)-dat1(i,3);

% FZmax(i,1)=Fmax
end

FF(:,1)=Fz_actual(:,1);
% FF(:,2)=FZmax(:,1);
save Force_Fz.dat FF -ASCII
```

Ft - End milling cutting HexMC :

```
clear all
clearvars;
close all
clc;

%loading the data file
addpath('C:\Users\Nishita\Desktop\Shanti\HEXMC TXT');
no=2;

for i=1:8
i
clear o p t Ft ch6 pks ch6_1 locs pks1 locs1 pks2 locs2 pks3 locs3 i1 i2 ii1 ii2 zeroshift zshift ttmax Ftmax Ftmax1
Fmax
name=sprintf('MAR 15 - Edge - HexMc - %d',i); %creating the name of the data file to be fetched
load(name,'-mat'); %fetching the data file ".mat files"

% hold all;
% plot(t,Ft);
% plot(t,ch6,'r');figure();
% grid on


%Specifying data
dat=xlsread('doe_hexmc.xlsx'); %reading the doe file
t=time;
for k=1:size(dat,1)
if dat(k,1)==i
   m=k;
end
end
res=1.25e-4;
rpm= dat(m,2);
feed= dat(m,3);
gap=(60/rpm); %time gap for each cutter rotation
loc=7; %length of cut in inches

% Finding the peaks in ch6
ch6_1 = ch6(1:2/res);
[pks,locs]=findpeaks(ch6_1,'MinPeakDistance',gap/res-10,'MinPeakHeight',100);
if i==5
   ch6_1=ch6(1:10/res);
   [pks,locs]=findpeaks(ch6_1,'MinPeakDistance',gap/res-100,'MinPeakHeight',100);
   %plot(t,ch6)
end
% hold all;
% plot(t(1:2/res),ch6_1,'r');
% plot(t(locs), ch6_1(locs), 'ob');
% figure();
%Zero Shift
i1=1; %starting index of initial zero shift data
i2=locs(1)-gap/res; %end index of initial zero shift data
width=floor( (i2-i1)/(gap/res) );%number of cutter rotations in zero shift data
```

```
i3= i1 + width*(gap/res);
zeroshift=mean(Ft(i1:i3));
if i2<gap/res   %this is different for other variables
   i2=1;
   zeroshift=0;
end

% if i==5 %signal at i5 is an exception
%     zeroshift=mean(Ft(i1:i1+gap/res));
% end

zshift(i,1)=zeroshift;
Ft=Ft-zshift(i,1);


% Selecting the cut to be analyzed
cut_gap=60*loc/feed; % Time range for conventional/climb
number=no;
% [pks1,locs1]=findpeaks(Ft,'MinPeakDistance',cut_gap/res);

%Exceptions
if i==1
clear locs1

locs1=floor([1.259703;18.158992;35.009734;51.90765;68.768376;85.616124;102.438288;119.344815;136.147011;
153.113815;169.715587
]/res);
elseif i==2
    clear locs1
    locs1=floor([0.253838;84.632597;168.540621;252.873955]/res);
elseif i==3
    clear locs1

locs1=floor([1.352303;18.241857;35.042805;51.899913;68.860726;85.648696;102.530368;119.357794;136.259453
;153.096718;169.837764]/res);
elseif i==4
    clear locs1
    locs1=floor([0.363534;84.226382;168.543117;252.692999]/res);
elseif i==5
   clear locs1
   locs1=floor(([9.9244498;94.217022;178.448646;262.491951])/res);
elseif i==6
    clear locs1

locs1=floor([0.011856;16.860726;33.726195;50.559341;67.455759;84.287158;101.184575;118.079246;134.925621
;151.807188;168.403345]/res);
elseif i==7
    clear locs1

locs1=floor([0.0463;16.702359;33.540122;50.434793;67.273056;84.162112;101.00287;117.890428;134.736553;15
1.618245;167.976164]/res);
elseif i==8
    clear locs1
    locs1=floor([0.025708;83.450768;167.801572;251.843754]/res);
end
```

```
ii1=locs1(number)+1.5/res;
ii2=locs1(number+1)-1.5/res;


[pks2,locs2]=findpeaks(ch6(ii1:ii2),'MinPeakDistance',gap/res-10,'MinPeakHeight',100);
if i==5
   [pks2,locs2]=findpeaks(ch6(ii1:ii2),'MinPeakDistance',gap/res-100,'MinPeakHeight',100);
end
hold all;
% plot(t(ii1:ii2),ch6(ii1:ii2),'r',t(locs2+ii1-1),ch6(locs2+ii1-1),'ob');figure();

%selecting maximum value in the identified range
Fmax=max(Ft(ii1:ii2));

%selecting maximum value in each cutter rotation
locs3=locs2+ii1-1;
for o=2:length(locs3)
   [Ftmax1 p]=max(Ft(locs3(o-1):locs3(o)));
   Ftmax(o-1)=Ftmax1;
   index(o-1)=locs3(o-1)+p;
   ttmax(o-1)=t(index(o-1));
end

% hold all
% grid on
% plot(ttmax,Ftmax);
% legend(name);
if i==3
   plot(t,Ft)
end
dat1=xlsread('zshift.xlsx');
FTavg(i,1)=mean(Ftmax)
FT_actual(i,1)=FTavg(i,1)-dat1(i,5);

% FTmax(i,1)=Fmax

end


FF(:,1)=FT_actual(:,1);
% FF(:,2)=FTmax(:,1);
save Force_Ft.dat FF -ASCII
```

Fr - End milling cutting HexMC :

```
clear all;
close all;
clc;

%loading the data file
addpath('C:\Users\Nishita\Desktop\Shanti\HEXMC TXT');
no=2;

for i=1:8
i
clear o p t Fr ch6 pks ch6_1 locs pks1 locs1 pks2 locs2 pks3 locs3 i1 i2 ii1 ii2 zeroshift zshift trmax Frmax Frmax1
Fmax
name=sprintf('MAR 15 - Edge - HexMc - %d',i); %creating the name of the data file to be fetched
load(name,'-mat'); %fetching the data file ".mat files"
% hold all;
% plot(t,Fr);
% plot(t,ch6,'r');figure();
% grid on



%Specifying data
dat=xlsread('doe_hexmc.xlsx'); %reading the doe file
t=time;
for k=1:size(dat,1)
if dat(k,1)==i
   m=k;
end
end
res=1.25e-4;
rpm= dat(m,2);
feed= dat(m,3);
gap=(60/rpm); %time gap for each cutter rotation
loc=7; %length of cut in inches

% Finding the peaks in ch6
ch6_1 = ch6(1:2/res);
[pks,locs]=findpeaks(ch6_1,'MinPeakDistance',gap/res-10,'MinPeakHeight',100);
if i==5
   ch6_1=ch6(1:10/res);
   [pks,locs]=findpeaks(ch6_1,'MinPeakDistance',gap/res-100,'MinPeakHeight',100);
   plot(t,ch6)
end
% hold all;
% plot(t(1:2/res),ch6_1,'r');
% plot(t(locs), ch6_1(locs), 'ob');
% figure();

%Zero Shift
i1=1; %starting index of initial zero shift data
i2=locs(1)-gap/res; %end index of initial zero shift data
width=floor( (i2-i1)/(gap/res) );%number of cutter rotations in zero shift data
i3= i1 + width*(gap/res);
```

```
zeroshift=mean(Fr(i1:i3));

if i2<gap/res  %this is different for other variables
   i2=1;
   zeroshift=0;
end
zeroshift=mean(Fr(i1:i2));
zshift(i,1)=zeroshift;
Fr=Fr-zshift(i,1);

% if i==5 %signal at i5 is an exception
%     zeroshift=mean(Fr(i1:i1+gap/res));
% end

% Selecting the cut to be analyzed
cut_gap=60*loc/feed; % Time range for conventional/climb
number=no;
% [pks1,locs1]=findpeaks(Fr,'MinPeakDistance',cut_gap/res);

%Exceptions
if i==1
   clear locs1

locs1=floor([1.259703;18.158992;35.009734;51.90765;68.768376;85.616124;102.438288;119.344815;136.147011;
153.113815;169.715587
]/res);
elseif i==2
    clear locs1
    locs1=floor([0.253838;84.632597;168.540621;252.873955]/res);
elseif i==3
    clear locs1

locs1=floor([1.352303;18.241857;35.042805;51.899913;68.860726;85.648696;102.530368;119.357794;136.259453
;153.096718;169.837764]/res);
elseif i==4
    clear locs1
    locs1=floor([0.363534;84.226382;168.543117;252.692999]/res);
elseif i==5
   clear locs1
   locs1=floor(([9.9244498;94.217022;178.448646;262.491951])/res);
elseif i==6
    clear locs1

locs1=floor([0.011856;16.860726;33.726195;50.559341;67.455759;84.287158;101.184575;118.079246;134.925621
;151.807188;168.403345]/res);
elseif i==7
    clear locs1

locs1=floor([0.0463;16.702359;33.540122;50.434793;67.273056;84.162112;101.00287;117.890428;134.736553;15
1.618245;167.976164]/res);
elseif i==8
    clear locs1
    locs1=floor([0.025708;83.450768;167.801572;251.843754]/res);
end
```

```
ii1=locs1(number)+1/res;
ii2=locs1(number+1)-1/res;

[pks2,locs2]=findpeaks(ch6(ii1:ii2),'MinPeakDistance',gap/res-10,'MinPeakHeight',100);
if i==5
   [pks2,locs2]=findpeaks(ch6(ii1:ii2),'MinPeakDistance',gap/res-100,'MinPeakHeight',100);
end
hold all;
% plot(t(ii1:ii2),ch6(ii1:ii2),'r',t(locs2+ii1-1),ch6(locs2+ii1-1),'ob');figure();

%selecting maximum value in the identified range
Fmax=max(Fr(ii1:ii2));

%selecting maximum value in each cutter rotation
locs3=locs2+ii1-1;
for o=2:length(locs3)
   [Frmax1 p]=max(Fr(locs3(o-1):locs3(o)));
   Frmax(o-1)=Frmax1;
   index(o-1)=locs3(o-1)+p;
   trmax(o-1)=t(index(o-1));
end

% hold all
% grid on
% plot(trmax,Frmax);
% legend(name);figure();
dat1=xlsread('zshift.xlsx');

FRavg(i,1)=mean(Frmax)
FR_actual(i,1)=FRavg(i,1)-dat1(i,6);
% FRmax(i,1)=Fmax
end


FF(:,1)=FR_actual(:,1);
% FF(:,2)=FRmax(:,1);
save Force_Fr.dat FF -ASCII
```

Appendix - C - CFRP End milling Dynoware Graphs

Experiment 1 : Speed - 6000 rpm; Feed - 635 mmpm; Depth Of Cut - 6.35 mm;

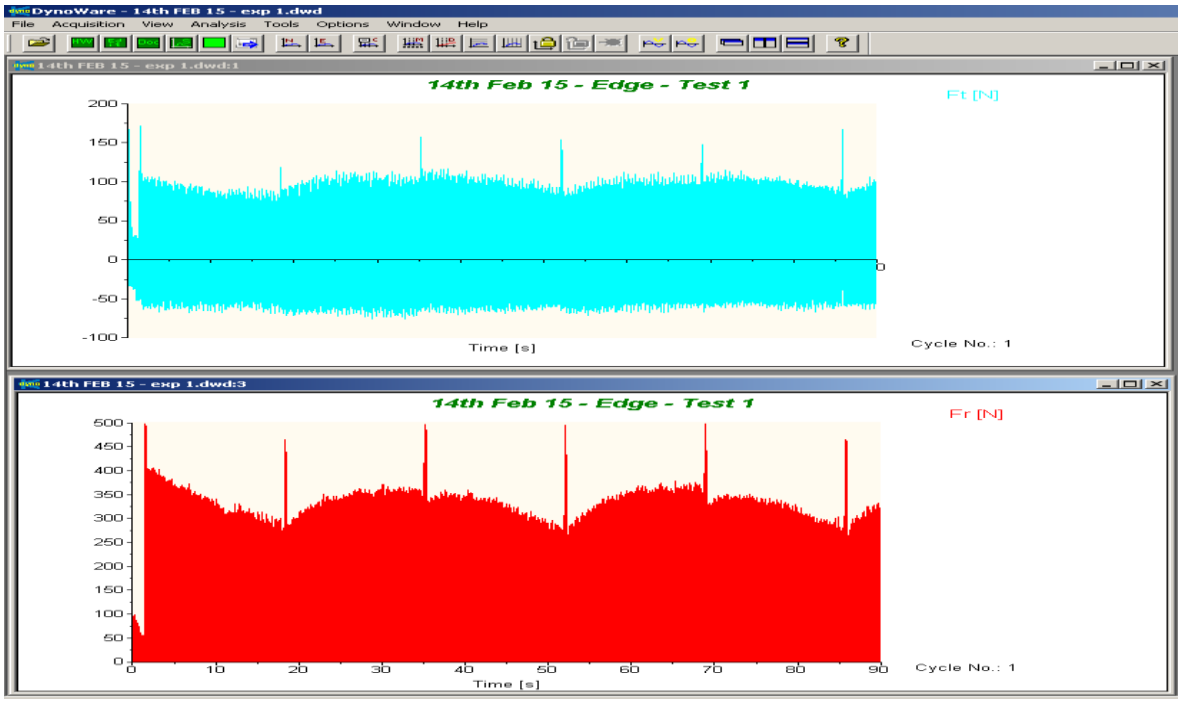

Experiment 2 : Speed - 6000 rpm; Feed - 635 mmpm; Depth Of Cut - 3.81 mm;

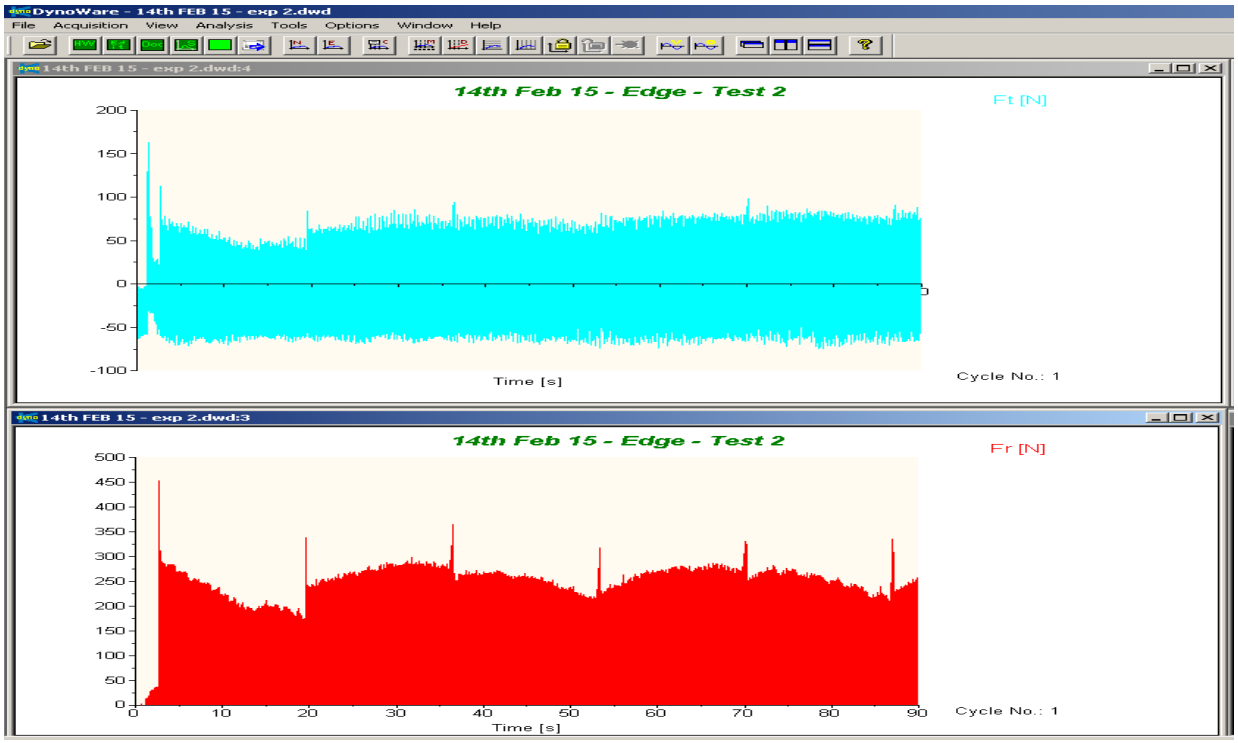

Experiment 3 : Speed - 3000 rpm; Feed - 635 mmpm; Depth Of Cut - 3.81 mm;

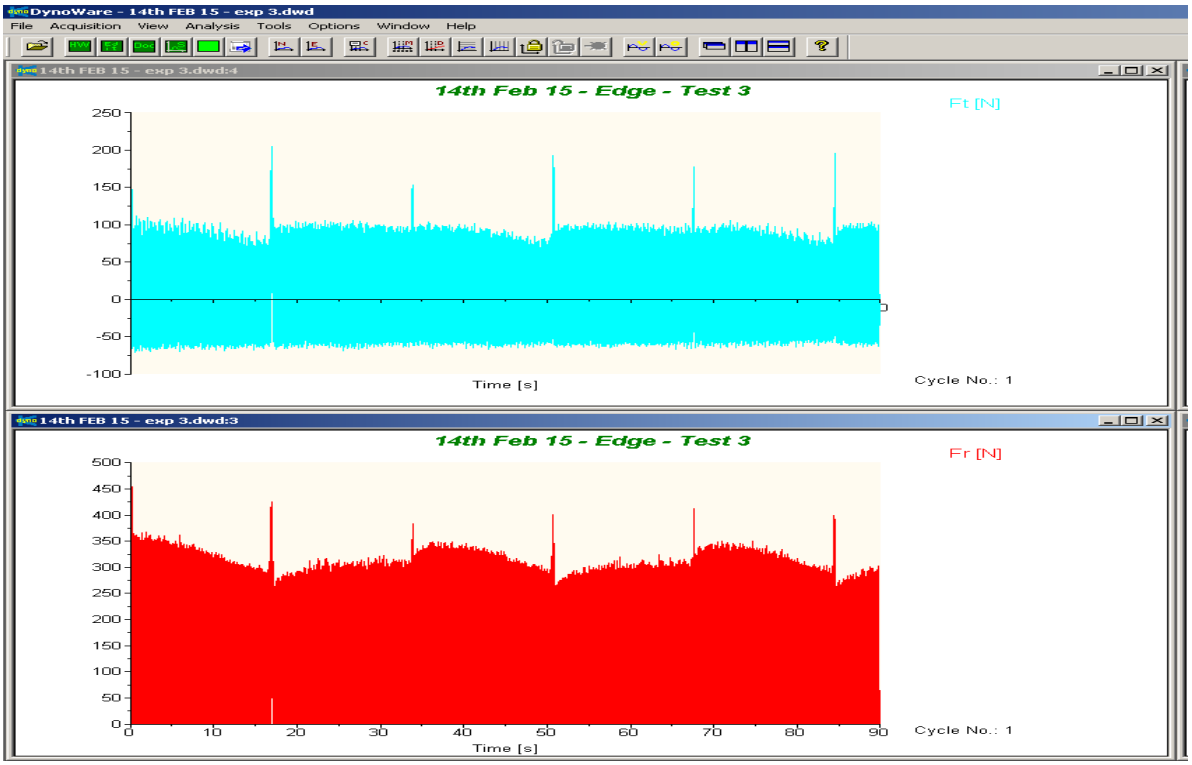

Experiment 4 : Speed - 6000 rpm; Feed - 635 mmpm; Depth Of Cut - 2.54 mm;

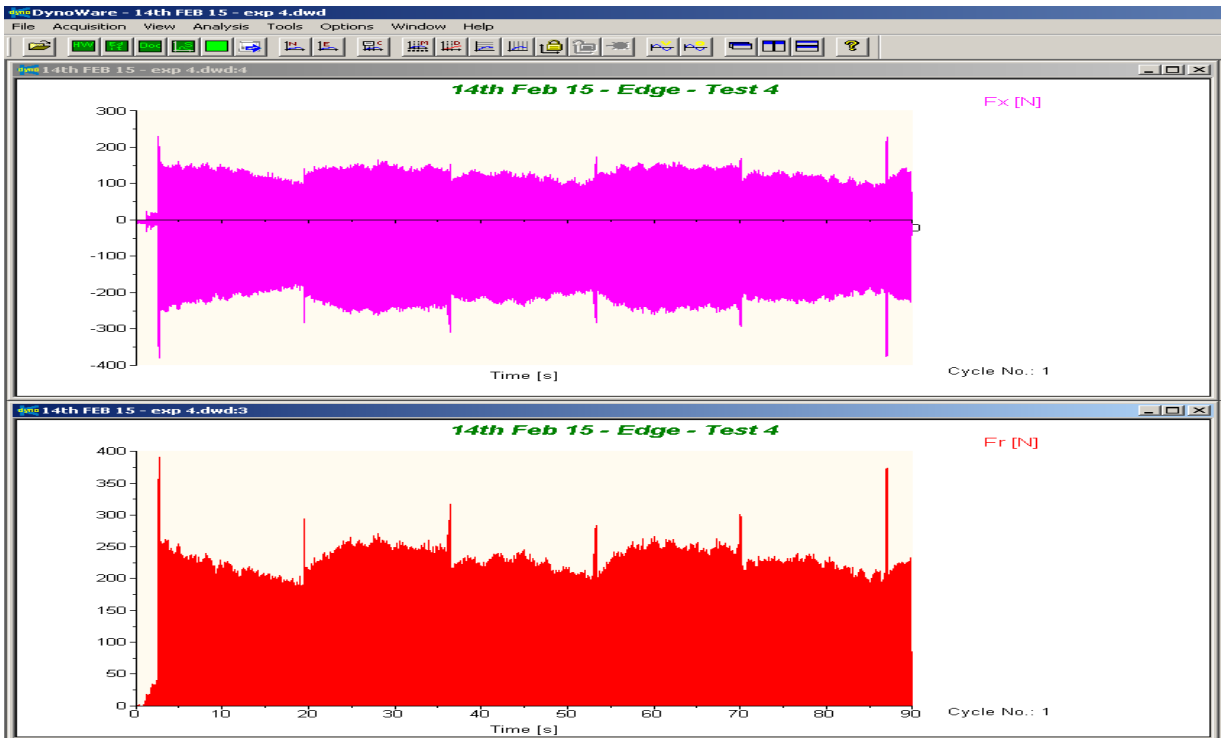

Experiment 5 : Speed - 3000 rpm; Feed - 635 mmpm; Depth Of Cut - 2.54 mm;

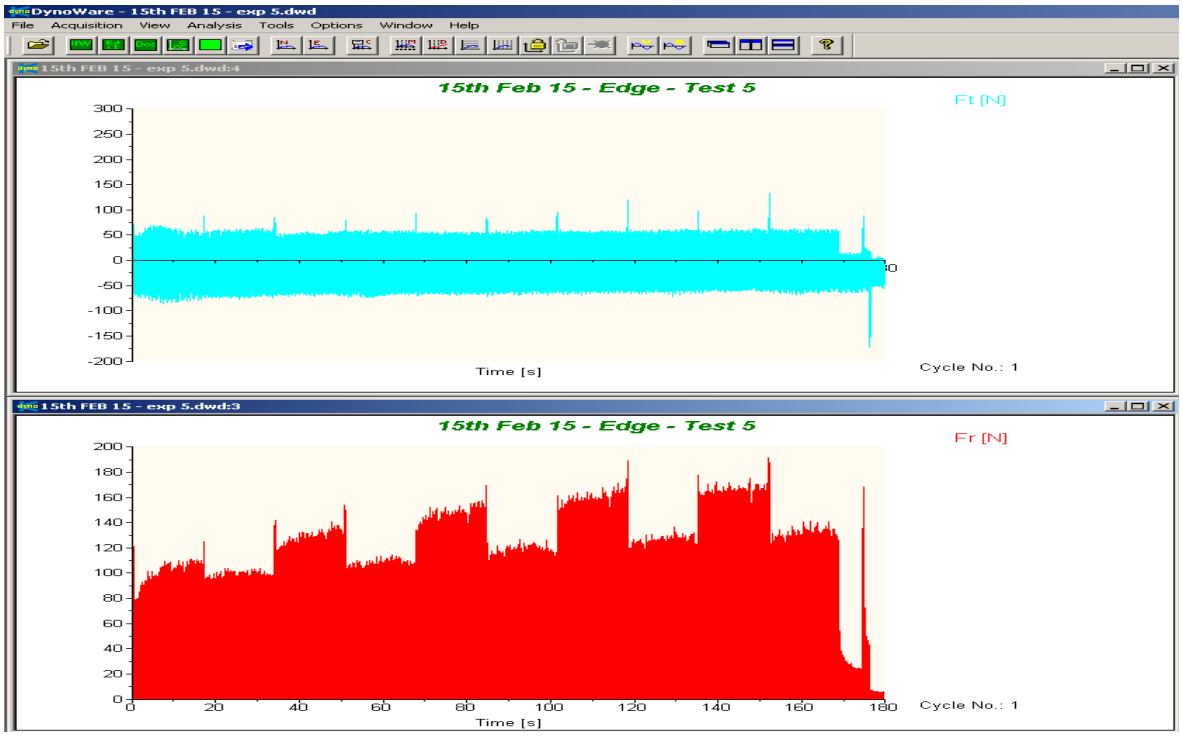

Experiment 6 : Speed - 1000 rpm; Feed - 635 mmpm; Depth Of Cut - 2.54 mm;

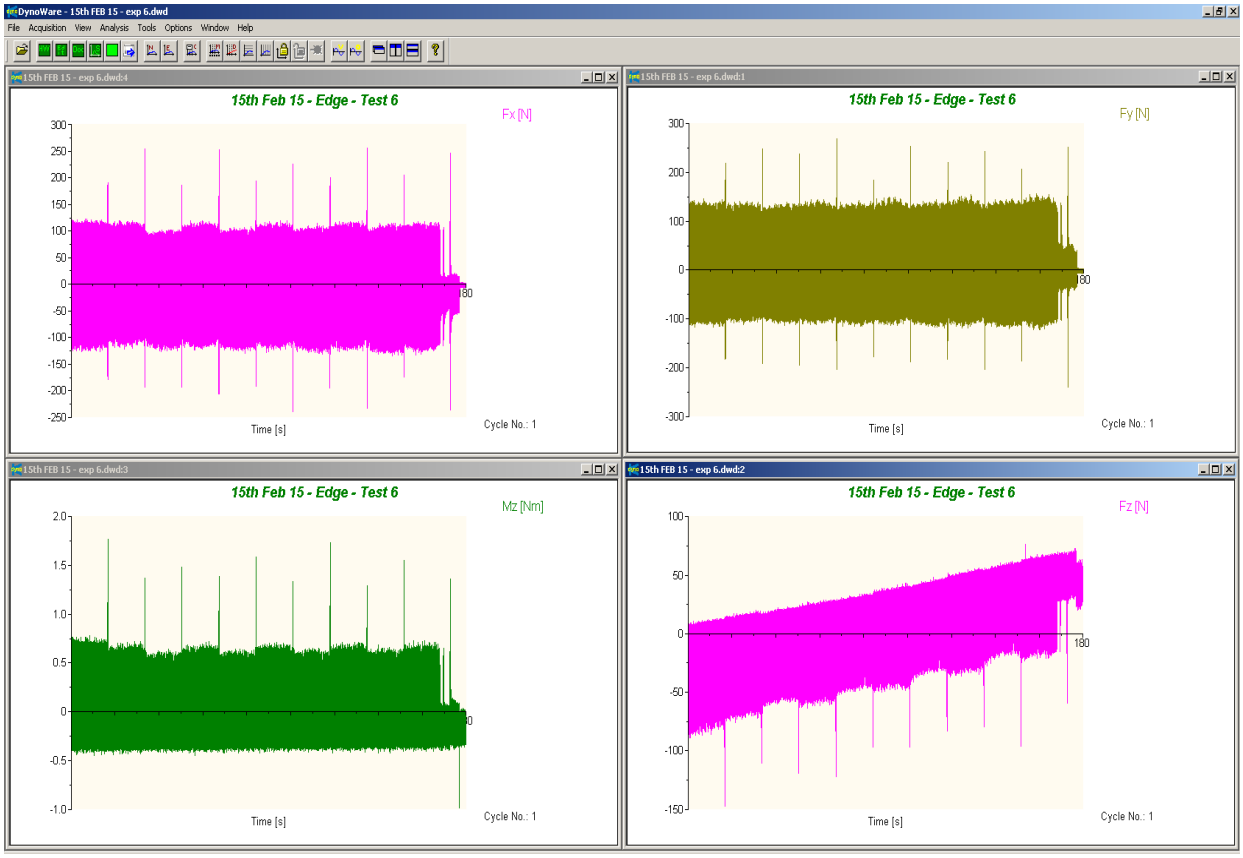

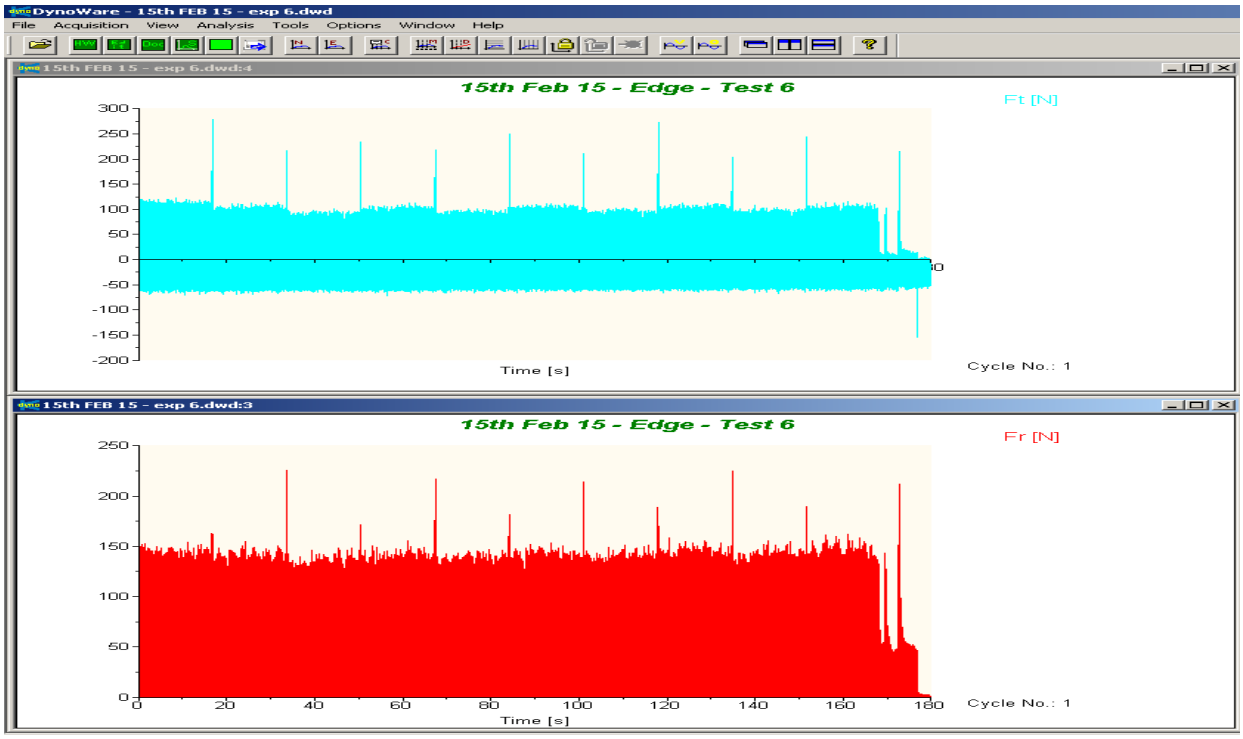

Experiment 7 : Speed - 1000 rpm; Feed - 635 mmpm; Depth Of Cut - 6.35 mm;

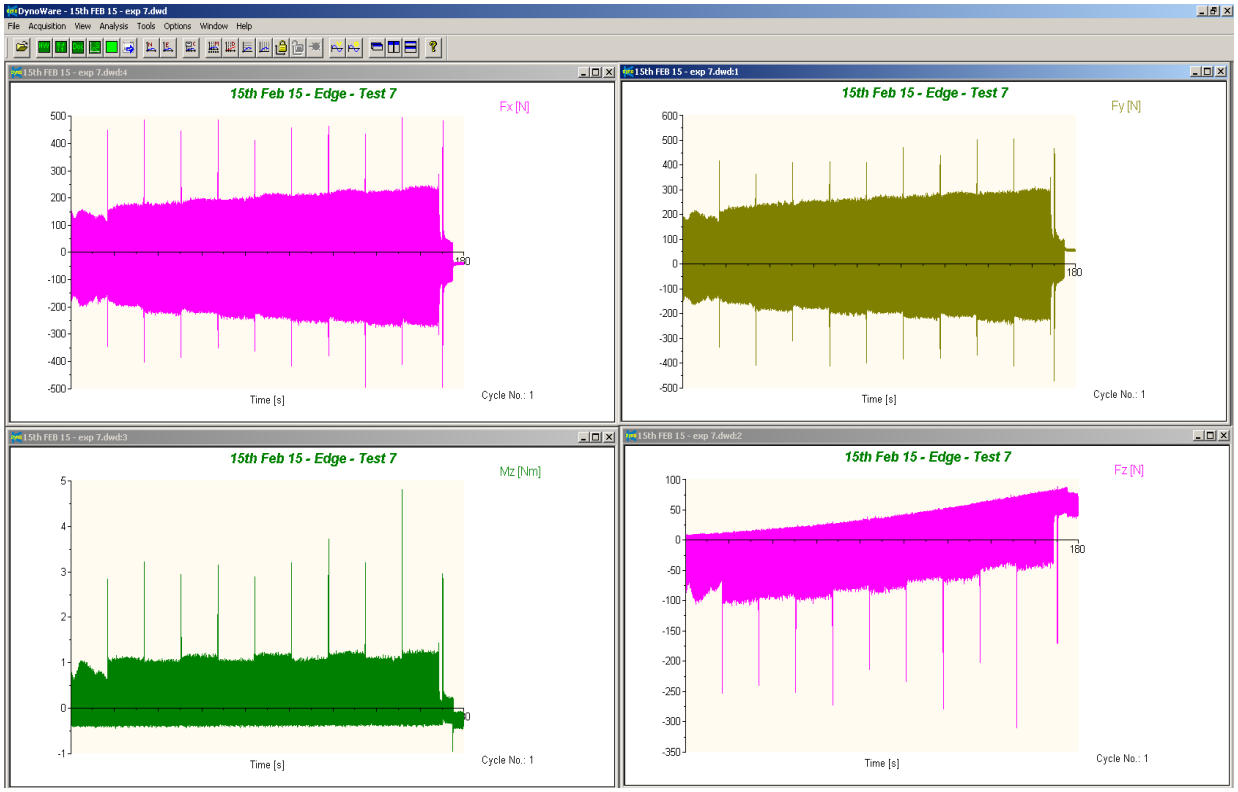

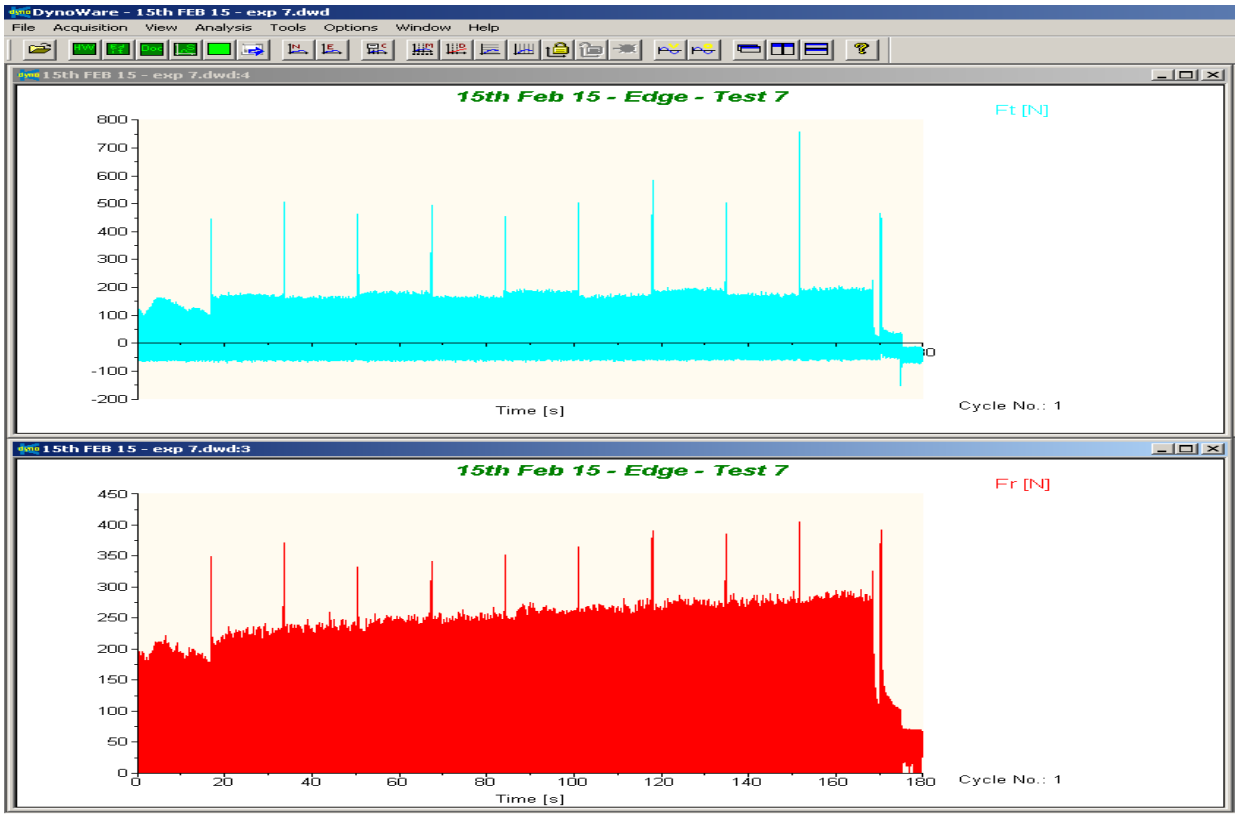

Experiment 8 : Speed - 1000 rpm; Feed - 635 mmpm; Depth Of Cut - 3.81 mm;

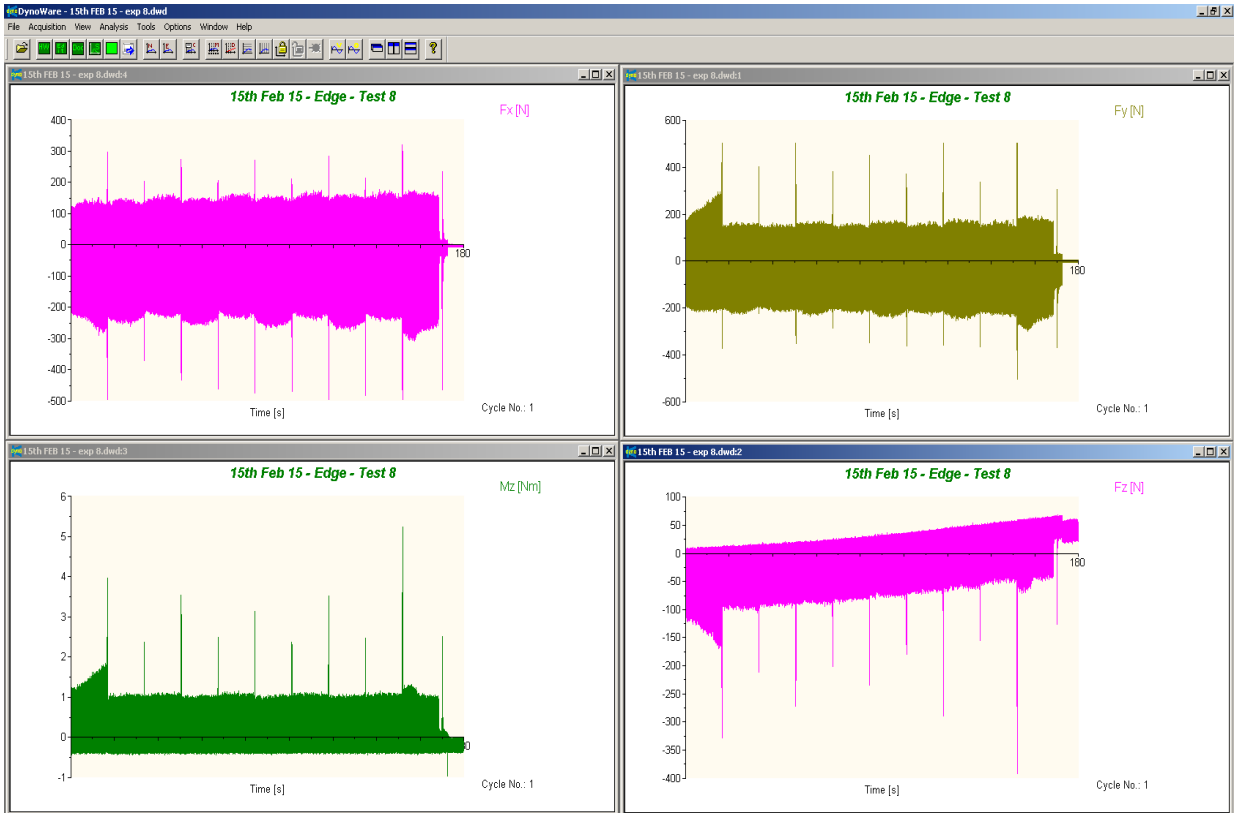

Experiment 9 : Speed - 6000 rpm; Feed - 381 mmpm; Depth Of Cut - 6.35 mm;

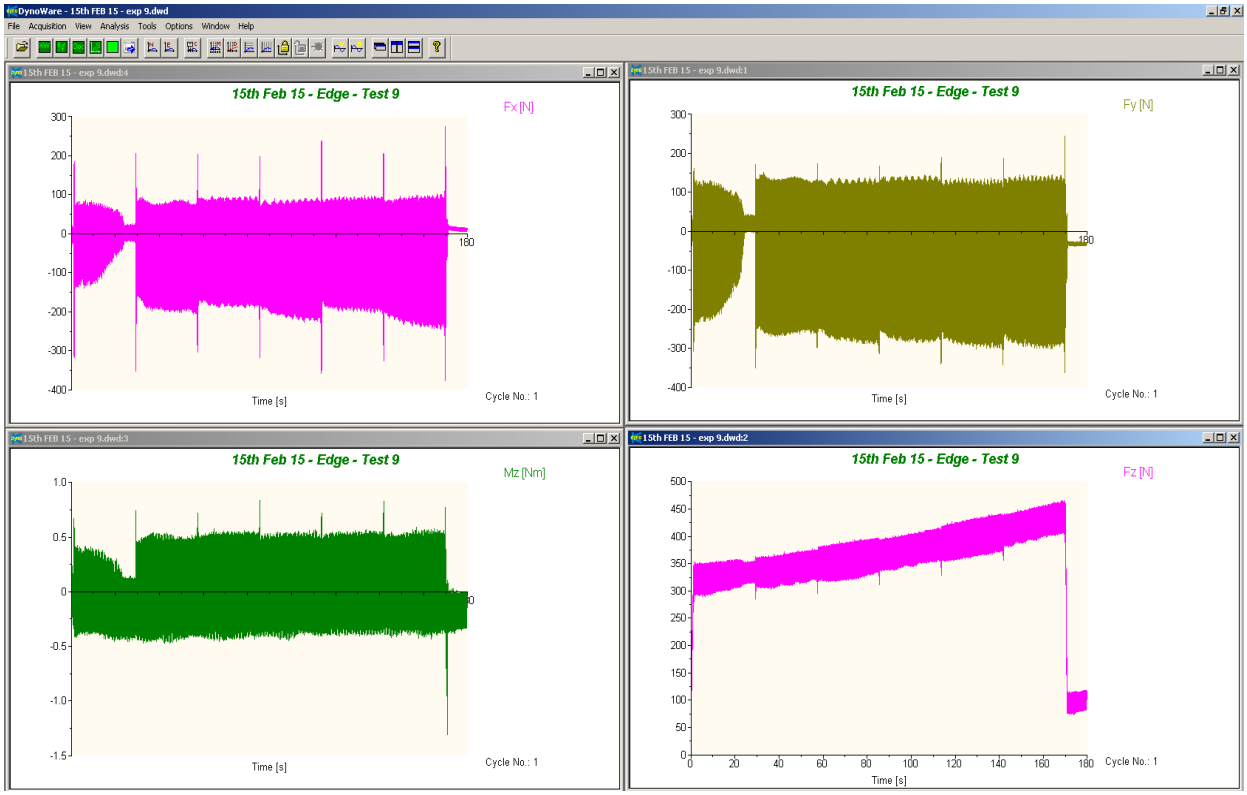

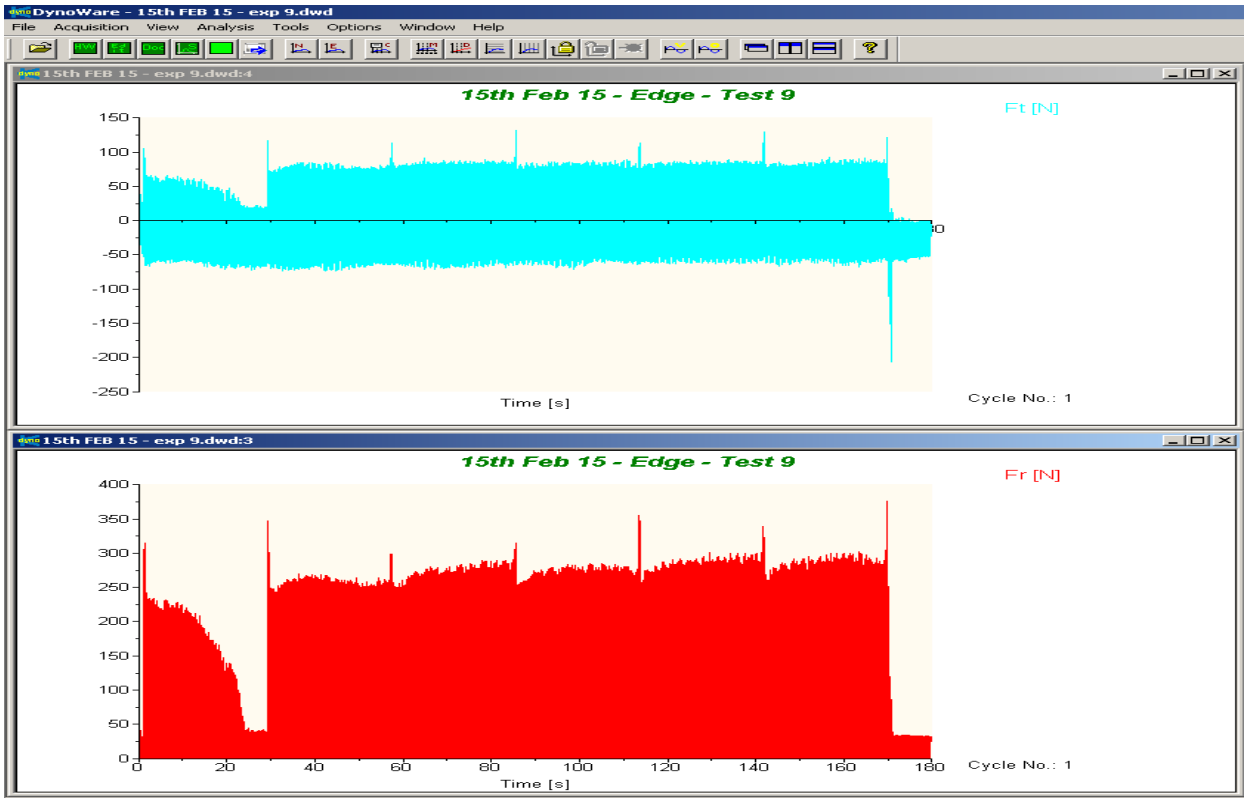

Experiment 10 : Speed - 6000 rpm; Feed - 381 mmpm; Depth Of Cut - 3.81 mm;

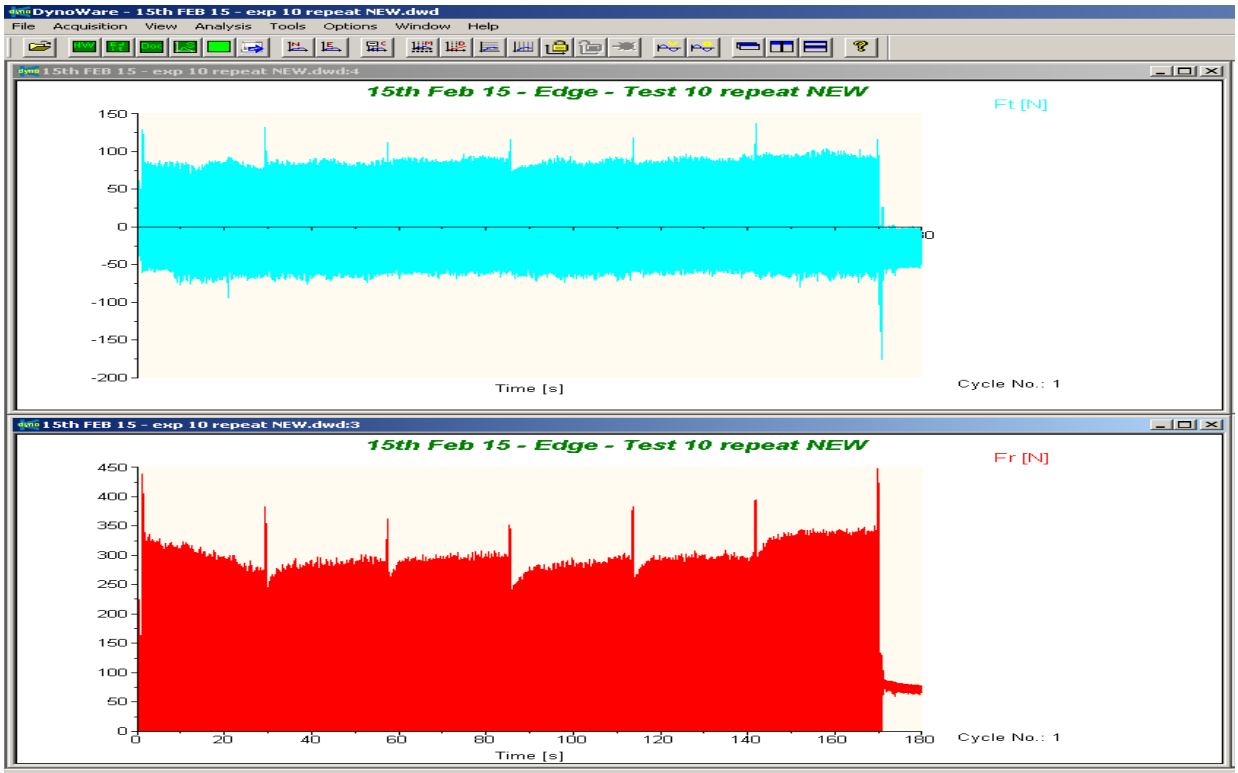

Experiment 11 : Speed - 6000 rpm; Feed - 381 mmpm; Depth Of Cut - 2.54 mm;

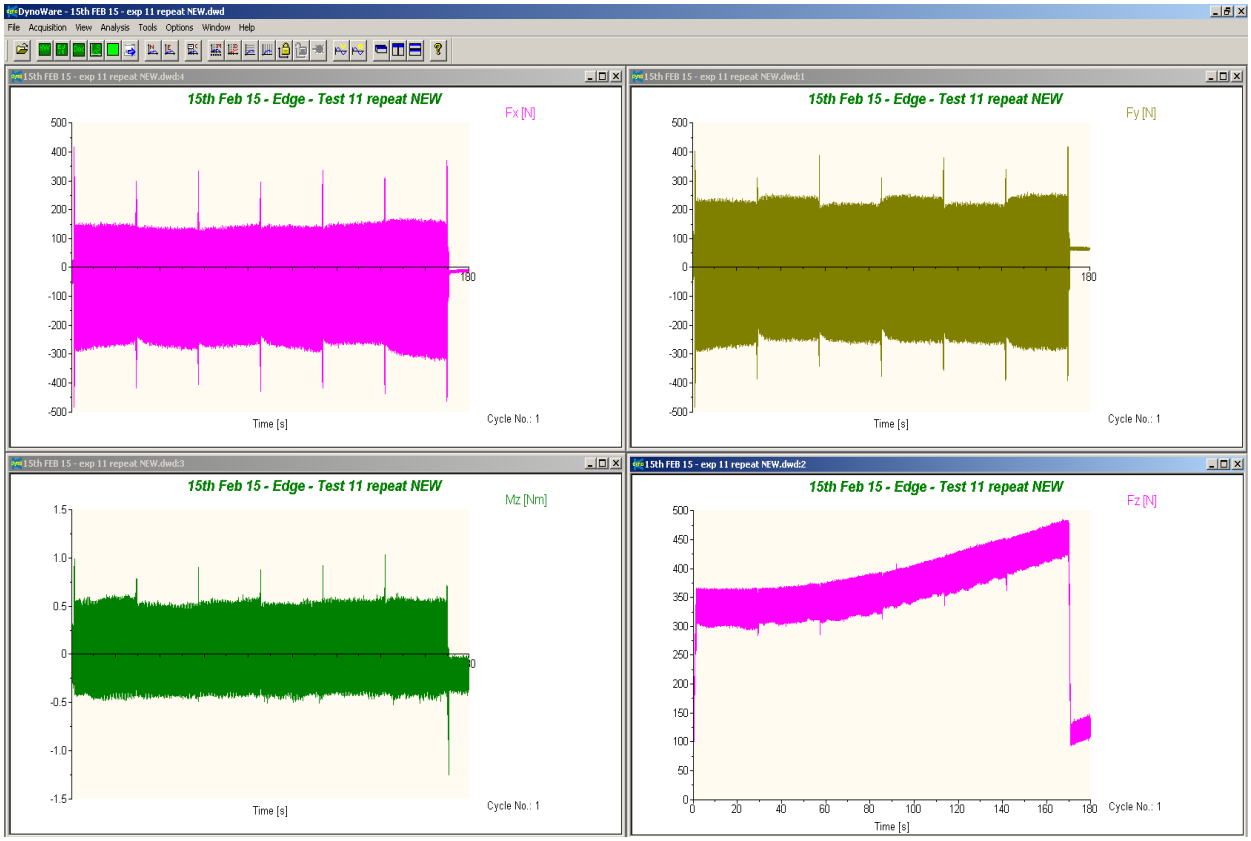

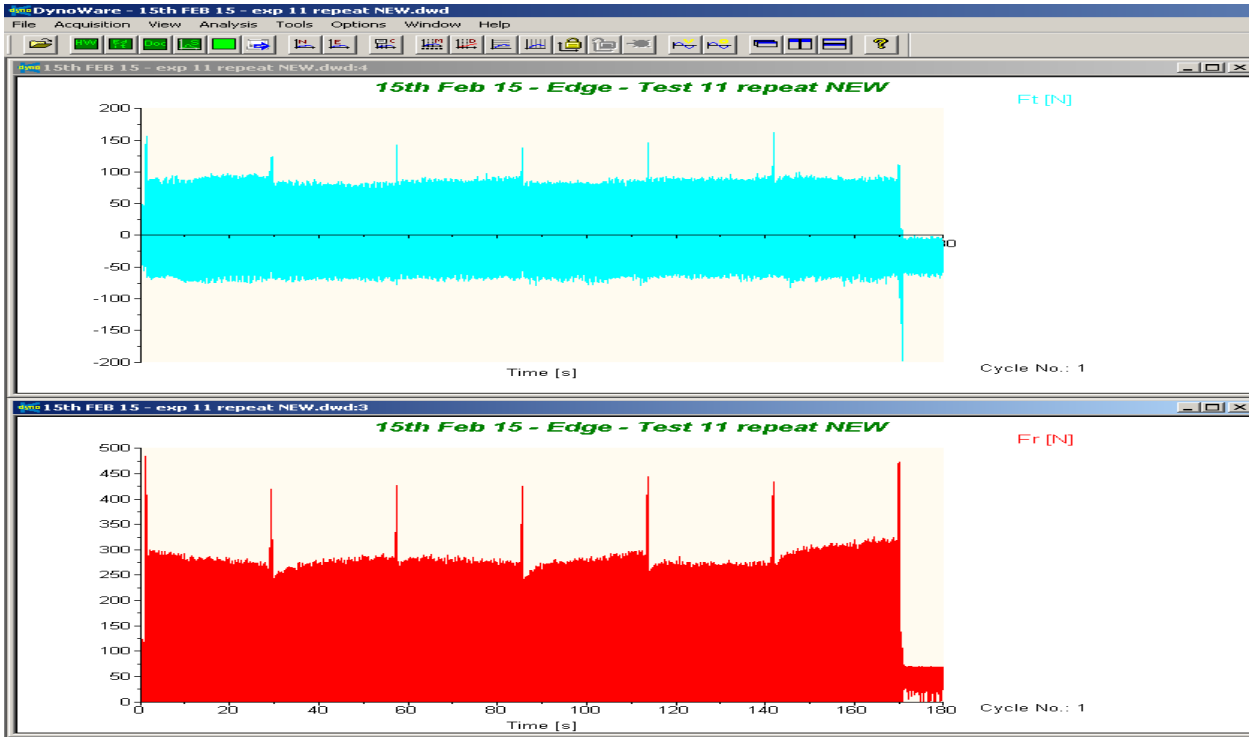

Experiment 12 : Speed - 3000 rpm; Feed - 381 mmpm; Depth Of Cut - 6.35 mm;

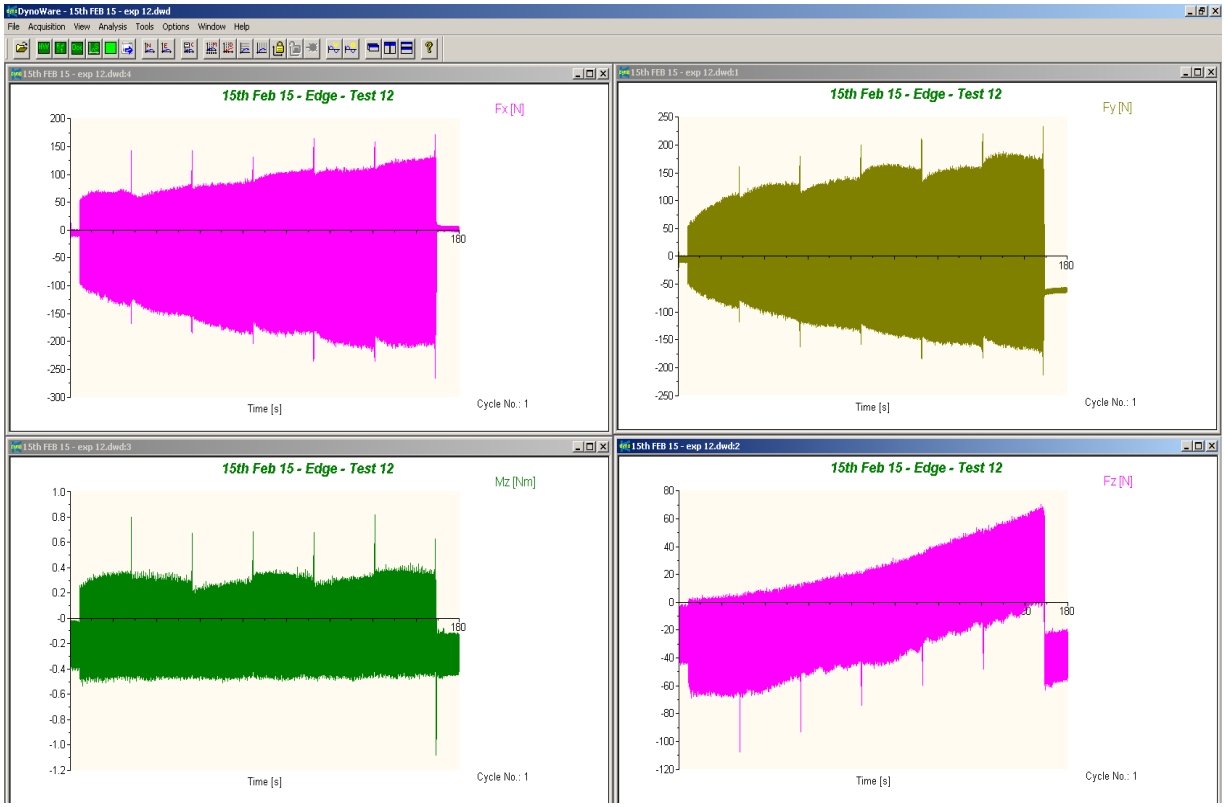

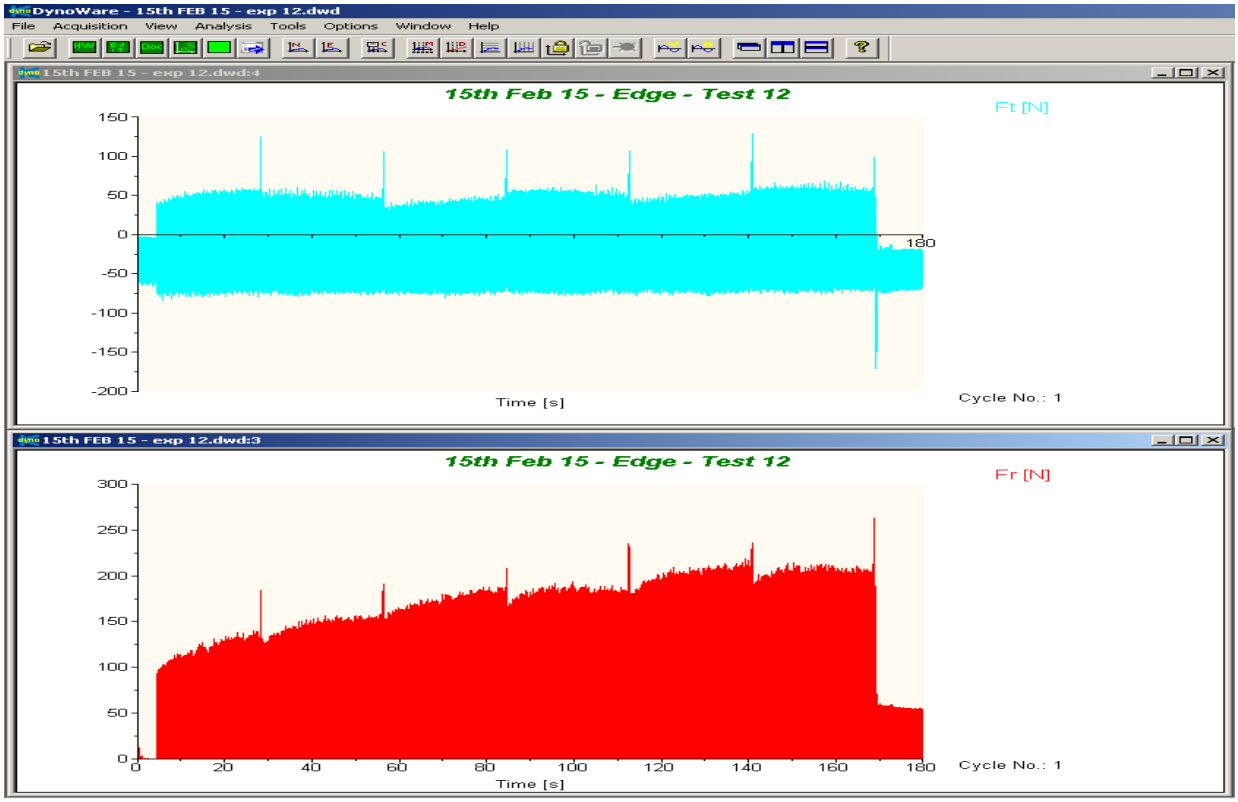

Experiment 13 : Speed - 3000 rpm; Feed - 381 mmpm; Depth Of Cut - 3.81 mm;

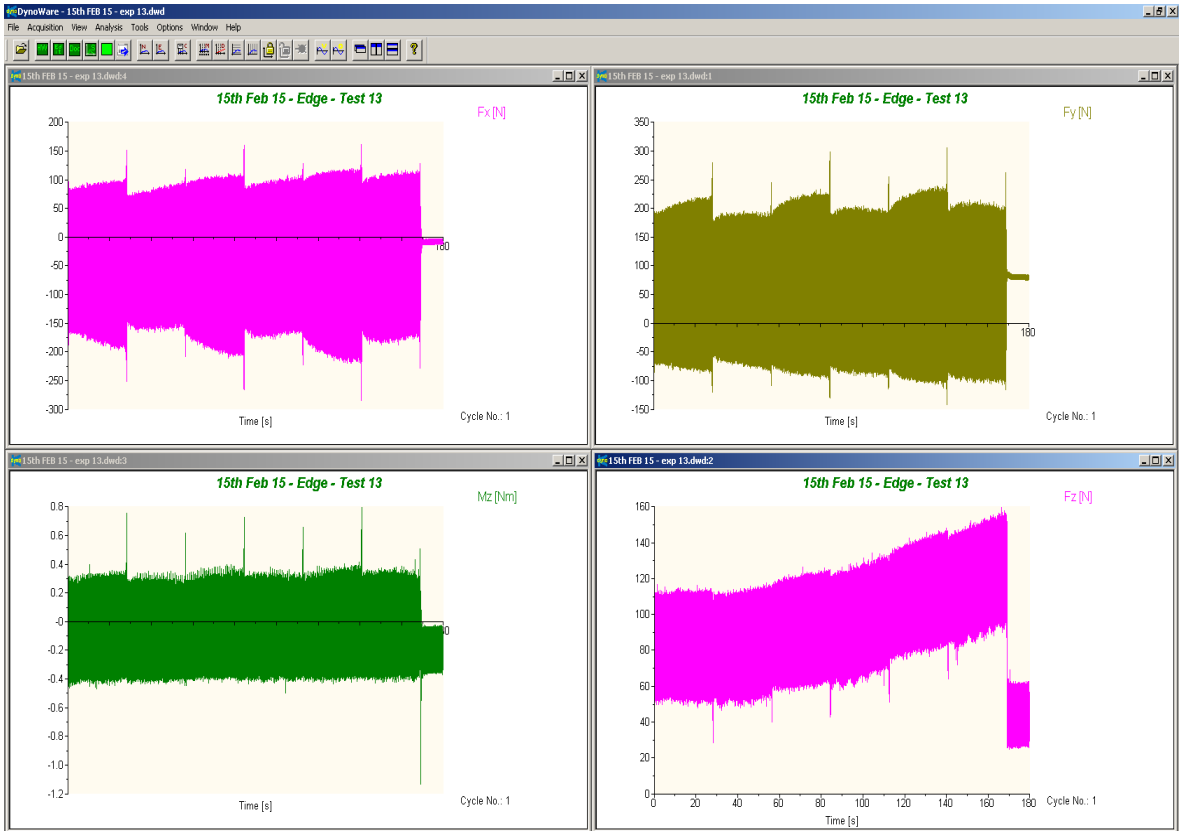

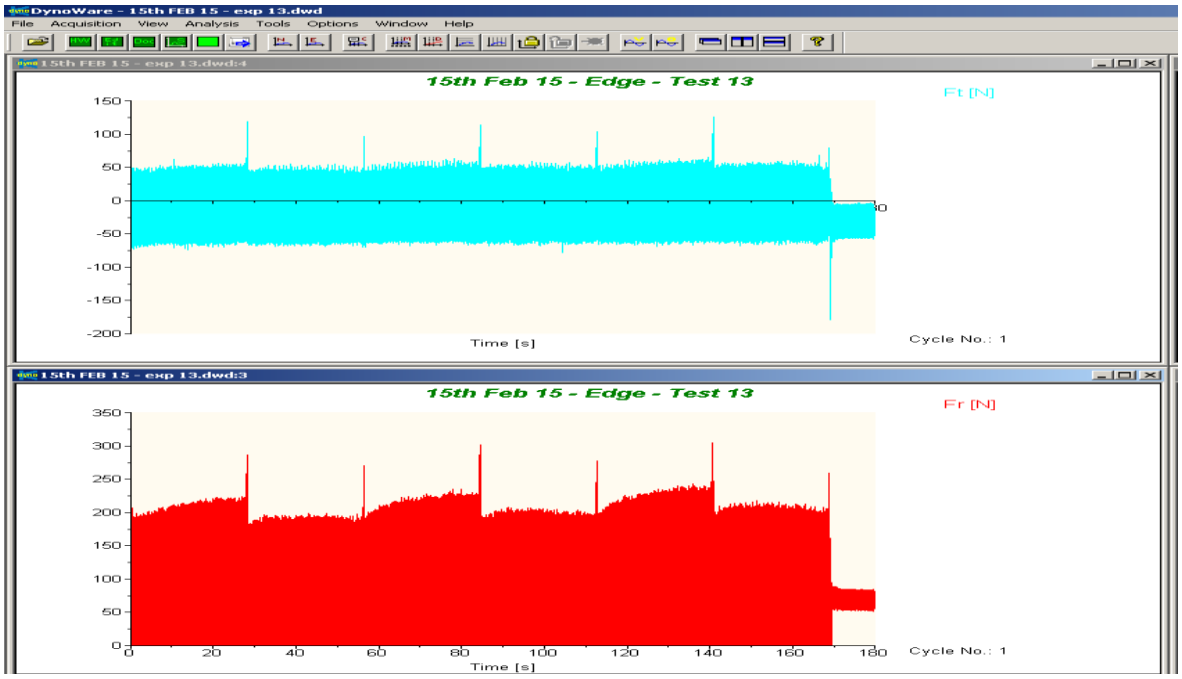

Experiment 14 : Speed - 3000 rpm; Feed - 381 mmpm; Depth Of Cut - 2.54 mm;

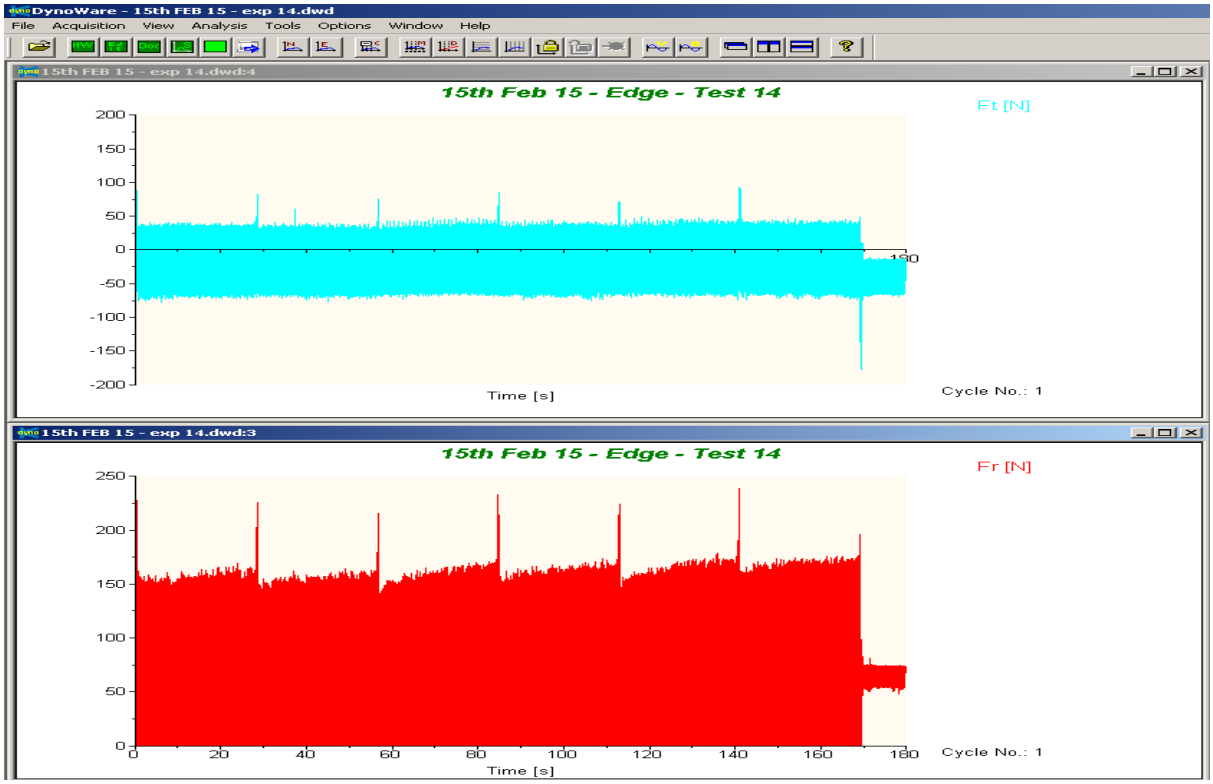

Experiment 15 : Speed - 1000 rpm; Feed - 381 mmpm; Depth Of Cut - 2.54 mm;

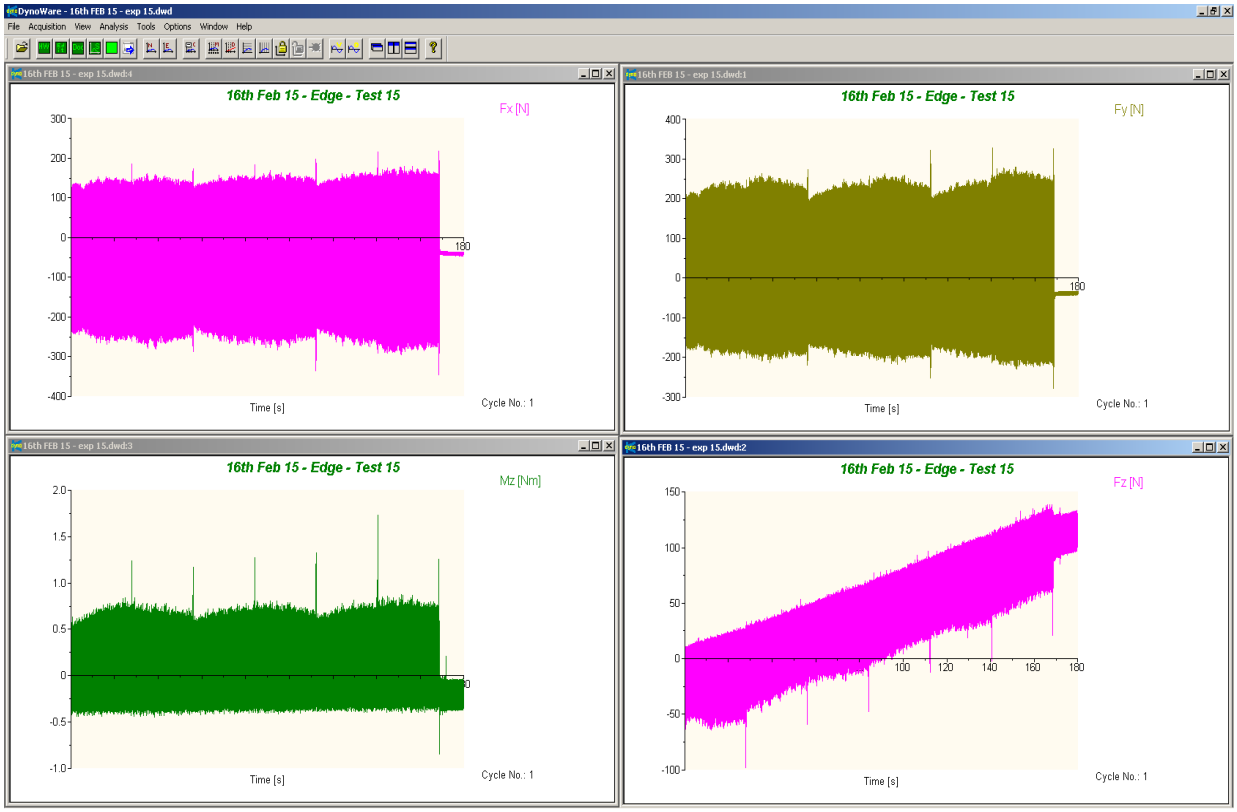

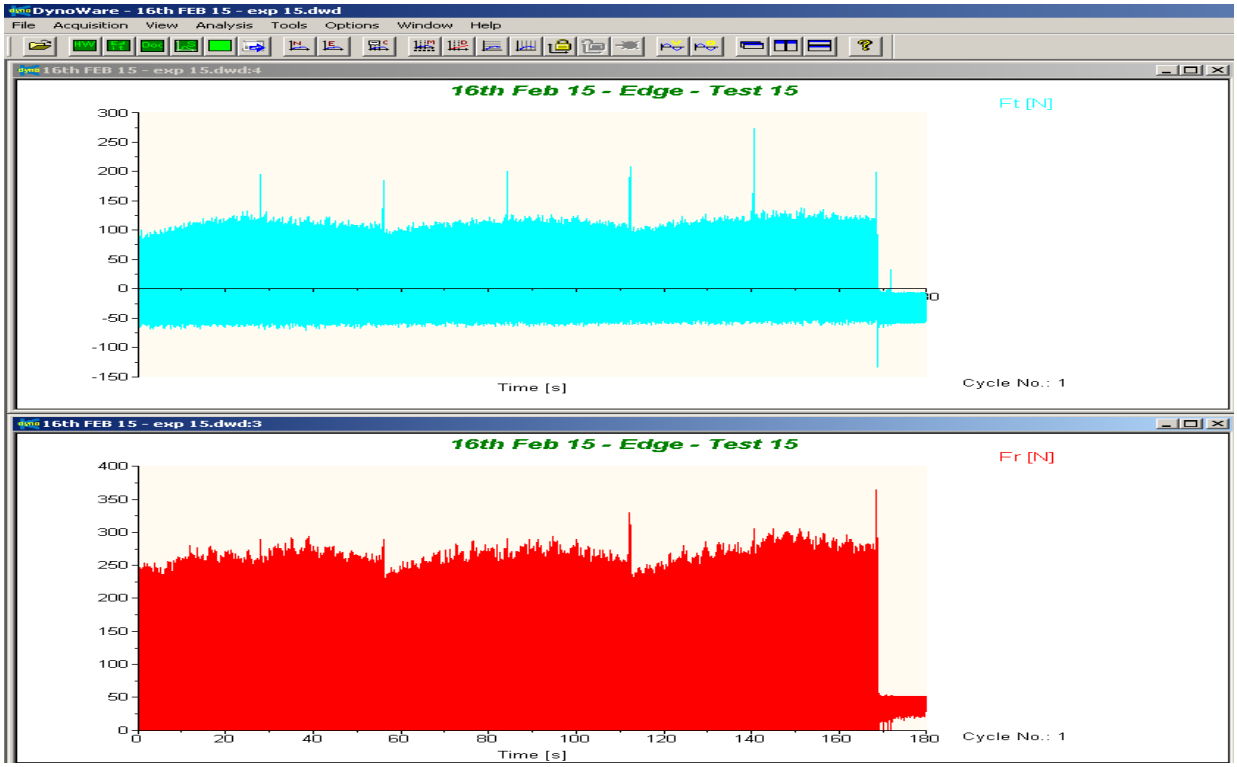

Experiment 16 : Speed - 1000 rpm; Feed - 381 mmpm; Depth Of Cut - 6.35 mm;

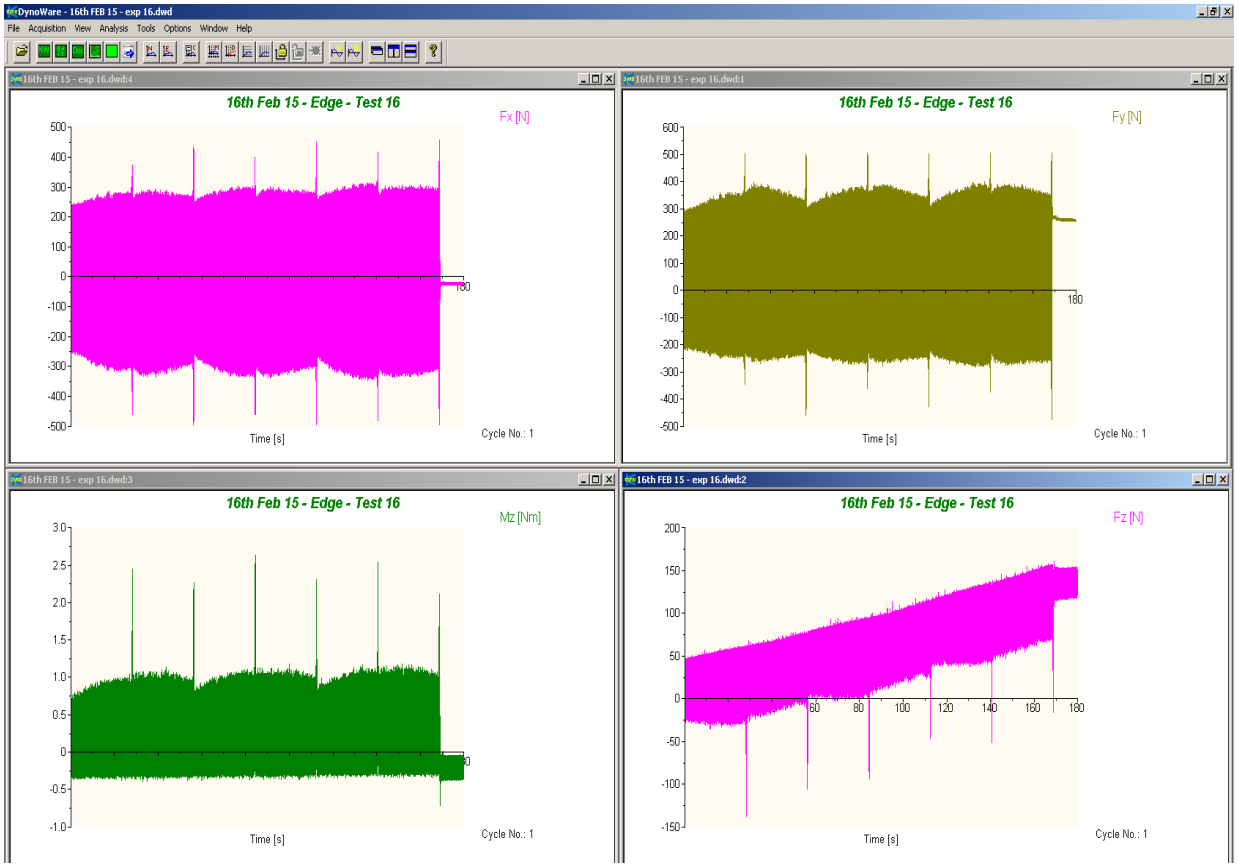

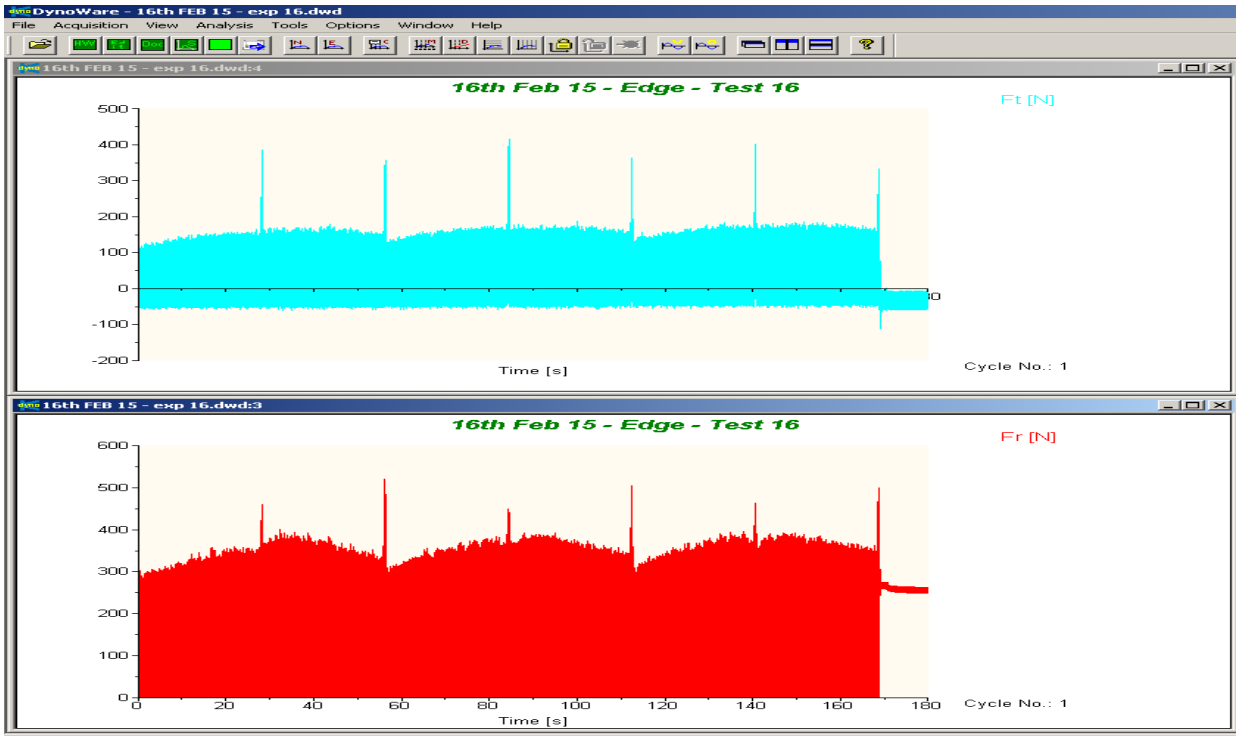

Experiment 17 : Speed - 6000 rpm; Feed - 127 mmpm; Depth Of Cut - 3.81 mm;

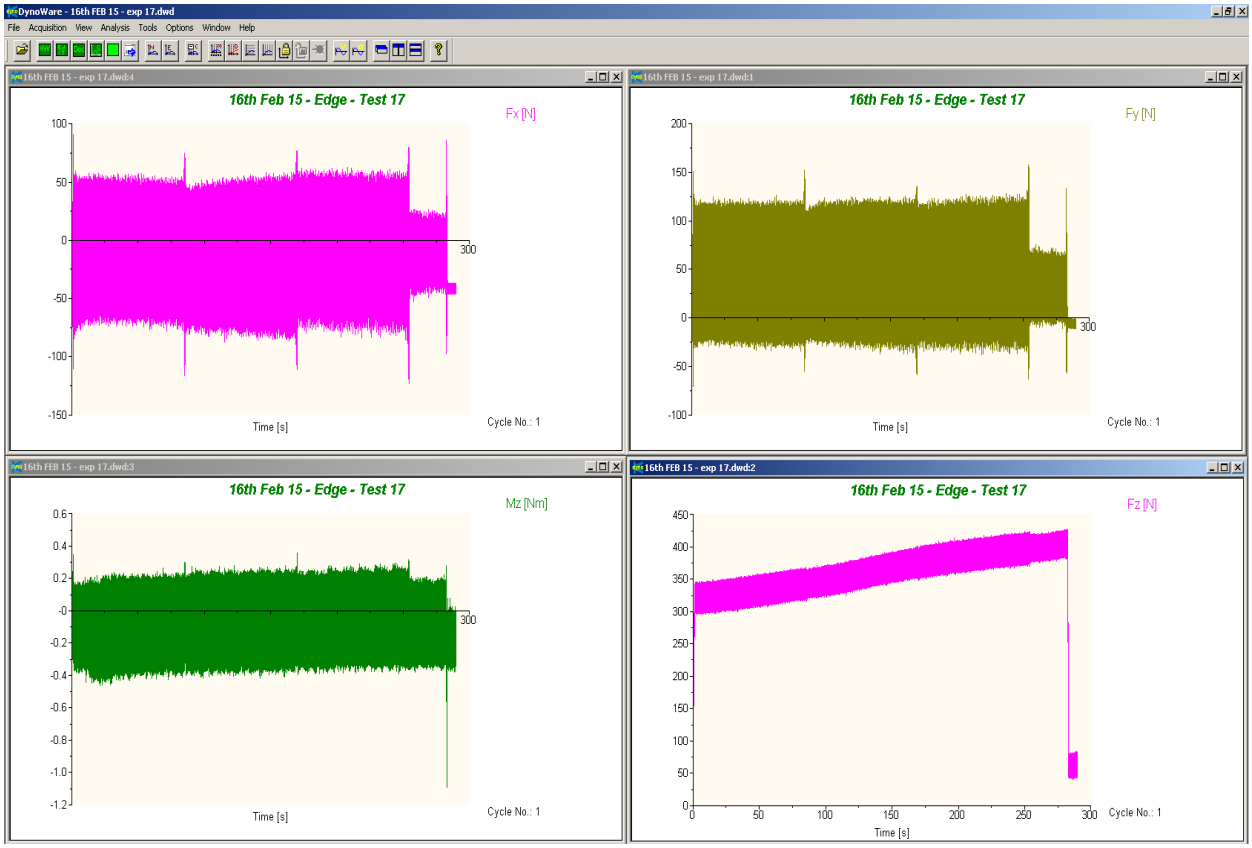

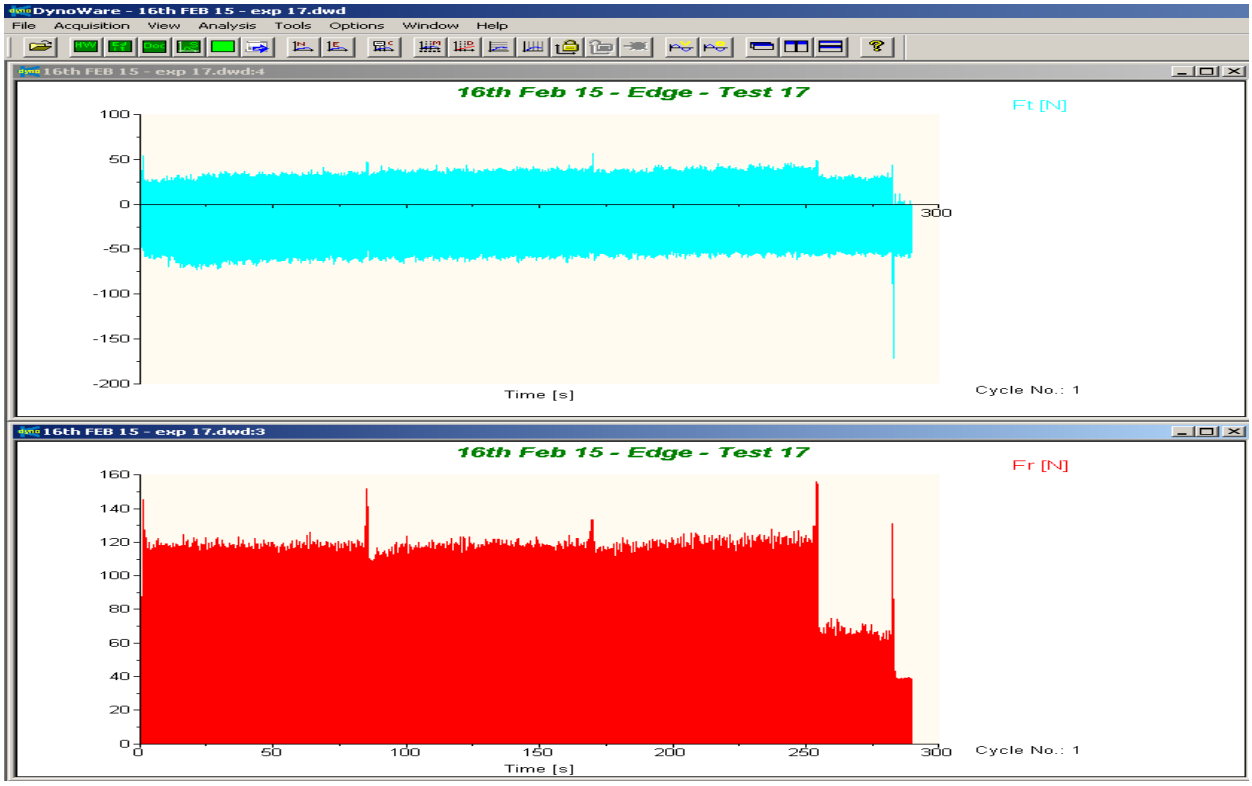

Experiment 18 : Speed - 3000 rpm; Feed - 127 mmpm; Depth Of Cut - 3.81 mm;

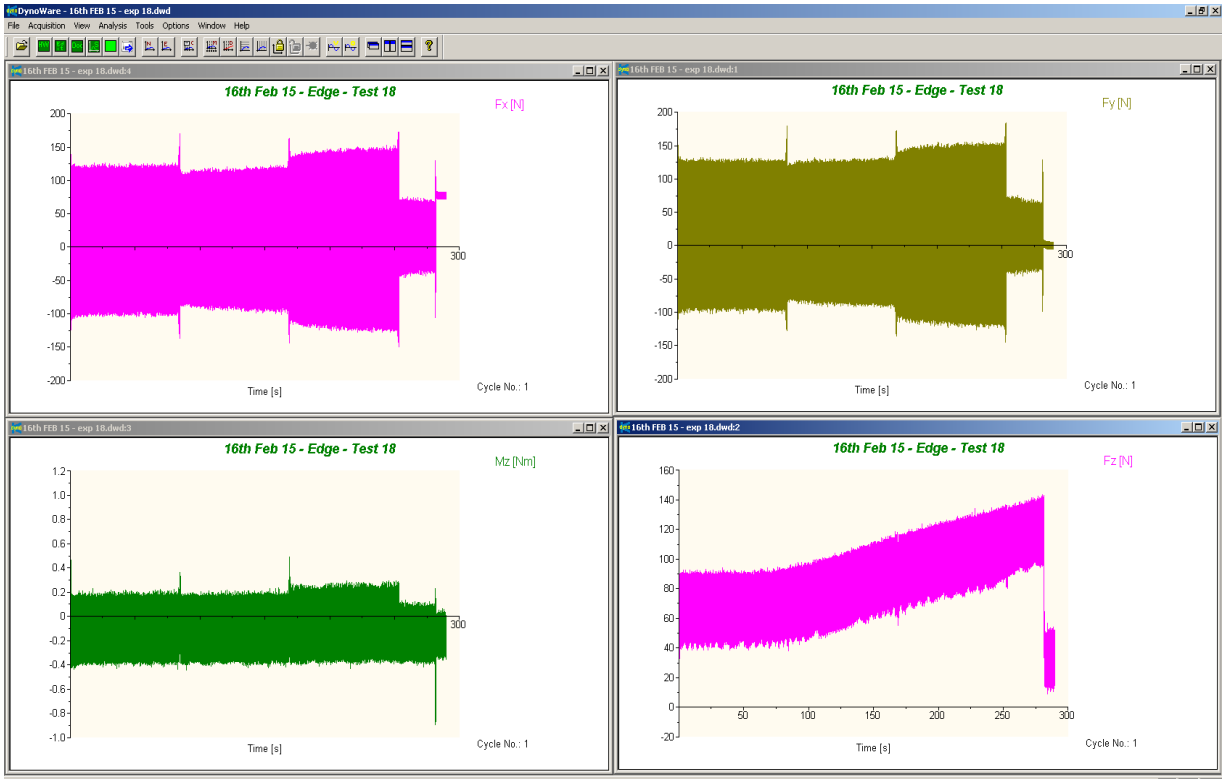

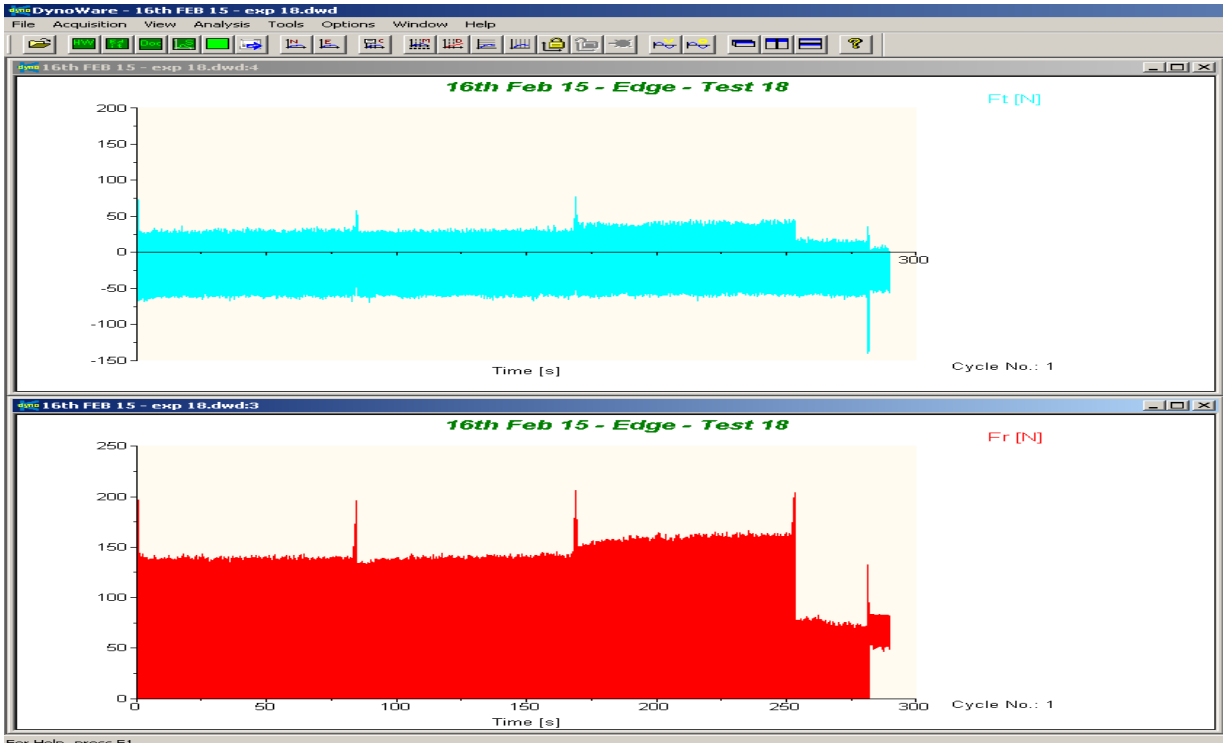

Experiment 19 : Speed - 1000 rpm; Feed - 127 mmpm; Depth Of Cut - 3.81 mm;

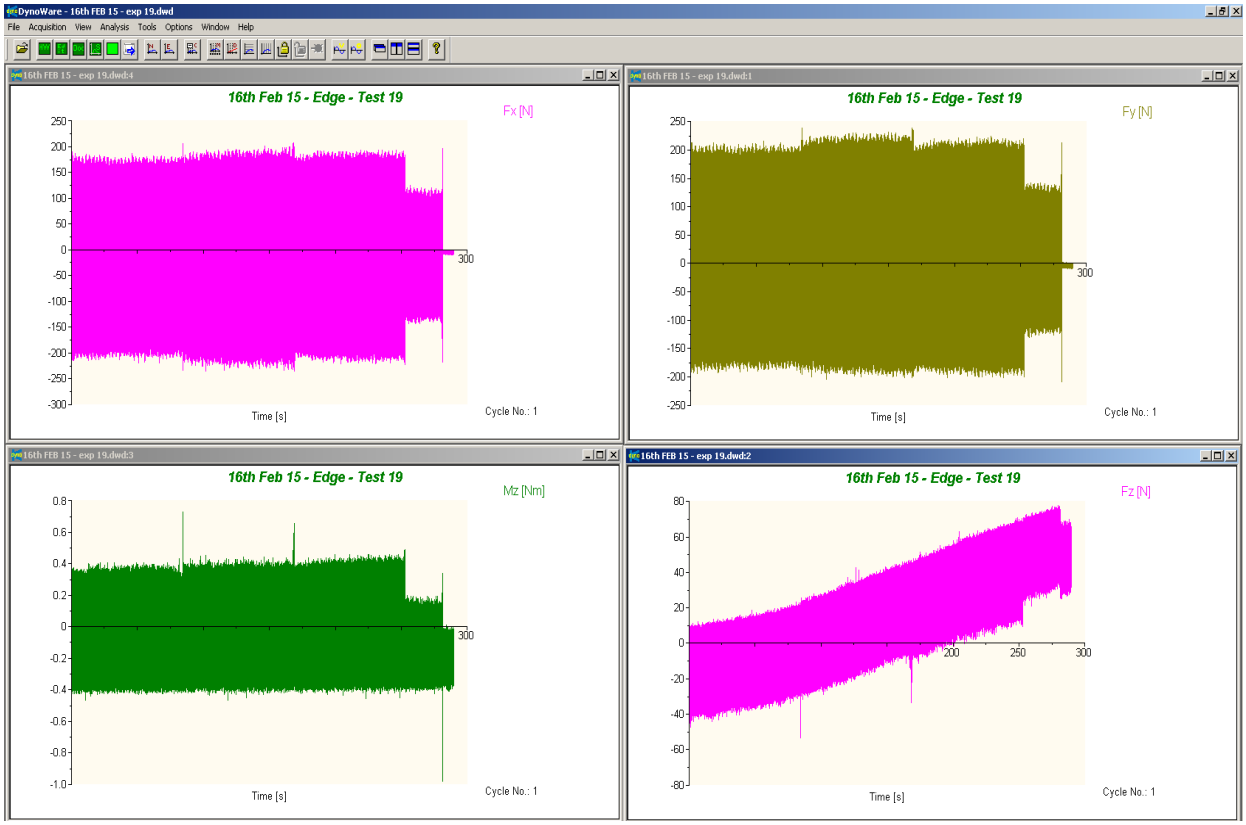

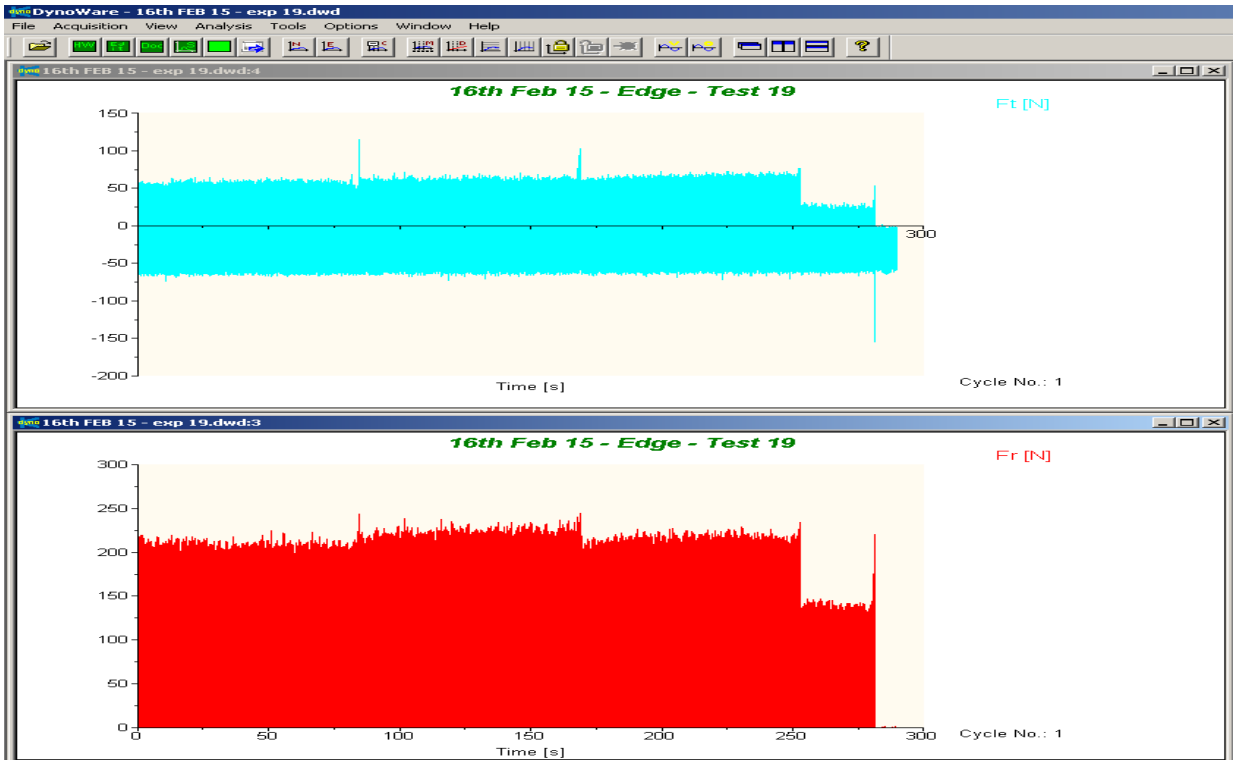

Experiment 20 : Speed - 1000 rpm; Feed - 127 mmpm; Depth Of Cut - 2.54 mm;

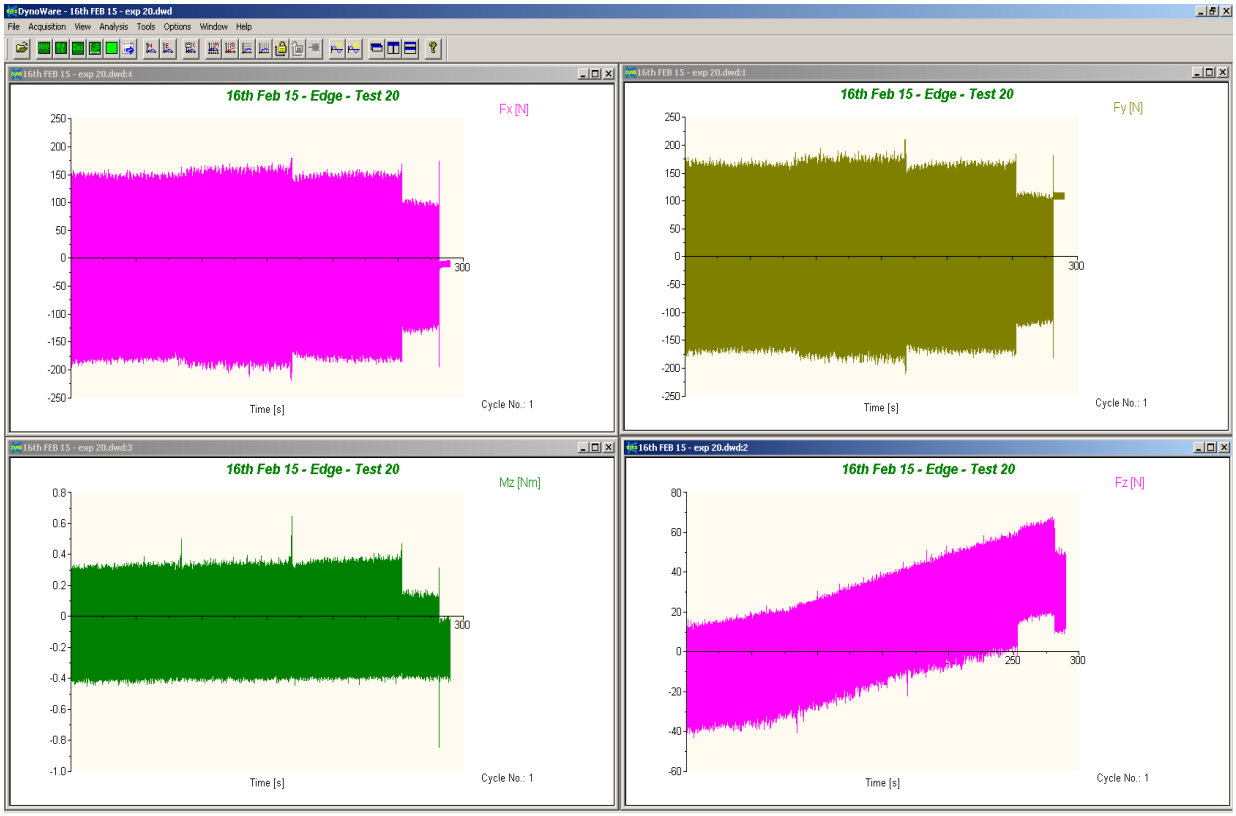

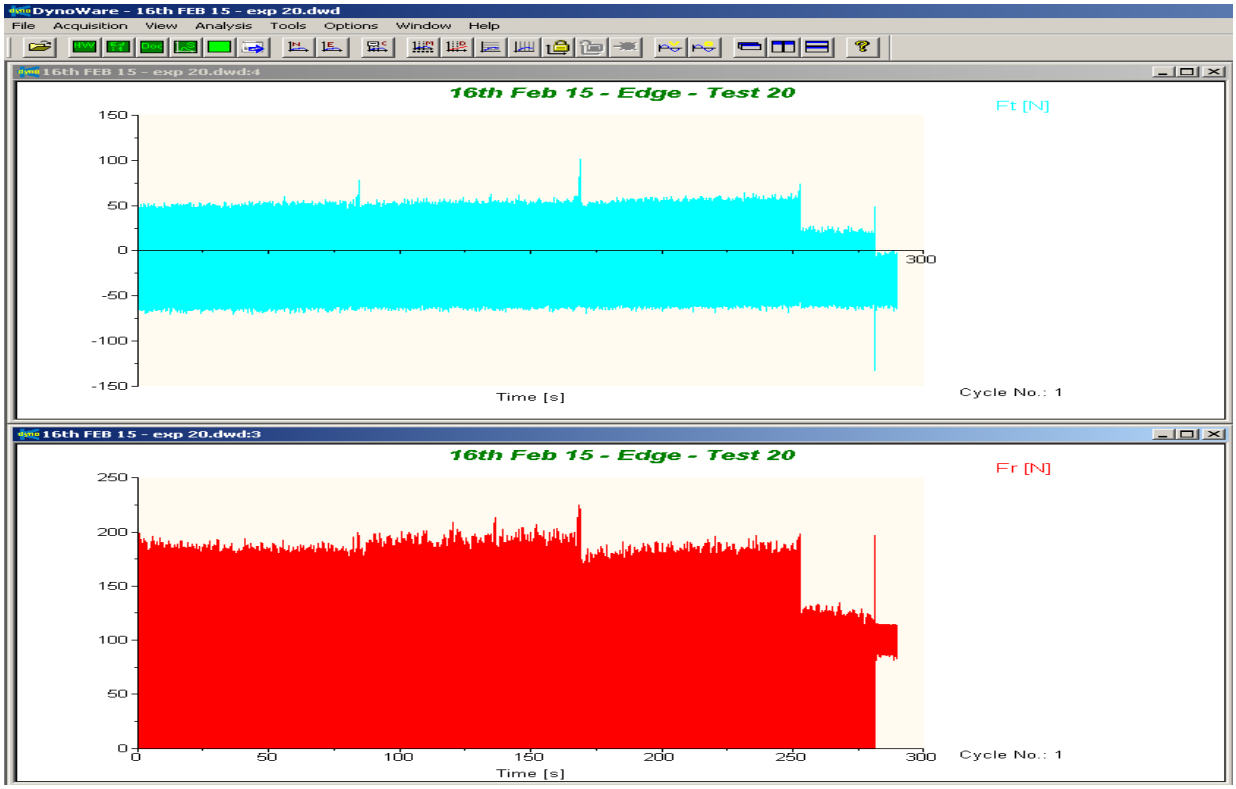

Experiment 21 : Speed - 3000 rpm; Feed - 127 mmpm; Depth Of Cut - 2.54 mm;

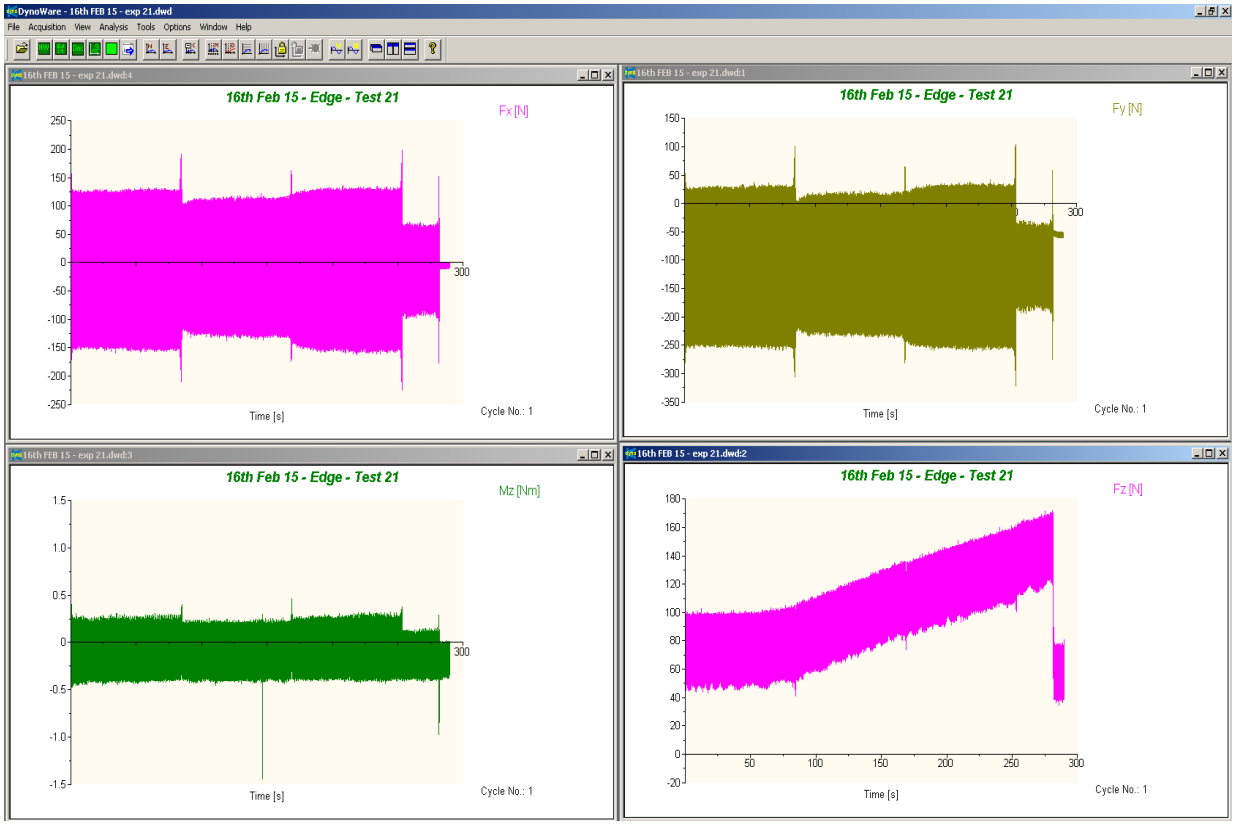

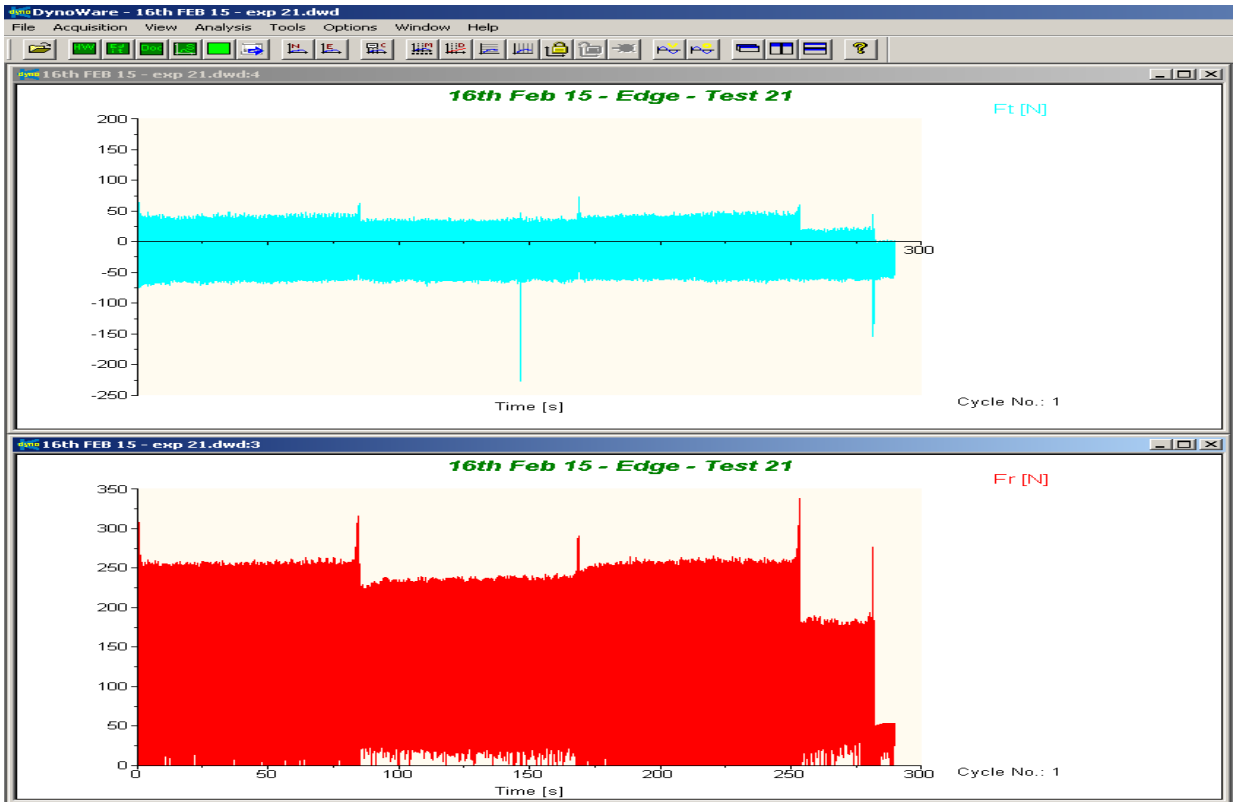

Experiment 22 : Speed - 6000 rpm; Feed - 127 mmpm; Depth Of Cut - 6.35 mm;

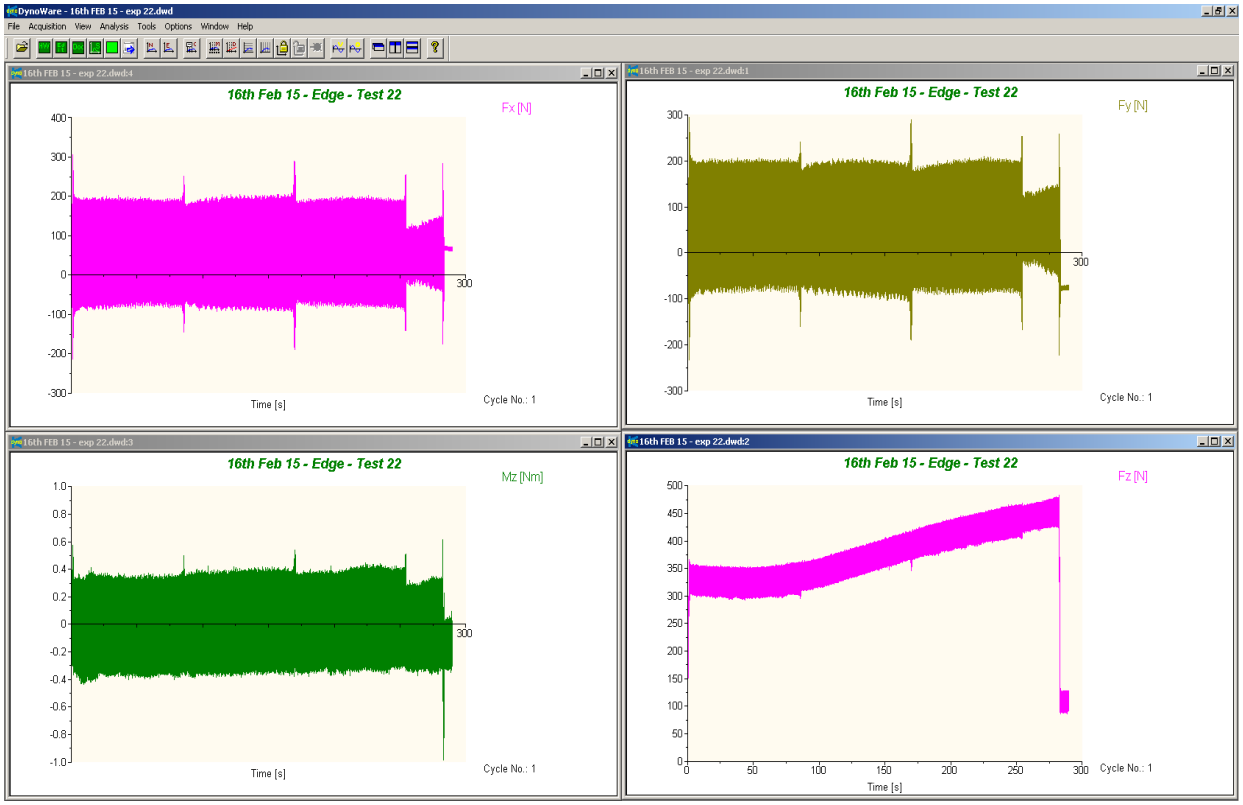

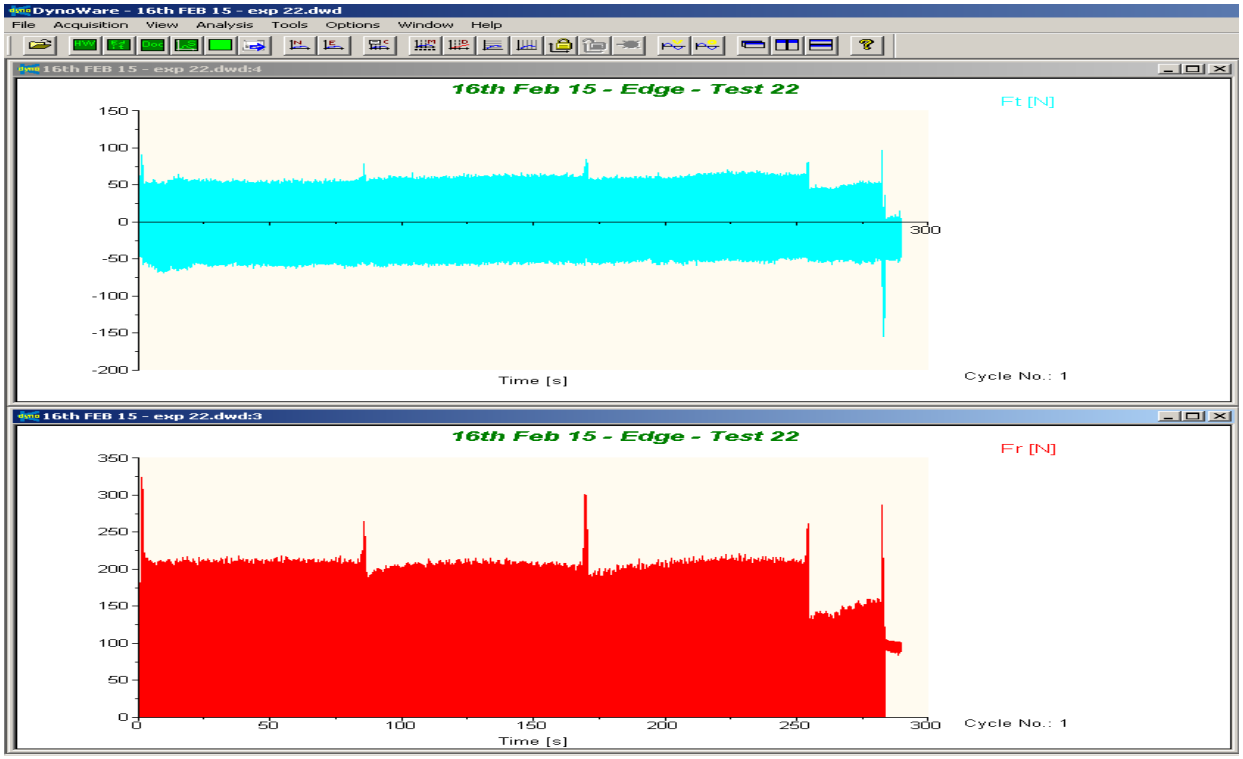

Experiment 23 : Speed - 3000 rpm; Feed - 127 mmpm; Depth Of Cut - 6.35 mm;

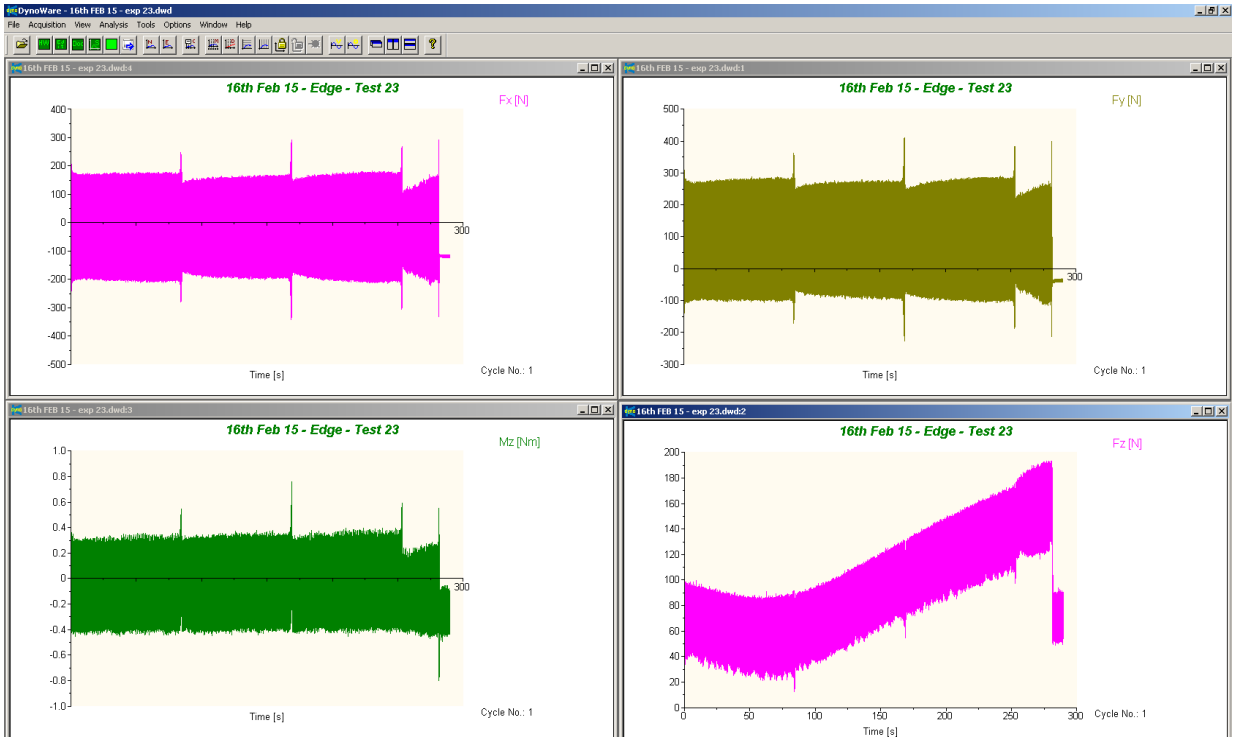

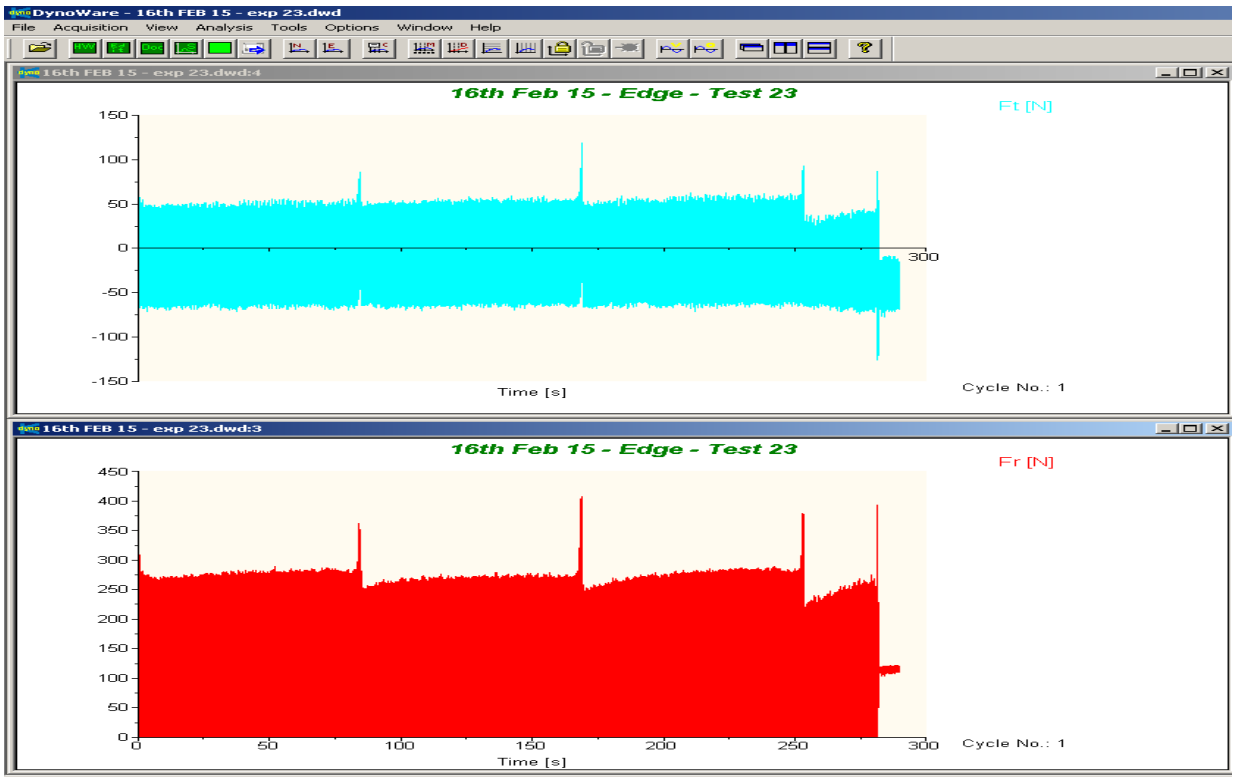

Experiment 24 : Speed - 1000 rpm; Feed - 127 mmpm; Depth Of Cut - 6.35 mm;

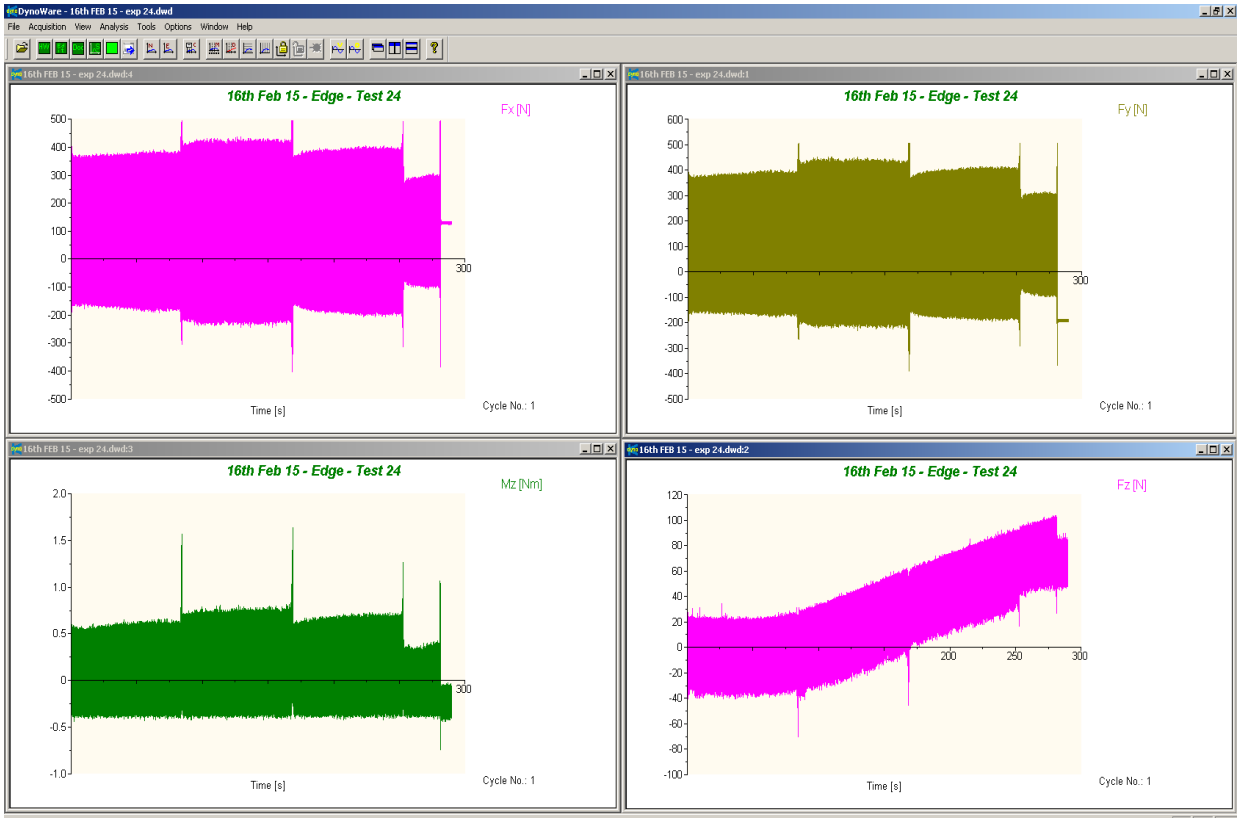

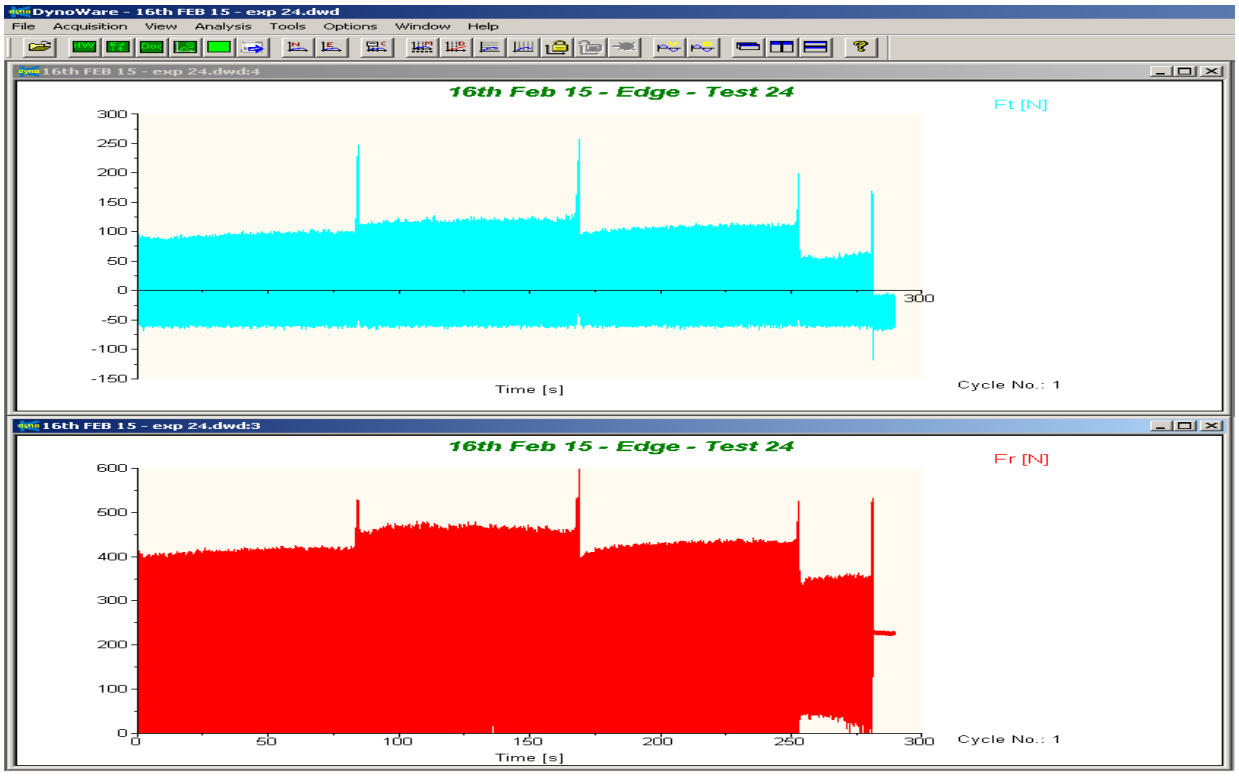

Appendix - D - HexMC End milling Dynoware Graphs

Experiment 1 : Speed - 1000 rpm; Feed - 127 mmpm; Depth Of Cut - 6.35 mm;

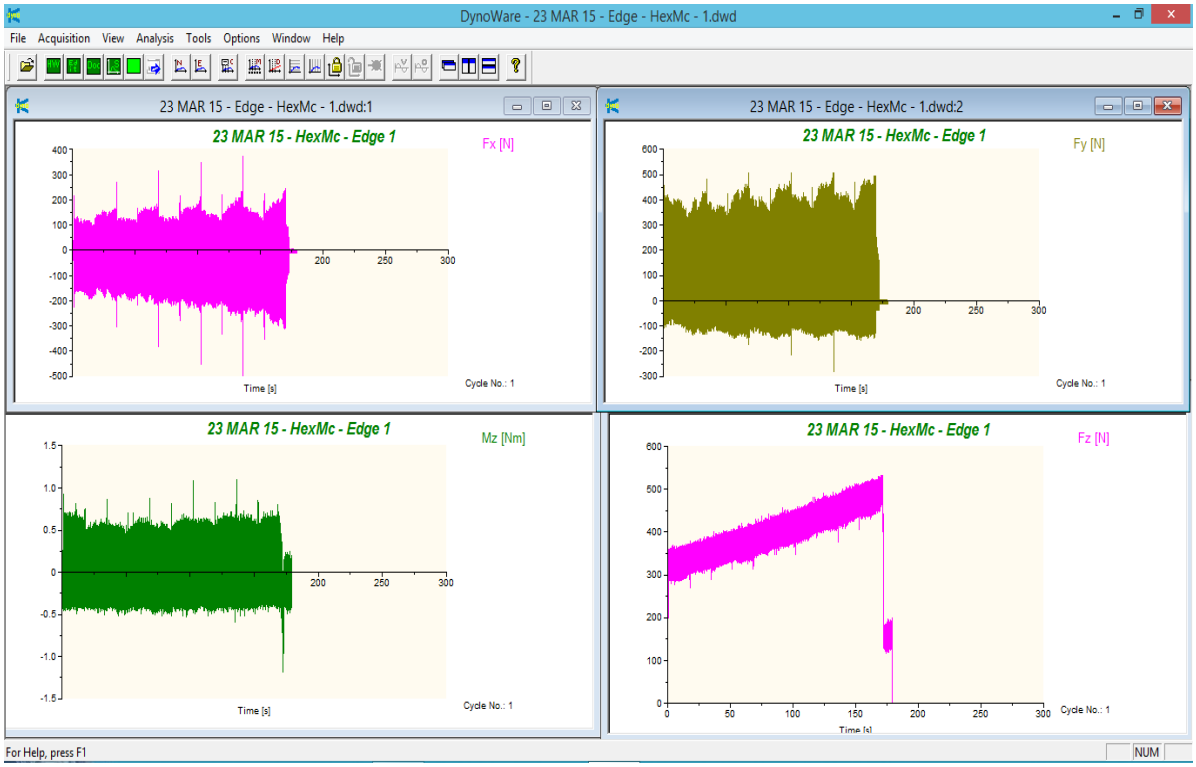

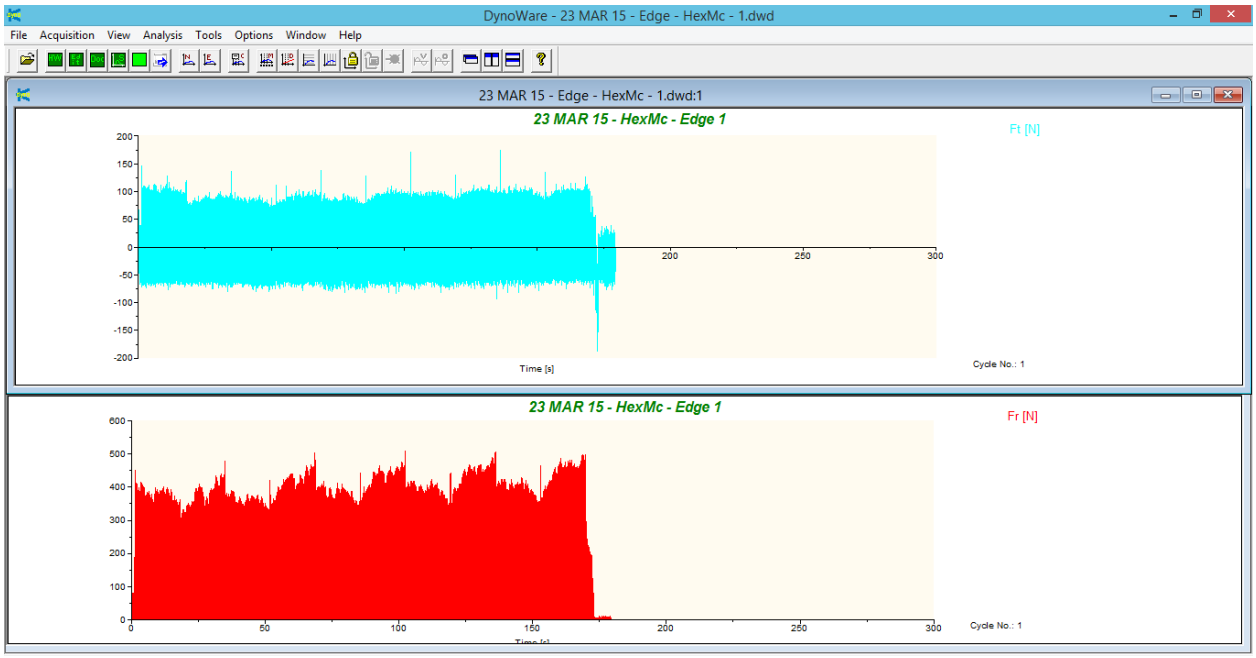

Experiment 2 : Speed - 6000 rpm; Feed - 127 mmpm; Depth Of Cut - 6.35 mm;

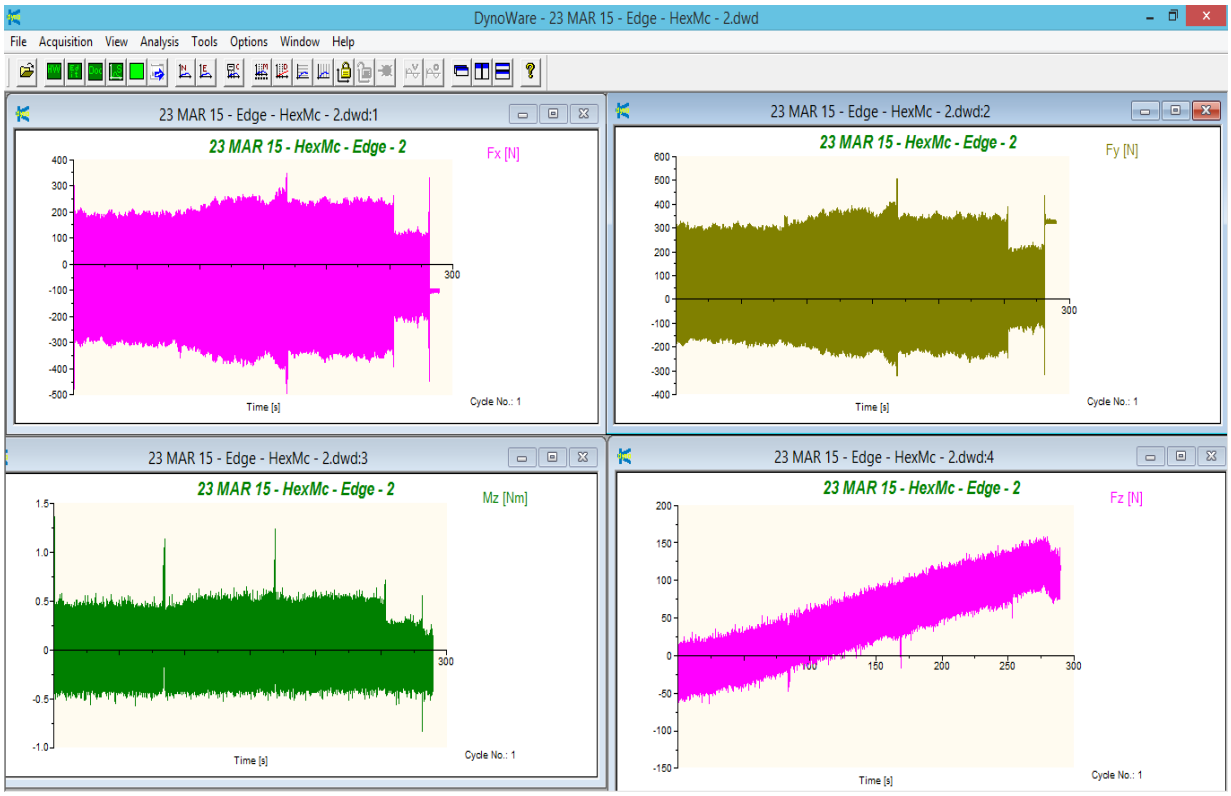

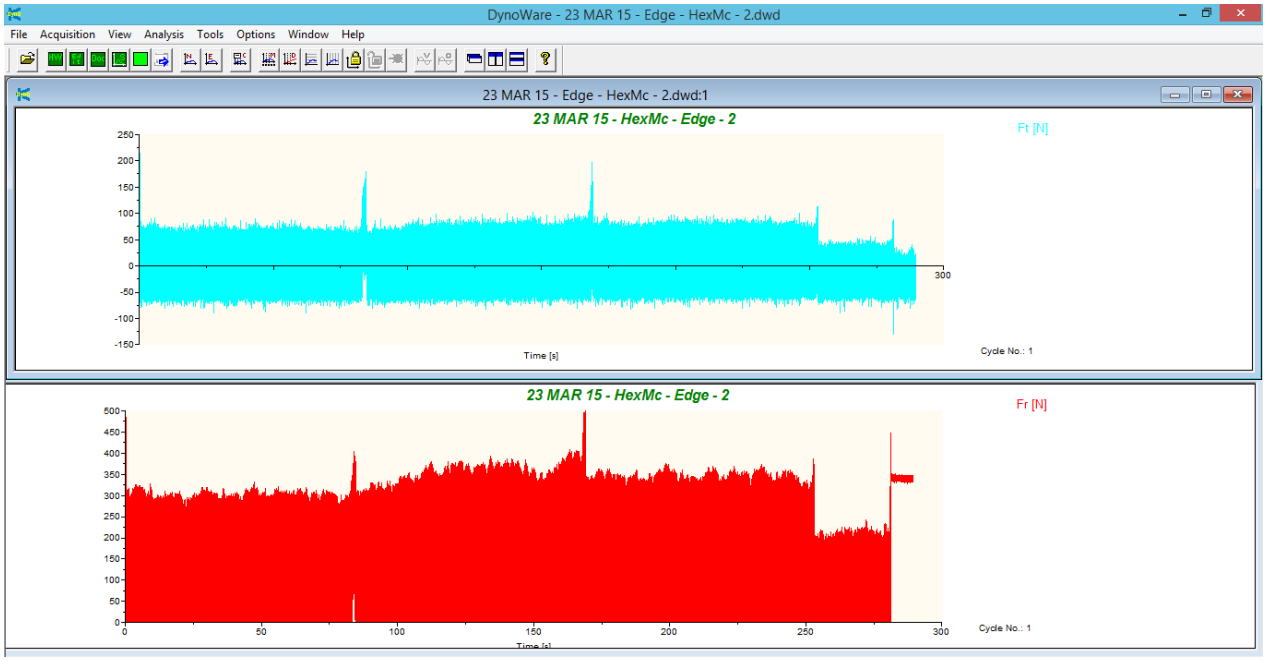

Experiment 3 : Speed - 6000 rpm; Feed - 635 mmpm; Depth Of Cut - 2.54 mm;

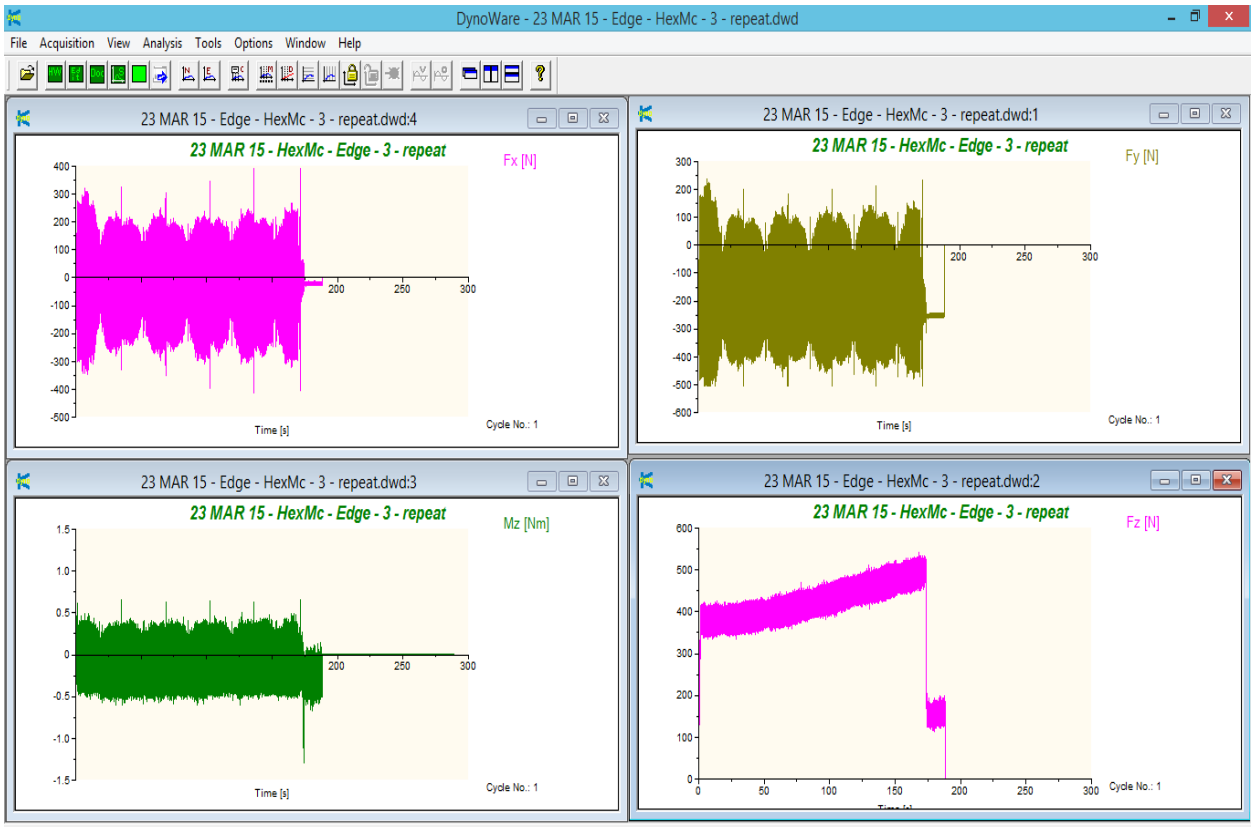

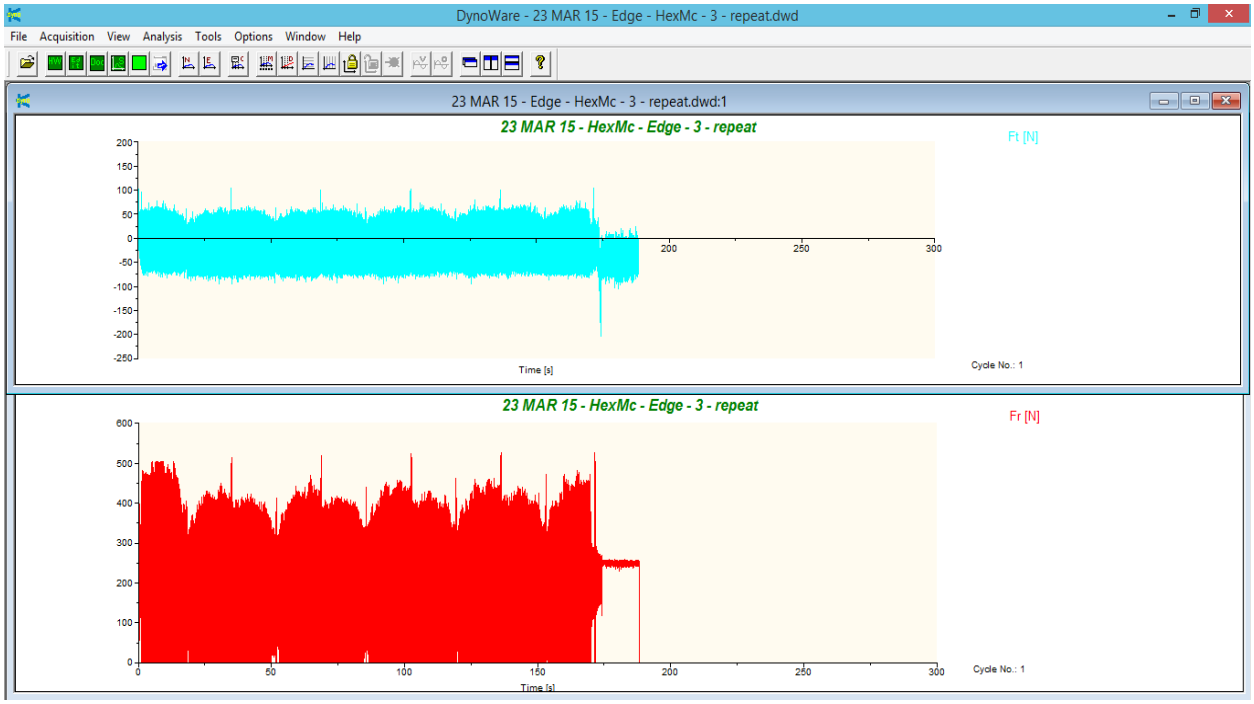

Experiment 4 : Speed - 6000 rpm; Feed - 127 mmpm; Depth Of Cut - 2.54 mm;

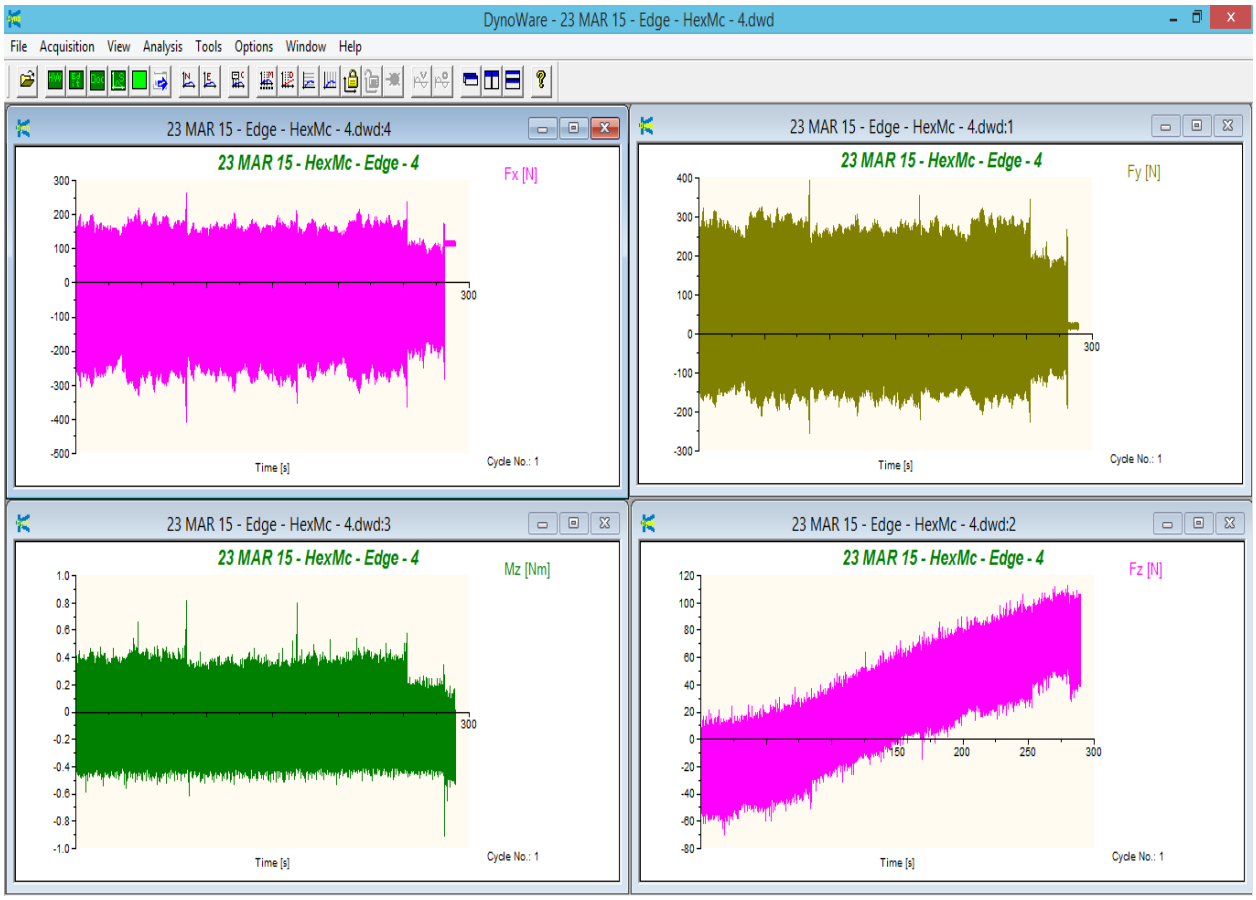

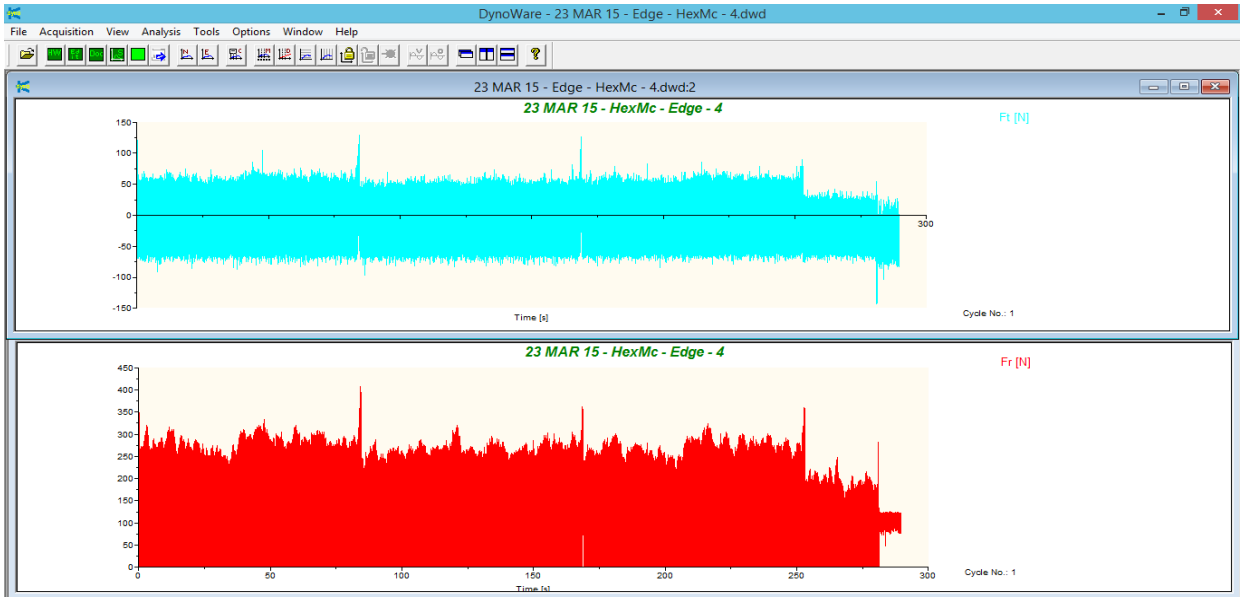

Experiment 5 : Speed - 1000 rpm; Feed - 127 mmpm; Depth Of Cut - 6.35 mm;

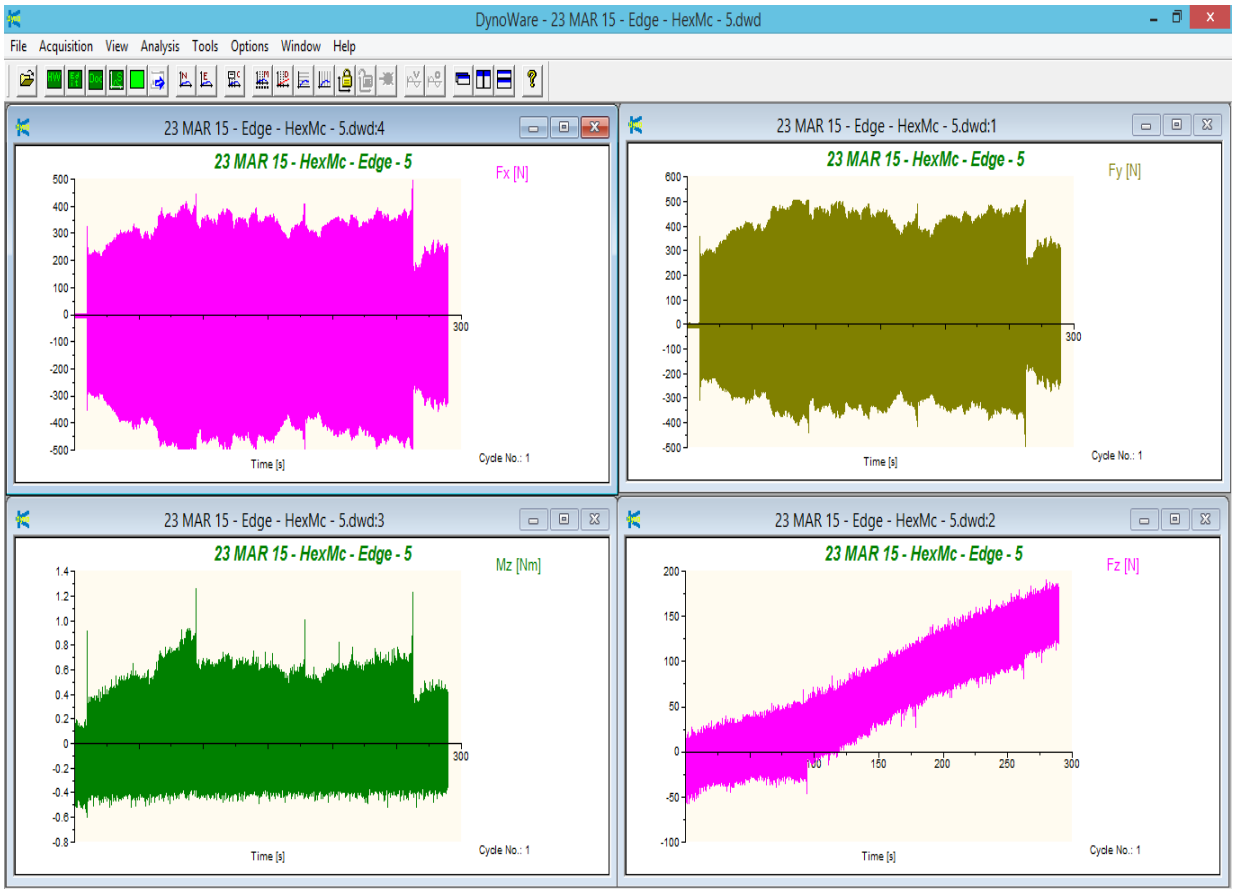

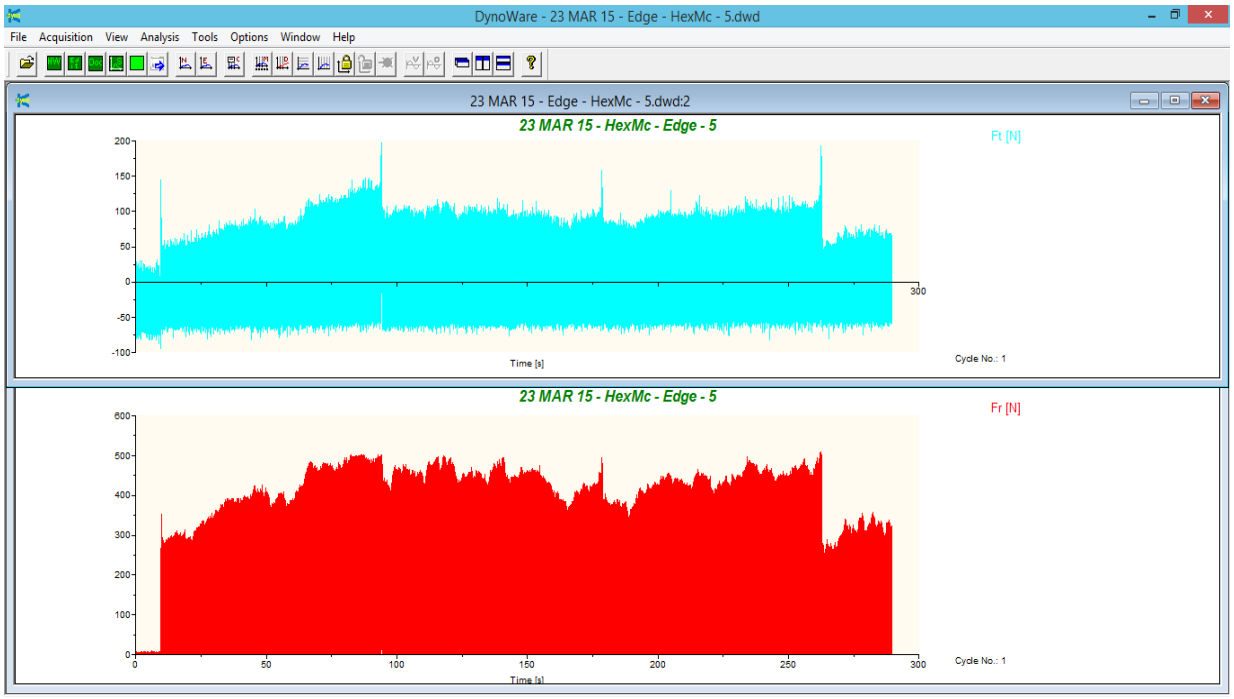

Experiment 6 : Speed - 1000 rpm; Feed - 635 mmpm; Depth Of Cut - 6.35 mm;

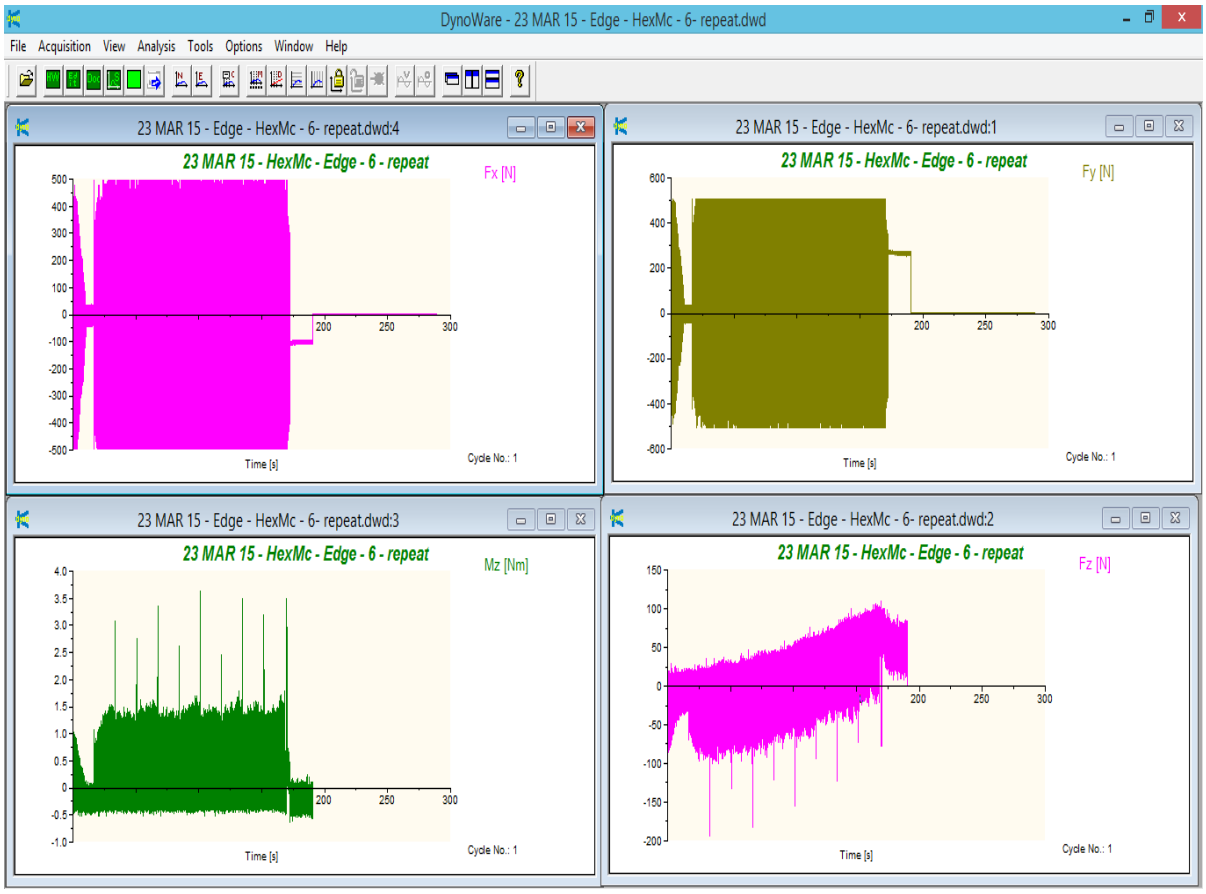

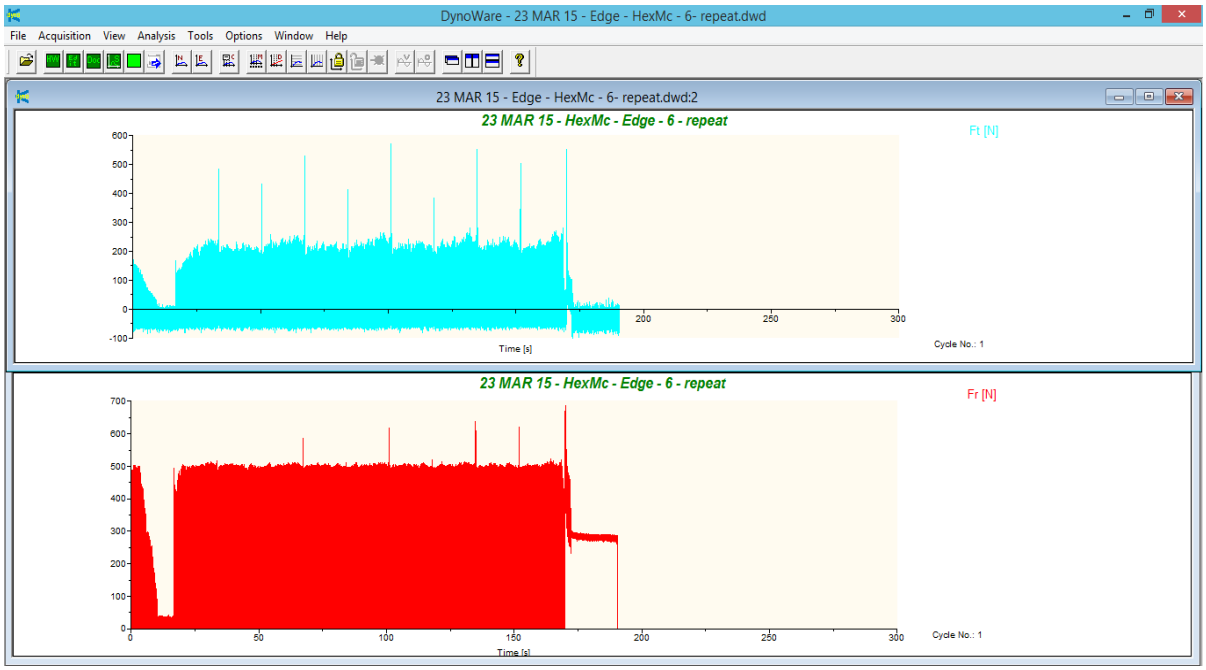

Experiment 7 : Speed - 1000 rpm; Feed - 635 mmpm; Depth Of Cut - 2.54 mm;

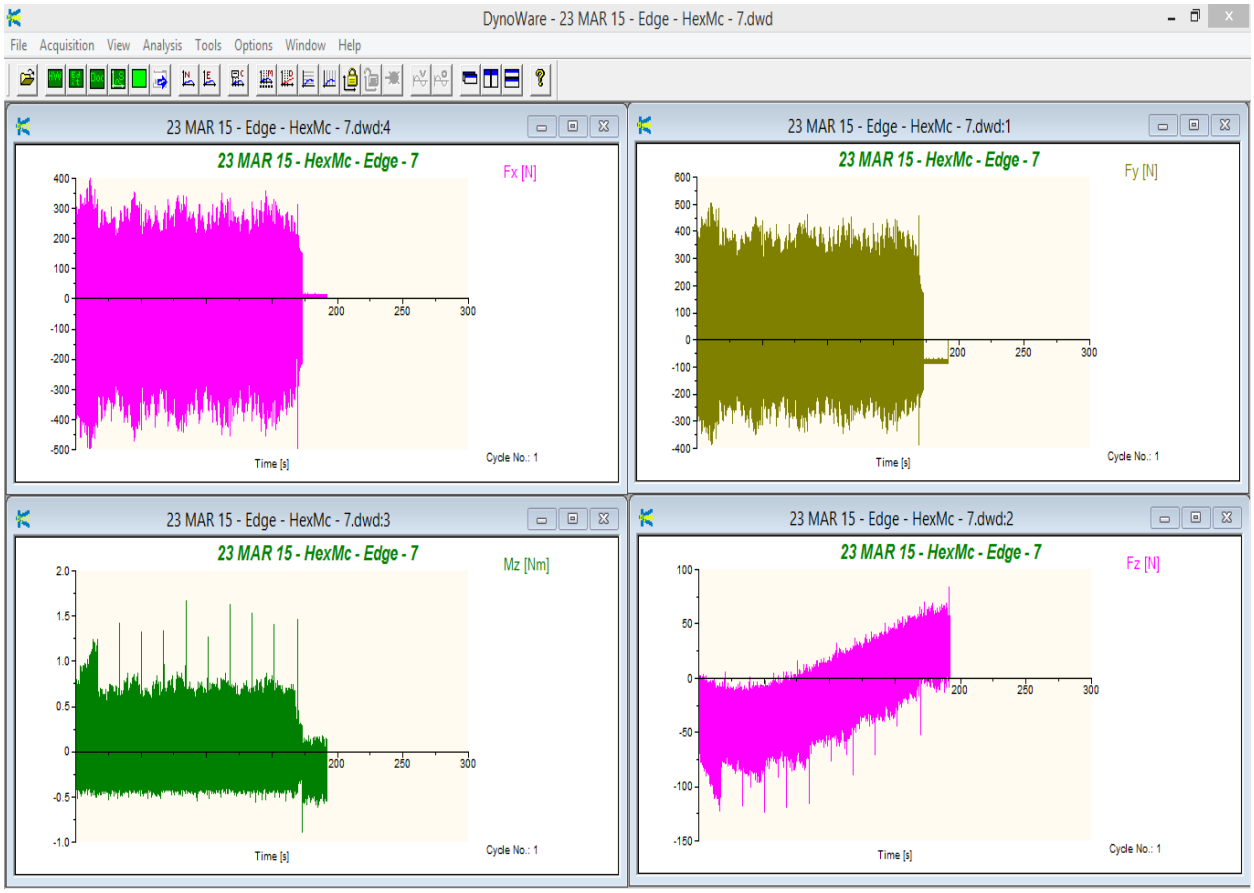

Experiment 8 : Speed - 1000 rpm; Feed - 127 mmpm; Depth Of Cut - 2.54 mm;

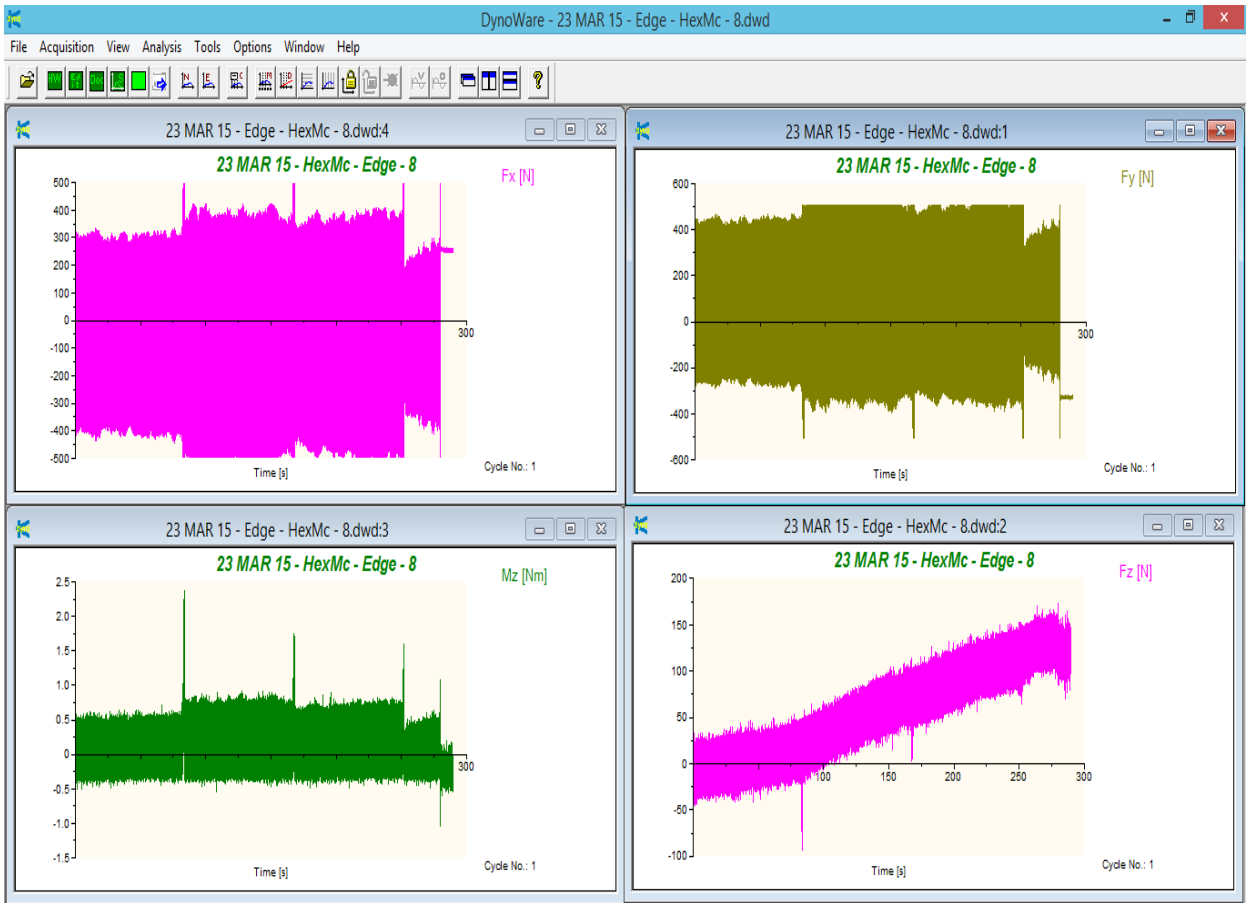

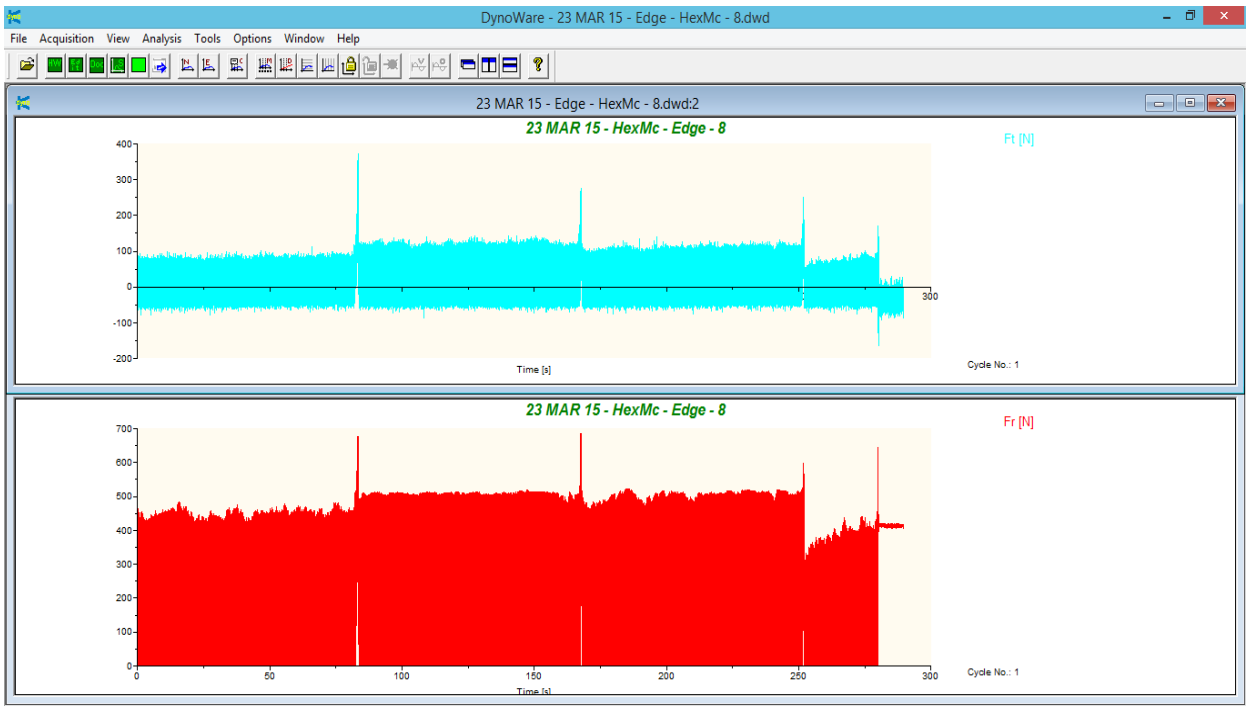

Appendix - E - Circular (CFRP) Slot milling Dynoware Graphs

Experiment C1 : Slot dia - 50.8 mm; Speed - 1000 rpm; Feed - 127 mmpm; DOC - 5.08 mm

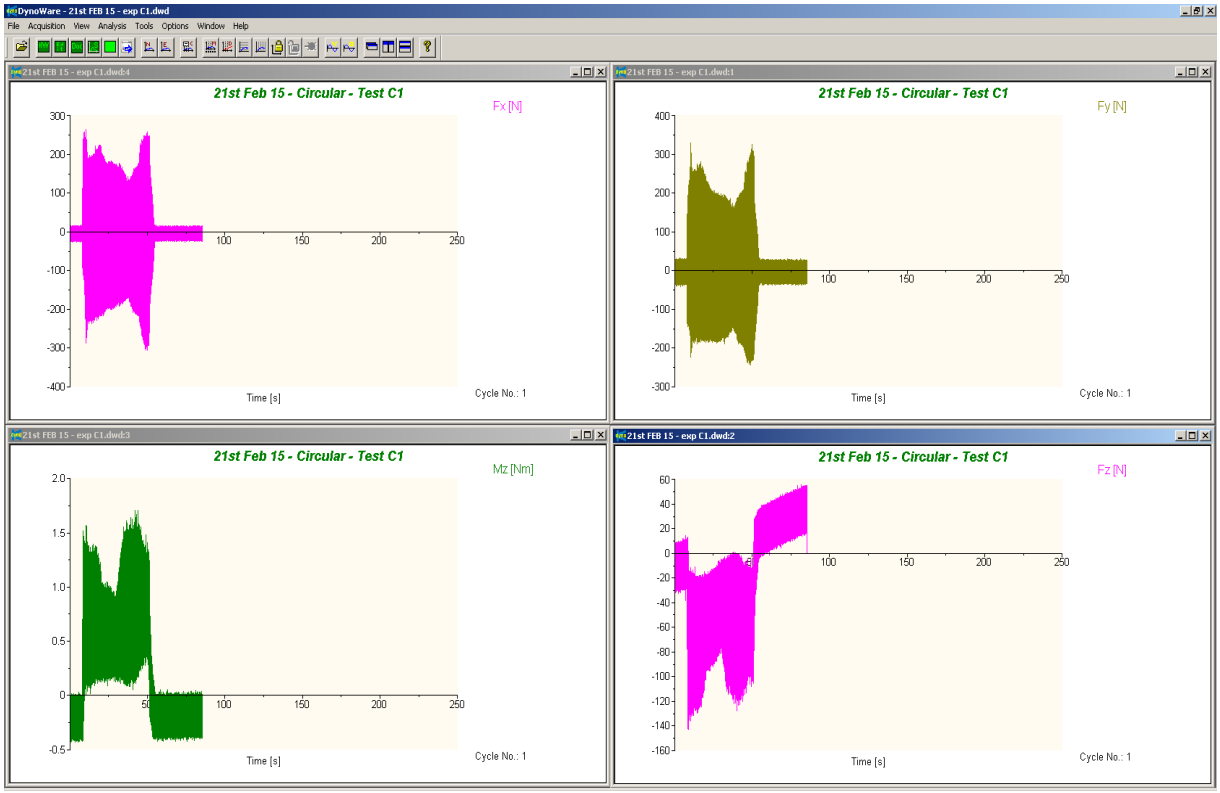

Experiment C2 : Slot dia - 82.55 mm; Speed - 6000 rpm; Feed - 254 mmpm; DOC - 5.08 mm

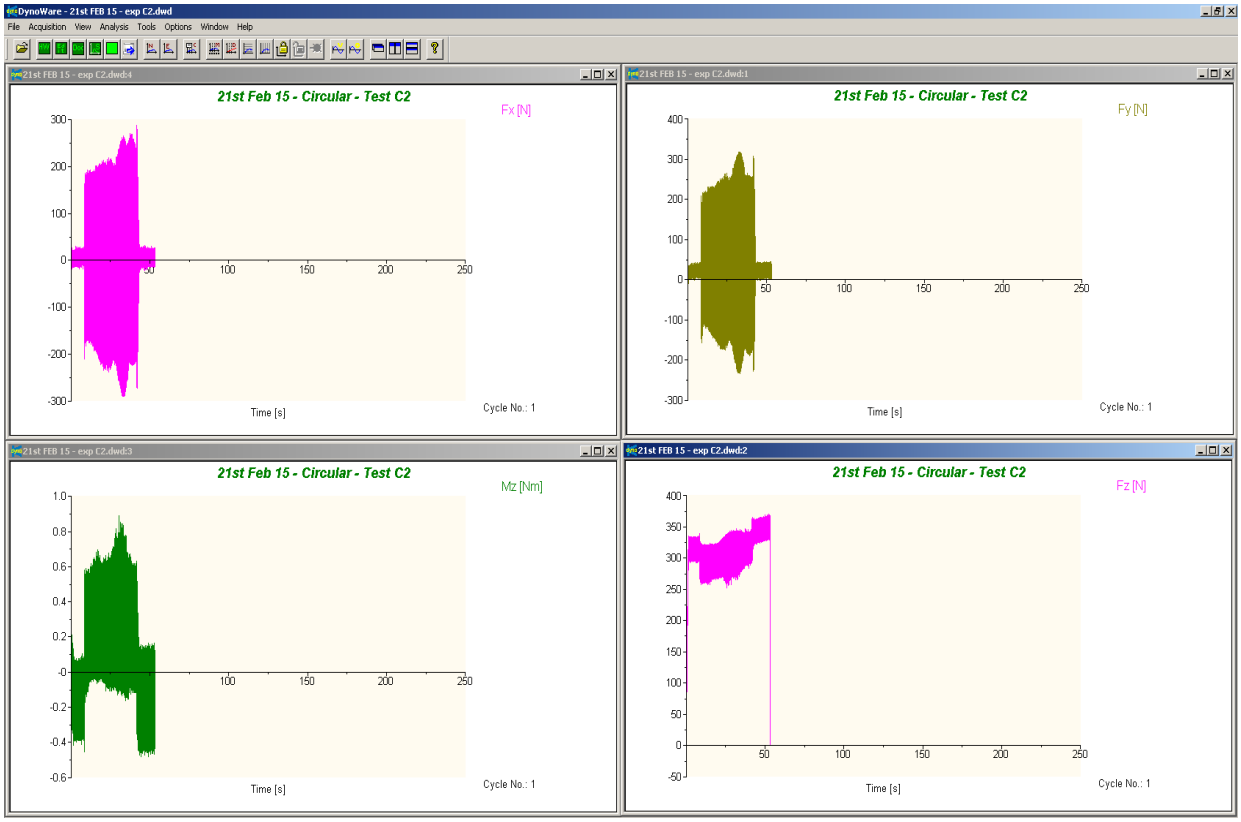

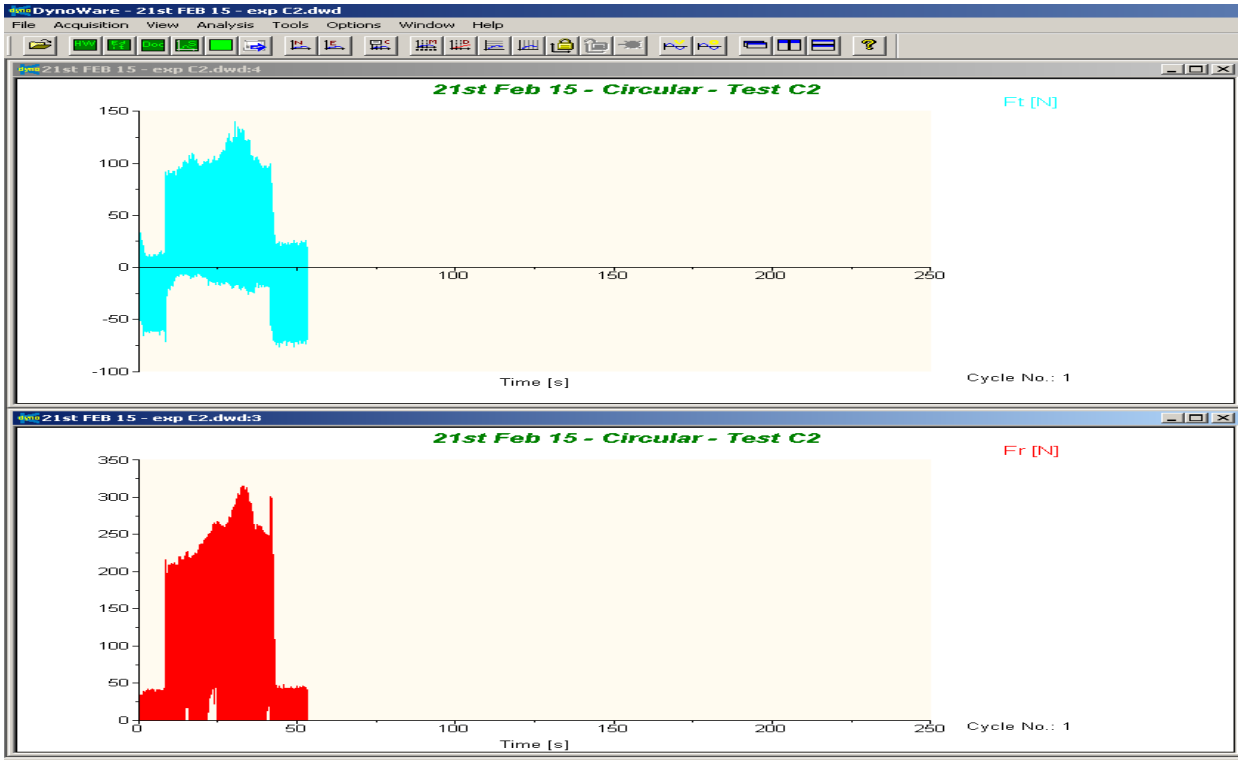

Experiment C3 : Slot dia - 114.3 mm; Speed - 6000 rpm; Feed - 381 mmpm; DOC - 5.08 mm

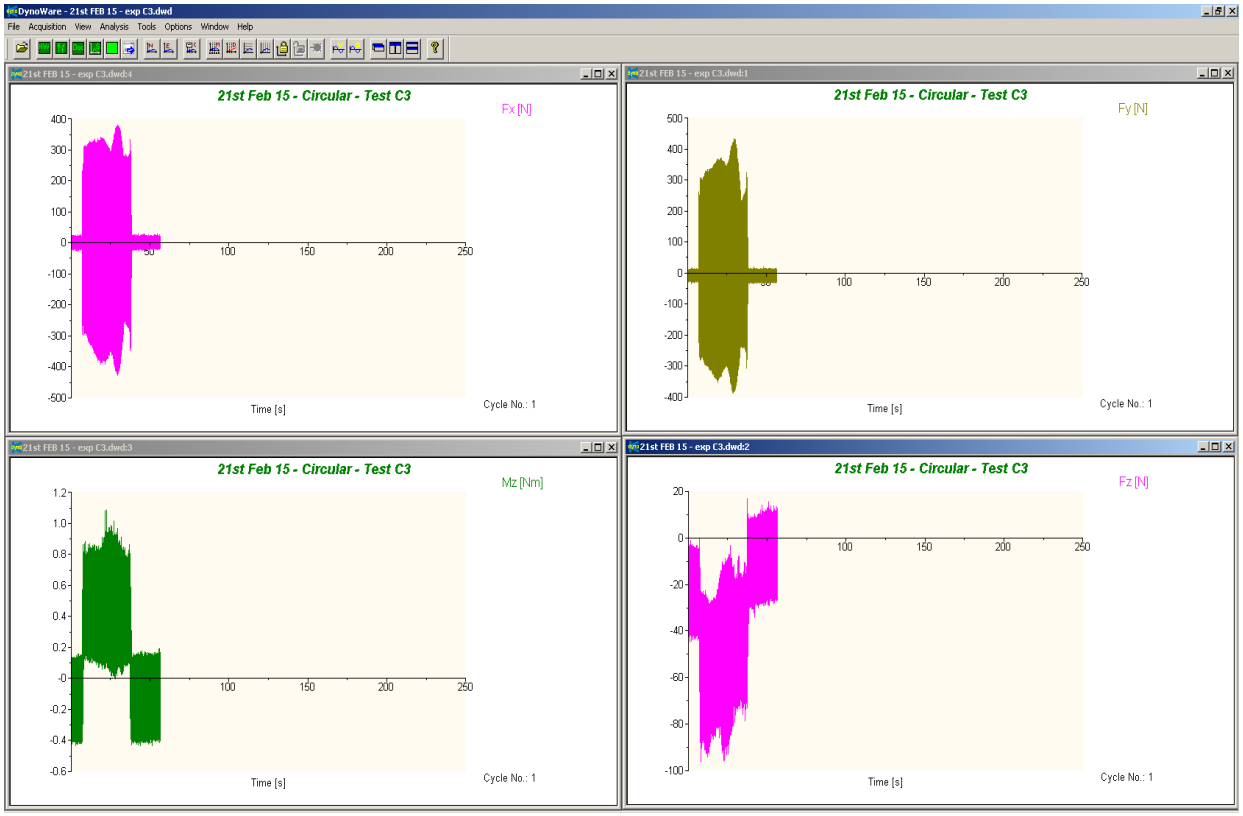

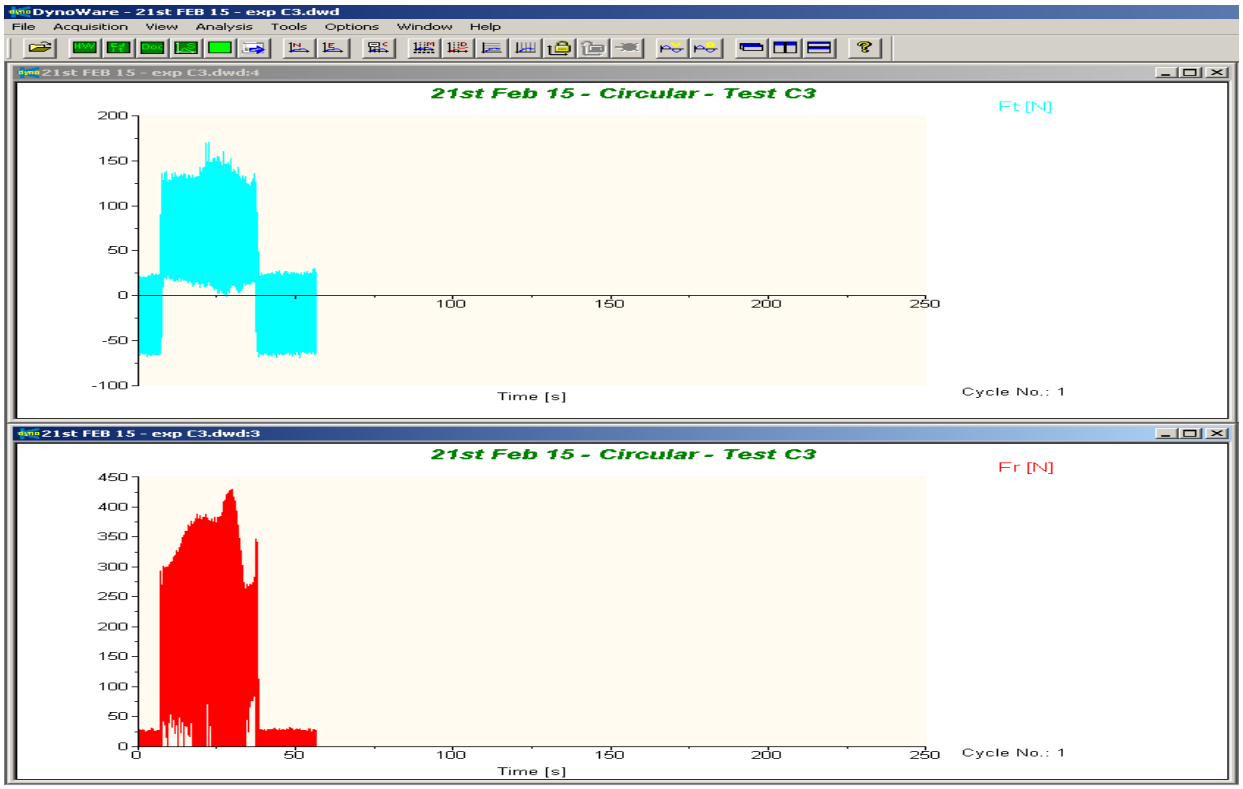

Experiment C4 : Slot dia - 146.05 mm; Speed - 3000 rpm; Feed - 508 mmpm; DOC - 5.08 mm

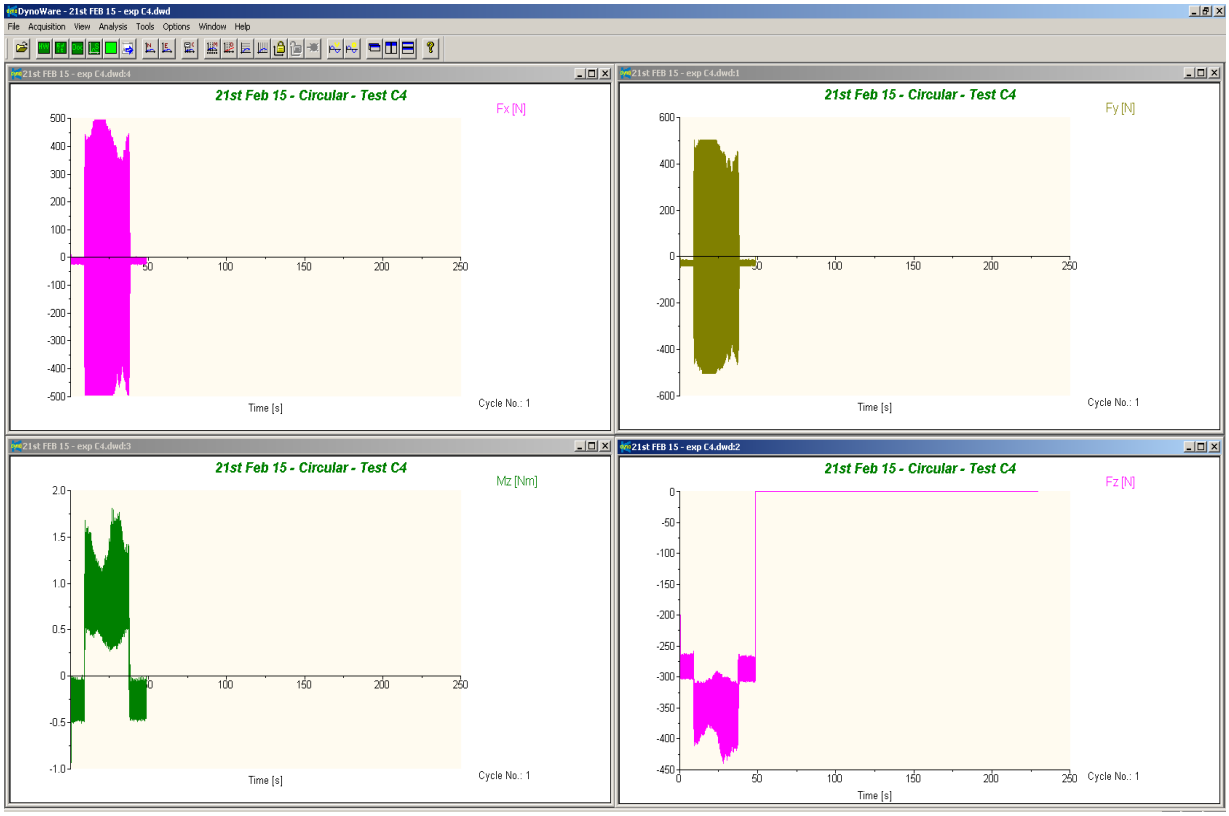

Experiment C5 : Slot dia - 177.8 mm; Speed - 3000 rpm; Feed - 635 mmpm; DOC - 5.08 mm

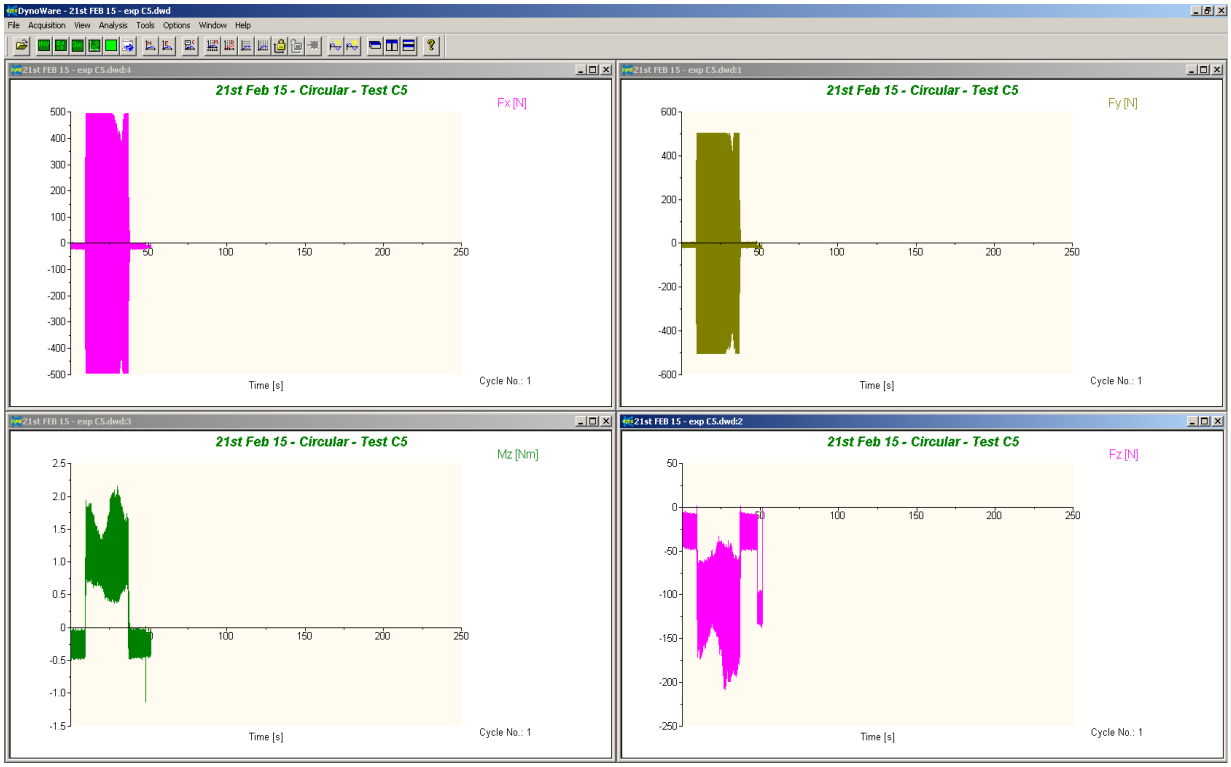

Appendix - F - Octagonal (CFRP) Slot milling Dynoware Graphs

Octagonal Slot test - Machining parameters

Slot No.	Slot Length (mm)	Speed (rpm)	Feed (mm/min)	DOC (mm)	Relative angle wrt Fiber direction (Degrees)
1	35.96	1000	25.4	5.08	0°
2	38.1	1000	25.4	5.08	45°
3	35.96	1000	25.4	5.08	90°
4	50.8	1000	25.4	5.08	135°
5	35.96	1000	25.4	5.08	180°
6	38.1	1000	25.4	5.08	225°
7	35.96	1000	25.4	5.08	270°
8	50.8	1000	25.4	5.08	315°

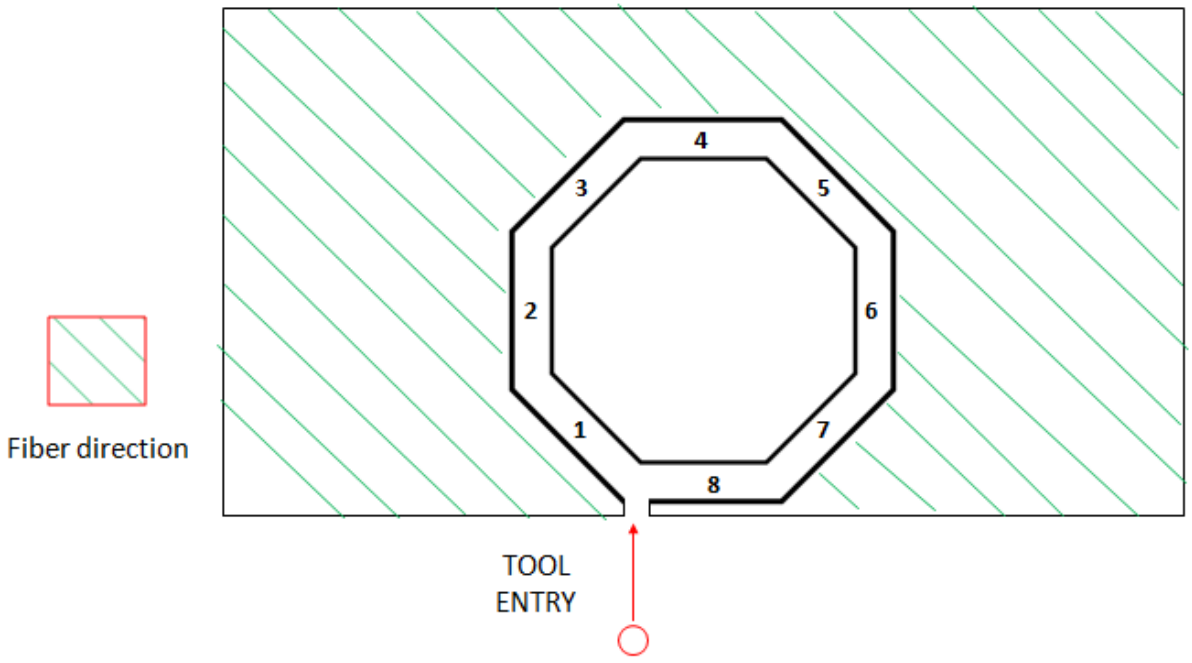

Schematic to show Circular slot test on UD CFRP

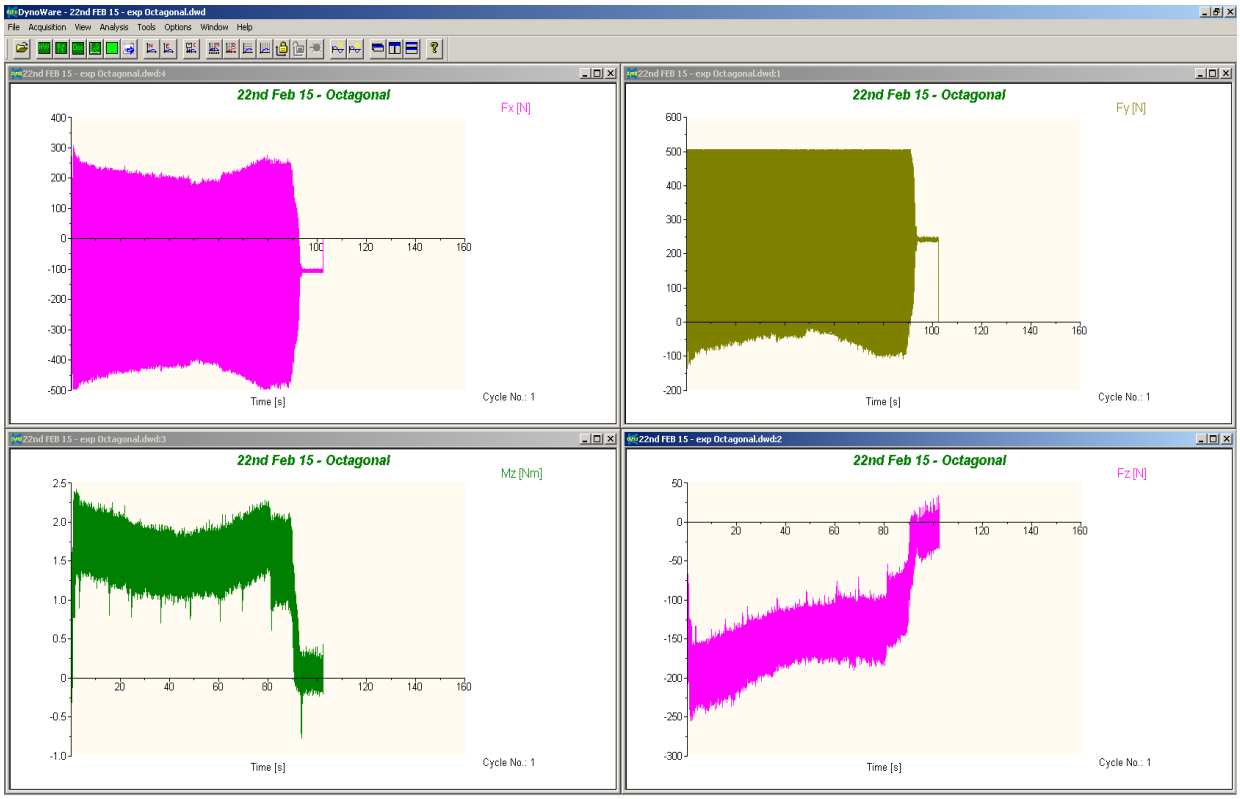
DynoWare - 22nd FEB 15 - exp Octagonal.dwd
File Acquisition View Analysis Tools Options Window Help
22nd FEB 15 - exp Octagonal.dwd:4
22nd Feb 15 - Octagonal
Fx [N]
Time [s]
Cycle No.: 1
22nd FEB 15 - exp Octagonal.dwd:1
22nd Feb 15 - Octagonal
Fy [N]
Time [s]
Cycle No.: 1
22nd FEB 15 - exp Octagonal.dwd:3
22nd Feb 15 - Octagonal
Mz [Nm]
Time [s]
Cycle No.: 1
22nd FEB 15 - exp Octagonal.dwd:2
22nd Feb 15 - Octagonal
Fz [N]
Time [s]
Cycle No.: 1

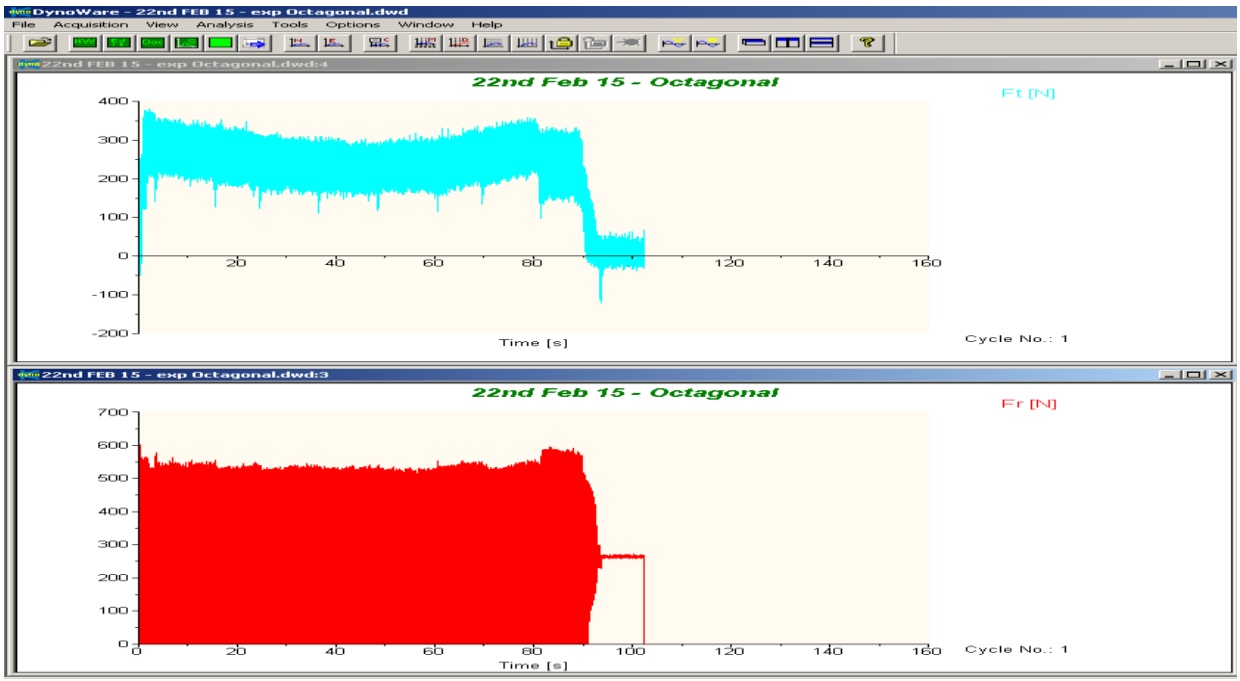
DynoWare - 22nd FEB 15 - exp Octagonal.dwd
File Acquisition View Analysis Tools Options Window Help
22nd FEB 15 - exp Octagonal.dwd:4
22nd Feb 15 - Octagonal
Ft [N]
Time [s]
Cycle No.: 1
22nd FEB 15 - exp Octagonal.dwd:3
22nd Feb 15 - Octagonal
Fr [N]
Time [s]
Cycle No.: 1

Appendix - G - Surface Roughness Pictures

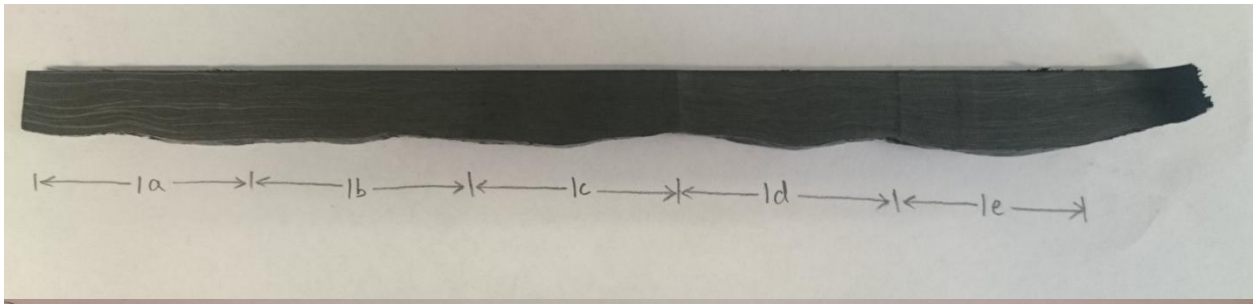

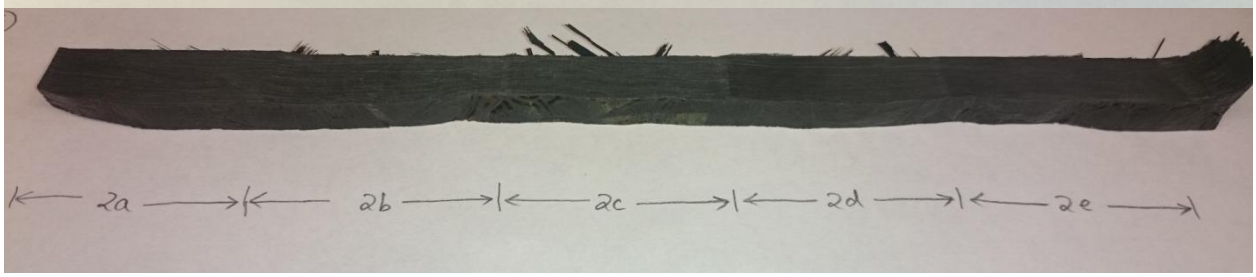

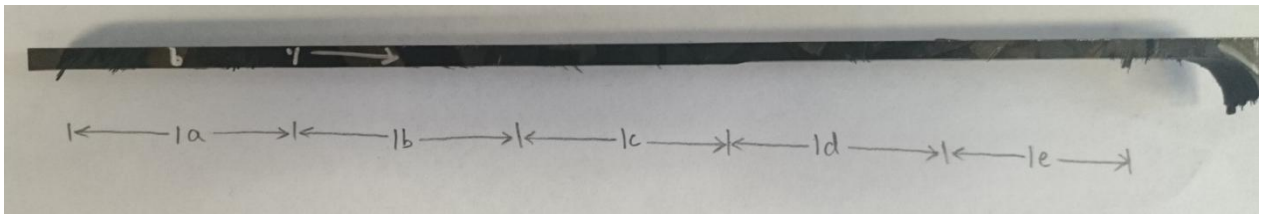

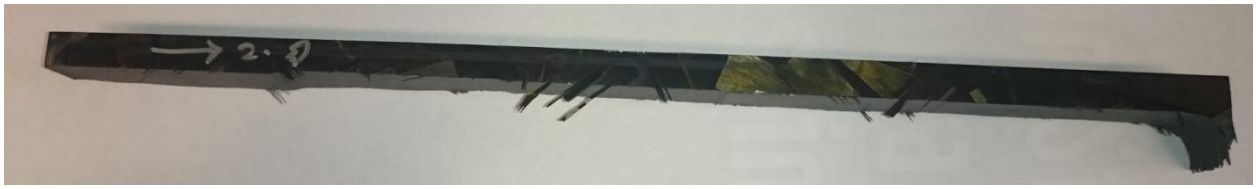

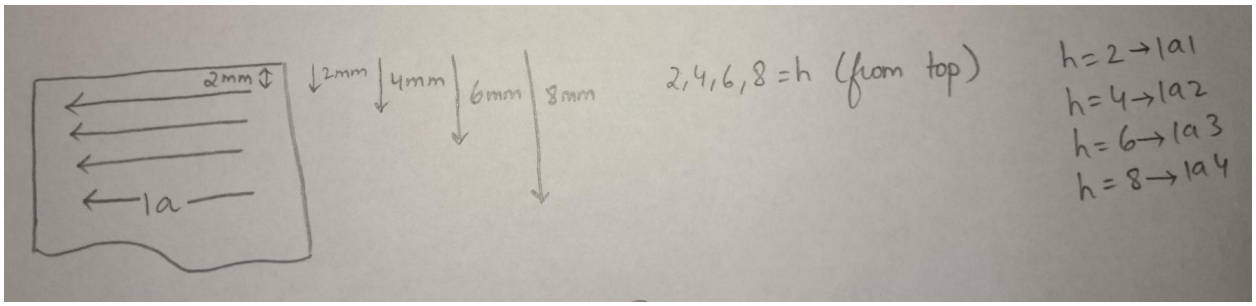

Experiment 1a : Speed - 6000 rpm; Feed - 15 mmpm;

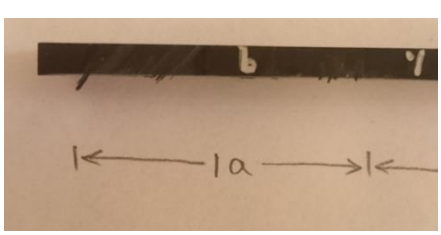

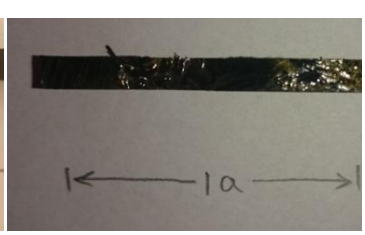

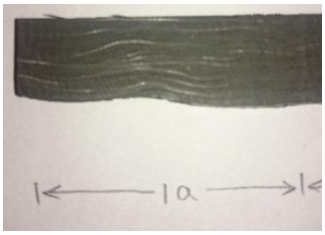

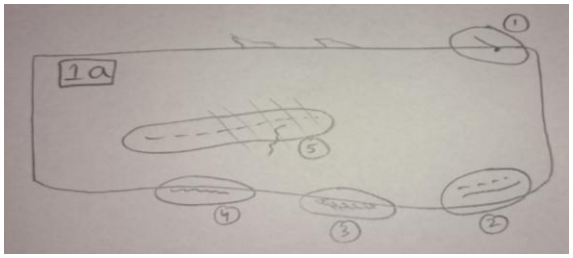

1a -top- 1x - H

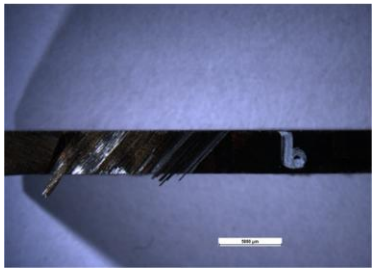

1a -1x - H

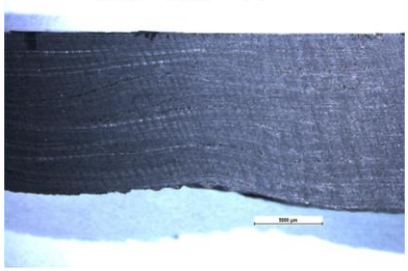

1a -1- 4x - H

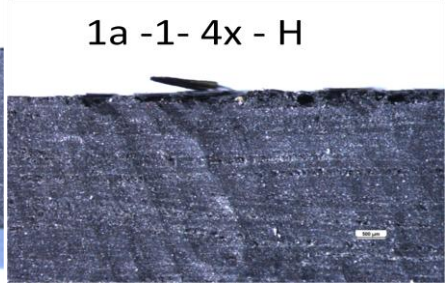

1a -2- 4x - H

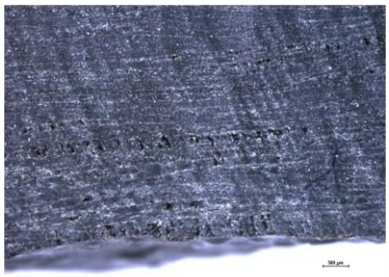

1a -3- 4x - H

1a -4- 4x - H

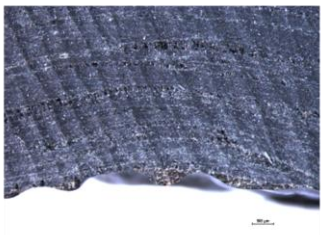

1a -5- 4x – H

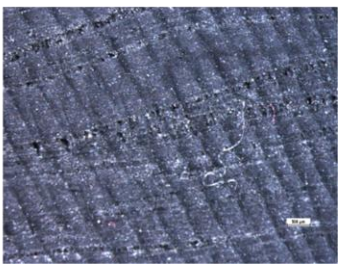

Experiment 1b : Speed - 6000 rpm; Feed - 10 mmpm;

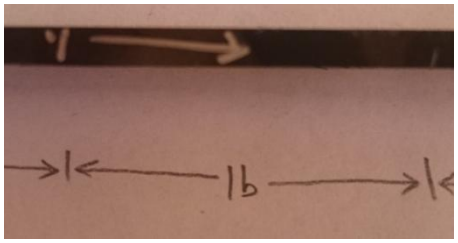

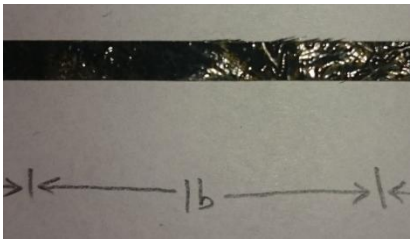

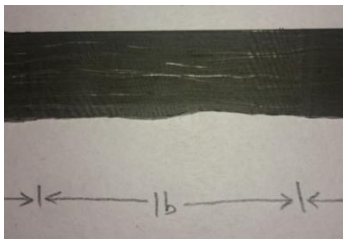

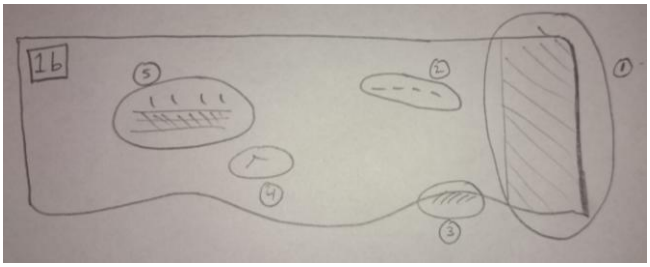

1b -1x - H

1b -1- 2x - H

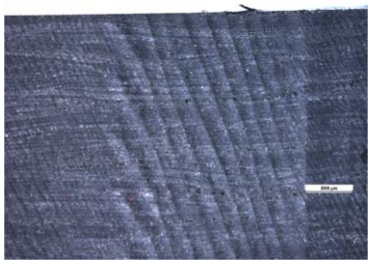

1b -2- 4x - H

1b -3- 4x - H

1b -4- 4x - H

1b -5- 4x - H

Experiment 1c : Speed - 6000 rpm; Feed - 5 mmpm;

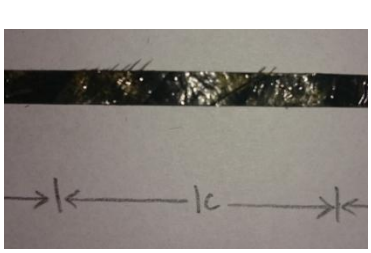

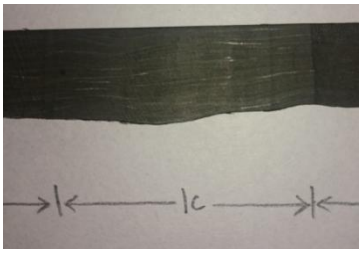

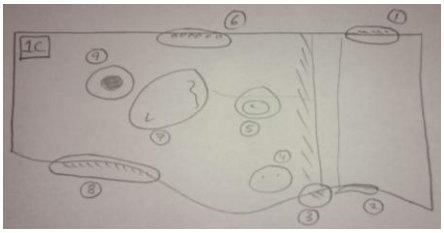

1c -1x - H

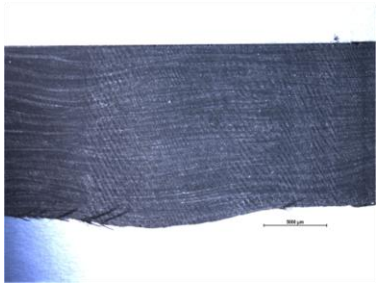

1c -1- 4x - H

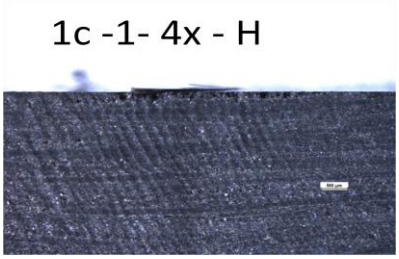

1c -2- 4x - H

1c -4- 8x - H

1c -5- 4x - H

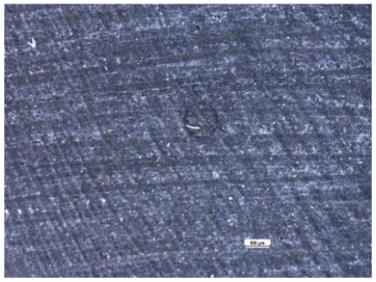

1c -6- 4x - H

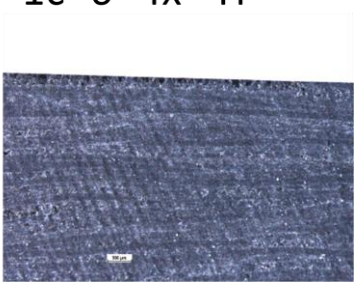

1c -7- 4x - H

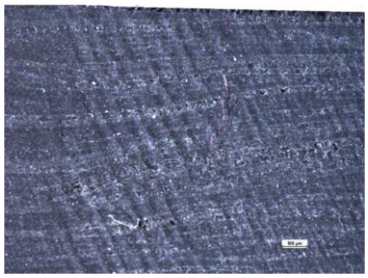

1c - 8 - 4x - H

1c - 9 - 4x - H

Experiment 1d : Speed - 3000 rpm; Feed - 15 mmpm;

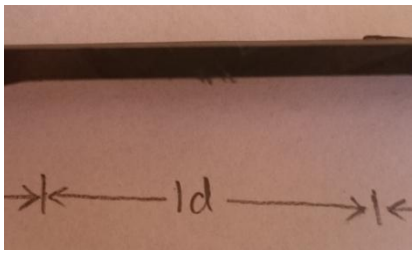

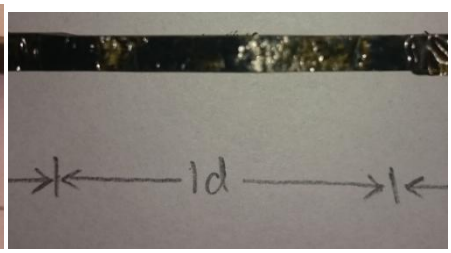

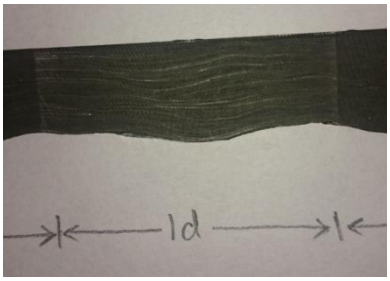

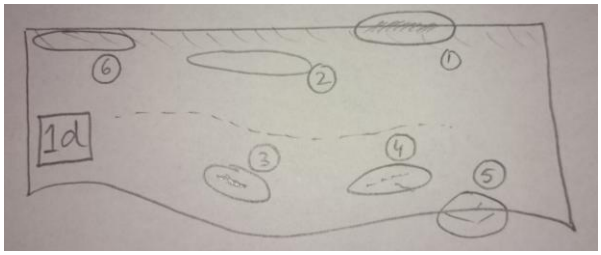

1d -1x - H

1d -1- 4x - H

1d -2- 4x - H

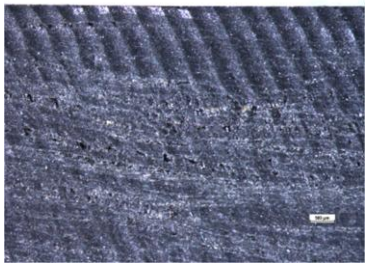

1d -3- 4x - H

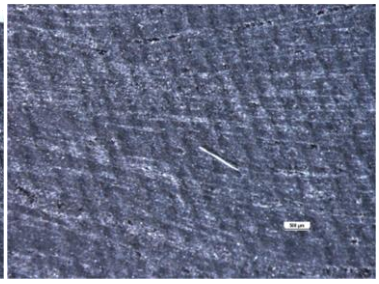

1d -4- 4x - H

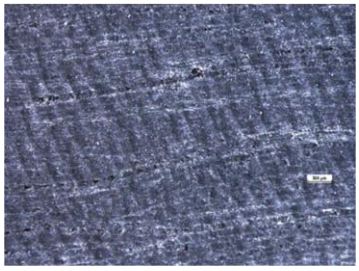

1d -5- 4x - H

1d -6- 4x - H

Experiment 1e : Speed - 3000 rpm; Feed - 10 mmpm;

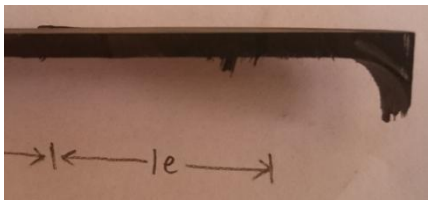

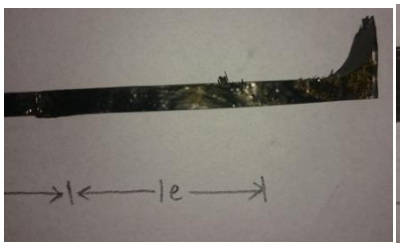

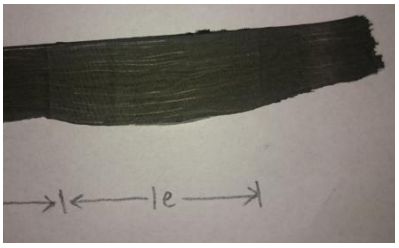

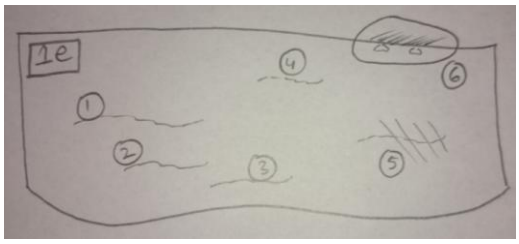

1e -1x - H

1e -1- 4x - H

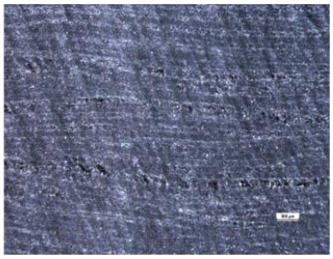

1e -2- 4x - H

1e -3- 4x - H

1e -4- 4x - H

1e -5- 4x - H

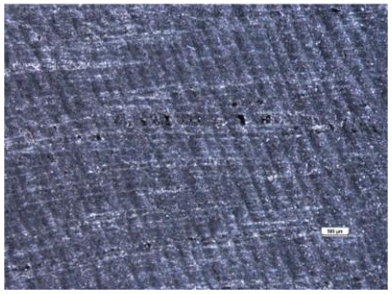

1e -6- 4x - H

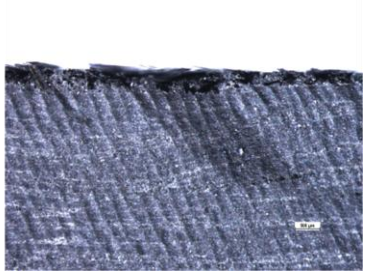

Experiment 2 a : Speed - 3000 rpm; Feed - 5 mmpm;

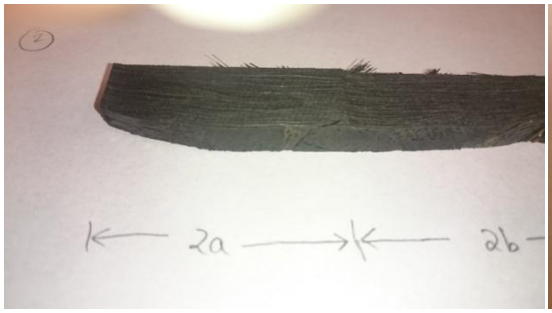

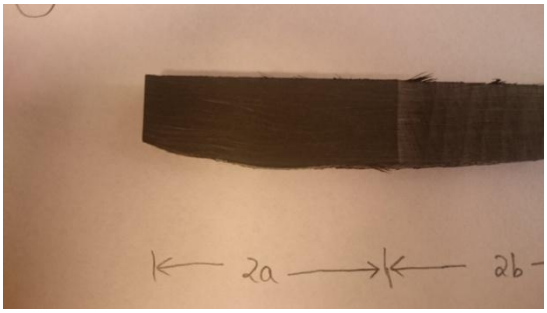

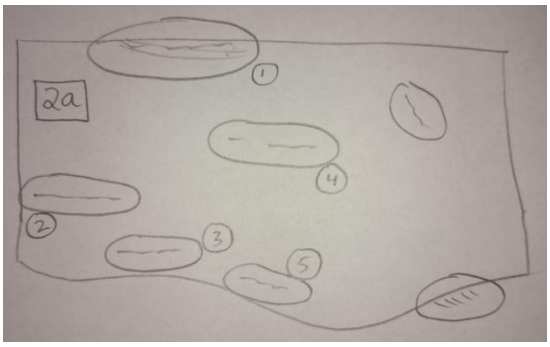

2a -1x - H

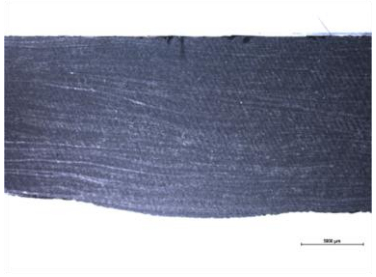

2a -1- 4x - H

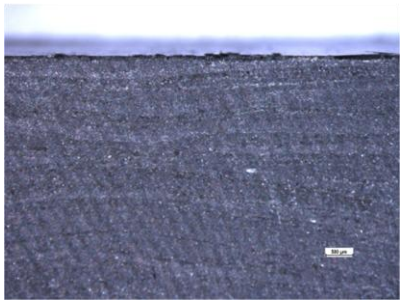

2a -2- 4x - H

2a -3- 4x - H

2a -4- 4x - H

2a -5- 4x - H

Experiment 2 b : Speed - 1000 rpm; Feed - 15 mmpm;

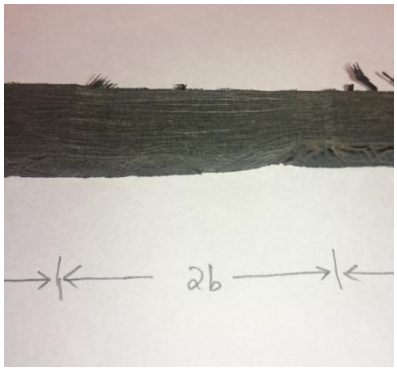

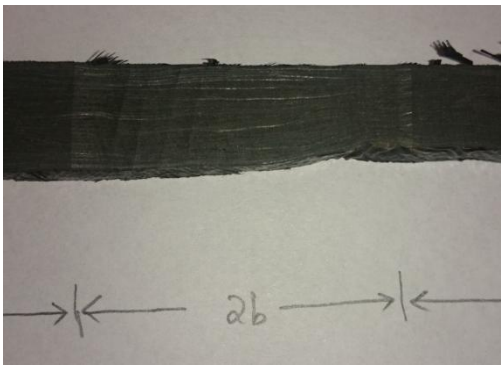

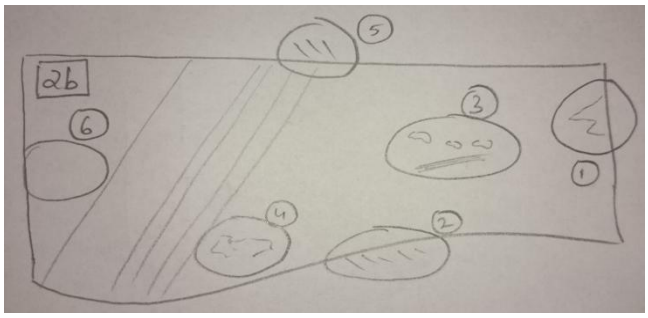

2b -1x - H

2b -1- 4x - H

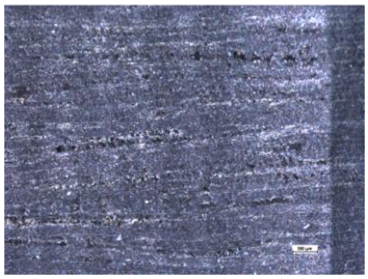

2b -2- 4x - H

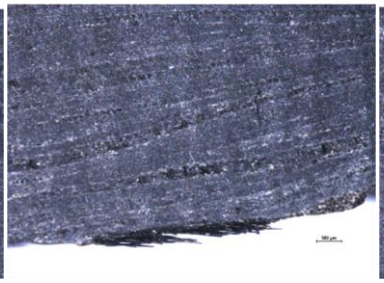

2b -3- 4x - H

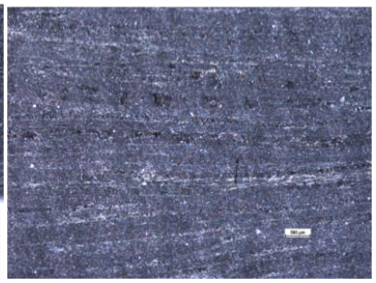

2b -4- 4x - H

2b -5- 4x - H

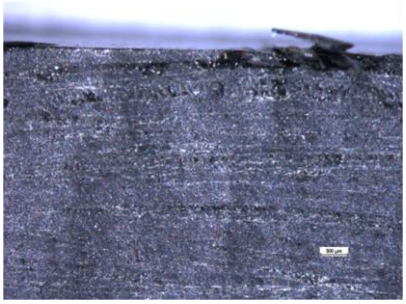

2b -6- 4x - H

Experiment 2 c : Speed - 1000 rpm; Feed - 10 mmpm;

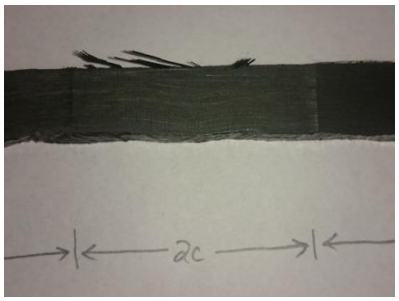

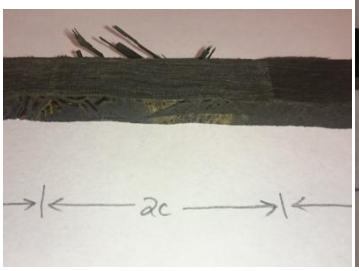

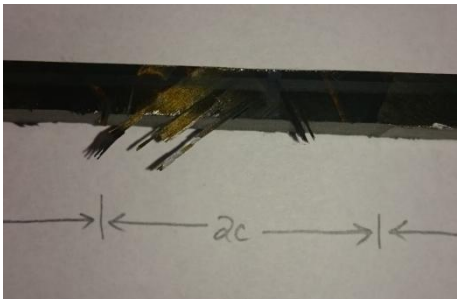

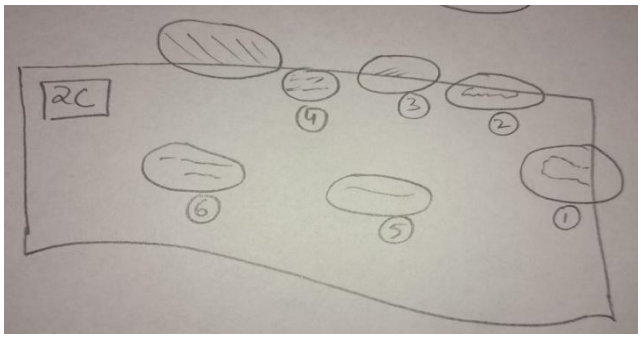

2c -1x - H

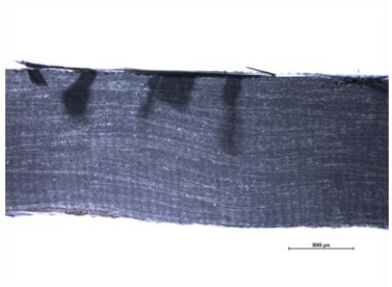

2c -1- 4x - H

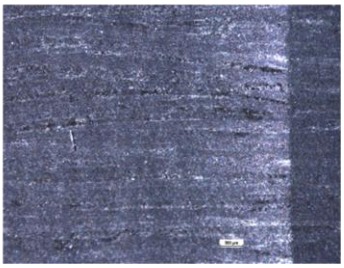

2c -2- 4x - H

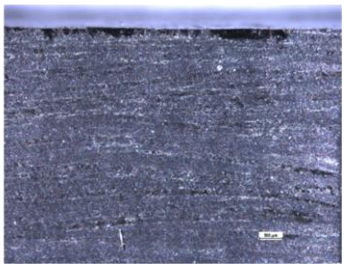

2c -3- 4x - H

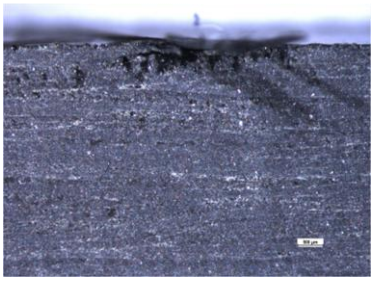

2c -4- 4x - H

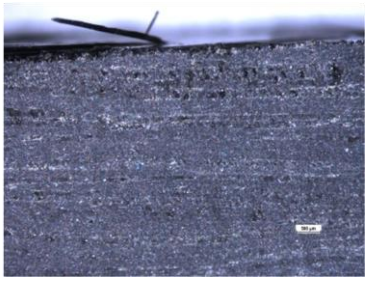

2c -5- 4x - H

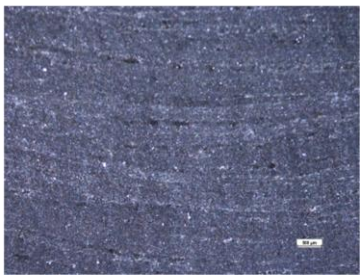

2c -6- 4x - H

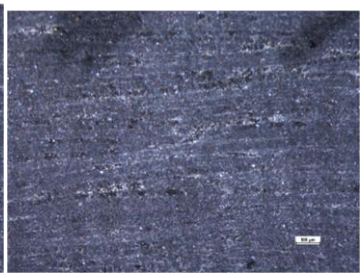

Experiment 2 d : Speed - 1000 rpm; Feed - 5 mmpm;

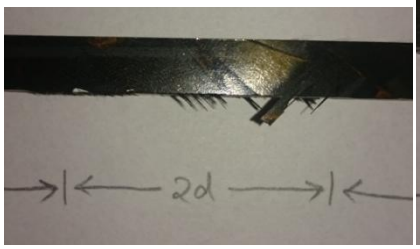

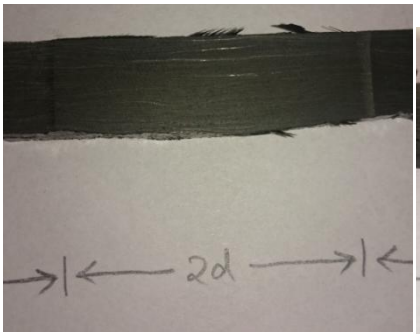

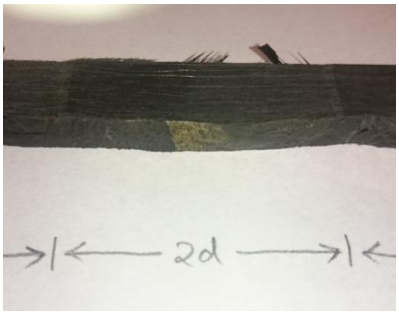

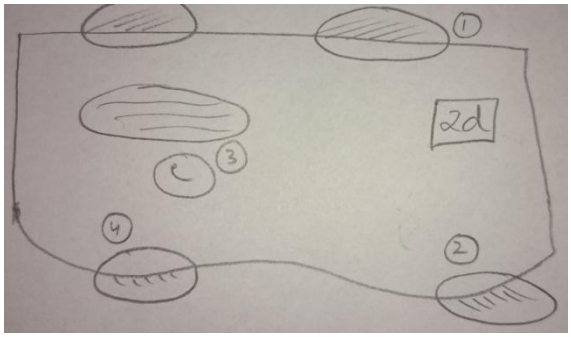

2d -1x - H

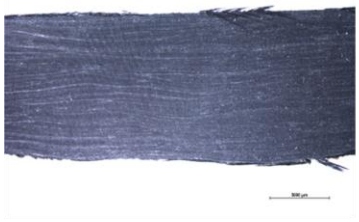

2d -1- 4x - H

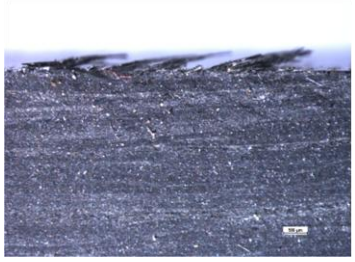

2d -2- 4x - H

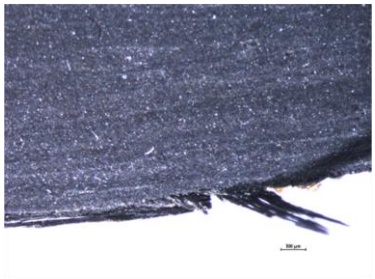

2d -3- 4x - H

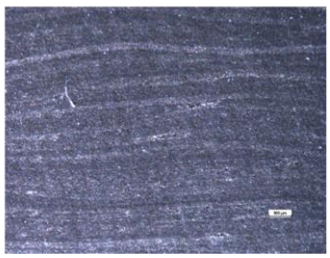

2d -4- 4x - H

Experiment 2 e : Speed - 1000 rpm; Feed - 2.12 mmpm;

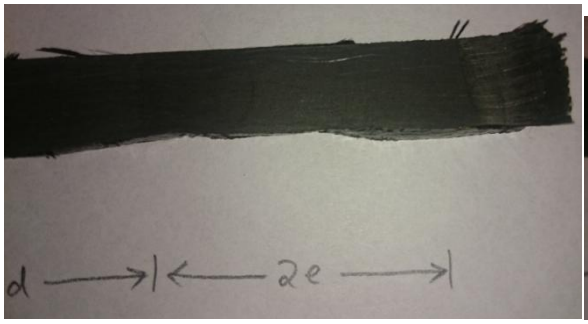

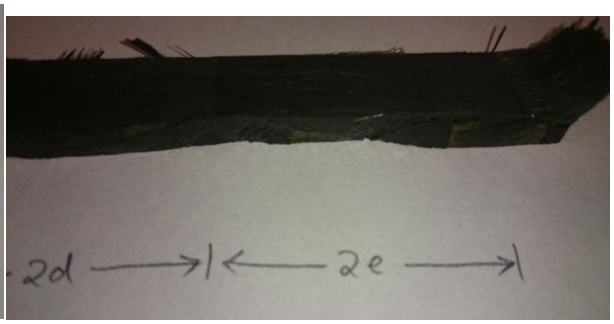

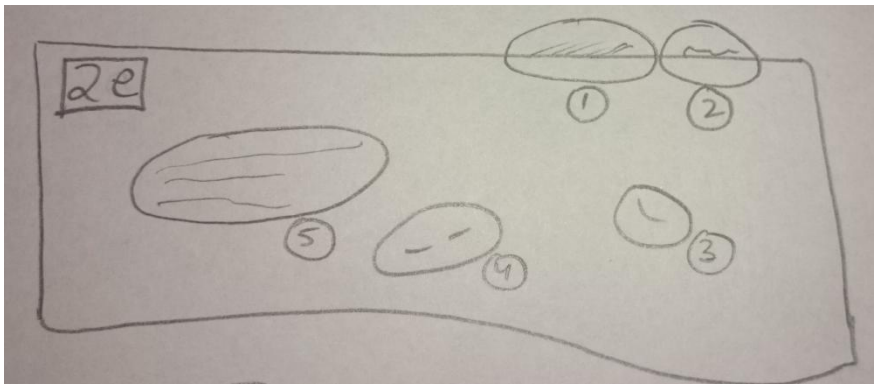

2e -1x - H

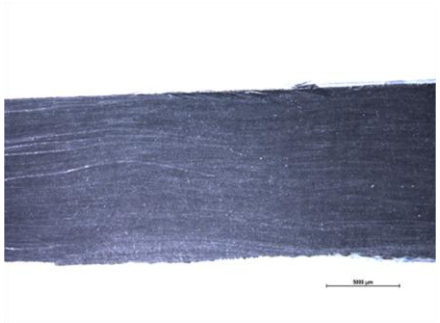

2e -1- 4x - H

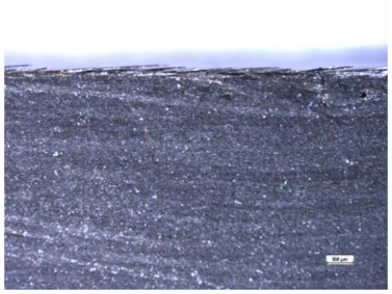

2e -2- 4x - H

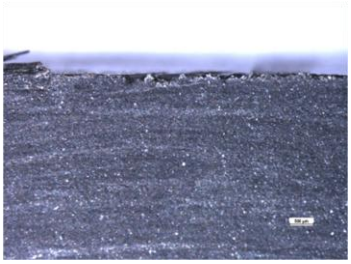

2e -3- 4x - H

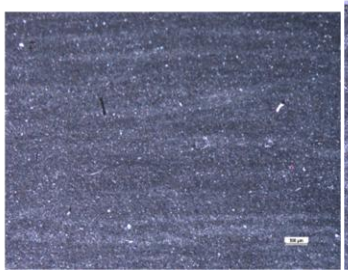

2e -4- 4x - H

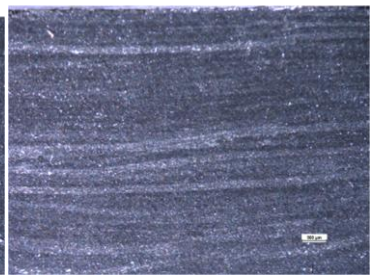

2e -5- 4x - H

Appendix - H - Roughness Profiles

h (from top) values: 1a1 = 2 mm; 1a2 = 4mm; 1a3 = 6 mm; 1a4 = 8 mm;

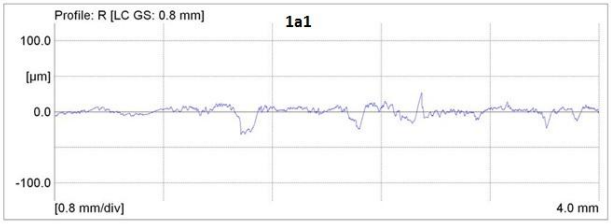

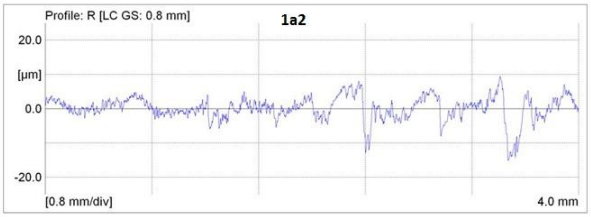

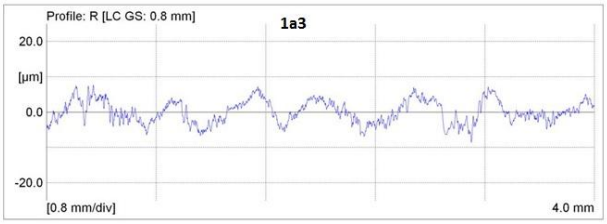

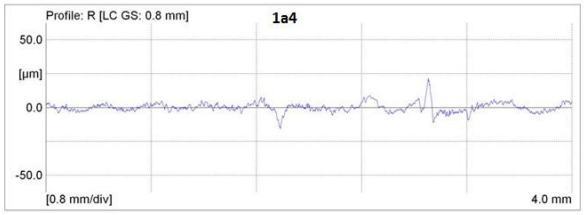

h (from top) values: 1b1 = 2 mm; 1b2 = 4mm; 1b3 = 6 mm; 1b4 = 8 mm;

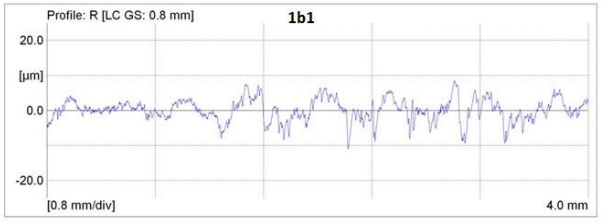

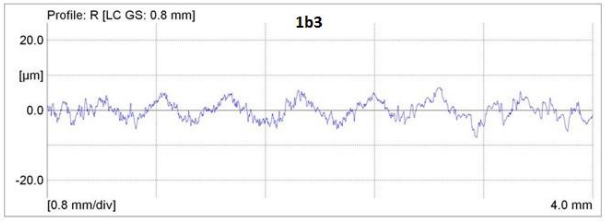

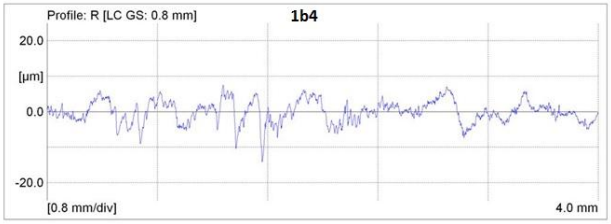

h (from top) values: 1c1 = 2 mm; 1c2 = 4mm; 1c3 = 6 mm; 1c4 = 8 mm;

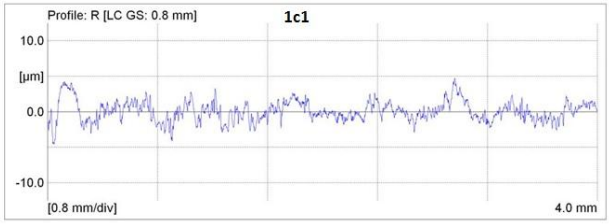

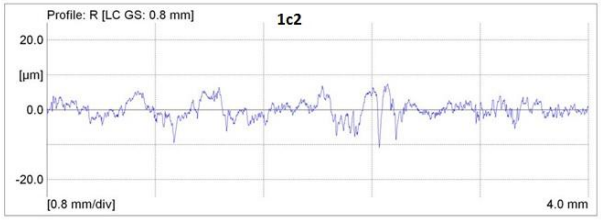

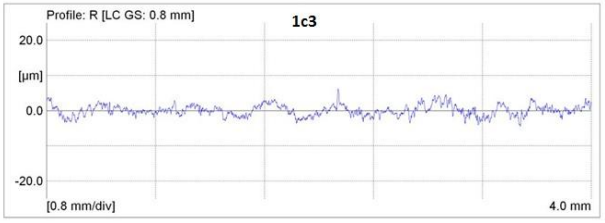

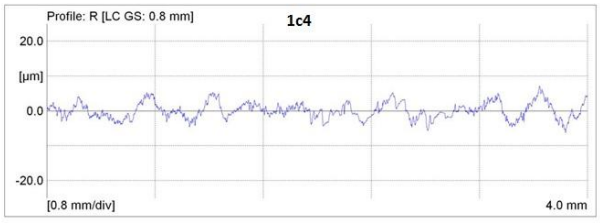

h (from top) values: 1d1 = 2 mm; 1d2 = 4mm; 1d3 = 6 mm; 1d4 = 8 mm;

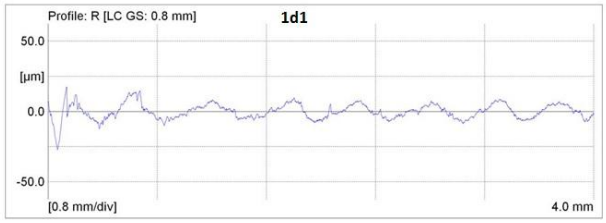

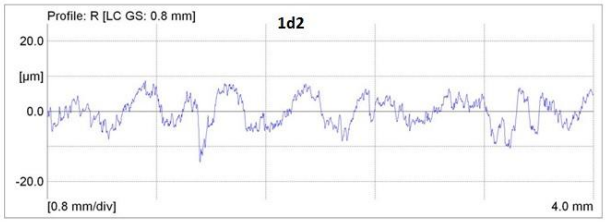

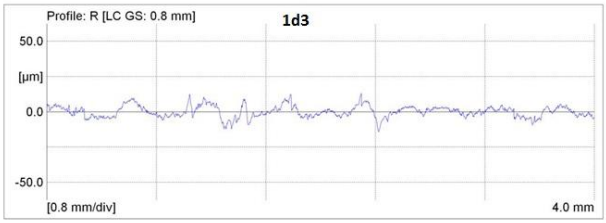

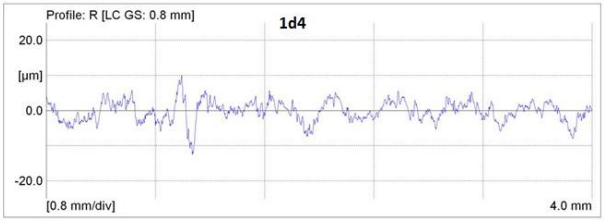

h (from top) values: 1e1 = 2 mm; 1e2 = 4mm; 1e3 = 6 mm; 1e4 = 8 mm;

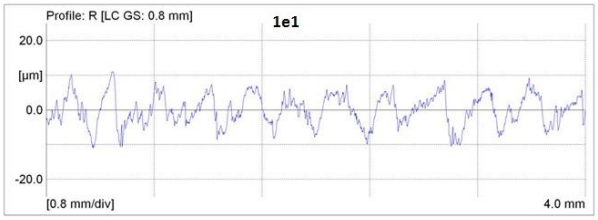

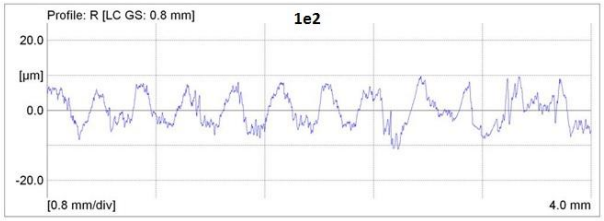

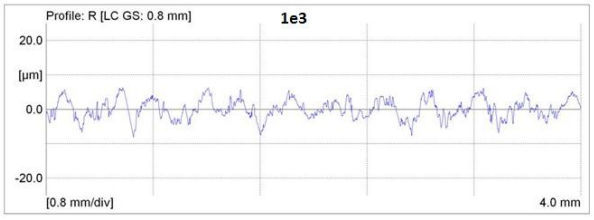

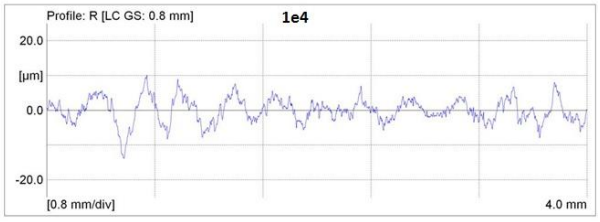

h (from top) values: 2a1 = 2 mm; 2a2 = 4mm; 2a3 = 6 mm; 2a4 = 8 mm;

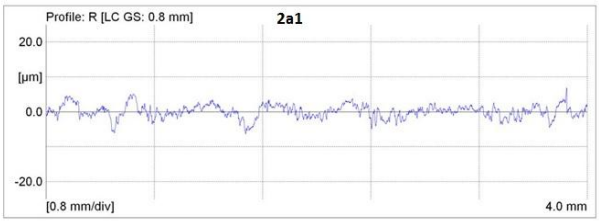

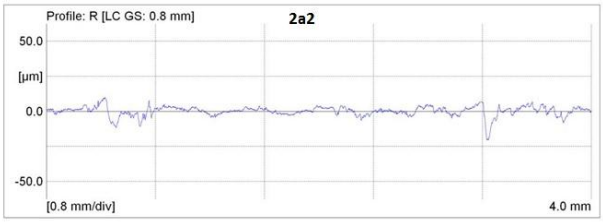

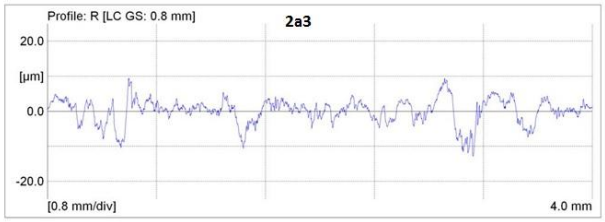

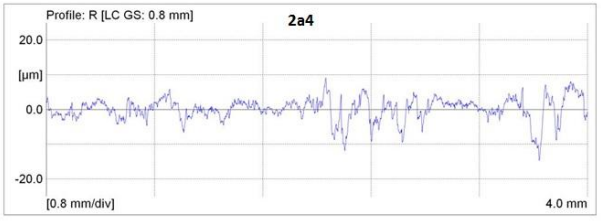

h (from top) values: 2b1 = 2 mm; 2b2 = 4mm; 2b3 = 6 mm; 2b4 = 8 mm;

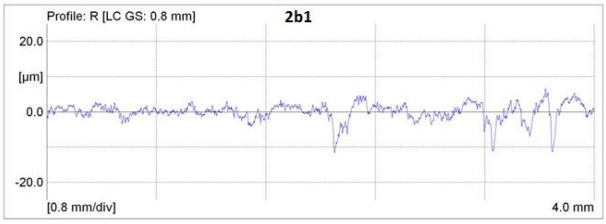

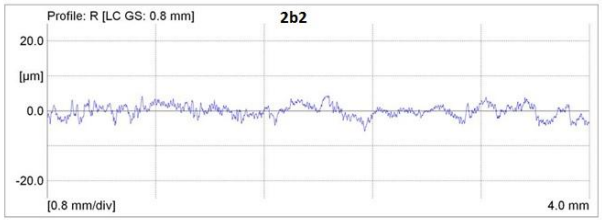

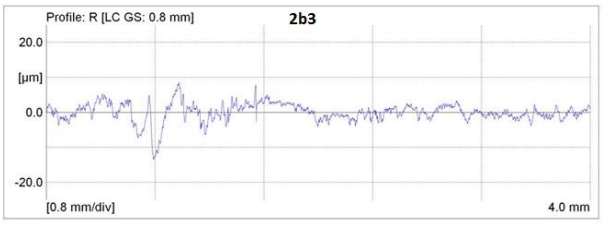

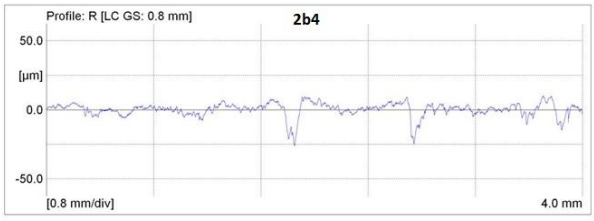

h (from top) values: 2c1 = 2 mm; 2c2 = 4mm; 2c3 = 6 mm; 2c4 = 8 mm;

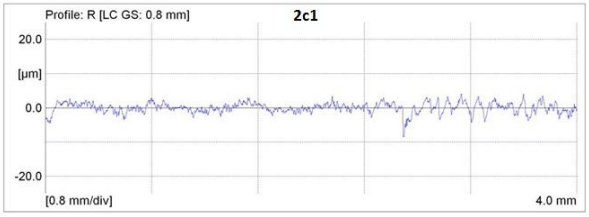

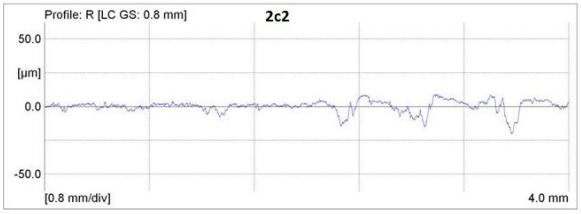

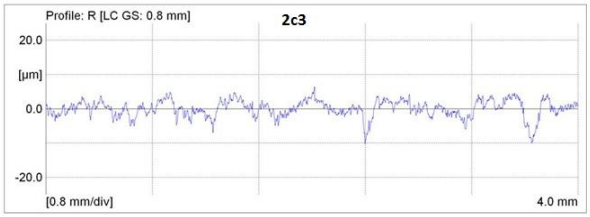

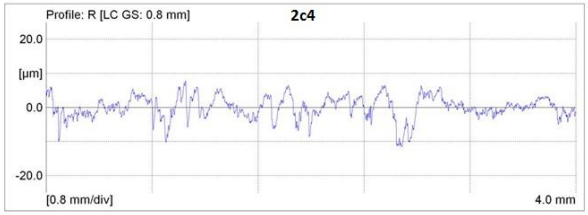

h (from top) values: 2d1 = 2 mm; 2d2 = 4mm; 2d3 = 6 mm; 2d4 = 8 mm;

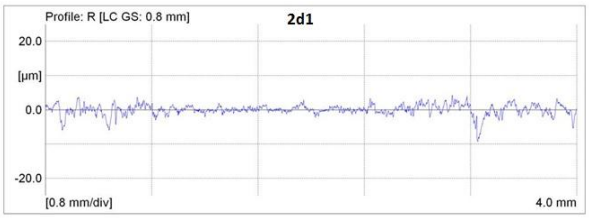

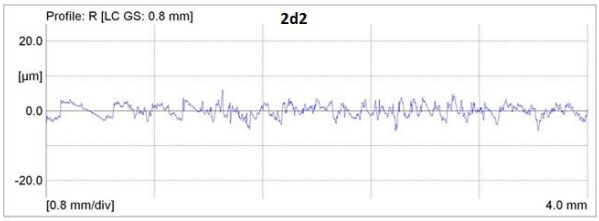

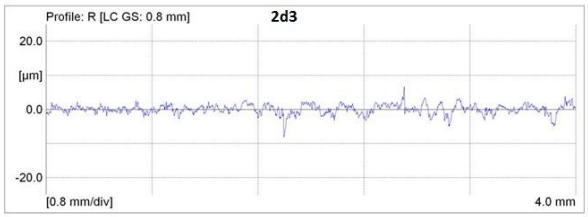

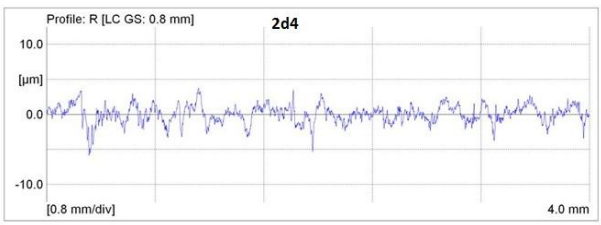

h (from top) values: 2e1 = 2 mm; 2e2 = 4mm; 2e3 = 6 mm; 2e4 = 8 mm;

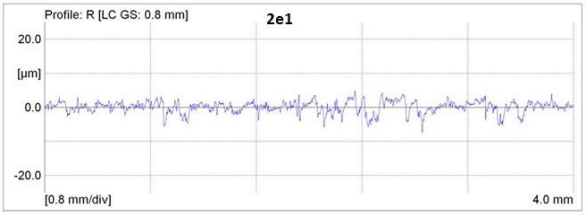

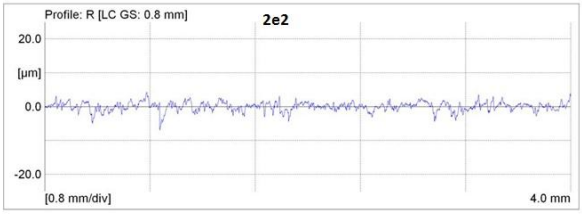

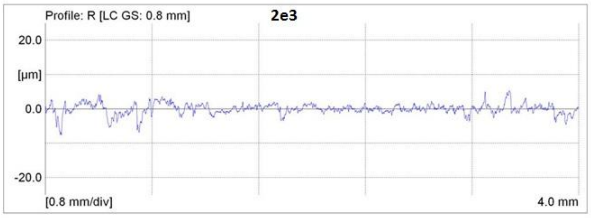

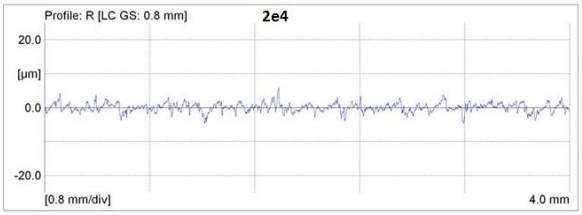

Appendix - I - CFRP – Climb (Even) – DOE Graphs etc

Fx

CFRP - Climb (Even) - Edge Trim ANOVA				
Experiment(s) Ignored	**Force**	**Model Used**		
		Process Order	**Selection**	**Alpha Out**
6,16,19,20	Fx	Cubic	Backward	0.05
6,16,19,20	Fy	Cubic	Backward	0.1
6,16,19,20	Fz	Quadratic	Backward	0.1
6,16,19,20	Ft	Quadratic	Backward	0.1
6,16,19,20	Fr	Cubic	Backward	0.05

Run	Factor 1 A : Speed rpm	Factor 2 B : Feed mm/min	Factor 3 C : DOC mm	Response 1 Fx N	Response 2 Fy N	Response 3 Fz N	Response 4 Ft N	Response 5 Fr N
1	6000	635	6.35	143.115	275.8503	364.7114	33.36993	311.1462
2	6000	635	3.81	101.5559	174.2728	368.1563	70.623	239.687
3	3000	635	3.81	153.2877	224.1279	112.6527	75.46583	316.3304
4	6000	635	2.54	104.6266	136.8084	356.0724	71.9315	210.8921
5	3000	635	2.54	59.06375	110.5862	113.7669	35.6466	119.7625
6	1000	635	2.54	94.42652	126.0127	22.12614	80.73293	140
7	1000	635	6.35	172.9833	235.1539	18.32296	152.8115	225
8	1000	635	3.81	143.6454	143.8556	20.28835	154.641	218.4237
9	6000	381	6.35	79.92946	115.9064	363.429	57.94921	258.9037
10	6000	381	3.81	112.8019	137.521	350.0182	65.67046	262.9074
11	6000	381	2.54	125.3633	203.2971	363.8001	64.58286	230.9507
12	3000	381	6.35	74.8513	124.6906	6.703777	34.27733	166.013
13	3000	381	3.81	96.40978	209.843	111.3645	43.47756	212.6087
14	3000	381	2.54	70.76549	98.6738	100.2196	42.63078	152.265
15	1000	381	2.54	139.5168	220.7682	23.96494	98.85523	260
16	1000	381	6.35	278.0024	346.8159	48.36253	147.822	320
17	6000	127	3.81	44.10433	109.1953	357.9492	25.8273	97.64605
18	3000	127	3.81	136.3261	141.4977	108.1768	30.9997	152.2137
19	1000	127	3.81	177.4816	204.8916	7.973164	61.44043	215
20	1000	127	2.54	142.0234	157.246	6.540984	51.1524	175
21	3000	127	2.54	120.9974	22.99295	85.52739	33.15409	247.9018
22	6000	127	6.35	177.6107	182.3015	354.4235	47.74905	194.4933
23	3000	127	6.35	161.991	267.6451	77.55997	46.26357	267.8589
24	1000	127	6.35	386.1639	396.624	20.56	102.1051	424.7395

Analysis of variance table [Partial sum of squares - Type III]

Source	Sum of Squares	df	Mean Square	F Value	p-value Prob> F	
Model	1.070E+005	10	10699.51	13.10	0.0003	significant
A-Speed	*1057.47*	*1*	*1057.47*	*1.30*	*0.2845*	
B-Feed	*752.48*	*1*	*752.48*	*0.92*	*0.3621*	
C-DOC	*614.67*	*1*	*614.67*	*0.75*	*0.4081*	
AB	*27465.41*	*1*	*27465.41*	*33.64*	*0.0003*	
BC	*1336.69*	*1*	*1336.69*	*1.64*	*0.2327*	
A^2	*13698.48*	*1*	*13698.48*	*16.78*	*0.0027*	
B^2	*13410.58*	*1*	*13410.58*	*16.42*	*0.0029*	
A^2B	*6307.15*	*1*	*6307.15*	*7.72*	*0.0214*	
AB^2	*5865.90*	*1*	*5865.90*	*7.18*	*0.0252*	
B^2C	*5827.25*	*1*	*5827.25*	*7.14*	*0.0256*	
Residual	7348.69	9	816.52			
Cor Total	1.143E+005	19				

Std. Dev.	28.57	R-Squared	0.9357
Mean	128.58	Adj R-Squared	0.8643
C.V. %	22.22	Pred R-Squared	0.5067
PRESS	56408.31	Adeq Precision	17.072

Fx =

+511.09110
-0.26418 * Speed
-0.81146 * Feed
+62.69661 * DOC
+5.92868E-004 * Speed * Feed
-0.33128 * Feed * DOC
+2.46841E-005 * Speed^2
+2.54741E-004 * Feed^2
-3.64656E-008 * Speed^2 * Feed
-3.06937E-007 * Speed * Feed^2
+3.94733E-004 * Feed^2 * DOC

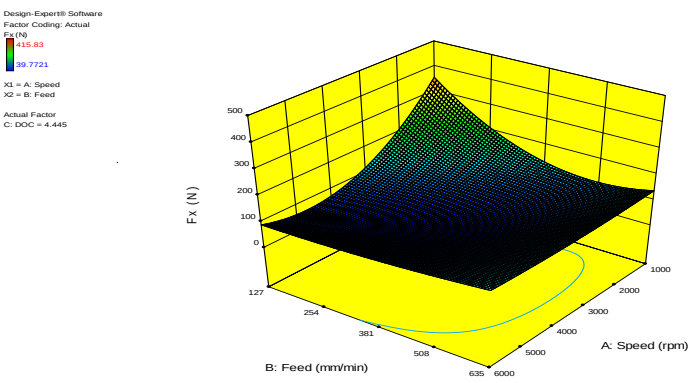
Design-Expert® Software
Factor Coding: Actual
Fx (N)
415.83
39.7721
X1 = A: Speed
X2 = B: Feed
Actual Factor
C: DOC = 4.445
F x (N)
500
400
300
200
100
0
127
254
381
508
635
B: Feed (mm/min)
1000
2000
3000
4000
5000
6000
A: Speed (rpm)

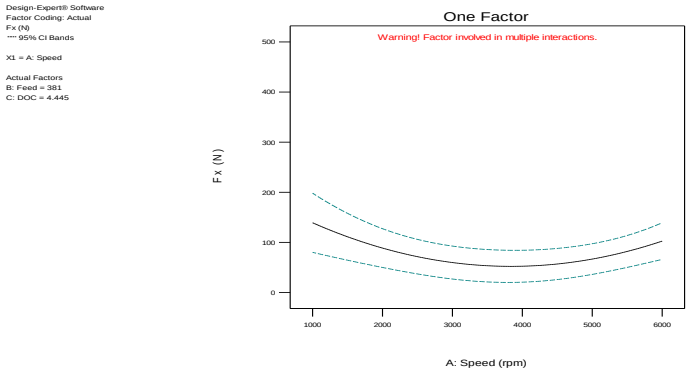
Design-Expert® Software
Factor Coding: Actual
Fx (N)
**** 95% CI Bands
X1 = A: Speed
Actual Factors
B: Feed = 381
C: DOC = 4.445
One Factor
Warning! Factor involved in multiple interactions.
F x (N)
500
400
300
200
100
0
1000
2000
3000
4000
5000
6000
A: Speed (rpm)

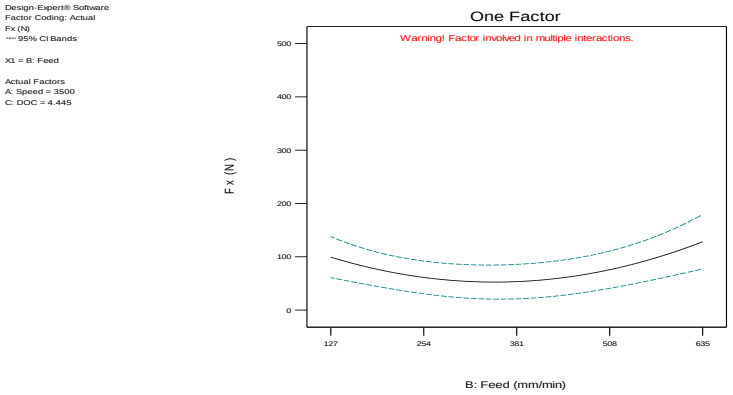
Design-Expert® Software
Factor Coding: Actual
Fx (N)
**** 95% CI Bands
X1 = B: Feed
Actual Factors
A: Speed = 3500
C: DOC = 4.445
One Factor
Warning! Factor involved in multiple interactions.
F x (N)
500
400
300
200
100
0
127
254
381
508
635
B: Feed (mm/min)

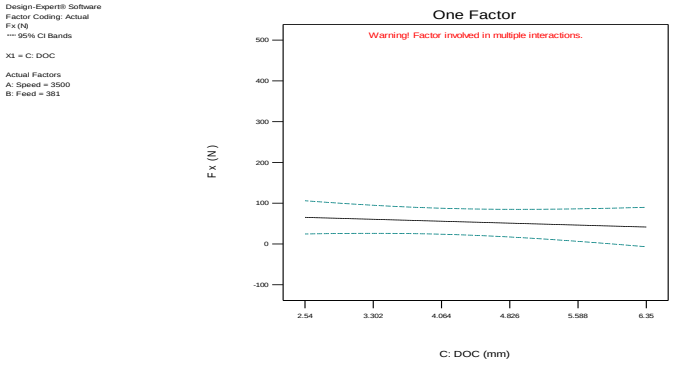
Design-Expert® Software
Factor Coding: Actual
Fx (N)
**** 95% CI Bands
X1 = C: DOC
Actual Factors
A: Speed = 3500
B: Feed = 381
One Factor
Warning! Factor involved in multiple interactions.
F x (N)
500
400
300
200
100
0
-100
2.54
3.302
4.064
4.826
5.588
6.35
C: DOC (mm)

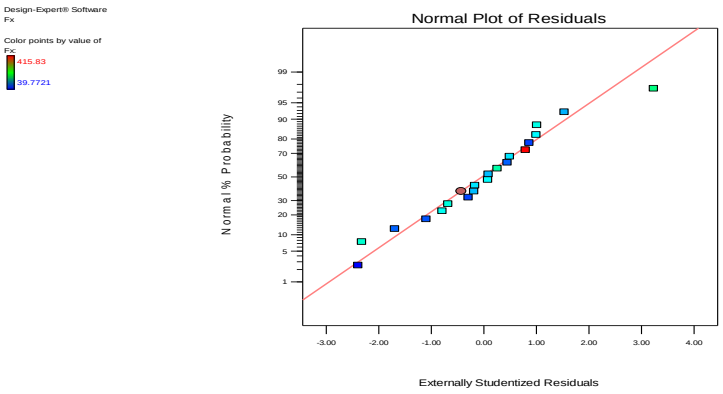
Design-Expert® Software
Fx
Color points by value of
Fx
415.83
39.7721
Normal Plot of Residuals
Normal % Probability
99
95
90
80
70
50
30
20
10
5
1
-3.00
-2.00
-1.00
0.00
1.00
2.00
3.00
4.00
Externally Studentized Residuals

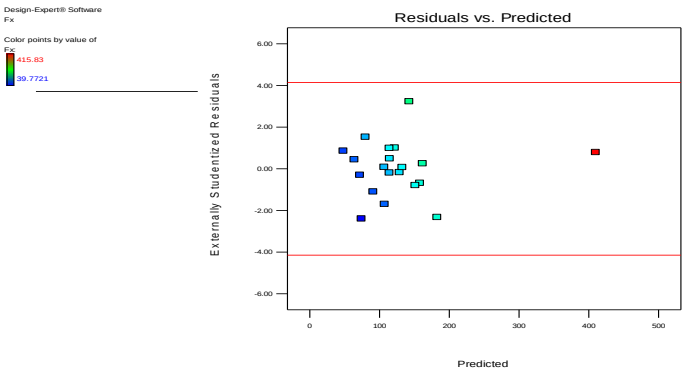
Design-Expert® Software
Fx
Color points by value of
Fx
415.83
39.7721
Residuals vs. Predicted
Externally Studentized Residuals
6.00
4.00
2.00
0.00
-2.00
-4.00
-6.00
0
100
200
300
400
500
Predicted

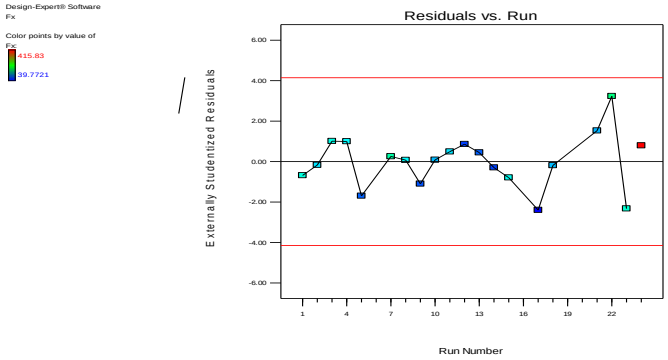
Design-Expert® Software
Fx
Color points by value of
Fx
415.83
39.7721
Residuals vs. Run
Externally Studentized Residuals
6.00
4.00
2.00
0.00
-2.00
-4.00
-6.00
1
4
7
10
13
16
19
22
Run Number

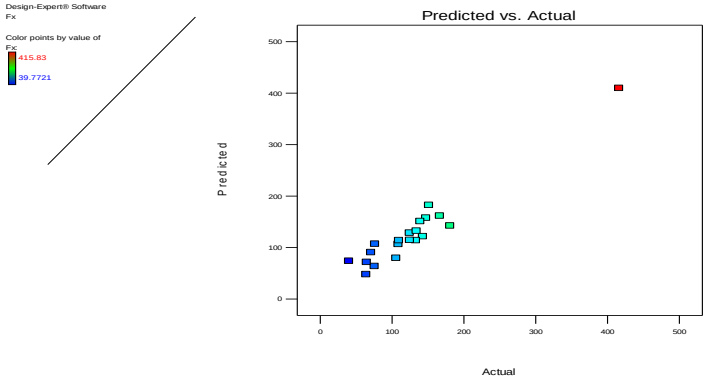
Design-Expert® Software
Fx
Color points by value of
Fx
415.83
39.7721
Predicted vs. Actual
Predicted
500
400
300
200
100
0
0
100
200
300
400
500
Actual

Fy

ANOVA for Response Surface Reduced Cubic model

Analysis of variance table [Partial sum of squares - Type III]

Source	Sum of Squares	df	Mean Square	F Value	p-value Prob> F	
Model	1.548E+005	12	12901.83	10.99	0.0020	significant
A-Speed	*16.55*	*1*	*16.55*	*0.014*	*0.9088*	
B-Feed	*14989.75*	*1*	*14989.75*	*12.76*	*0.0091*	
C-DOC	*1302.00*	*1*	*1302.00*	*1.11*	*0.3273*	
AB	*36946.52*	*1*	*36946.52*	*31.46*	*0.0008*	
AC	*514.66*	*1*	*514.66*	*0.44*	*0.5292*	
BC	*770.11*	*1*	*770.11*	*0.66*	*0.4447*	
A^2	*5103.06*	*1*	*5103.06*	*4.35*	*0.0756*	
B^2	*9131.71*	*1*	*9131.71*	*7.78*	*0.0270*	
A^2B	*15461.73*	*1*	*15461.73*	*13.17*	*0.0084*	
A^2C	*10564.38*	*1*	*10564.38*	*9.00*	*0.0200*	
AB^2	*4708.19*	*1*	*4708.19*	*4.01*	*0.0853*	
B^2C	*34894.40*	*1*	*34894.40*	*29.71*	*0.0010*	
Residual	8220.45	7	1174.35			
Cor Total	1.630E+005	19				

Std. Dev.	34.27	R-Squared	0.9496
Mean	177.70	Adj R-Squared	0.8631
C.V. %	19.28	Pred R-Squared	0.7173
PRESS	46100.19	Adeq Precision	14.855

Fy =
+688.97572
-0.56769 * Speed
+0.58712 * Feed
+46.53942 * DOC
+8.64030E-004 * Speed * Feed
+0.054463 * Speed * DOC
-0.72770 * Feed * DOC
+6.56662E-005 * Speed^2
-2.22853E-003 * Feed^2
-6.74273E-008 * Speed^2 * Feed
-7.47015E-006 * Speed^2 * DOC
-3.44241E-007 * Speed * Feed^2
+9.90311E-004 * Feed^2 * DOC

Design-Expert® Software
Factor Coding: Actual
Fy (N)
431.279
9.28259

X1 = A: Speed
X2 = B: Feed

Actual Factor
C: DOC = 4.445

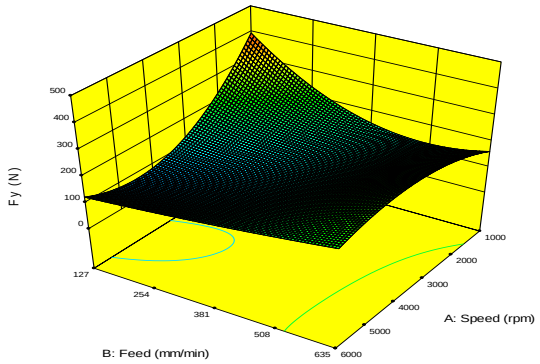

Design-Expert® Software
Factor Coding: Actual
Fy (N)
95% CI Bands

X1 = A: Speed

Actual Factors
B: Feed = 381
C: DOC = 4.445

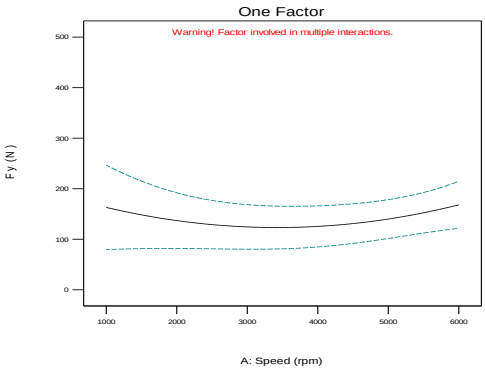

Design-Expert® Software
Factor Coding: Actual
Fy (N)
95% CI Bands

X1 = B: Feed

Actual Factors
A: Speed = 3500
C: DOC = 4.445

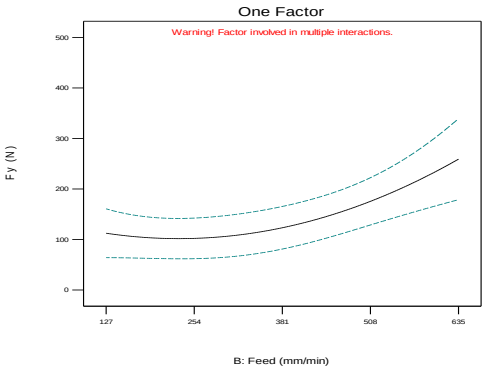

Design-Expert® Software
Factor Coding: Actual
Fy (N)
95% CI Bands

X1 = C: DOC

Actual Factors
A: Speed = 3500
B: Feed = 381

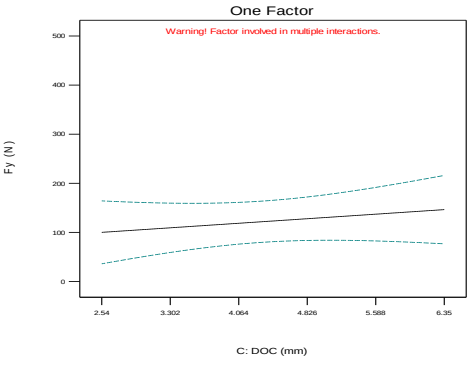


Design-Expert® Software
Fy
Color points by value of
Fy:
431.279
9.28259

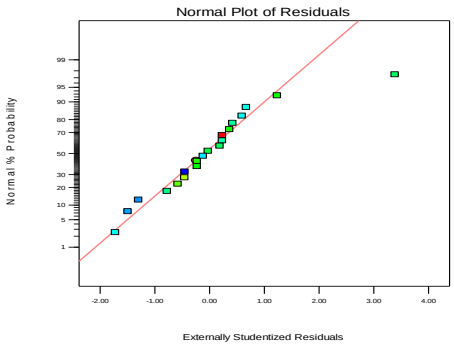
Normal Plot of Residuals
Normal % Probability
99
95
90
80
70
50
30
20
10
5
1
-2.00
-1.00
0.00
1.00
2.00
3.00
4.00
Externally Studentized Residuals


Design-Expert® Software
Fy
Color points by value of
Fy:
431.279
9.28259

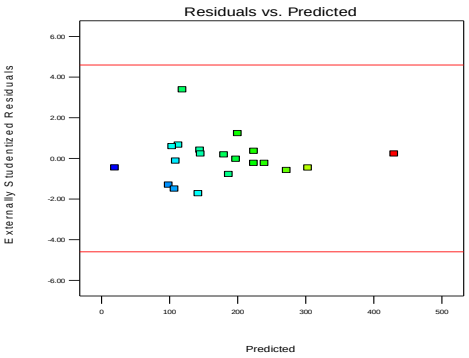
Residuals vs. Predicted
Externally Studentized Residuals
6.00
4.00
2.00
0.00
-2.00
-4.00
-6.00
0
100
200
300
400
500
Predicted


Design-Expert® Software
Fy
Color points by value of
Fy:
431.279
9.28259

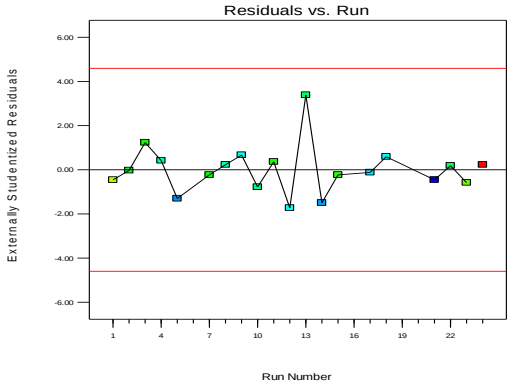
Residuals vs. Run
Externally Studentized Residuals
6.00
4.00
2.00
0.00
-2.00
-4.00
-6.00
1
4
7
10
13
16
19
22
Run Number


Design-Expert® Software
Fy
Color points by value of
Fy:
431.279
9.28259

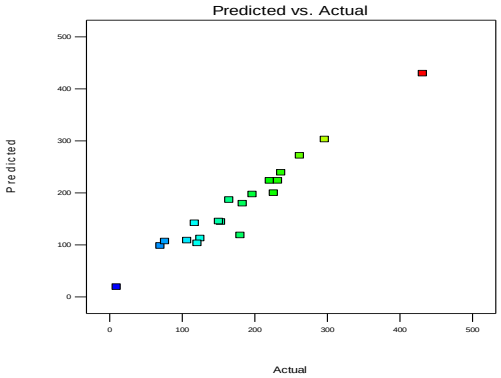
Predicted vs. Actual
Predicted
500
400
300
200
100
0
0
100
200
300
400
500
Actual

Fz

ANOVA for Response Surface Reduced Cubic model

Analysis of variance table [Partial sum of squares - Type III]

Source	Sum of Squares	df	Mean Square	F Value	p-value Prob> F	
Model	4.244E+005	5	84881.67	261.74	< 0.0001	significant
A-Speed	*2.932E+005*	*1*	*2.932E+005*	*904.14*	*< 0.0001*	
C-DOC	*4900.55*	*1*	*4900.55*	*15.11*	*0.0016*	
AC	*0.41*	*1*	*0.41*	*1.268E-003*	*0.9721*	
A^2	*22619.03*	*1*	*22619.03*	*69.75*	*< 0.0001*	
A^2C	*2307.15*	*1*	*2307.15*	*7.11*	*0.0184*	
Residual	4540.09	14	324.29			
Cor Total	4.289E+005	19				

Std. Dev.	18.01	R-Squared	0.9894
Mean	175.21	Adj R-Squared	0.9856
C.V. %	10.28	Pred R-Squared	0.9753
PRESS	10592.56	Adeq Precision	34.792

Fz =

-36.41485

+0.057510 * Speed

+13.26182 * DOC

-0.017622 * Speed * DOC

+1.40543E-006 * Speed^2

+2.51052E-006 * Speed^2 * DOC

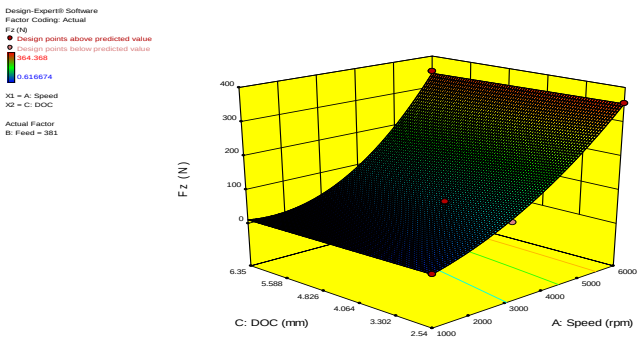
Design-Expert® Software
Factor Coding: Actual
Fz (N)
Design points above predicted value
Design points below predicted value
364.368
0.616674
X1 = A: Speed
X2 = C: DOC
Actual Factor
B: Feed = 381
F z (N)
400
300
200
100
0
6.35
5.588
4.826
4.064
3.302
2.54
C: DOC (mm)
1000
2000
3000
4000
5000
6000
A: Speed (rpm)

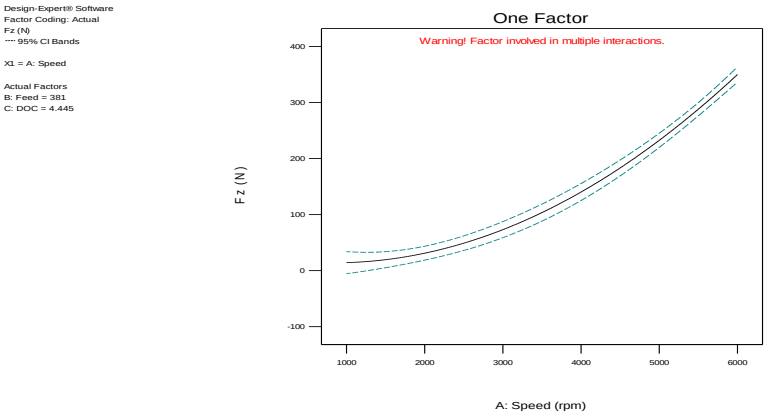
Design-Expert® Software
Factor Coding: Actual
Fz (N)
95% CI Bands
X1 = A: Speed
Actual Factors
B: Feed = 381
C: DOC = 4.445
One Factor
Warning! Factor involved in multiple interactions.
F z (N)
400
300
200
100
0
-100
1000
2000
3000
4000
5000
6000
A: Speed (rpm)

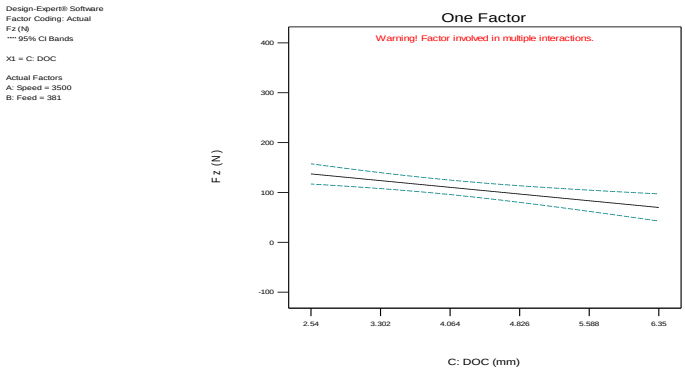
Design-Expert® Software
Factor Coding: Actual
Fz (N)
95% CI Bands
X1 = C: DOC
Actual Factors
A: Speed = 3500
B: Feed = 381
One Factor
Warning! Factor involved in multiple interactions.
F z (N)
400
300
200
100
0
-100
2.54
3.302
4.064
4.826
5.588
6.35
C: DOC (mm)


Design-Expert® Software
Fz
Color points by value of
Fz
364.368
0.616674

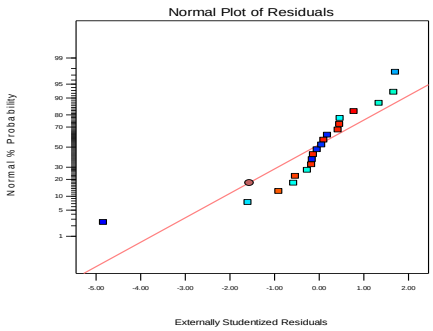
Normal Plot of Residuals
Normal % Probability
99
95
90
80
70
50
30
20
10
5
1
-5.00
-4.00
-3.00
-2.00
-1.00
0.00
1.00
2.00
Externally Studentized Residuals

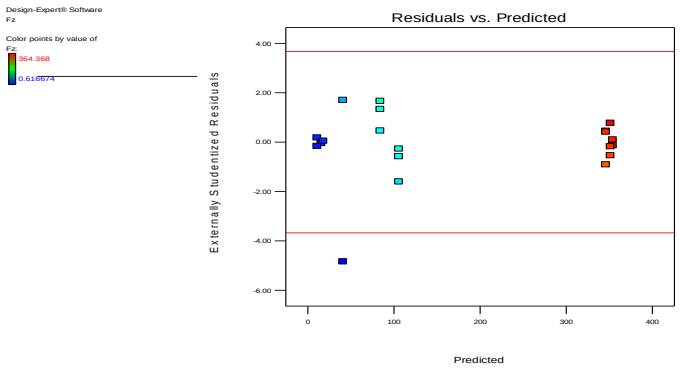
Design-Expert® Software
Fz
Color points by value of
Fz:
364.368
0.616674
Residuals vs. Predicted
Externally Studentized Residuals
4.00
2.00
0.00
-2.00
-4.00
-6.00
0
100
200
300
400
Predicted

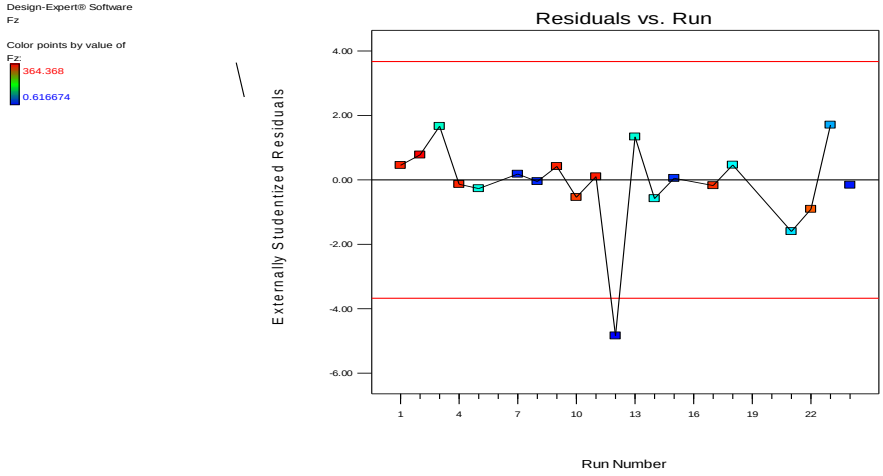
Design-Expert® Software
Fz
Color points by value of
Fz:
364.368
0.616674
Residuals vs. Run
Externally Studentized Residuals
4.00
2.00
0.00
-2.00
-4.00
-6.00
1
4
7
10
13
16
19
22
Run Number

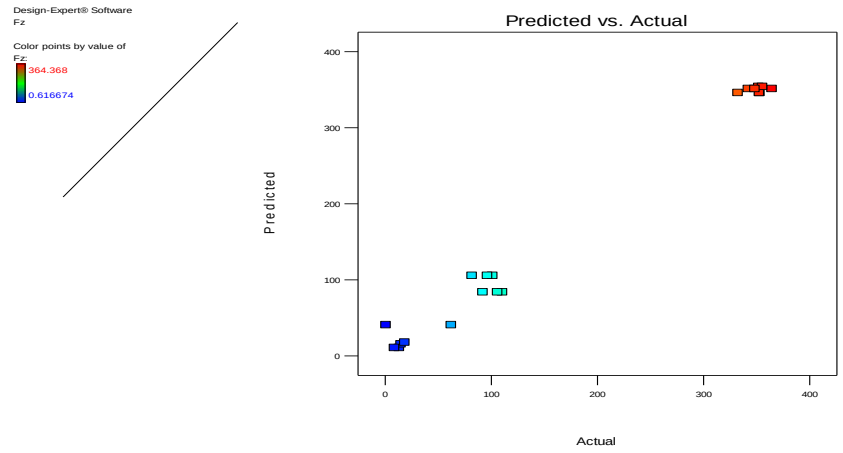
Design-Expert® Software
Fz
Color points by value of
Fz:
364.368
0.616674
Predicted vs. Actual
Predicted
400
300
200
100
0
0
100
200
300
400
Actual

Ft

ANOVA for Response Surface Reduced Quadratic model
Analysis of variance table [Partial sum of squares - Type III]

Source	Sum of Squares	df	Mean Square	F Value	p-value Prob> F	
Model	26800.90	5	5360.18	25.23	< 0.0001	significant
A-Speed	*14713.87*	*1*	*14713.87*	*69.24*	*< 0.0001*	
B-Feed	*2858.25*	*1*	*2858.25*	*13.45*	*0.0025*	
C-DOC	*237.50*	*1*	*237.50*	*1.12*	*0.3083*	
AC	*761.93*	*1*	*761.93*	*3.59*	*0.0791*	
A^2	*9426.49*	*1*	*9426.49*	*44.36*	*< 0.0001*	
Residual	2974.88	14	212.49			
Cor Total	29775.79	19				

Std. Dev.	14.58	R-Squared	0.9001
Mean	63.52	Adj R-Squared	0.8644
C.V. %	22.95	Pred R-Squared	0.7690
PRESS	6877.41	Adeq Precision	16.393

Ft =
+124.94383
-0.064078 * Speed
+0.060951 * Feed
+9.30673 * DOC
-2.00161E-003 * Speed * DOC
+8.27937E-006 * Speed^2

Design-Expert® Software
Factor Coding: Actual
Ft (N)
Design points above predicted value
Design points below predicted value
155.962
22.4976

X1 = A: Speed
X2 = C: DOC

Actual Factor
B: Feed = 381

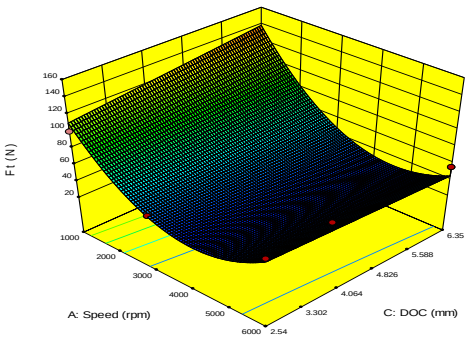

Design-Expert® Software
Factor Coding: Actual
Ft (N)
95% CI Bands

X1 = A: Speed

Actual Factors
B: Feed = 381
C: DOC = 4.445

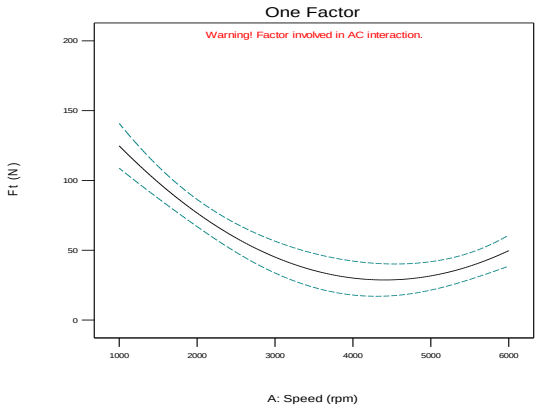

Design-Expert® Software
Factor Coding: Actual
Ft (N)
95% CI Bands

X1 = B: Feed

Actual Factors
A: Speed = 3500
C: DOC = 4.445

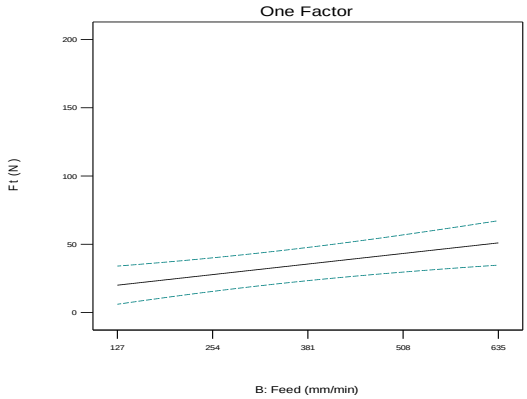

Design-Expert® Software
Factor Coding: Actual
Ft (N)
95% CI Bands

X1 = C: DOC

Actual Factors
A: Speed = 3500
B: Feed = 381

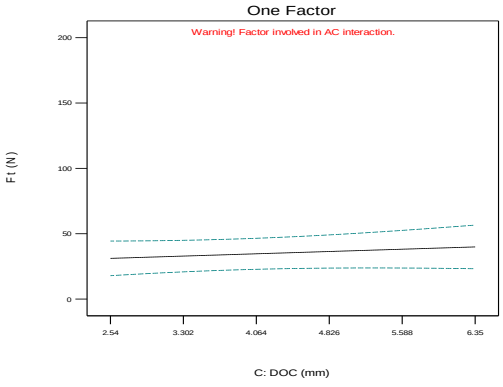

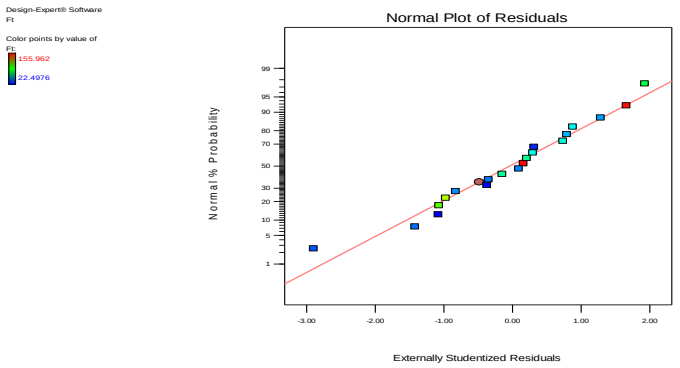
Design-Expert® Software
Ft
Color points by value of
Ft:
155.962
22.4976
Normal Plot of Residuals
Normal % Probability
99
95
90
80
70
50
30
20
10
5
1
-3.00
-2.00
-1.00
0.00
1.00
2.00
Externally Studentized Residuals

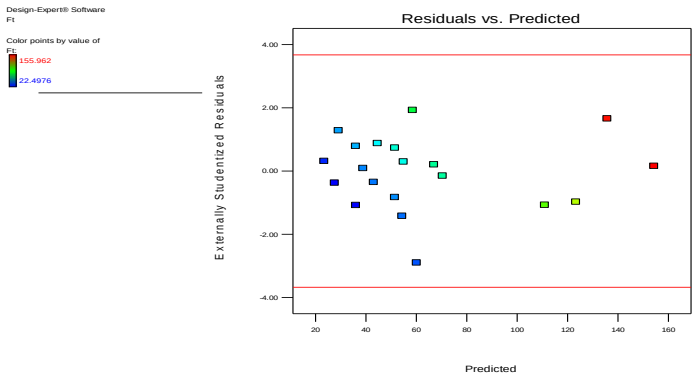
Design-Expert® Software
Ft
Color points by value of
Ft:
155.962
22.4976
Residuals vs. Predicted
Externally Studentized Residuals
4.00
2.00
0.00
-2.00
-4.00
20
40
60
80
100
120
140
160
Predicted

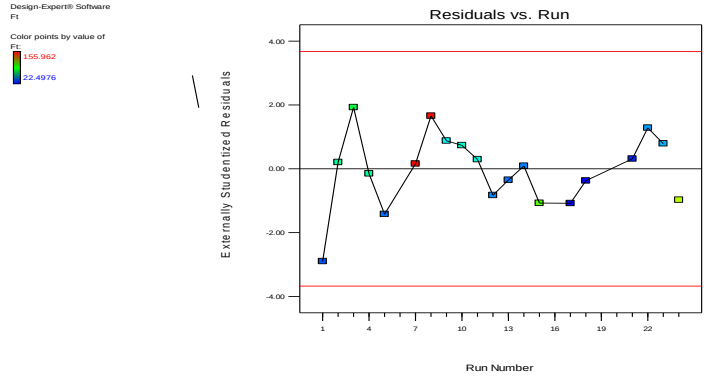
Design-Expert® Software
Ft
Color points by value of
Ft:
155.962
22.4976
Residuals vs. Run
Externally Studentized Residuals
4.00
2.00
0.00
-2.00
-4.00
1
4
7
10
13
16
19
22
Run Number

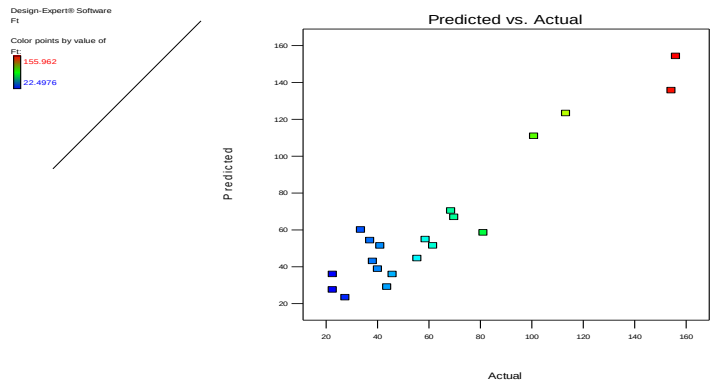
Design-Expert® Software
Ft
Color points by value of
Ft:
155.962
22.4976
Predicted vs. Actual
Predicted
160
140
120
100
80
60
40
20
20
40
60
80
100
120
140
160
Actual

Fr

ANOVA for Response Surface Reduced Cubic model
Analysis of variance table [Partial sum of squares - Type III]

Source	Sum of Squares	df	Mean Square	F Value	p-value Prob> F	
Model	1.351E+005	10	13509.40	5.36	0.0094	significant
A-Speed	*479.58*	*1*	*479.58*	*0.19*	*0.6729*	
B-Feed	*16682.47*	*1*	*16682.47*	*6.62*	*0.0300*	
C-DOC	*4222.48*	*1*	*4222.48*	*1.68*	*0.2277*	
AB	*24293.13*	*1*	*24293.13*	*9.64*	*0.0126*	
AC	*1540.45*	*1*	*1540.45*	*0.61*	*0.4544*	
BC	*232.07*	*1*	*232.07*	*0.092*	*0.7684*	
A^2	*7714.42*	*1*	*7714.42*	*3.06*	*0.1141*	
C^2	*7.54*	*1*	*7.54*	*2.991E-003*	*0.9576*	
ABC	*12009.29*	*1*	*12009.29*	*4.77*	*0.0569*	
BC^2	*28846.39*	*1*	*28846.39*	*11.45*	*0.0081*	
Residual	22678.93	9	2519.88			
Cor Total	1.578E+005	19				

Std. Dev.	50.20	R-Squared	0.8563
Mean	211.68	Adj R-Squared	0.6965
C.V. %	23.71	Pred R-Squared	0.0680
PRESS	1.470E+005	Adeq Precision	9.663

Fr =
+922.16037
+1.32701E-003 * Speed
-1.99878 * Feed
-370.35294 * DOC
-9.90762E-005 * Speed * Feed
-0.020657 * Speed * DOC
+1.03791 * Feed * DOC
+7.62361E-006 * Speed^2
+51.44809 * DOC^2
+4.60416E-005 * Speed * Feed * DOC
-0.13624 * Feed * DOC^2

Design-Expert® Software
Factor Coding: Actual
Fr (N)
459.998
75.8946

X1 = A: Speed
X2 = B: Feed

Actual Factor
C: DOC = 4.445

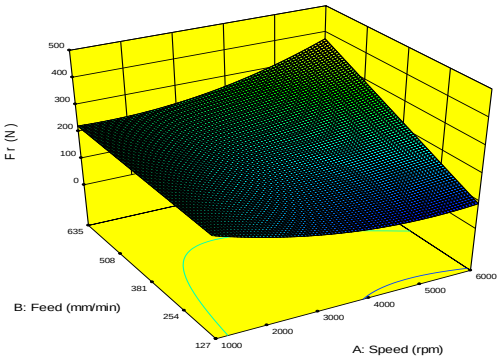

Design-Expert® Software
Factor Coding: Actual
Fr (N)
---- 95% CI Bands

X1 = A: Speed

Actual Factors
B: Feed = 381
C: DOC = 4.445

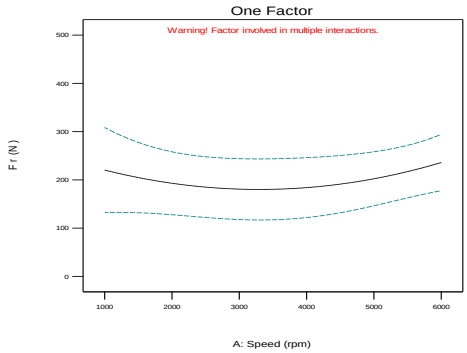

Design-Expert® Software
Factor Coding: Actual
Fr (N)
---- 95% CI Bands

X1 = B: Feed

Actual Factors
A: Speed = 3500
C: DOC = 4.445

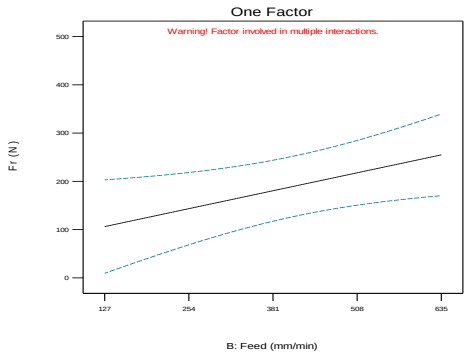

Design-Expert® Software
Factor Coding: Actual
Fr (N)
---- 95% CI Bands

X1 = C: DOC

Actual Factors
A: Speed = 3500
B: Feed = 381

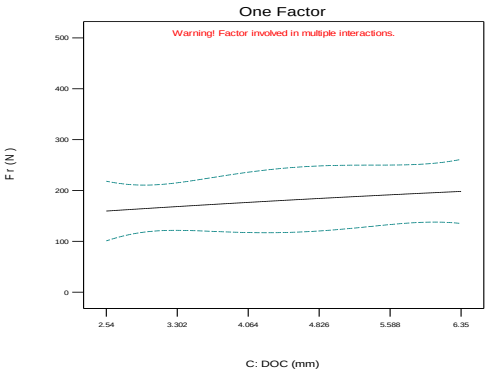

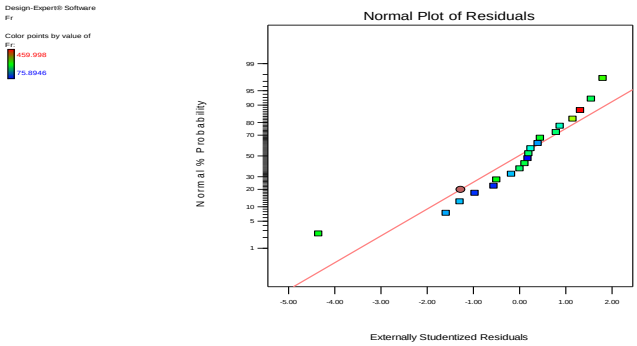
Design-Expert® Software
Fr
Color points by value of
Fr:
459.998
75.8946
Normal Plot of Residuals
Normal % Probability
99
95
90
80
70
50
30
20
10
5
1
-5.00
-4.00
-3.00
-2.00
-1.00
0.00
1.00
2.00
Externally Studentized Residuals

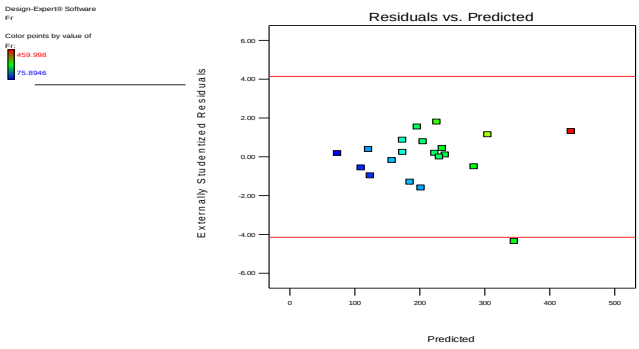
Design-Expert® Software
Fr
Color points by value of
Fr:
459.998
75.8946
Residuals vs. Predicted
Externally Studentized Residuals
6.00
4.00
2.00
0.00
-2.00
-4.00
-6.00
0
100
200
300
400
500
Predicted

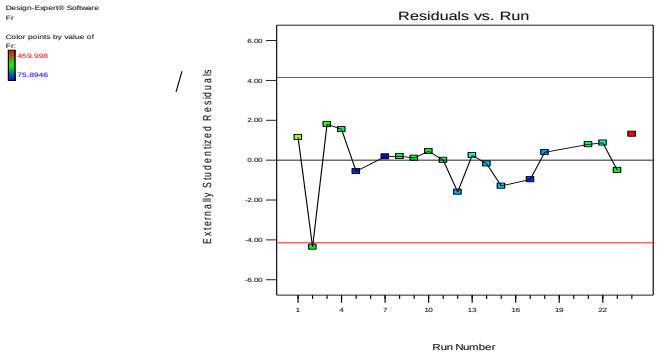
Design-Expert® Software
Fr
Color points by value of
Fr:
459.998
75.8946
Residuals vs. Run
Externally Studentized Residuals
6.00
4.00
2.00
0.00
-2.00
-4.00
-6.00
1
4
7
10
13
16
19
22
Run Number

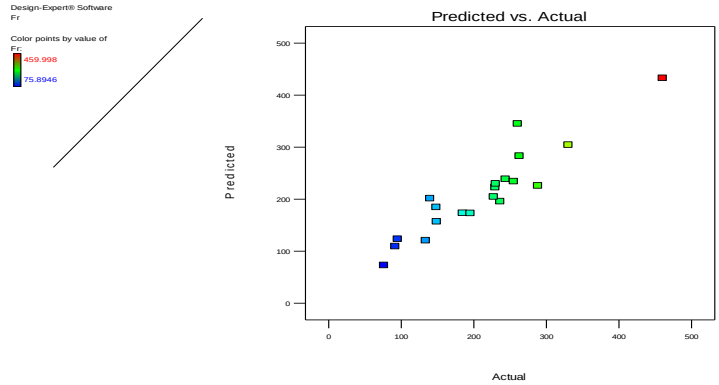
Design-Expert® Software
Fr
Color points by value of
Fr:
459.998
75.8946
Predicted vs. Actual
Predicted
500
400
300
200
100
0
0
100
200
300
400
500
Actual

Appendix - J - CFRP – Conventional (odd) – DOE Graphs etc

CFRP – Conventional (Odd) - Edge Trim ANOVA				
Experiment(s) Ignored	**Force**	**Model Used**		
		Process Order	**Selection**	**Alpha Out**
16,18,22,24	Fx	Cubic	Backward	0.05
16,18,22,24	Fy	Cubic	Backward	0.15
16,18,22,24	Fz	Cubic	Backward	0.15
16,18,22,24	Ft	Cubic	Backward	0.15
16,18,22,24	Fr	Quadratic	Backward	0.15

Run	Factor 1 A : Speed rpm	Factor 2 B : Feed mm/min	Factor 3 C : DOC mm	Response 1 Fx N	Response 2 Fy N	Response 3 Fz N	Response 4 Ft N	Response 5 Fr N
1	6000	635	6.35	143.115	275.8503	364.7114	33.36993	311.1462
2	6000	635	3.81	101.5559	174.2728	368.1563	70.623	239.687
3	3000	635	3.81	153.2877	224.1279	112.6527	75.46583	316.3304
4	6000	635	2.54	104.6266	136.8084	356.0724	71.9315	210.8921
5	3000	635	2.54	59.06375	110.5862	113.7669	35.6466	119.7625
6	1000	635	2.54	94.42652	126.0127	22.12614	80.73293	140
7	1000	635	6.35	172.9833	235.1539	18.32296	152.8115	225
8	1000	635	3.81	143.6454	143.8556	20.28835	154.641	218.4237
9	6000	381	6.35	79.92946	115.9064	363.429	57.94921	258.9037
10	6000	381	3.81	112.8019	137.521	350.0182	65.67046	262.9074
11	6000	381	2.54	125.3633	203.2971	363.8001	64.58286	230.9507
12	3000	381	6.35	74.8513	124.6906	6.703777	34.27733	166.013
13	3000	381	3.81	96.40978	209.843	111.3645	43.47756	212.6087
14	3000	381	2.54	70.76549	98.6738	100.2196	42.63078	152.265
15	1000	381	2.54	139.5168	220.7682	23.96494	98.85523	260
16	1000	381	6.35	278.0024	346.8159	48.36253	147.822	320
17	6000	127	3.81	44.10433	109.1953	357.9492	25.8273	97.64605
18	3000	127	3.81	136.3261	141.4977	108.1768	30.9997	152.2137
19	1000	127	3.81	177.4816	204.8916	7.973164	61.44043	215
20	1000	127	2.54	142.0234	157.246	6.540984	51.1524	175
21	3000	127	2.54	120.9974	22.99295	85.52739	33.15409	247.9018
22	6000	127	6.35	177.6107	182.3015	354.4235	47.74905	194.4933
23	3000	127	6.35	161.991	267.6451	77.55997	46.26357	267.8589
24	1000	127	6.35	386.1639	396.624	20.56	102.1051	424.7395

Fx

ANOVA for Response Surface Reduced Cubic model
Analysis of variance table [Partial sum of squares - Type III]

Source	Sum of Squares	df	Mean Square	F Value	p-value Prob> F	
Model	21332.80	8	2666.60	4.38	0.0134	significant
A-Speed	*21.57*	*1*	*21.57*	*0.035*	*0.8540*	
B-Feed	*187.03*	*1*	*187.03*	*0.31*	*0.5903*	
C-DOC	*1459.81*	*1*	*1459.81*	*2.40*	*0.1496*	
AB	*4797.16*	*1*	*4797.16*	*7.89*	*0.0170*	
BC	*96.92*	*1*	*96.92*	*0.16*	*0.6974*	
B^2	*3396.91*	*1*	*3396.91*	*5.58*	*0.0376*	
AB^2	*3535.24*	*1*	*3535.24*	*5.81*	*0.0346*	
B^2C	*6571.91*	*1*	*6571.91*	*10.80*	*0.0072*	
Residual	6690.76	11	608.25			
Cor Total	28023.56	19				

Std. Dev.	24.66	R-Squared	0.7612
Mean	115.95	Adj R-Squared	0.5876
C.V. %	21.27	Pred R-Squared	0.3535
PRESS	18116.99	Adeq Precision	7.541

Fx =
+124.70475
-0.048965 * Speed
+0.20683 * Feed
+45.83631 * DOC
+2.21629E-004 * Speed * Feed
-0.29795 * Feed * DOC
-4.81235E-004 * Feed^2
-2.37650E-007 * Speed * Feed^2
+4.01325E-004 * Feed^2 * DOC

Design-Expert® Software
Factor Coding: Actual
Fx (N)
177.482
44.1043

X1 = A: Speed
X2 = B: Feed

Actual Factor
C: DOC = 4.445

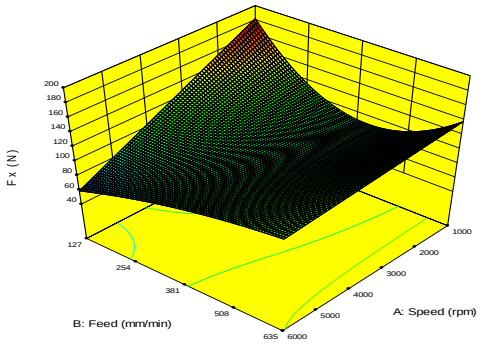

Design-Expert® Software
Factor Coding: Actual
Fx (N)
95% CI Bands

X1 = A: Speed

Actual Factors
B: Feed = 381
C: DOC = 4.445

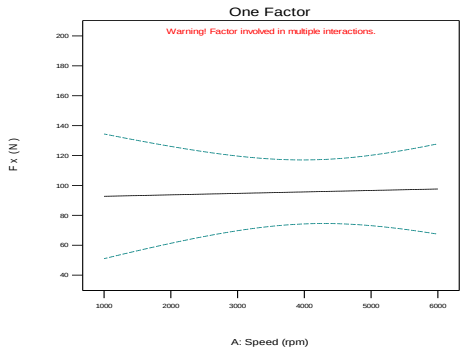

Design-Expert® Software
Factor Coding: Actual
Fx (N)
95% CI Bands

X1 = B: Feed

Actual Factors
A: Speed = 3500
C: DOC = 4.445

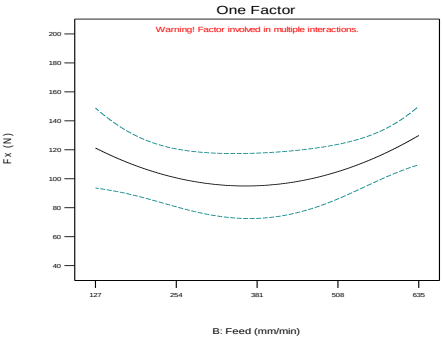

Design-Expert® Software
Factor Coding: Actual
Fx (N)
95% CI Bands

X1 = C: DOC

Actual Factors
A: Speed = 3500
B: Feed = 381

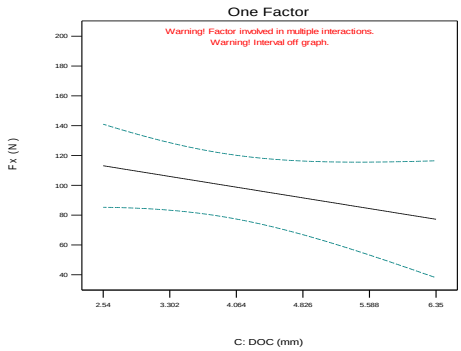

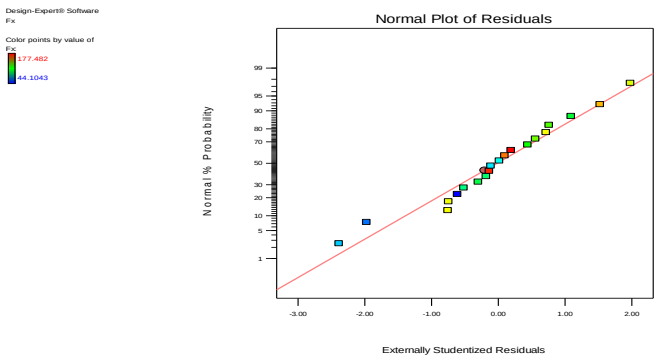
Design-Expert® Software
Fx
Color points by value of
Fx
177.482
44.1043
Normal Plot of Residuals
Normal % Probability
99
95
90
80
70
50
30
20
10
5
1
-3.00
-2.00
-1.00
0.00
1.00
2.00
Externally Studentized Residuals

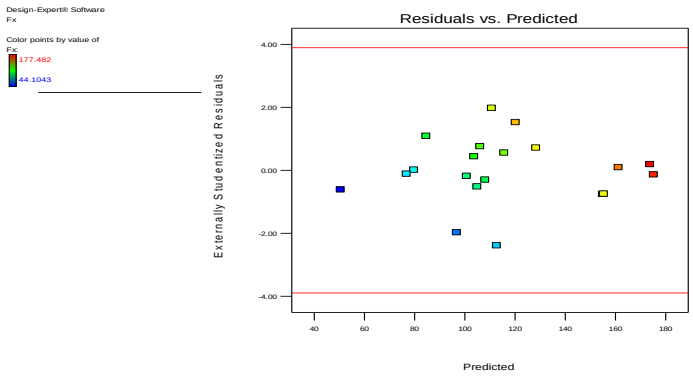
Design-Expert® Software
Fx
Color points by value of
Fx
177.482
44.1043
Residuals vs. Predicted
Externally Studentized Residuals
4.00
2.00
0.00
-2.00
-4.00
40
60
80
100
120
140
160
180
Predicted

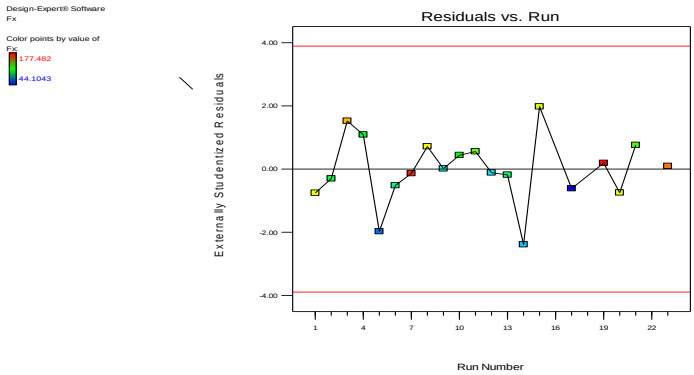
Design-Expert® Software
Fx
Color points by value of
Fx
177.482
44.1043
Residuals vs. Run
Externally Studentized Residuals
4.00
2.00
0.00
-2.00
-4.00
1
4
7
10
13
16
19
22
Run Number

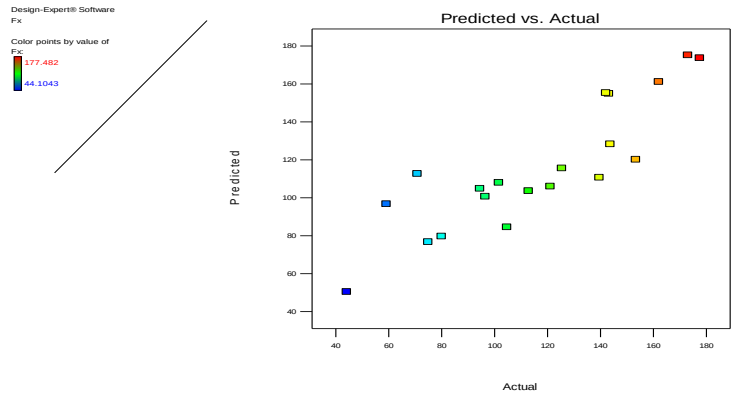
Design-Expert® Software
Fx
Color points by value of
Fx
177.482
44.1043
Predicted vs. Actual
Predicted
180
160
140
120
100
80
60
40
40
60
80
100
120
140
160
180
Actual

Fy

ANOVA for Response Surface Reduced Cubic model
Analysis of variance table [Partial sum of squares - Type III]

Source	Sum of Squares	df	Mean Square	F Value	p-value Prob> F	
Model	68553.59	11	6232.14	5.42	0.0120	significant
A-Speed	*865.91*	*1*	*865.91*	*0.75*	*0.4109*	
B-Feed	*9158.05*	*1*	*9158.05*	*7.96*	*0.0225*	
C-DOC	*103.14*	*1*	*103.14*	*0.090*	*0.7723*	
AB	*5029.49*	*1*	*5029.49*	*4.37*	*0.0699*	
AC	*353.49*	*1*	*353.49*	*0.31*	*0.5945*	
BC	*65.15*	*1*	*65.15*	*0.057*	*0.8179*	
A^2	*4.93*	*1*	*4.93*	*4.283E-003*	*0.9494*	
B^2	*4443.06*	*1*	*4443.06*	*3.86*	*0.0850*	
A^2B	*6484.24*	*1*	*6484.24*	*5.64*	*0.0450*	
A^2C	*3849.99*	*1*	*3849.99*	*3.35*	*0.1048*	
B^2C	*34558.61*	*1*	*34558.61*	*30.03*	*0.0006*	
Residual	9205.18	8	1150.65			
Cor Total	77758.77	19				

Std. Dev.	33.92	R-Squared	0.8816
Mean	164.97	Adj R-Squared	0.7188
C.V. %	20.56	Pred R-Squared	0.1126
PRESS	69002.14	Adeq Precision	10.111

Fy =
+15.32671
-0.26756 * Speed
+2.50400 * Feed
+83.28673 * DOC
+2.86183E-004 * Speed * Feed
+0.034262 * Speed * DOC
-0.74043 * Feed * DOC
+3.41569E-005 * Speed^2
-3.69419E-003 * Feed^2
-3.46856E-008 * Speed^2 * Feed
-4.65582E-006 * Speed^2 * DOC
+9.60132E-004 * Feed^2 * DOC

Design-Expert® Software
Factor Coding: Actual
Fy (N)
275.85
22.993

X1 = A: Speed
X2 = B: Feed

Actual Factor
C: DOC = 4.445

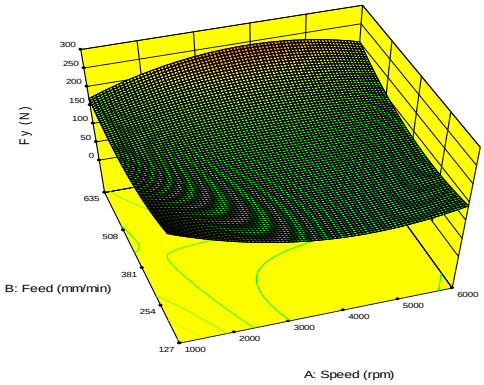

Design-Expert® Software
Factor Coding: Actual
Fy (N)
**** 95% CI Bands

X1 = A: Speed

Actual Factors
B: Feed = 381
C: DOC = 4.445

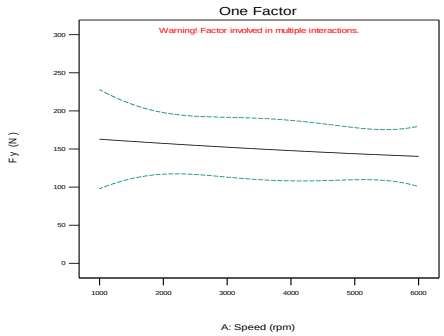

Design-Expert® Software
Factor Coding: Actual
Fy (N)
**** 95% CI Bands

X1 = B: Feed

Actual Factors
A: Speed = 3500
C: DOC = 4.445

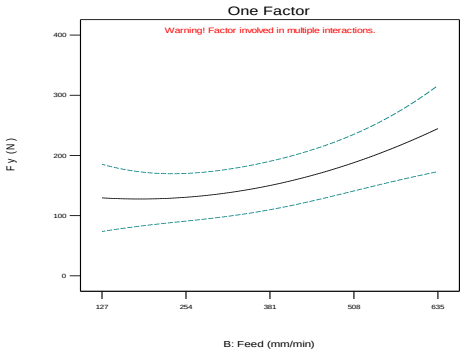

Design-Expert® Software
Factor Coding: Actual
Fy (N)
**** 95% CI Bands

X1 = C: DOC

Actual Factors
A: Speed = 3500
B: Feed = 381

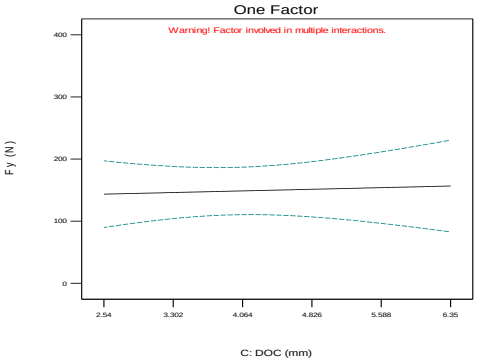

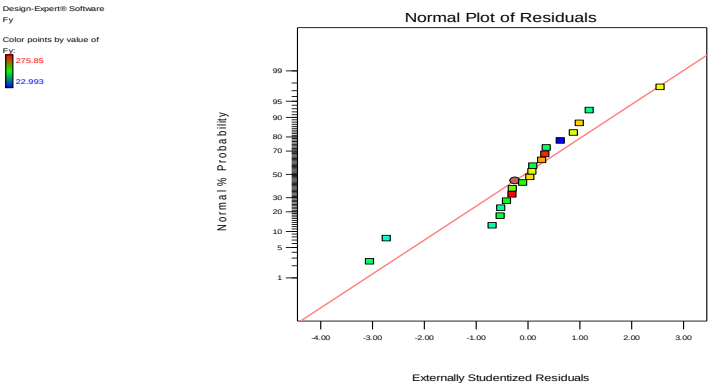
Design-Expert® Software
Fy
Color points by value of
Fy:
275.85
22.993
Normal Plot of Residuals
Normal % Probability
99
95
90
80
70
50
30
20
10
5
1
-4.00
-3.00
-2.00
-1.00
0.00
1.00
2.00
3.00
Externally Studentized Residuals

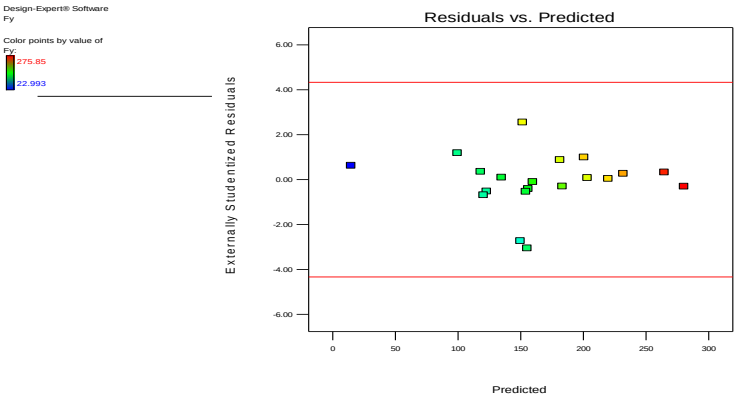
Design-Expert® Software
Fy
Color points by value of
Fy:
275.85
22.993
Residuals vs. Predicted
Externally Studentized Residuals
6.00
4.00
2.00
0.00
-2.00
-4.00
-6.00
0
50
100
150
200
250
300
Predicted

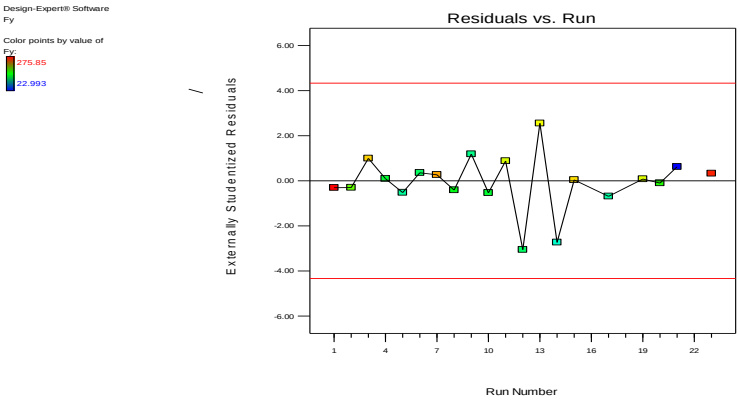
Design-Expert® Software
Fy
Color points by value of
Fy:
275.85
22.993
Residuals vs. Run
Externally Studentized Residuals
6.00
4.00
2.00
0.00
-2.00
-4.00
-6.00
1
4
7
10
13
16
19
22
Run Number

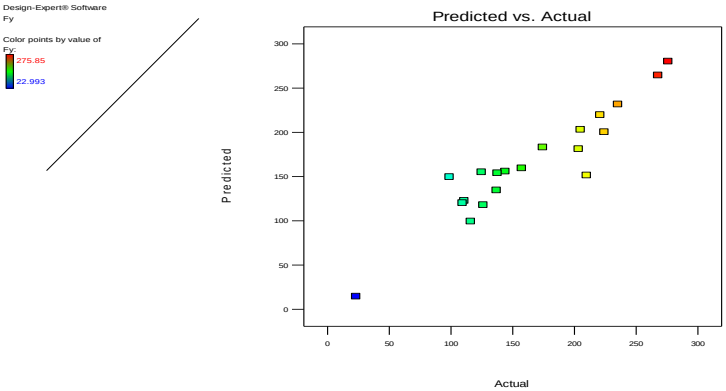
Design-Expert® Software
Fy
Color points by value of
Fy:
275.85
22.993
Predicted vs. Actual
Predicted
300
250
200
150
100
50
0
0
50
100
150
200
250
300
Actual

Fz

ANOVA for Response Surface Reduced Cubic model

Analysis of variance table [Partial sum of squares - Type III]

Source	Sum of Squares	df	Mean Square	F Value	p-value Prob> F	
Model	4.505E+005	13	34650.97	159.11	< 0.0001	significant
A-Speed	*87112.34*	*1*	*87112.34*	*400.01*	*< 0.0001*	
B-Feed	*1.96*	*1*	*1.96*	*8.999E-003*	*0.9275*	
C-DOC	*5630.53*	*1*	*5630.53*	*25.85*	*0.0023*	
AB	*1091.47*	*1*	*1091.47*	*5.01*	*0.0665*	
AC	*3239.64*	*1*	*3239.64*	*14.88*	*0.0084*	
BC	*273.26*	*1*	*273.26*	*1.25*	*0.3055*	
A^2	*4379.03*	*1*	*4379.03*	*20.11*	*0.0042*	
B^2	*2291.04*	*1*	*2291.04*	*10.52*	*0.0176*	
C^2	*807.45*	*1*	*807.45*	*3.71*	*0.1025*	
ABC	*1844.02*	*1*	*1844.02*	*8.47*	*0.0270*	
AB^2	*674.46*	*1*	*674.46*	*3.10*	*0.1289*	
B^2C	*4068.38*	*1*	*4068.38*	*18.68*	*0.0050*	
BC^2	*368.14*	*1*	*368.14*	*1.69*	*0.2412*	
Residual	1306.67	6	217.78			
Cor Total	4.518E+005	19				

Std. Dev.	14.76	R-Squared	0.9971
Mean	161.56	Adj R-Squared	0.9908
C.V. %	9.13	Pred R-Squared	0.9377
PRESS	28152.14	Adeq Precision	29.535

```
Fz =
    -86.75309
    -0.060428 * Speed
     +0.70960 * Feed
     +66.98427 * DOC
+1.92065E-004 * Speed * Feed
     +0.019625 * Speed * DOC
      -0.35025 * Feed * DOC
+6.99467E-006 * Speed^2
 -9.22620E-004 * Feed^2
      -10.55455 * DOC^2
 -2.96631E-005 * Speed * Feed * DOC
 -1.12207E-007 * Speed * Feed^2
+3.93269E-004 * Feed^2 * DOC
     +0.015680 * Feed * DOC^2
```

Design-Expert® Software
Factor Coding: Actual
Fz (N)
368.156
6.54098

X1 = A: Speed
X2 = B: Feed

Actual Factor
C: DOC = 4.445

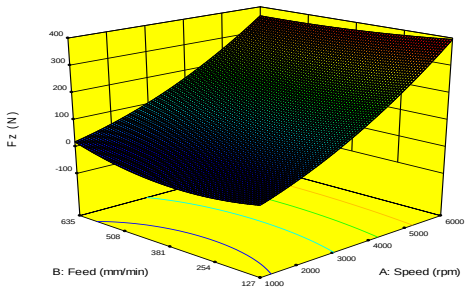

Design-Expert® Software
Factor Coding: Actual
Fz (N)
95% CI Bands

X1 = A: Speed

Actual Factors
B: Feed = 381
C: DOC = 4.445

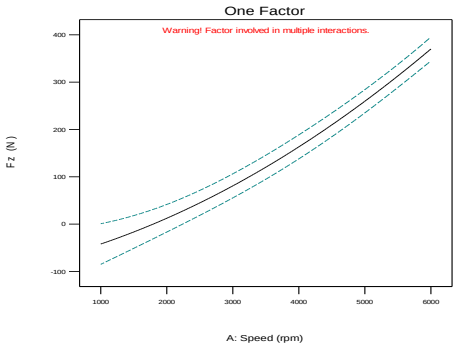

Design-Expert® Software
Factor Coding: Actual
Fz (N)
95% CI Bands

X1 = B: Feed

Actual Factors
A: Speed = 3500
C: DOC = 4.445

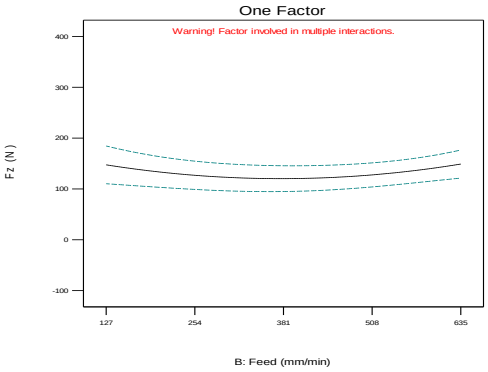

Design-Expert® Software
Factor Coding: Actual
Fz (N)
95% CI Bands

X1 = C: DOC

Actual Factors
A: Speed = 3500
B: Feed = 381

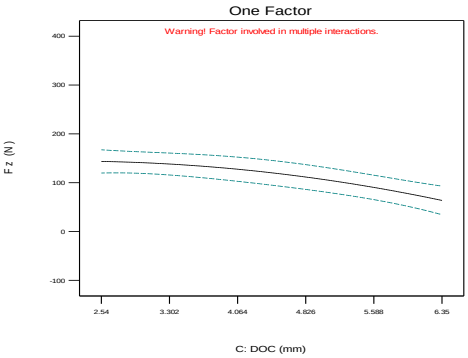

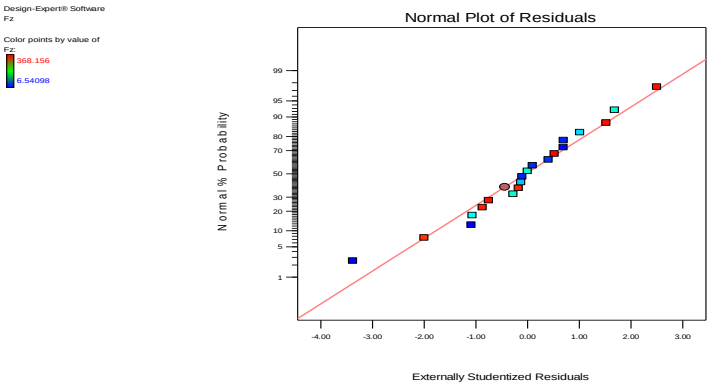
Design-Expert® Software
Fz
Color points by value of
Fz
368.156
6.54098
Normal Plot of Residuals
Normal % Probability
99
95
90
80
70
50
30
20
10
5
1
-4.00
-3.00
-2.00
-1.00
0.00
1.00
2.00
3.00
Externally Studentized Residuals

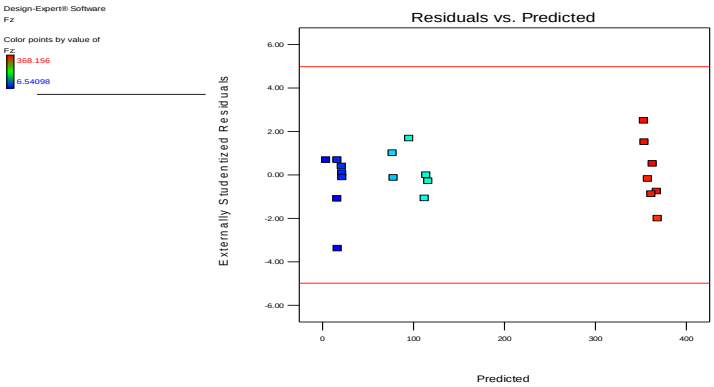
Design-Expert® Software
Fz
Color points by value of
Fz
368.156
6.54098
Residuals vs. Predicted
Externally Studentized Residuals
6.00
4.00
2.00
0.00
-2.00
-4.00
-6.00
0
100
200
300
400
Predicted

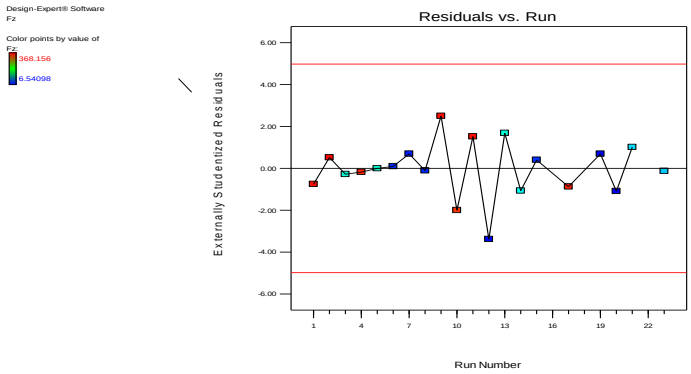
Design-Expert® Software
Fz
Color points by value of
Fz
368.156
6.54098
Residuals vs. Run
Externally Studentized Residuals
6.00
4.00
2.00
0.00
-2.00
-4.00
-6.00
1
4
7
10
13
16
19
22
Run Number

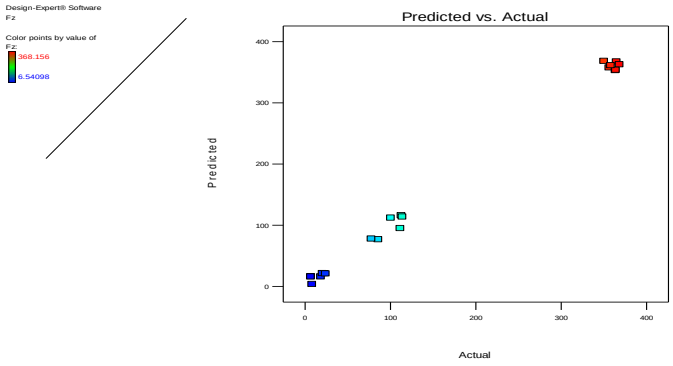
Design-Expert® Software
Fz
Color points by value of
Fz
368.156
6.54098
Predicted vs. Actual
Predicted
400
300
200
100
0
0
100
200
300
400
Actual

Ft

ANOVA for Response Surface Reduced Cubic model

Analysis of variance table [Partial sum of squares - Type III]

Source	Sum of Squares	df	Mean Square	F Value	p-value Prob> F	
Model	23743.29	14	1695.95	16.63	0.0029	significant
A-Speed	*2593.85*	*1*	*2593.85*	*25.43*	*0.0040*	
B-Feed	*553.52*	*1*	*553.52*	*5.43*	*0.0673*	
C-DOC	*116.88*	*1*	*116.88*	*1.15*	*0.3334*	
AB	*1750.78*	*1*	*1750.78*	*17.16*	*0.0090*	
AC	*8.816E-003*	*1*	*8.816E-003*	*8.643E-005*	*0.9929*	
BC	*97.27*	*1*	*97.27*	*0.95*	*0.3736*	
A^2	*3042.28*	*1*	*3042.28*	*29.83*	*0.0028*	
B^2	*0.59*	*1*	*0.59*	*5.759E-003*	*0.9425*	
C^2	*225.96*	*1*	*225.96*	*2.22*	*0.1968*	
ABC	*837.59*	*1*	*837.59*	*8.21*	*0.0352*	
A^2B	*290.10*	*1*	*290.10*	*2.84*	*0.1525*	
AC^2	*681.80*	*1*	*681.80*	*6.68*	*0.0491*	
B^2C	*546.54*	*1*	*546.54*	*5.36*	*0.0685*	
BC^2	*799.55*	*1*	*799.55*	*7.84*	*0.0380*	
Residual	510.01	5	102.00			
Cor Total	24253.30	19				

Std. Dev.	10.10	R-Squared	0.9790
Mean	65.03	Adj R-Squared	0.9201
C.V. %	15.53	Pred R-Squared	0.6529
PRESS	8418.31	Adeq Precision	14.709

Ft =

+71.16062
-0.013088 * Speed
-9.49021E-004 * Feed
-6.69459 * DOC
-9.30215E-007 * Speed * Feed
-9.65593E-003 * Speed * DOC
+0.18570 * Feed * DOC
+2.52158E-006 * Speed^2
-6.28867E-004 * Feed^2
-0.15919 * DOC^2
-2.15946E-005 * Speed * Feed * DOC
+8.90823E-009 * Speed^2 * Feed
+2.01329E-003 * Speed * DOC^2
+1.39935E-004 * Feed^2 * DOC

-0.025388 * Feed * DOC^2

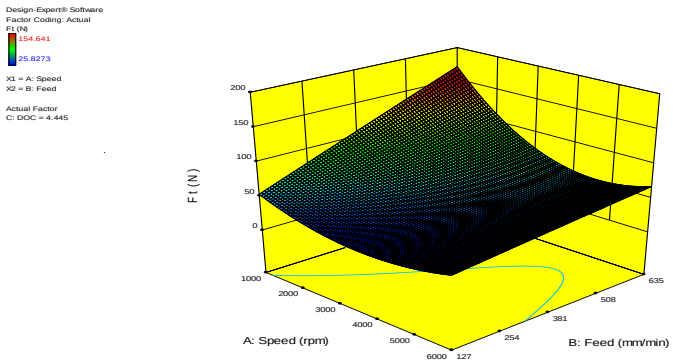

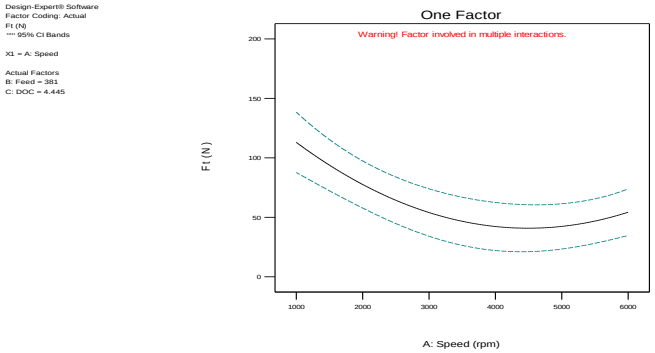

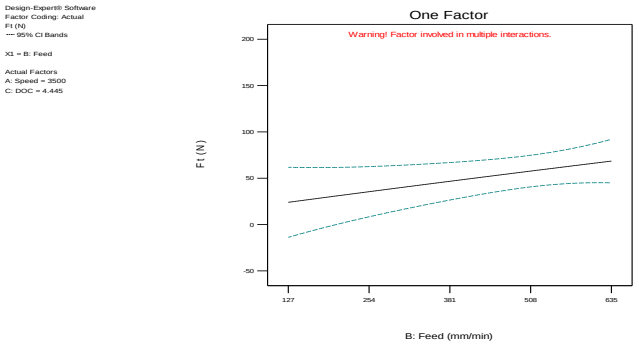

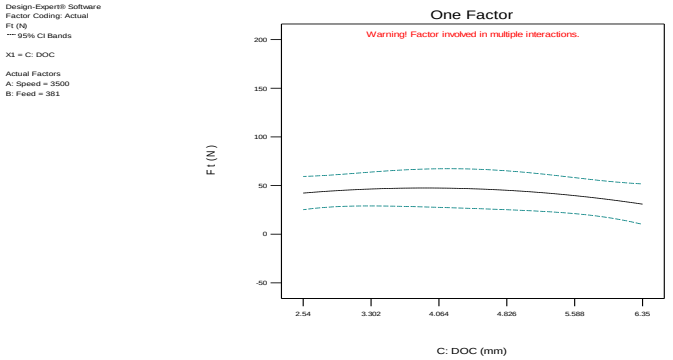

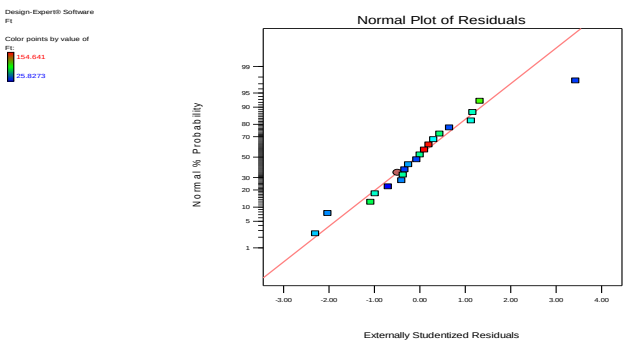
Design-Expert® Software
Ft
Color points by value of
Ft:
154.641
25.8273
Normal Plot of Residuals
Normal % Probability
99
95
90
80
70
50
30
20
10
5
1
-3.00
-2.00
-1.00
0.00
1.00
2.00
3.00
4.00
Externally Studentized Residuals

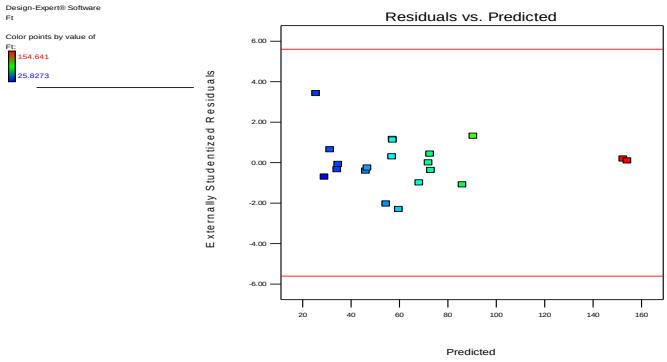
Design-Expert® Software
Ft
Color points by value of
Ft:
154.641
25.8273
Residuals vs. Predicted
Externally Studentized Residuals
6.00
4.00
2.00
0.00
-2.00
-4.00
-6.00
20
40
60
80
100
120
140
160
Predicted

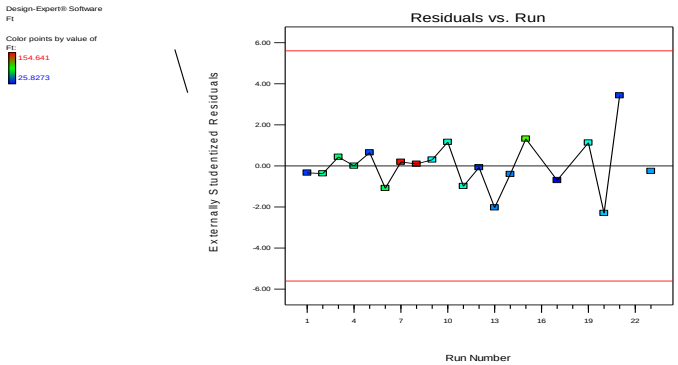
Design-Expert® Software
Ft
Color points by value of
Ft:
154.641
25.8273
Residuals vs. Run
Externally Studentized Residuals
6.00
4.00
2.00
0.00
-2.00
-4.00
-6.00
1
4
7
10
13
16
19
22
Run Number

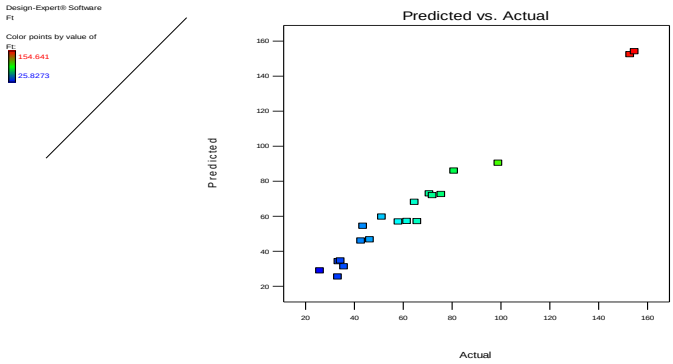
Design-Expert® Software
Ft
Color points by value of
Ft:
154.641
25.8273
Predicted vs. Actual
Predicted
160
140
120
100
80
60
40
20
20
40
60
80
100
120
140
160
Actual

Fr

ANOVA for Response Surface Reduced 2FI model
Analysis of variance table [Partial sum of squares - Type III]

Source	Sum of Squares	df	Mean Square	F Value	p-value Prob> F	
Model	19915.19	4	4978.80	1.59	0.2291	not significant
A-Speed	*0.11*	*1*	*0.11*	*3.472E-005*	*0.9954*	
B-Feed	*2521.49*	*1*	*2521.49*	*0.80*	*0.3843*	
C-DOC	*8805.25*	*1*	*8805.25*	*2.81*	*0.1147*	
AB	*9328.98*	*1*	*9328.98*	*2.97*	*0.1052*	
Residual	47081.69	15	3138.78			
Cor Total	66996.89	19				

Std. Dev.	56.02	R-Squared	0.2973
Mean	216.41	Adj R-Squared	0.1099
C.V. %	25.89	Pred R-Squared	-0.2548
PRESS	84070.68	Adeq Precision	4.771

Fr =
+206.61415
-0.020555 * Speed
-0.13115 * Feed
+14.22590 * DOC
+5.38482E-005 * Speed * Feed

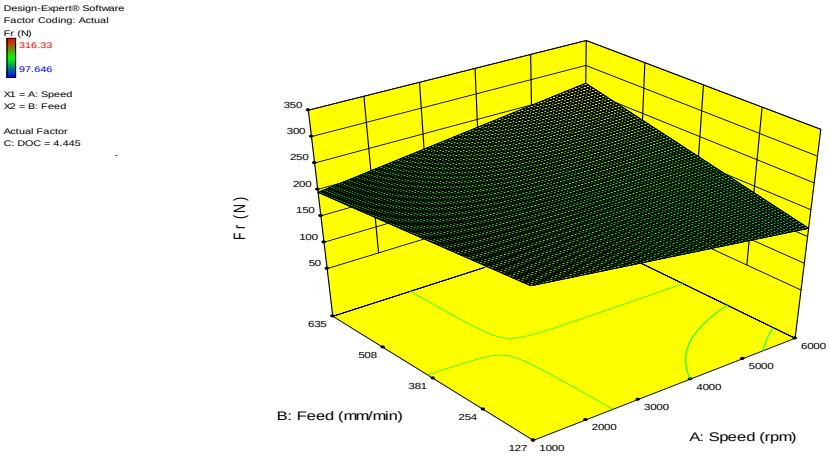
Design-Expert® Software
Factor Coding: Actual
Fr (N)
316.33
97.646
X1 = A: Speed
X2 = B: Feed
Actual Factor
C: DOC = 4.445
Fr (N)
350
300
250
200
150
100
50
B: Feed (mm/min)
635
508
381
254
127
A: Speed (rpm)
1000
2000
3000
4000
5000
6000

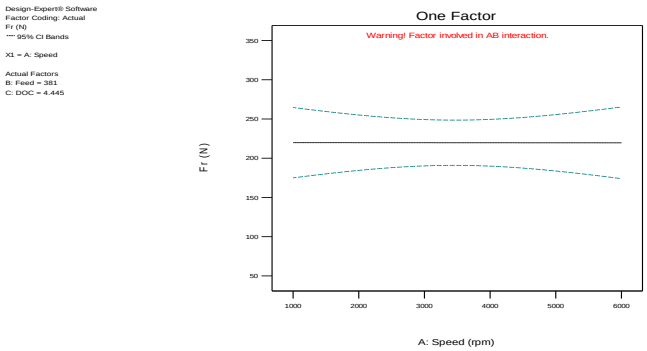
Design-Expert® Software
Factor Coding: Actual
Fr (N)
95% CI Bands
X1 = A: Speed
Actual Factors
B: Feed = 381
C: DOC = 4.445
One Factor
Warning! Factor involved in AB interaction.
Fr (N)
A: Speed (rpm)

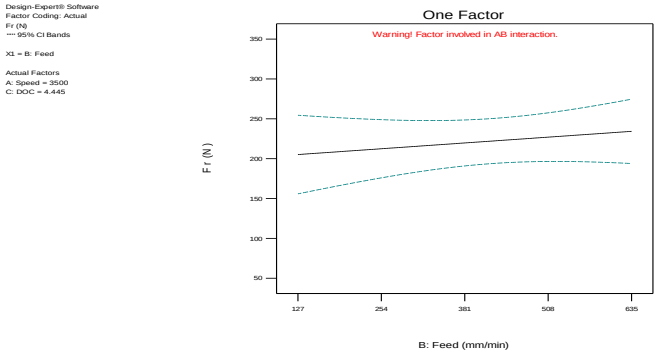
Design-Expert® Software
Factor Coding: Actual
Fr (N)
95% CI Bands
X1 = B: Feed
Actual Factors
A: Speed = 3500
C: DOC = 4.445
One Factor
Warning! Factor involved in AB interaction.
Fr (N)
B: Feed (mm/min)

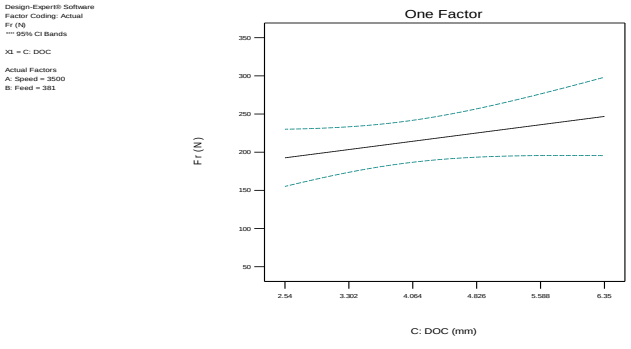
Design-Expert® Software
Factor Coding: Actual
Fr (N)
95% CI Bands
X1 = C: DOC
Actual Factors
A: Speed = 3500
B: Feed = 381
One Factor
Fr (N)
C: DOC (mm)

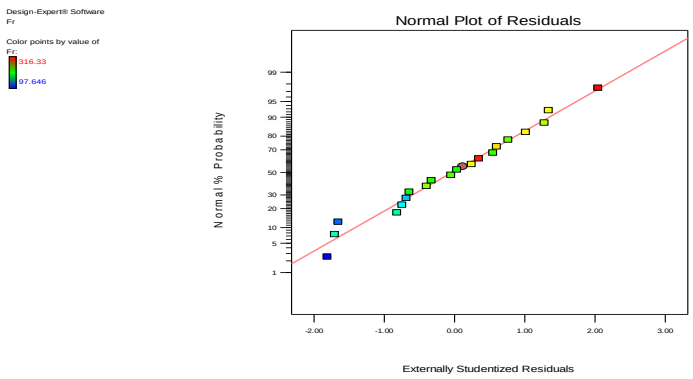
Design-Expert® Software
Fr
Color points by value of
Fr:
316.33
97.646
Normal Plot of Residuals
Normal % Probability
99
95
90
80
70
50
30
20
10
5
1
-2.00
-1.00
0.00
1.00
2.00
3.00
Externally Studentized Residuals

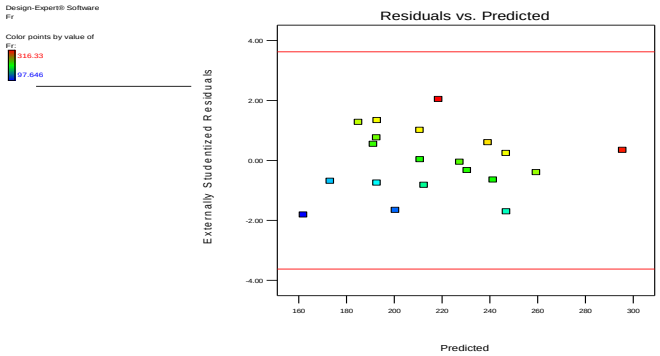
Design-Expert® Software
Fr
Color points by value of
Fr:
316.33
97.646
Residuals vs. Predicted
Externally Studentized Residuals
4.00
2.00
0.00
-2.00
-4.00
160
180
200
220
240
260
280
300
Predicted

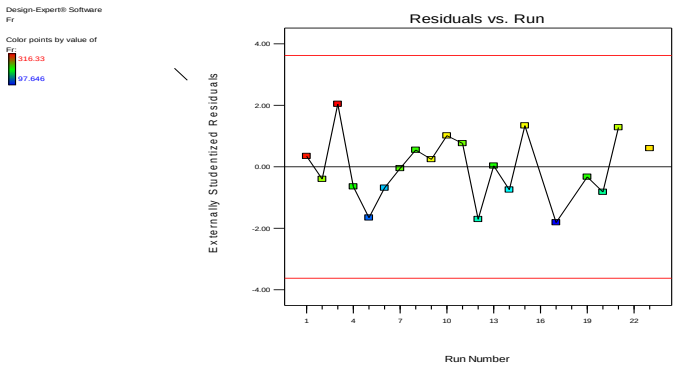
Design-Expert® Software
Fr
Color points by value of
Fr:
316.33
97.646
Residuals vs. Run
Externally Studentized Residuals
4.00
2.00
0.00
-2.00
-4.00
1
4
7
10
13
16
19
22
Run Number

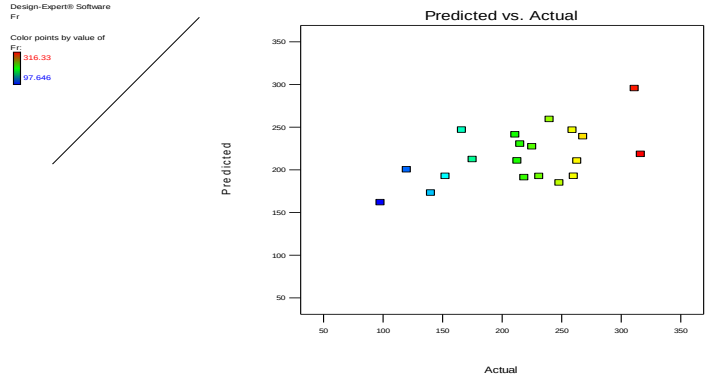
Design-Expert® Software
Fr
Color points by value of
Fr:
316.33
97.646
Predicted vs. Actual
Predicted
350
300
250
200
150
100
50
50
100
150
200
250
300
350
Actual

Appendix - K - HEXMC – Climb (Even) – DOE Graphs etc

HexMC – Climb (Even) – DOE Graphs etc

HexMC – Climb (Even) - Edge Trim ANOVA				
Experiment(s) Ignored	**Force**	**Model Used**		
		Process Order	**Selection**	**Alpha Out**
3,6	Fx	Quadratic	Backward	0.1
3,6	Fy	Quadratic	Backward	0.1
3,6	Fz	Quadratic	Backward	0.1
3,6	Ft	Quadratic	Backward	0.1
3	Fr	Quadratic	Backward	0.1

Run	Factor 1 A : Speed rpm	Factor 2 B : Feed mm/min	Factor 3 C : DOC mm	Response 1 Fx N	Response 2 Fy N	Response 3 Fz N	Response 4 Ft N	Response 5 Fr N
1	6000	635	6.35	133.2376	364.2612	373.23637	70.154	366.63047
2	6000	127	6.35	220.748	350.7327	28.679959	75.548463	380.30959
3	6000	635	2.54	200.4337	105.7998	392.96902	69.497331	400.933151
4	6000	127	2.54	162.3139	260.1835	25.484417	55.1144513	257.617251
5	1000	127	6.35	351.0996	451.1789	25.3152836	86.54677	459.32525
6	1000	635	6.35	454.3612	494.6293	93.10847	183.60054	496.472899
7	1000	635	2.54	249.8575	357.024	7.9711415	90.848156	380.52993
8	1000	127	2.54	387.6653	502.3149	19.3138315	124.37951	499.54867

Fx

ANOVA for Response Surface Reduced Linear model
Analysis of variance table [Partial sum of squares - Type III]

Source	Sum of Squares	df	Mean Square	F Value	p-value Prob > F	
Model	47721.28	2	23860.64	19.74	0.0188	significant
A-Speed	*37181.48*	*1*	*37181.48*	*30.77*	*0.0116*	
B-Feed	*10539.79*	*1*	*10539.79*	*8.72*	*0.0599*	
Residual	3625.57	3	1208.52			
Cor Total	51346.84	5				

Std. Dev.	34.76	R-Squared	0.9294
Mean	250.82	Adj R-Squared	0.8823
C.V. %	13.86	Pred R-Squared	0.6941
PRESS	15704.82	Adeq Precision	10.022

Fx =
+412.89266
-0.031488 * Speed
-0.17502 * Feed

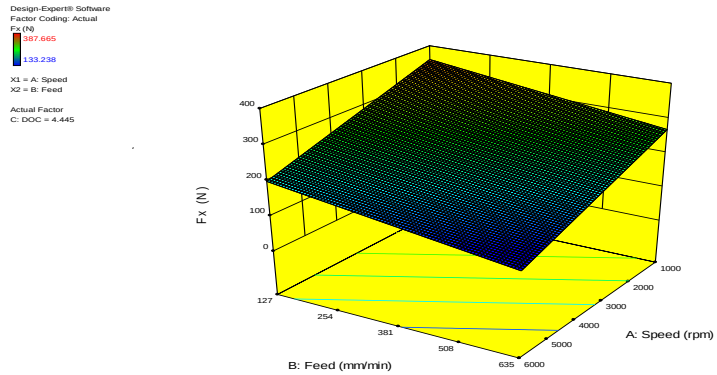
Design-Expert® Software
Factor Coding: Actual
Fx (N)
387.665
133.238
X1 = A: Speed
X2 = B: Feed
Actual Factor
C: DOC = 4.445
Fx (N)
400
300
200
100
0
127
254
381
508
635
B: Feed (mm/min)
1000
2000
3000
4000
5000
6000
A: Speed (rpm)

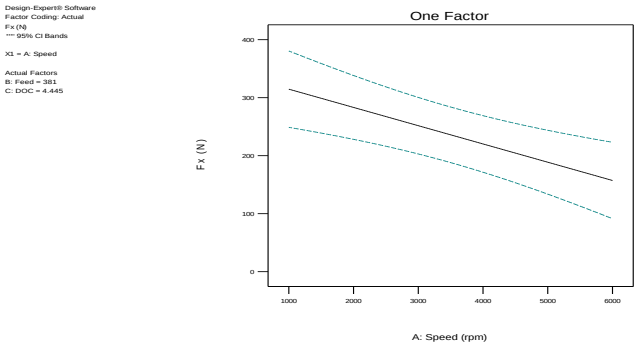
Design-Expert® Software
Factor Coding: Actual
Fx (N)
95% CI Bands
X1 = A: Speed
Actual Factors
B: Feed = 381
C: DOC = 4.445
One Factor
Fx (N)
400
300
200
100
0
1000
2000
3000
4000
5000
6000
A: Speed (rpm)

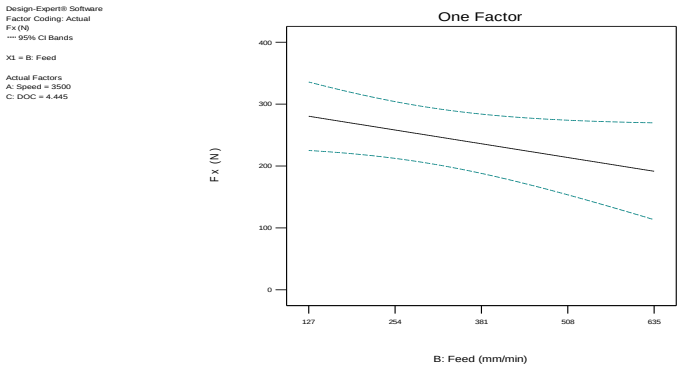
Design-Expert® Software
Factor Coding: Actual
Fx (N)
95% CI Bands
X1 = B: Feed
Actual Factors
A: Speed = 3500
C: DOC = 4.445
One Factor
Fx (N)
400
300
200
100
0
127
254
381
508
635
B: Feed (mm/min)

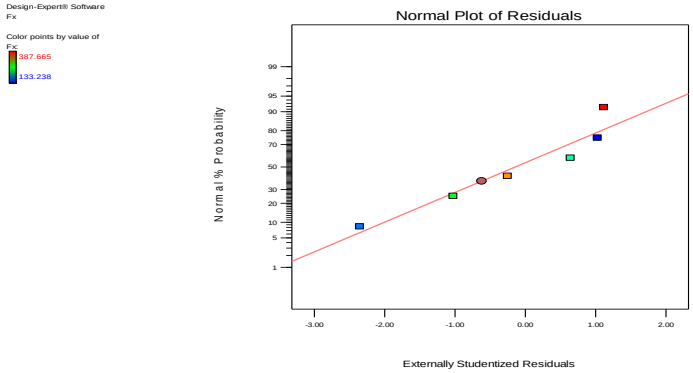
Design-Expert® Software
Fx
Color points by value of
Fx
387.665
133.238
Normal Plot of Residuals
Normal % Probability
99
95
90
80
70
50
30
20
10
5
1
-3.00
-2.00
-1.00
0.00
1.00
2.00
Externally Studentized Residuals

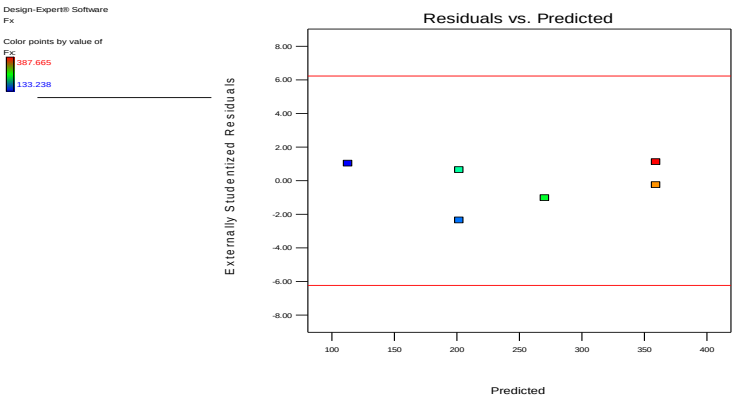
Design-Expert® Software
Fx
Color points by value of
Fx:
387.665
133.238
Residuals vs. Predicted
Externally Studentized Residuals
8.00
6.00
4.00
2.00
0.00
-2.00
-4.00
-6.00
-8.00
100
150
200
250
300
350
400
Predicted

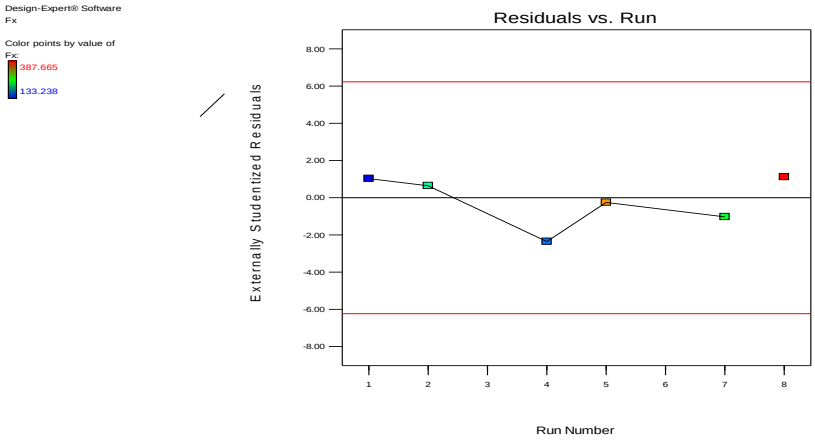
Design-Expert® Software
Fx
Color points by value of
Fx:
387.665
133.238
Residuals vs. Run
Externally Studentized Residuals
8.00
6.00
4.00
2.00
0.00
-2.00
-4.00
-6.00
-8.00
1
2
3
4
5
6
7
8
Run Number

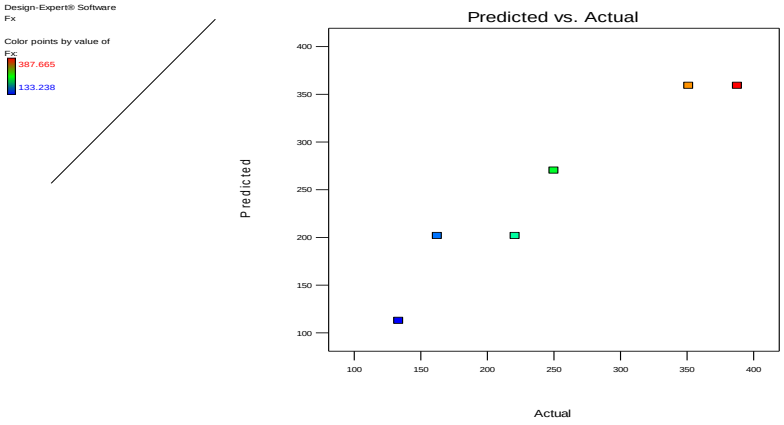
Design-Expert® Software
Fx
Color points by value of
Fx:
387.665
133.238
Predicted vs. Actual
Predicted
400
350
300
250
200
150
100
100
150
200
250
300
350
400
Actual

Fy

ANOVA for Response Surface Reduced 2FI model
Analysis of variance table [Partial sum of squares - Type III]

Source	Sum of Squares	df	Mean Square	F Value	p-value Prob > F	
Model	30603.12	3	10201.04	3.77	0.2165	not significant
A-Speed	*8970.98*	*1*	*8970.98*	*3.32*	*0.2101*	
B-Feed	*1237.07*	*1*	*1237.07*	*0.46*	*0.5685*	
AB	*10623.85*	*1*	*10623.85*	*3.93*	*0.1859*	
Residual	5407.02	2	2703.51			
Cor Total	36010.14	5				

Std. Dev.	52.00	R-Squared	0.8498
Mean	380.95	Adj R-Squared	0.6246
C.V. %	13.65	Pred R-Squared	N/A
PRESS	N/A	Adeq Precision	4.035

Fy =
+549.86170
-0.043184 * Speed
-0.30596 * Feed
+7.02858E-005 * Speed * Feed

Design-Expert® Software
Factor Coding: Actual
Fy (N)
502.315
260.184

X1 = A: Speed
X2 = B: Feed

Actual Factor
C: DOC = 4.445

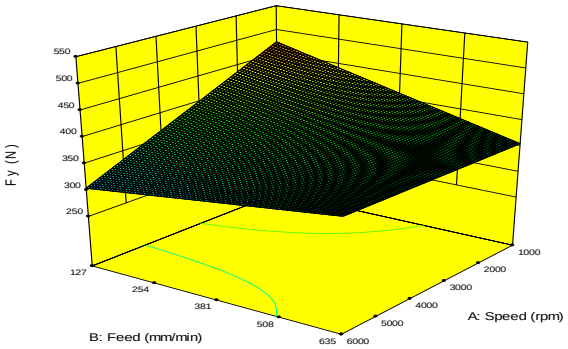

Design-Expert® Software
Factor Coding: Actual
Fy (N)
----- 95% CI Bands

X1 = A: Speed

Actual Factors
B: Feed = 381
C: DOC = 4.445

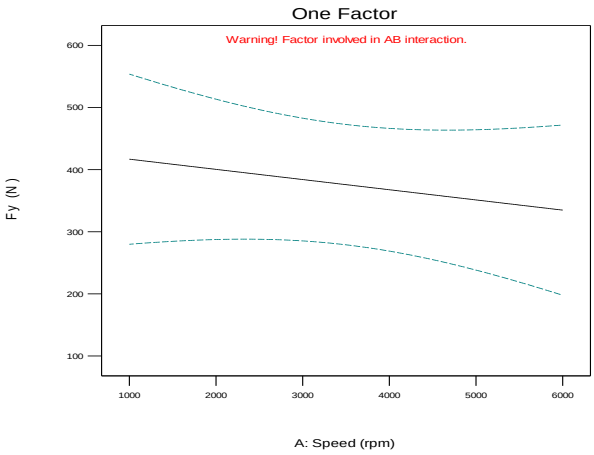

Design-Expert® Software
Factor Coding: Actual
Fy (N)
----- 95% CI Bands

X1 = B: Feed

Actual Factors
A: Speed = 3500
C: DOC = 4.445

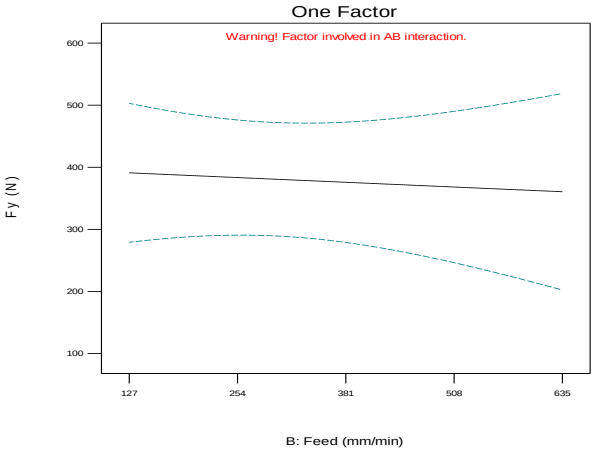

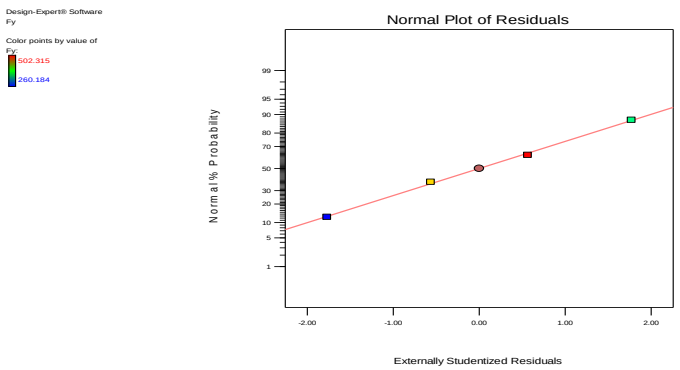
Design-Expert® Software
Fy
Color points by value of
Fy:
502.315
260.184
Normal Plot of Residuals
Normal% Probability
99
95
90
80
70
50
30
20
10
5
1
-2.00
-1.00
0.00
1.00
2.00
Externally Studentized Residuals

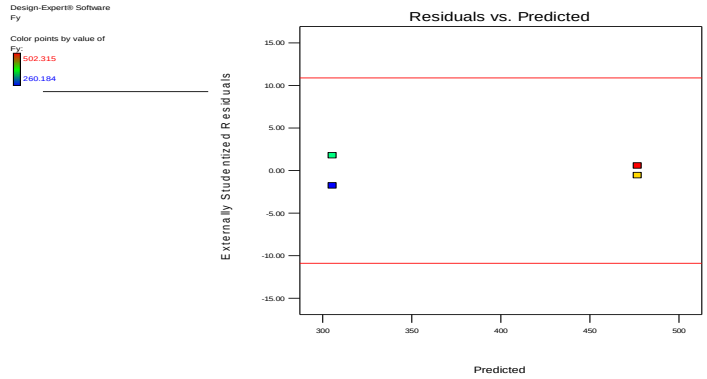
Design-Expert® Software
Fy
Color points by value of
Fy:
502.315
260.184
Residuals vs. Predicted
Externally Studentized Residuals
15.00
10.00
5.00
0.00
-5.00
-10.00
-15.00
300
350
400
450
500
Predicted

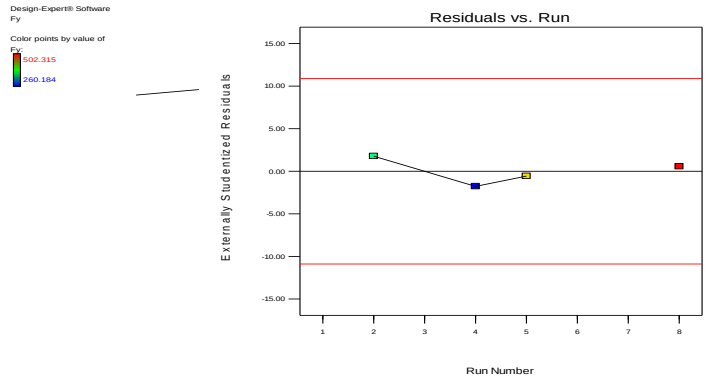
Design-Expert® Software
Fy
Color points by value of
Fy:
502.315
260.184
Residuals vs. Run
Externally Studentized Residuals
15.00
10.00
5.00
0.00
-5.00
-10.00
-15.00
1
2
3
4
5
6
7
8
Run Number

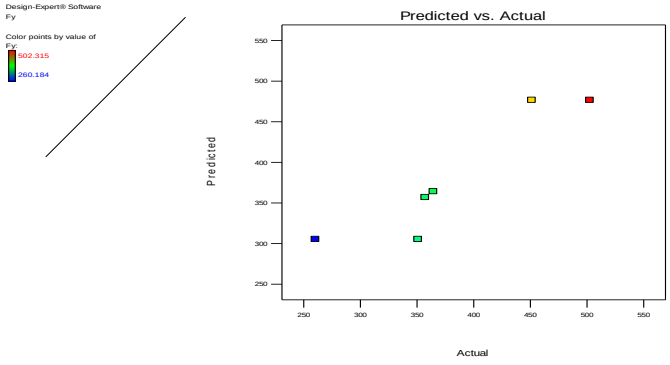
Design-Expert® Software
Fy
Color points by value of
Fy:
502.315
260.184
Predicted vs. Actual
Predicted
550
500
450
400
350
300
250
250
300
350
400
450
500
550
Actual

Fz

ANOVA for Response Surface Reduced 2FI model
Analysis of variance table [Partial sum of squares - Type III]

Source	Sum of Squares	df	Mean Square	F Value	p-value Prob > F	
Model	1.034E+005	3	34477.18	2983.17	0.0003	significant
A-Speed	*45641.44*	*1*	*45641.44*	*3949.17*	*0.0003*	
B-Feed	*36699.46*	*1*	*36699.46*	*3175.46*	*0.0003*	
AB	*43319.51*	*1*	*43319.51*	*3748.26*	*0.0003*	
Residual	23.11	2	11.56			
Cor Total	1.035E+005	5				

Std. Dev.	3.40	R-Squared	0.9998
Mean	80.00	Adj R-Squared	0.9994
C.V. %	4.25	Pred R-Squared	N/A
PRESS	N/A	Adeq Precision	131.591

Fz =
+42.97177
-0.017071 * Speed
-0.17016 * Feed
+1.41928E-004 * Speed * Feed

Design-Expert® Software
Factor Coding: Actual
Fz (N)
373.236
7.97114

X1 = A: Speed
X2 = B: Feed

Actual Factor
C: DOC = 4.445

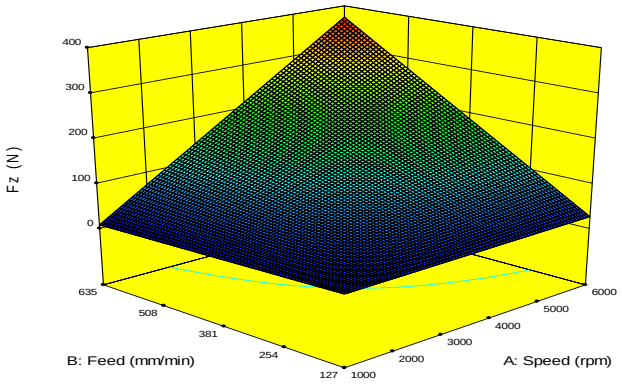

Design-Expert® Software
Factor Coding: Actual
Fz (N)
---- 95% CI Bands

X1 = A: Speed

Actual Factors
B: Feed = 381
C: DOC = 4.445

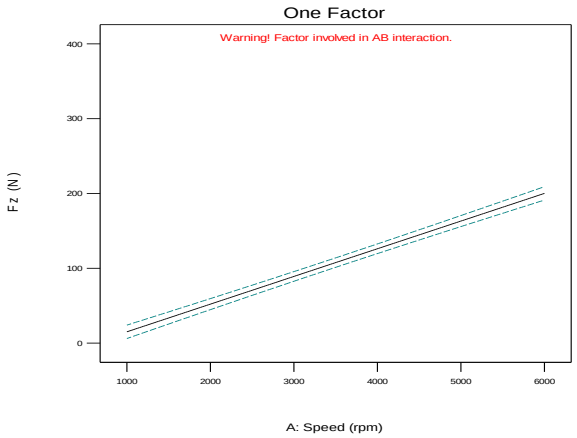

Design-Expert® Software
Factor Coding: Actual
Fz (N)
---- 95% CI Bands

X1 = B: Feed

Actual Factors
A: Speed = 3500
C: DOC = 4.445

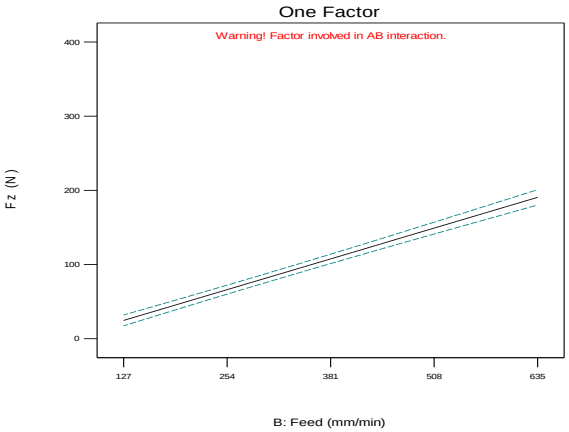

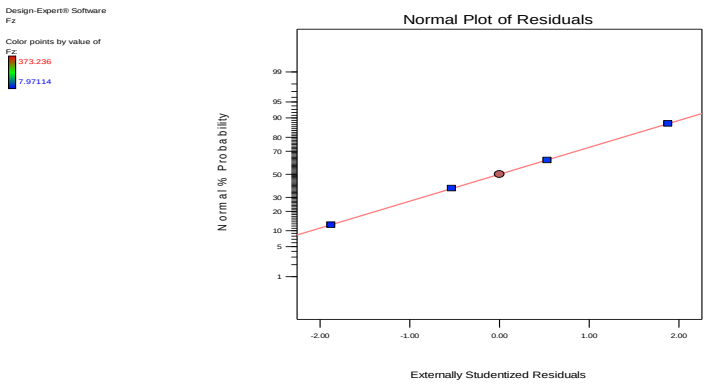
Design-Expert® Software
Fz
Color points by value of
Fz
373.236
7.97114
Normal Plot of Residuals
Normal% Probability
99
95
90
80
70
50
30
20
10
5
1
-2.00
-1.00
0.00
1.00
2.00
Externally Studentized Residuals

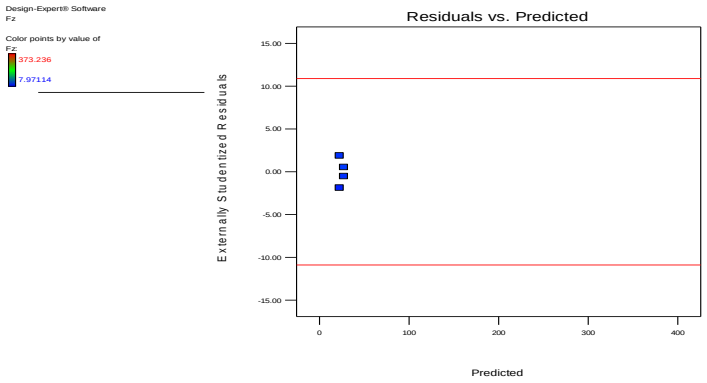
Design-Expert® Software
Fz
Color points by value of
Fz
373.236
7.97114
Residuals vs. Predicted
Externally Studentized Residuals
15.00
10.00
5.00
0.00
-5.00
-10.00
-15.00
0
100
200
300
400
Predicted

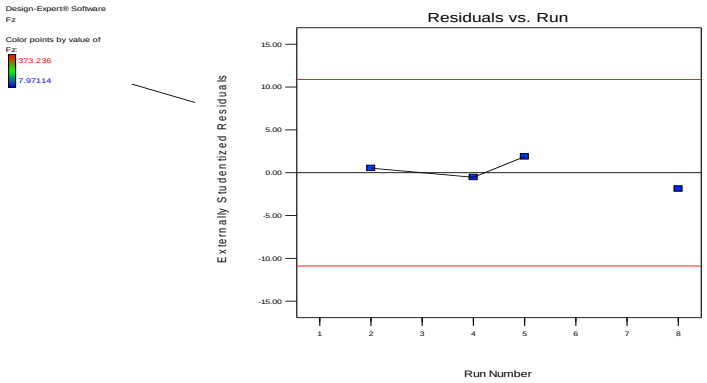
Design-Expert® Software
Fz
Color points by value of
Fz
373.236
7.97114
Residuals vs. Run
Externally Studentized Residuals
15.00
10.00
5.00
0.00
-5.00
-10.00
-15.00
1
2
3
4
5
6
7
8
Run Number

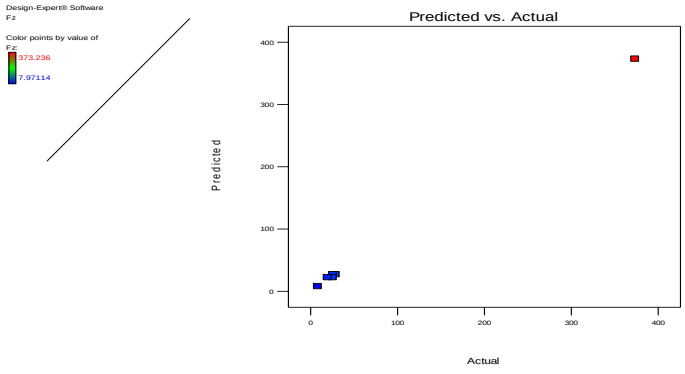
Design-Expert® Software
Fz
Color points by value of
Fz
373.236
7.97114
Predicted vs. Actual
Predicted
400
300
200
100
0
0
100
200
300
400
Actual

Ft

ANOVA for Response Surface Reduced Linear model
Analysis of variance table [Partial sum of squares - Type III]

Source	Sum of Squares	df	Mean Square	F Value	p-value Prob > F	
Model	1698.74	1	1698.74	6.28	0.0664	not significant
A-Speed	*1698.74*	*1*	*1698.74*	*6.28*	*0.0664*	
Residual	1082.34	4	270.58			
Cor Total	2781.07	5				

Std. Dev.	16.45	R-Squared	0.6108
Mean	83.77	Adj R-Squared	0.5135
C.V. %	19.64	Pred R-Squared	0.1243
PRESS	2435.26	Adeq Precision	3.543

Ft =
+107.32198
-6.73050E-003 * Speed

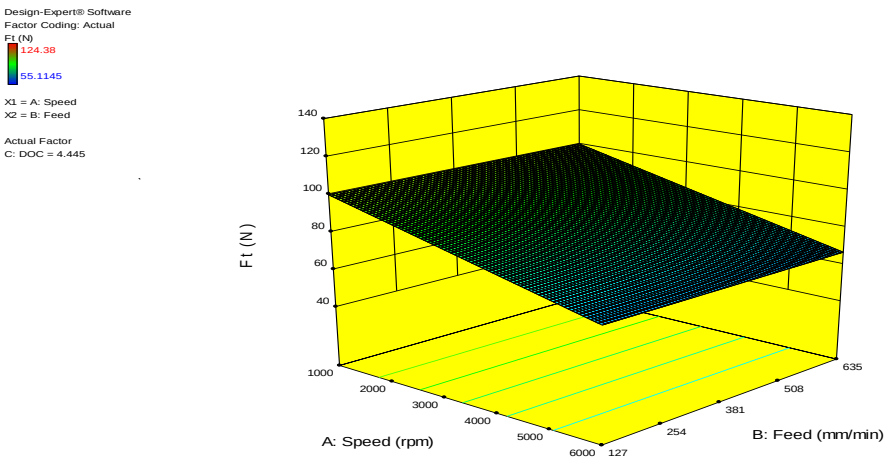

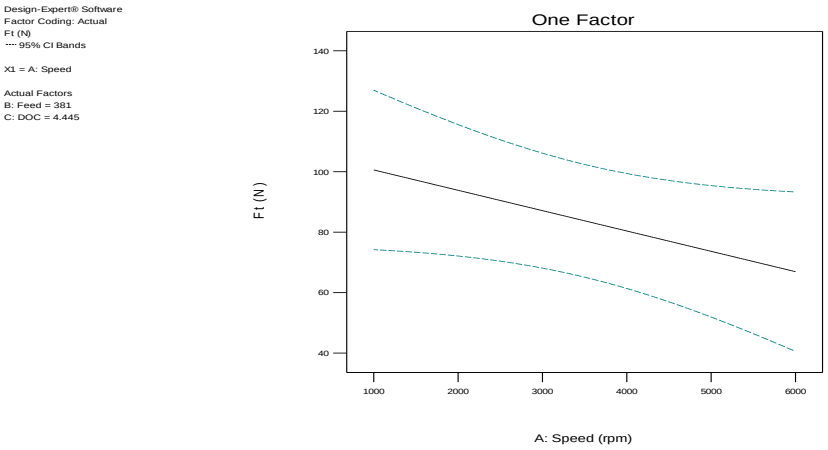
Design-Expert® Software
Factor Coding: Actual
Ft (N)
95% CI Bands
X1 = A: Speed
Actual Factors
B: Feed = 381
C: DOC = 4.445
One Factor
Ft (N)
140
120
100
80
60
40
1000
2000
3000
4000
5000
6000
A: Speed (rpm)

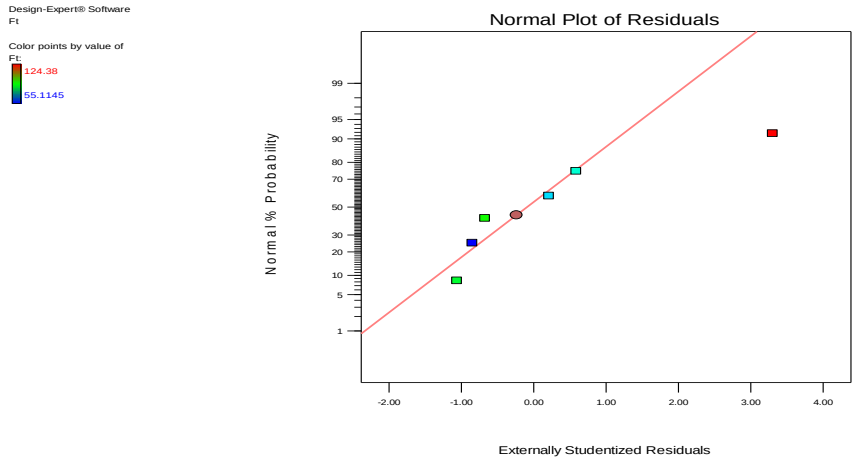
Design-Expert® Software
Ft
Color points by value of
Ft:
124.38
55.1145
Normal Plot of Residuals
Normal % Probability
99
95
90
80
70
50
30
20
10
5
1
-2.00
-1.00
0.00
1.00
2.00
3.00
4.00
Externally Studentized Residuals

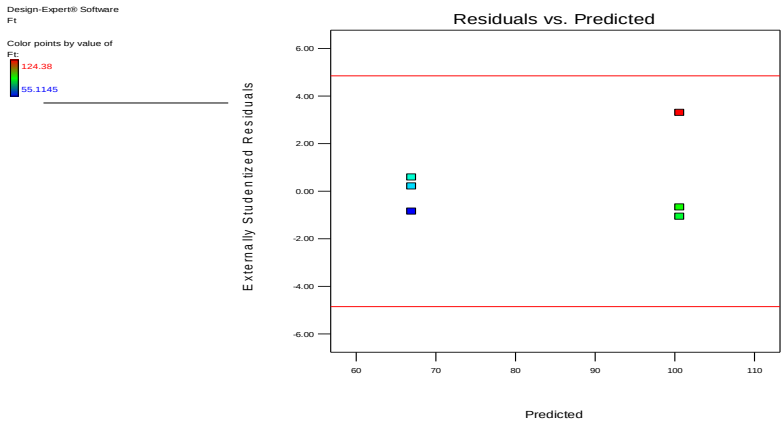
Design-Expert® Software
Ft
Color points by value of
Ft:
124.38
55.1145
Residuals vs. Predicted
Externally Studentized Residuals
6.00
4.00
2.00
0.00
-2.00
-4.00
-6.00
60
70
80
90
100
110
Predicted

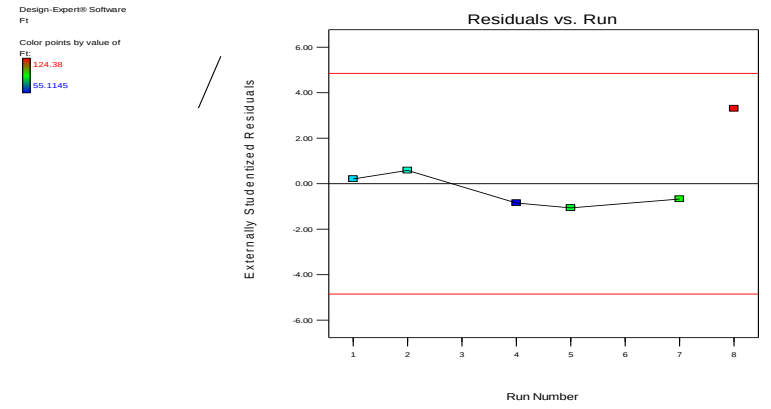
Design-Expert® Software
Ft
Color points by value of
Ft:
124.38
55.1145
Residuals vs. Run
Externally Studentized Residuals
6.00
4.00
2.00
0.00
-2.00
-4.00
-6.00
1
2
3
4
5
6
7
8
Run Number

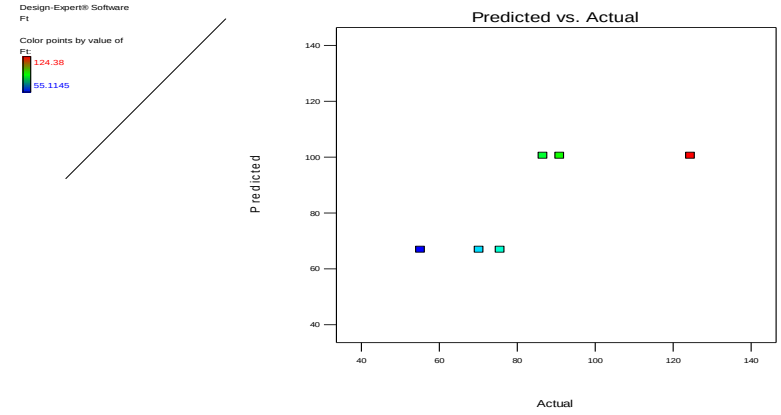
Design-Expert® Software
Ft
Color points by value of
Ft:
124.38
55.1145
Predicted vs. Actual
Predicted
140
120
100
80
60
40
40
60
80
100
120
140
Actual

Fr

ANOVA for Response Surface Reduced Linear model
Analysis of variance table [Partial sum of squares - Type III]

Source	Sum of Squares	df	Mean Square	F Value	p-value Prob > F	
Model	26408.52	1	26408.52	7.24	0.0433	significant
A-Speed	*26408.52*	*1*	*26408.52*	*7.24*	*0.0433*	
Residual	18247.54	5	3649.51			
Cor Total	44656.05	6				

Std. Dev.	60.41	R-Squared	0.5914
Mean	405.78	Adj R-Squared	0.5097
C.V. %	14.89	Pred R-Squared	0.1779
PRESS	36709.65	Adeq Precision	3.844

Fr =
+483.79254
-0.024823 * Speed

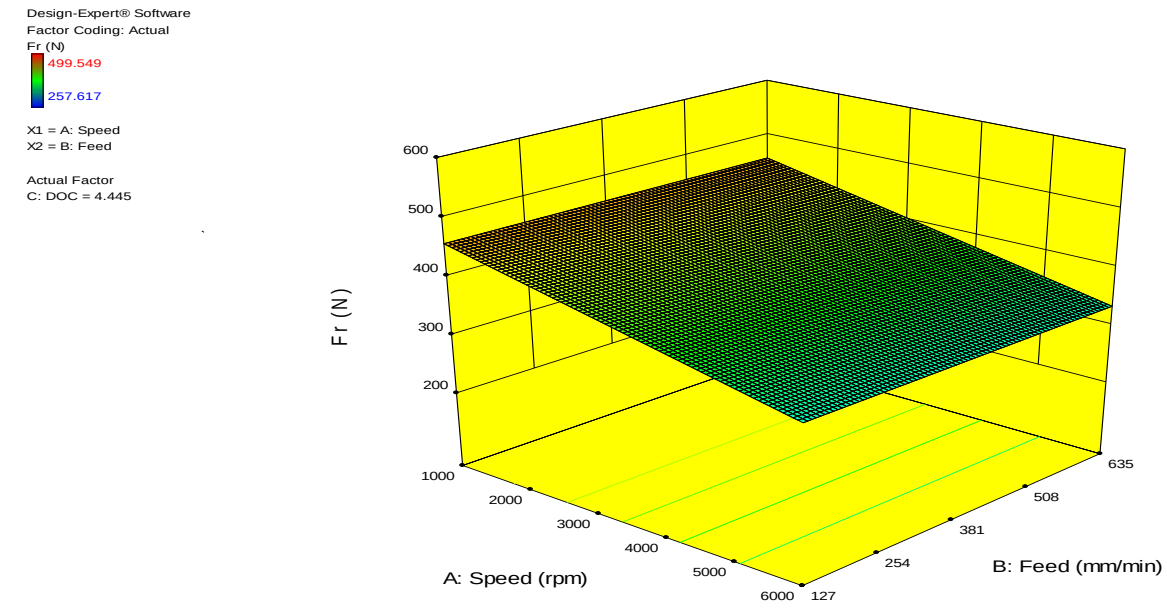

Design-Expert® Software
Factor Coding: Actual
Fr (N)
---- 95% CI Bands

X1 = A: Speed

Actual Factors
B: Feed = 381
C: DOC = 4.445

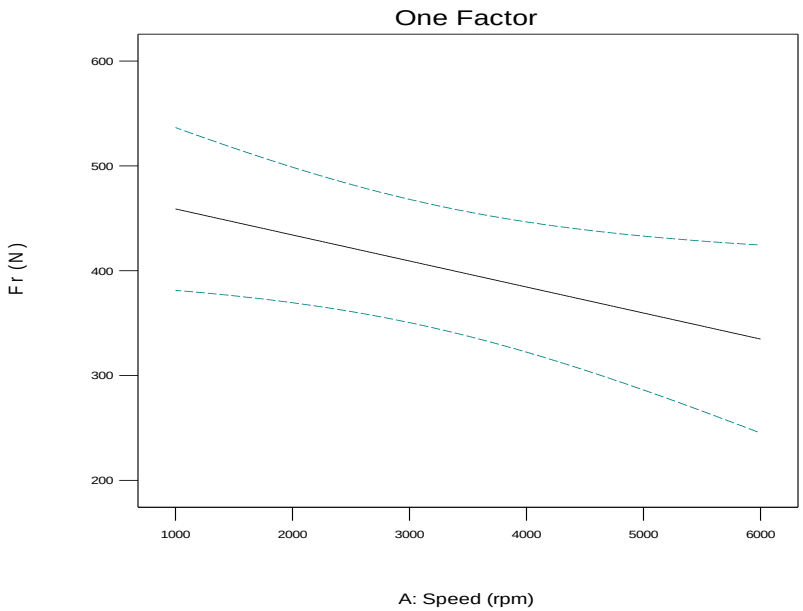

Design-Expert® Software
Fr

Color points by value of
Fr:
499.549
257.617

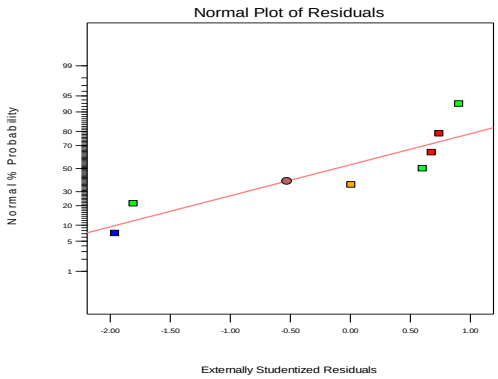

Design-Expert® Software
Fr

Color points by value of
Fr:
499.549
257.617

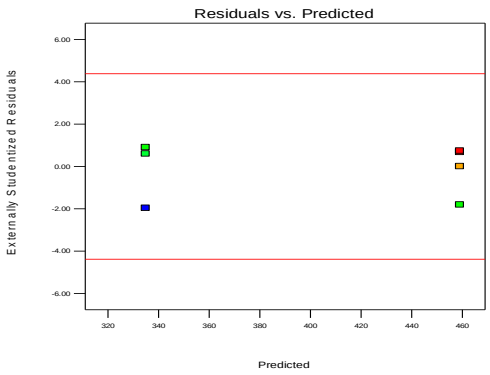

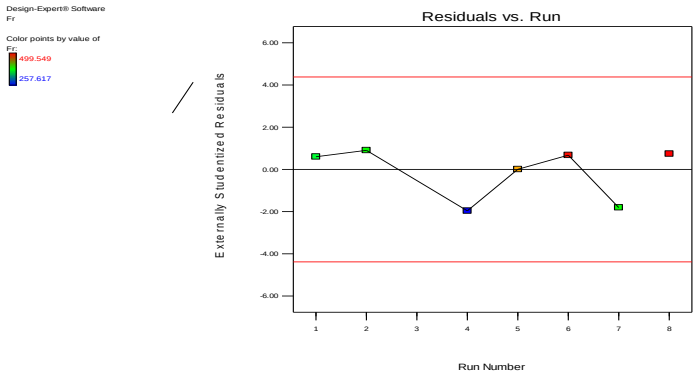
Design-Expert® Software
Fr
Color points by value of
Fr:
499.549
257.617
Residuals vs. Run
Externally Studentized Residuals
6.00
4.00
2.00
0.00
-2.00
-4.00
-6.00
1
2
3
4
5
6
7
8
Run Number

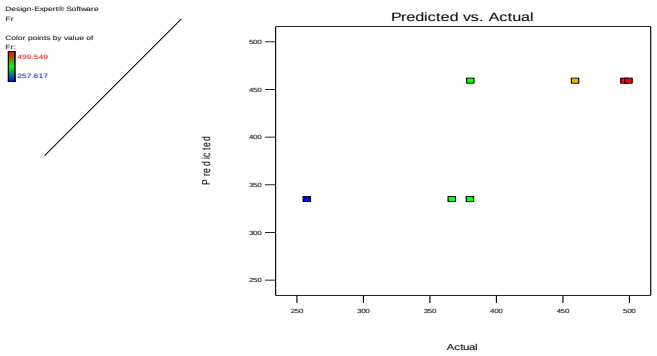
Design-Expert® Software
Fr
Color points by value of
Fr:
499.549
257.617
Predicted vs. Actual
Predicted
500
450
400
350
300
250
250
300
350
400
450
500
Actual

Appendix - L - HEXMC – Conventional (Odd) – DOE Graphs etc

HexMC – Conventional (Odd) – DOE Graphs etc

HexMC – Conventional (Odd) - Edge Trim ANOVA				
Experiment(s) Ignored	**Force**	**Model Used**		
		Process Order	**Selection**	**Alpha Out**
3,6	Fx	Quadratic	Backward	0.1
6	Fy	2FI	Manual	- (Terms taken A,B,C,BC)
6	Fz	Cubic	Backward	0.15
6	Ft	Quadratic	Backward	0.1
6	Fr	Cubic	Backward	0.15

Run	Factor 1 A : Speed rpm	Factor 2 B : Feed mm/min	Factor 3 C : DOC mm	Response 1 Fx N	Response 2 Fy N	Response 3 Fz N	Response 4 Ft N	Response 5 Fr N
1	6000	25	0.25	119.73684	373.11918	392.11682	60.385502	362.50328
2	6000	5	0.25	220.4424	351.31099	30.069604	55.415462	340.35353
3	6000	25	0.1	187.60634	100.31868	435.22236	67.162829	399.590897
4	6000	5	0.1	172.65266	285.55477	26.629158	59.419908	262.775458
5	1000	5	0.25	341.62139	430.39882	15.747067	96.80027	428.78717
6	1000	25	0.25	483.50717	502.8593	99.342005	205.56577	501.794256
7	1000	25	0.1	310.36221	399.993	4.9071033	124.91106	389.1026
8	1000	5	0.1	367.23959	495.02711	22.432769	107.56642	494.15034

Fx

ANOVA for Response Surface Reduced Linear model

Analysis of variance table [Partial sum of squares - Type III]

Source	**Sum of Squares**	**df**	**Mean Square**	**F Value**	**p-value Prob > F**	
Model	47609.27	2	23804.63	39.08	0.0071	significant
A-Speed	*42738.69*	*1*	*42738.69*	*70.16*	*0.0036*	
B-Feed	*4870.57*	*1*	*4870.57*	*8.00*	*0.0663*	
Residual	1827.43	3	609.14			
Cor Total	49436.70	5				

Std. Dev.	24.68	R-Squared	0.9630
Mean	255.34	Adj R-Squared	0.9384
C.V. %	9.67	Pred R-Squared	0.8622

Fx =
+408.75685
-0.033759 * Speed
-0.11898 * Feed

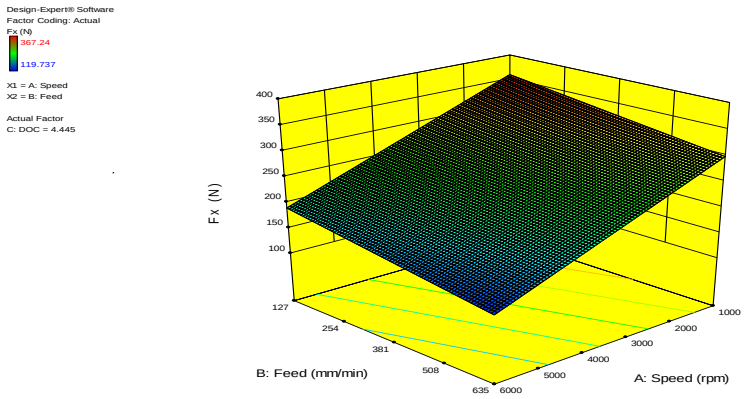

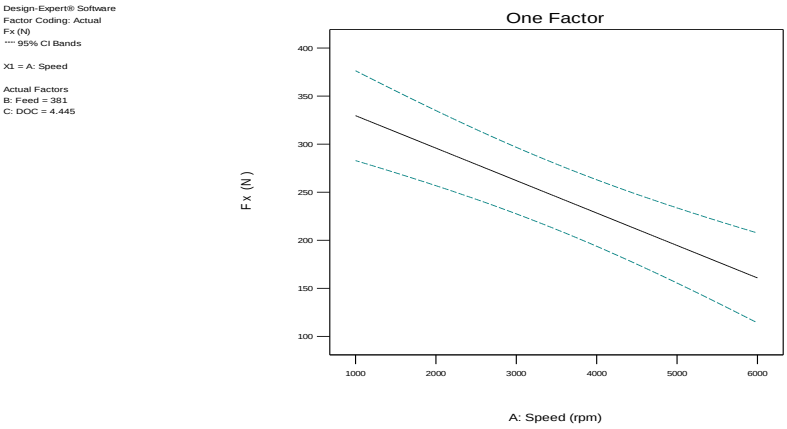

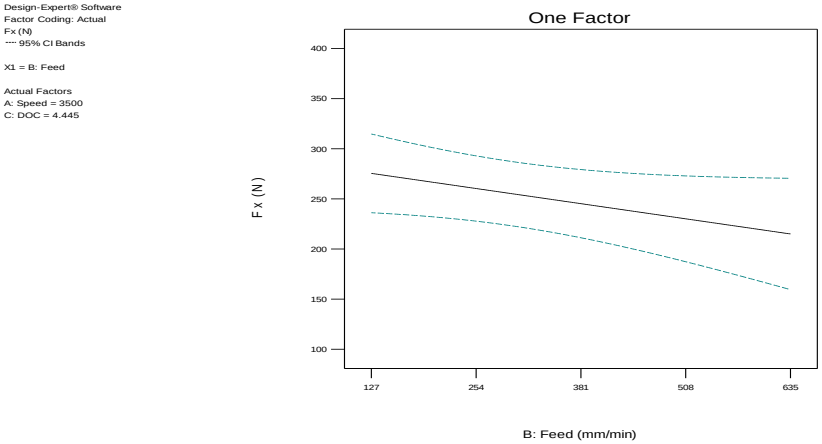

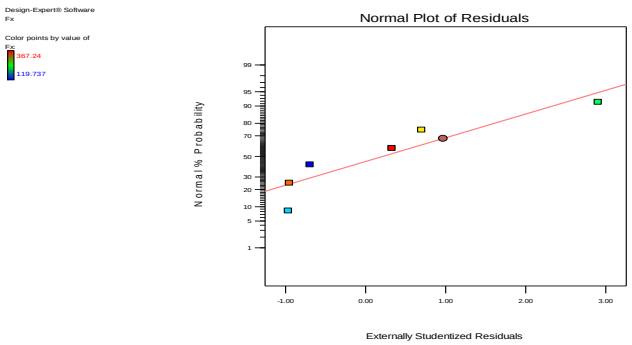
Design-Expert® Software
Fx
Color points by value of
Fx
367.24
119.737
Normal Plot of Residuals
Normal % Probability
99
95
90
80
70
50
30
20
10
5
1
-1.00
0.00
1.00
2.00
3.00
Externally Studentized Residuals

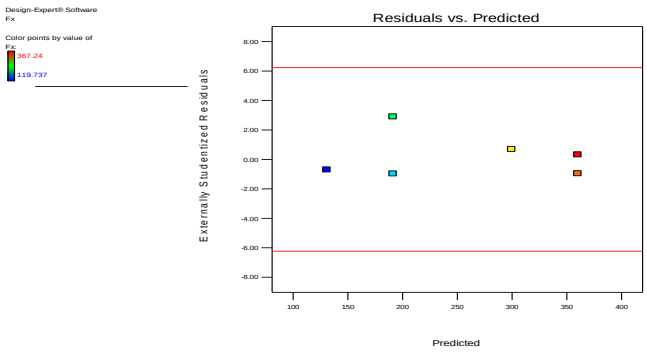
Design-Expert® Software
Fx
Color points by value of
Fx
367.24
119.737
Residuals vs. Predicted
Externally Studentized Residuals
8.00
6.00
4.00
2.00
0.00
-2.00
-4.00
-6.00
-8.00
100
150
200
250
300
350
400
Predicted

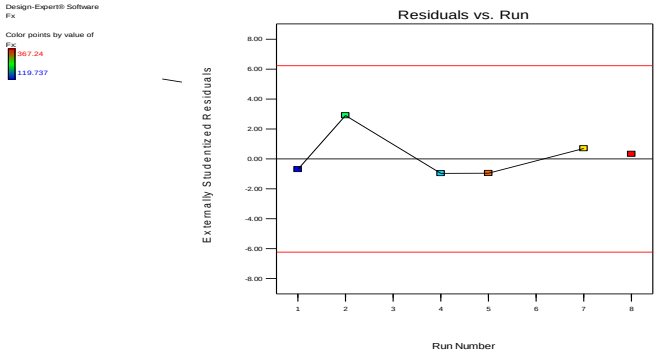
Design-Expert® Software
Fx
Color points by value of
Fx
367.24
119.737
Residuals vs. Run
Externally Studentized Residuals
8.00
6.00
4.00
2.00
0.00
-2.00
-4.00
-6.00
-8.00
1
2
3
4
5
6
7
8
Run Number

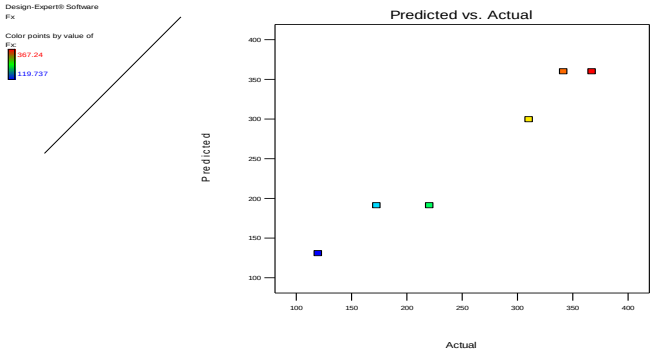
Design-Expert® Software
Fx
Color points by value of
Fx
367.24
119.737
Predicted vs. Actual
Predicted
400
350
300
250
200
150
100
100
150
200
250
300
350
400
Actual

Fy

ANOVA for Response Surface Reduced 2FI model
Analysis of variance table [Partial sum of squares - Type III]

Source	Sum of Squares	df	Mean Square	F Value	p-value Prob > F	
Model	84698.02	4	21174.51	3.44	0.2375	not significant
A-Speed	*57669.97*	*1*	*57669.97*	*9.38*	*0.0921*	
B-Feed	*1342.44*	*1*	*1342.44*	*0.22*	*0.6863*	
C-DOC	*18409.37*	*1*	*18409.37*	*2.99*	*0.2257*	
BC	*18222.42*	*1*	*18222.42*	*2.96*	*0.2273*	
Residual	12299.15	2	6149.58			
Cor Total	96997.18	6				

Std. Dev.	78.42	R-Squared	0.8732
Mean	347.96	Adj R-Squared	0.6196
C.V. %	22.54	Pred R-Squared	N/A
PRESS	N/A	Adeq Precision	5.081

Fy =
+598.94320
-0.039216 * Speed
-0.56515 * Feed
-14.31644 * DOC
+0.11389 * Feed * DOC

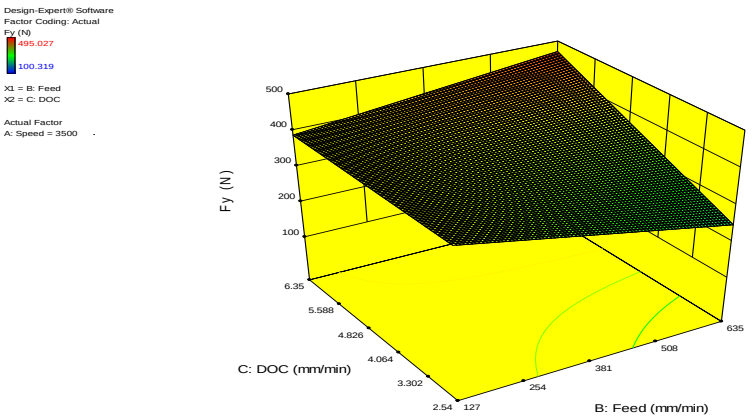

Design-Expert® Software
Factor Coding: Actual
Fy (N)
**** 95% CI Bands

X1 = A: Speed

Actual Factors
B: Feed = 381
C: DOC = 4.445

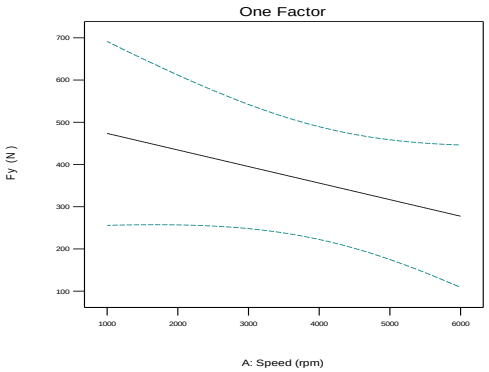

Design-Expert® Software
Factor Coding: Actual
Fy (N)
**** 95% CI Bands

X1 = B: Feed

Actual Factors
A: Speed = 3500
C: DOC = 4.445

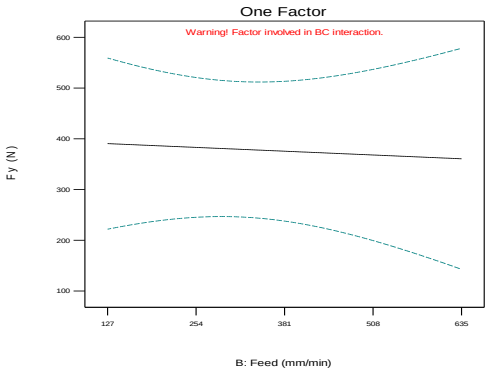

Design-Expert® Software
Factor Coding: Actual
Fy (N)
**** 95% CI Bands

X1 = C: DOC

Actual Factors
A: Speed = 3500
B: Feed = 381

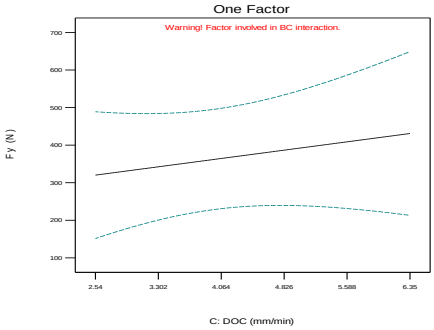

Design-Expert® Software
Fy

Color points by value of
Fy:
495.027
100.319

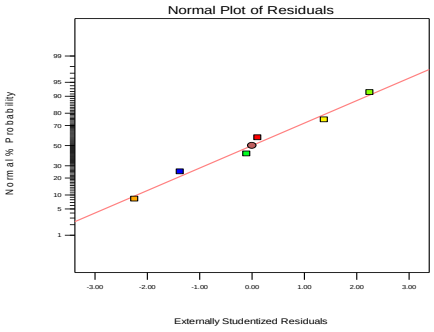

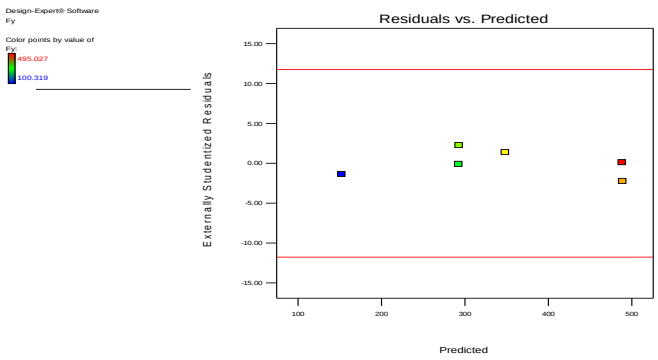
Design-Expert® Software
Fy
Color points by value of
Fy:
495.027
100.319
Residuals vs. Predicted
Externally Studentized Residuals
15.00
10.00
5.00
0.00
-5.00
-10.00
-15.00
100
200
300
400
500
Predicted

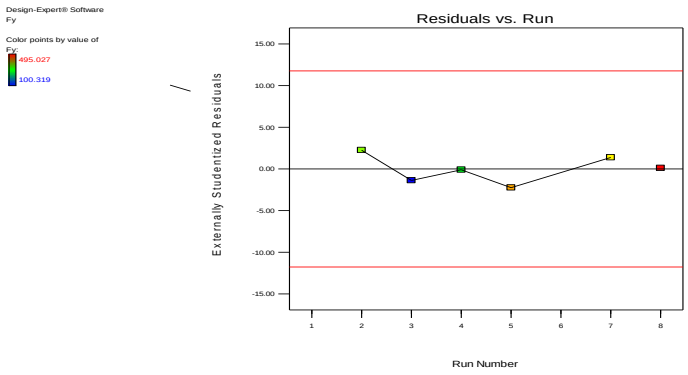
Design-Expert® Software
Fy
Color points by value of
Fy:
495.027
100.319
Residuals vs. Run
Externally Studentized Residuals
15.00
10.00
5.00
0.00
-5.00
-10.00
-15.00
1
2
3
4
5
6
7
8
Run Number

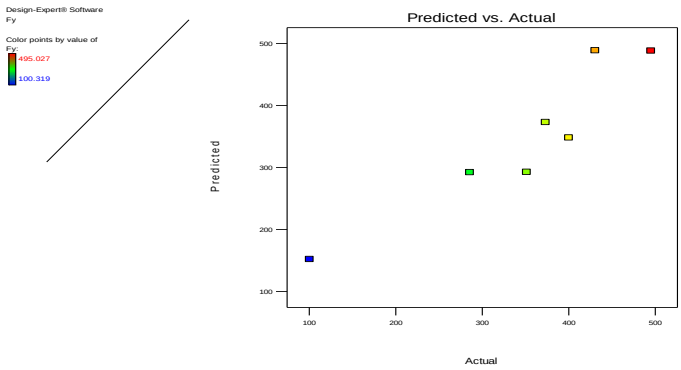
Design-Expert® Software
Fy
Color points by value of
Fy:
495.027
100.319
Predicted vs. Actual
Predicted
500
400
300
200
100
100
200
300
400
500
Actual

Fz

ANOVA for Response Surface Reduced 2FI model
Analysis of variance table [Partial sum of squares - Type III]

Source	Sum of Squares	df	Mean Square	F Value	p-value Prob > F	
Model	2.227E+005	5	44548.54	1737.82	0.0182	significant
A-Speed	*64408.64*	*1*	*64408.64*	*2512.56*	*0.0127*	
B-Feed	*40736.47*	*1*	*40736.47*	*1589.11*	*0.0160*	
C-DOC	*666.87*	*1*	*666.87*	*26.01*	*0.1233*	
AB	*59095.99*	*1*	*59095.99*	*2305.31*	*0.0133*	
BC	*573.61*	*1*	*573.61*	*22.38*	*0.1326*	
Residual	25.63	1	25.63			
Cor Total	2.228E+005	6				

Std. Dev.	5.06	R-Squared	0.9999
Mean	132.45	Adj R-Squared	0.9993
C.V. %	3.82	Pred R-Squared	N/A
PRESS	N/A	Adeq Precision	91.801

Fz =
+37.01859
-0.019201 * Speed
-0.14085 * Feed
+2.29609 * DOC
+1.65770E-004 * Speed * Feed
-0.021433 * Feed * DOC

Design-Expert® Software
Factor Coding: Actual
Fz (N)
435.222
4.9071

X1 = A: Speed
X2 = B: Feed

Actual Factor
C: DOC = 4.445

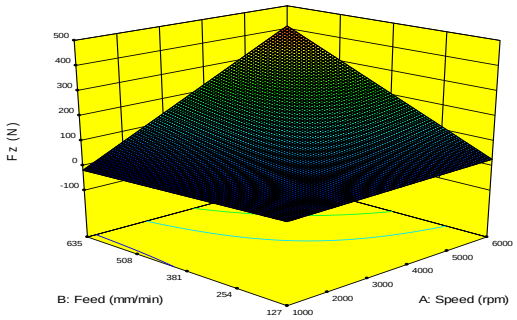

Design-Expert® Software
Factor Coding: Actual
Fz (N)
---- 95% CI Bands

X1 = A: Speed

Actual Factors
B: Feed = 381
C: DOC = 4.445

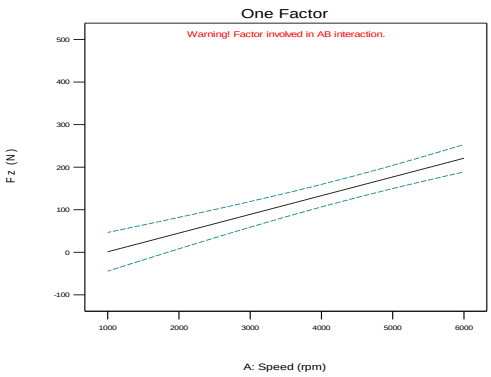

Design-Expert® Software
Factor Coding: Actual
Fz (N)
---- 95% CI Bands

X1 = B: Feed

Actual Factors
A: Speed = 3500
C: DOC = 4.445

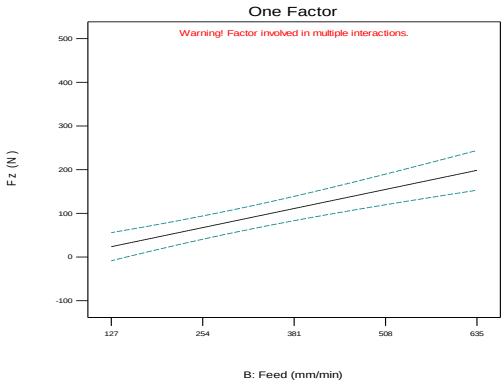

Design-Expert® Software
Factor Coding: Actual
Fz (N)
---- 95% CI Bands

X1 = C: DOC

Actual Factors
A: Speed = 3500
B: Feed = 381

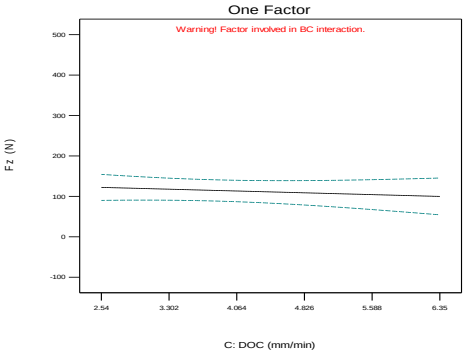

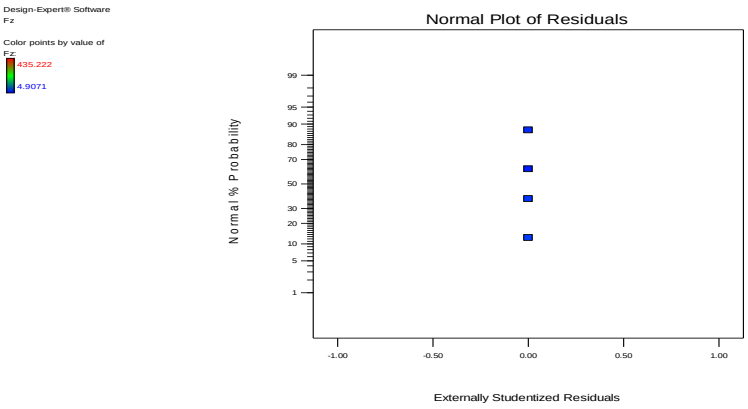
Design-Expert® Software
Fz
Color points by value of
Fz:
435.222
4.9071
Normal Plot of Residuals
Normal % Probability
99
95
90
80
70
50
30
20
10
5
1
-1.00
-0.50
0.00
0.50
1.00
Externally Studentized Residuals

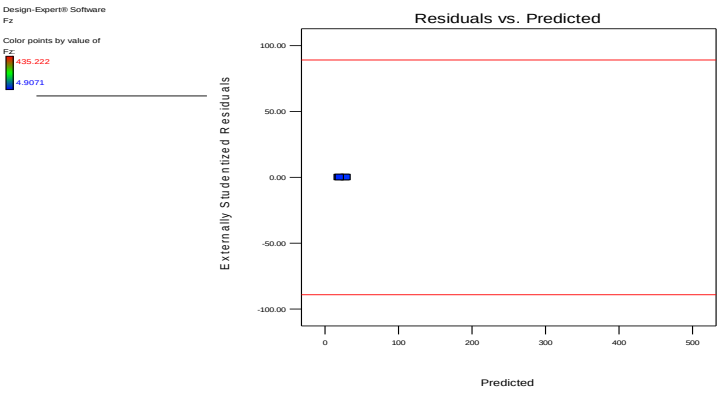
Design-Expert® Software
Fz
Color points by value of
Fz:
435.222
4.9071
Residuals vs. Predicted
Externally Studentized Residuals
100.00
50.00
0.00
-50.00
-100.00
0
100
200
300
400
500
Predicted

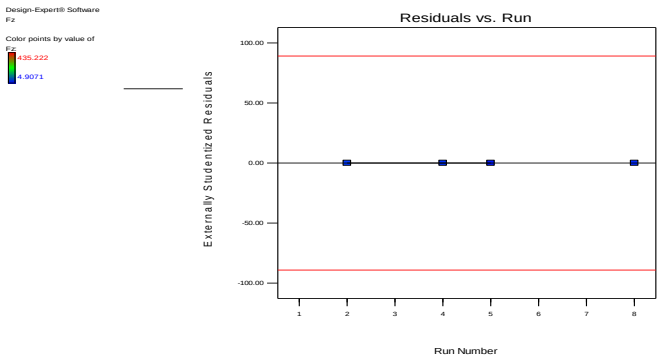
Design-Expert® Software
Fz
Color points by value of
Fz:
435.222
4.9071
Residuals vs. Run
Externally Studentized Residuals
100.00
50.00
0.00
-50.00
-100.00
1
2
3
4
5
6
7
8
Run Number

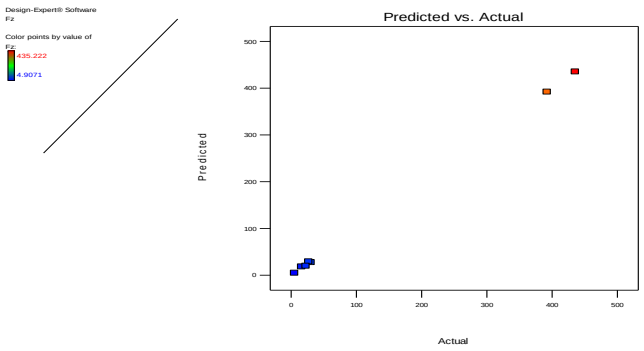
Design-Expert® Software
Fz
Color points by value of
Fz:
435.222
4.9071
Predicted vs. Actual
Predicted
500
400
300
200
100
0
0
100
200
300
400
500
Actual

Ft

ANOVA for Response Surface Reduced 2FI model
Analysis of variance table [Partial sum of squares - Type III]

Source	Sum of Squares	df	Mean Square	F Value	p-value Prob > F	
Model	4605.64	4	1151.41	199.32	0.0050	significant
A-Speed	*3925.35*	*1*	*3925.35*	*679.52*	*0.0015*	
B-Feed	*243.71*	*1*	*243.71*	*42.19*	*0.0229*	
C-DOC	*77.39*	*1*	*77.39*	*13.40*	*0.0672*	
AB	*61.25*	*1*	*61.25*	*10.60*	*0.0828*	
Residual	11.55	2	5.78			
Cor Total	4617.19	6				

Std. Dev.	2.40	R-Squared	0.9975
Mean	81.67	Adj R-Squared	0.9925
C.V. %	2.94	Pred R-Squared	N/A
PRESS	N/A	Adeq Precision	34.995

Ft =
+114.09313
-8.31414E-003 * Speed
+0.042702 * Feed
-1.88521 * DOC
-5.03146E-006 * Speed * Feed

Design-Expert® Software
Factor Coding: Actual
Ft (N)
124.911
55.4155

X1 = A: Speed
X2 = B: Feed

Actual Factor
C: DOC = 4.445

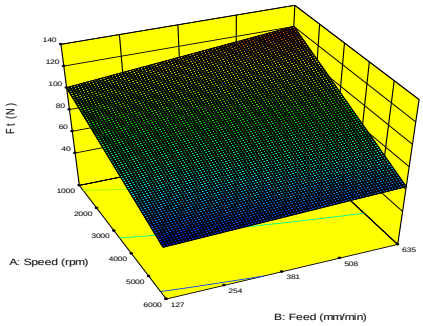

Design-Expert® Software
Factor Coding: Actual
Ft (N)
95% CI Bands

X1 = A: Speed

Actual Factors
B: Feed = 381
C: DOC = 4.445

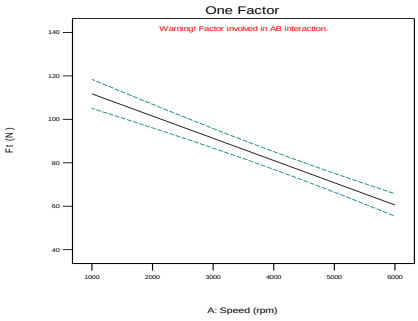

Design-Expert® Software
Factor Coding: Actual
Ft (N)
95% CI Bands

X1 = B: Feed

Actual Factors
A: Speed = 3500
C: DOC = 4.445

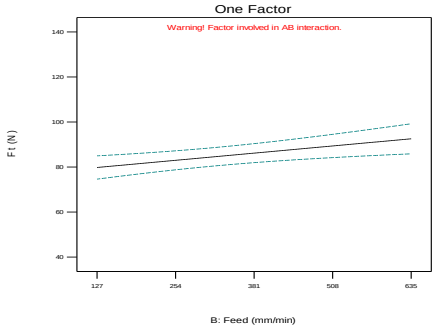

Design-Expert® Software
Factor Coding: Actual
Ft (N)
95% CI Bands

X1 = C: DOC

Actual Factors
A: Speed = 3500
B: Feed = 381

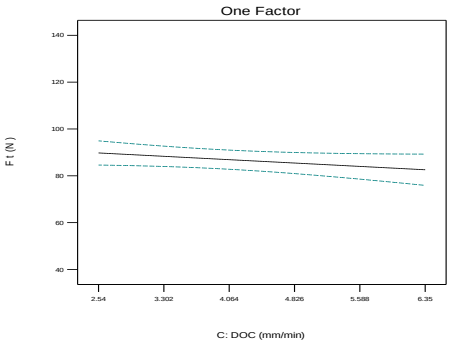

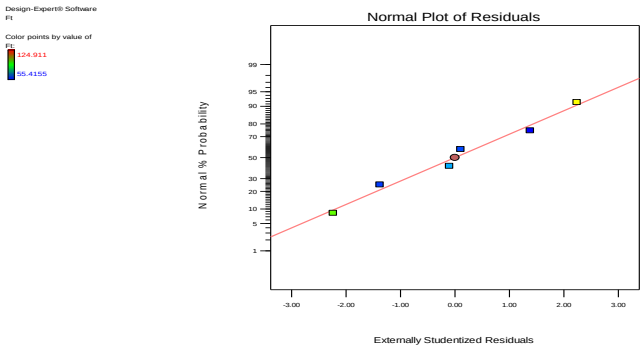
Design-Expert® Software
Ft
Color points by value of
Ft:
124.911
55.4155
Normal Plot of Residuals
Normal % Probability
99
95
90
80
70
50
30
20
10
5
1
-3.00
-2.00
-1.00
0.00
1.00
2.00
3.00
Externally Studentized Residuals

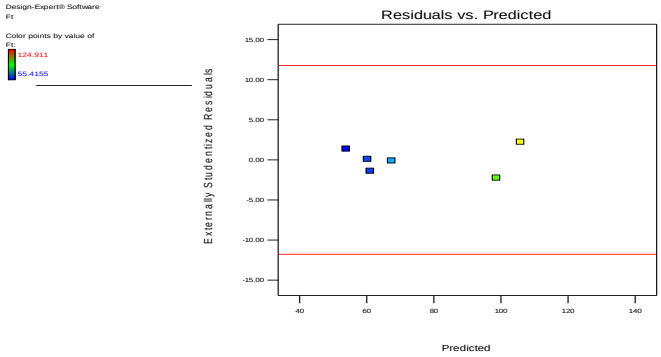
Design-Expert® Software
Ft
Color points by value of
Ft:
124.911
55.4155
Residuals vs. Predicted
Externally Studentized Residuals
15.00
10.00
5.00
0.00
-5.00
-10.00
-15.00
40
60
80
100
120
140
Predicted

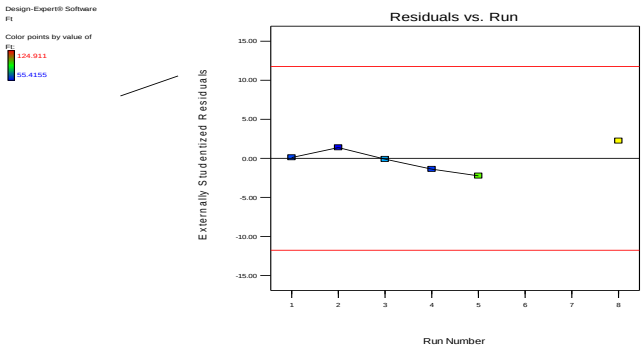
Design-Expert® Software
Ft
Color points by value of
Ft:
124.911
55.4155
Residuals vs. Run
Externally Studentized Residuals
15.00
10.00
5.00
0.00
-5.00
-10.00
-15.00
1
2
3
4
5
6
7
8
Run Number

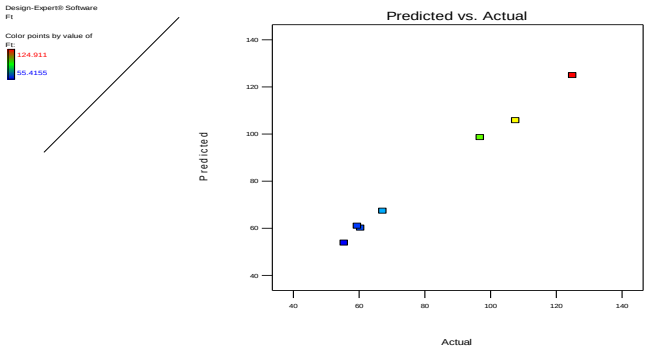
Design-Expert® Software
Ft
Color points by value of
Ft:
124.911
55.4155
Predicted vs. Actual
Predicted
140
120
100
80
60
40
40
60
80
100
120
140
Actual

Fr

ANOVA for Response Surface Reduced 2FI model
Analysis of variance table [Partial sum of squares - Type III]

Source	Sum of Squares	df	Mean Square	F Value	p-value Prob > F	
Model	25621.05	3	8540.35	4.39	0.1278	not significant
A-Speed	*11284.19*	*1*	*11284.19*	*5.80*	*0.0951*	
B-Feed	*20.26*	*1*	*20.26*	*0.010*	*0.9251*	
AB	*9223.22*	*1*	*9223.22*	*4.74*	*0.1176*	
Residual	5833.10	3	1944.37			
Cor Total	31454.15	6				

Std. Dev.	44.09	R-Squared	0.8146
Mean	382.47	Adj R-Squared	0.6291
C.V. %	11.53	Pred R-Squared	N/A
PRESS	N/A	Adeq Precision	4.797

Fr =
+519.13358
-0.039573 * Speed
-0.20224 * Feed
+5.97830E-005 * Speed * Feed

Design-Expert® Software
Factor Coding: Actual
Fr (N)
494.15
262.775

X1 = A: Speed
X2 = B: Feed

Actual Factor
C: DOC = 4.445

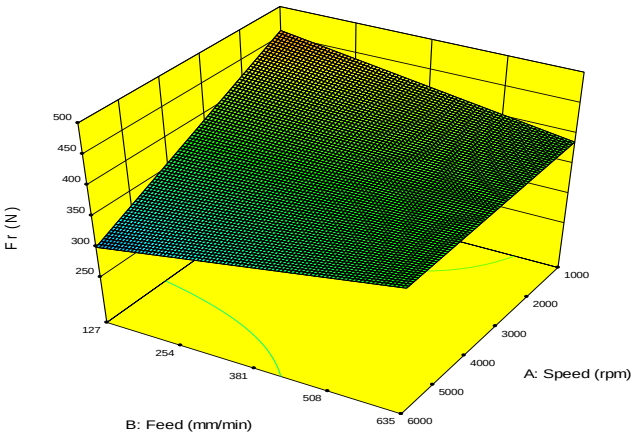

Design-Expert® Software
Factor Coding: Actual
Fr (N)
95% CI Bands

X1 = A: Speed

Actual Factors
B: Feed = 381
C: DOC = 4.445

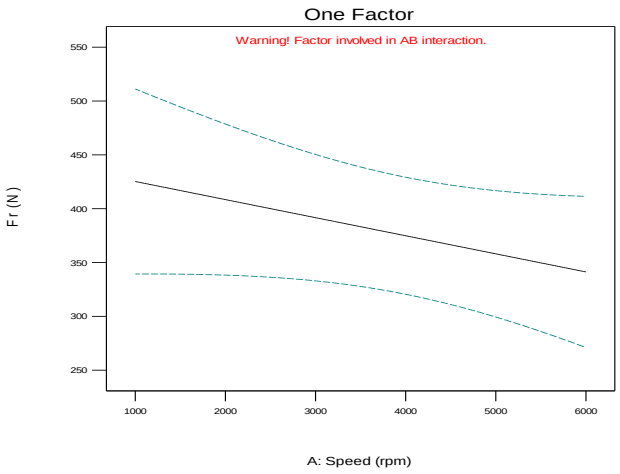

Design-Expert® Software
Factor Coding: Actual
Fr (N)
95% CI Bands

X1 = B: Feed

Actual Factors
A: Speed = 3500
C: DOC = 4.445

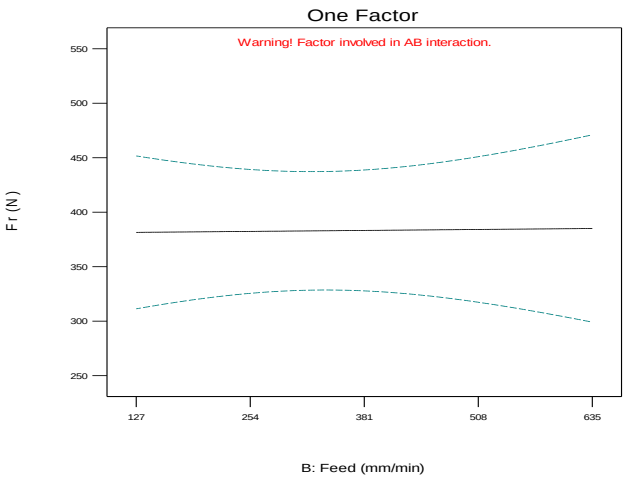

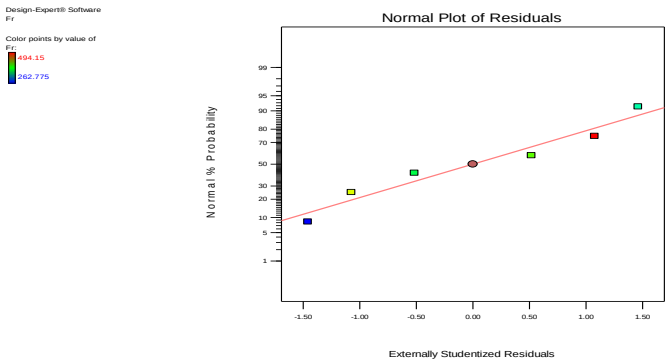
Design-Expert® Software
Fr
Color points by value of
Fr:
494.15
262.775
Normal Plot of Residuals
Normal % Probability
99
95
90
80
70
50
30
20
10
5
1
-1.50
-1.00
-0.50
0.00
0.50
1.00
1.50
Externally Studentized Residuals

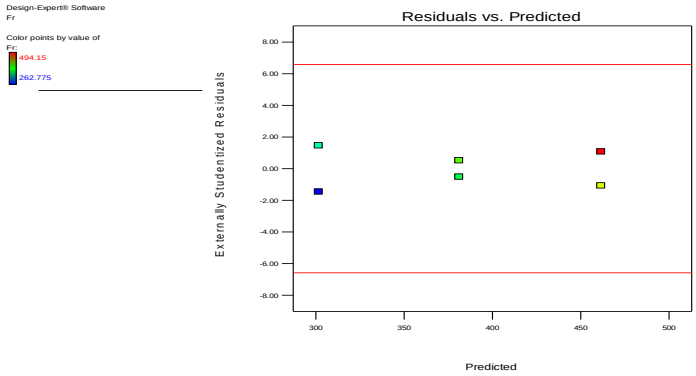
Design-Expert® Software
Fr
Color points by value of
Fr:
494.15
262.775
Residuals vs. Predicted
Externally Studentized Residuals
8.00
6.00
4.00
2.00
0.00
-2.00
-4.00
-6.00
-8.00
300
350
400
450
500
Predicted

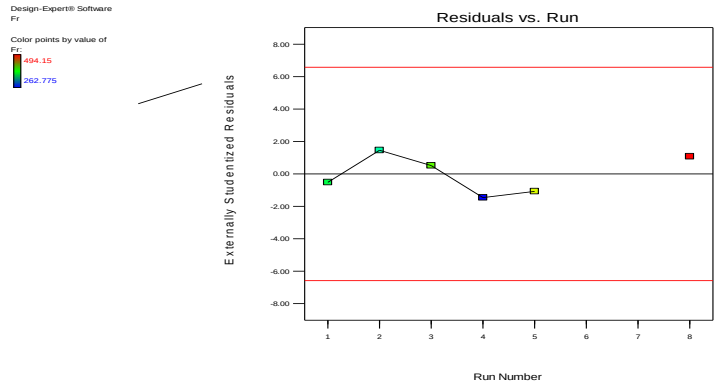
Design-Expert® Software
Fr
Color points by value of
Fr:
494.15
262.775
Residuals vs. Run
Externally Studentized Residuals
8.00
6.00
4.00
2.00
0.00
-2.00
-4.00
-6.00
-8.00
1
2
3
4
5
6
7
8
Run Number

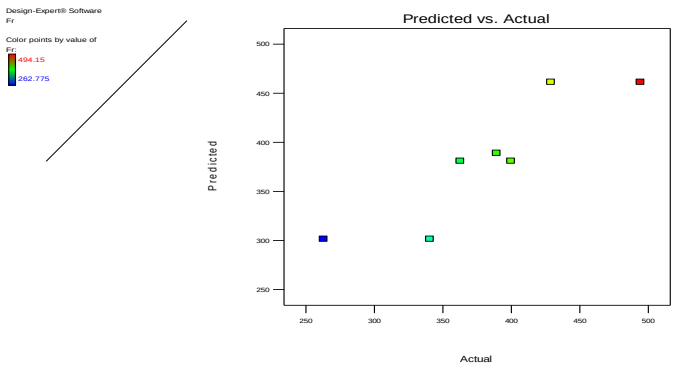
Design-Expert® Software
Fr
Color points by value of
Fr:
494.15
262.775
Predicted vs. Actual
Predicted
500
450
400
350
300
250
250
300
350
400
450
500
Actual

Appendix - M - Background equations for UD composites

The nomenclature used in this paper [34] is given by the following table.

Table M1 : Nomenclature used in [34] paper

Symbol	*Description*
β	Fiber cutting angle
θ	Fiber direction of the laminate
φ	Tool rotation angle
α	Rake angle of the tool
δ	Clearance angle of the tool
F_t	Tangential forces
F_r	Radial forces
K_{tc}	Cutting force coefficient - material's resistance to machining in tangential direction
K_{rc}	Cutting force coefficient - material's resistance to machining in radial direction
K_{te}	Rubbing force coefficient in tangential direction
K_{re}	Rubbing force coefficient in radial direction
r_e	Edge radius
γ	Helix angle
a_p	Axial depth of cut
h	Instantaneous chip thickness
f	feed
s	No. of teeth on the cutter
j	Index to represent no. of teeth on the tool
a_e	Radial depth of cut
φ_s	Entry angle
φ_e	Exit angle
$\varphi_j(t)$	Instantaneous location of the tooth
g	Control function to define if the tool is in cut or not
e_0	Magnitude of eccentricity wrt cutter
ϕ	Angle of eccentricity wrt cutter
$d\varphi$	Incremental cutter rotation angle
D	Tool Diameter

The background for the equations mentioned in Chapter 2 , in a more detailed is given (derived) from Faassen et al [53]. The nomenclature used in this paper is as follows and differs slightly from [34].

Faassen paper:

Symbol	*Description*
$\boldsymbol{\Omega}$	Spindle speed (rpm)
$\mathbf{f_z}$	Feed/tooth or chip load
$\mathbf{a_e}$	Radial depth of cut
$\mathbf{a_p}$	Axial depth of cut
$\mathbf{h}$	Chip thickness
$\mathbf{h_{stat}}$	Static chip thickness
$\mathbf{h_{dyn}}$	Dynamic chip thickness
$\boldsymbol{\tau}$	Delay time
$\mathbf{z}$	No. of teeth on the cutter
$\boldsymbol{\varphi_j}$	Rotation angle of tooth 'j'
$\mathbf{U_x(t)}$, $\mathbf{U_y(t)}$, $\boldsymbol{\varphi_j}$ **(t)**	Vibration of current tooth
$\mathbf{U_x(t-\tau)}$, $\mathbf{U_y(t-\tau)}$, $\boldsymbol{\varphi_j}$ **(t-** $\boldsymbol{\tau}$**)**	Vibration of previous tooth
$\boldsymbol{\vartheta}$	Angle b/w two subsequent teeth
$\boldsymbol{\varphi_s}$	Start angles
$\boldsymbol{\varphi_e}$	End angles

chip thickness = static chip thickness + dynamic chip thickness

$$h = h_{stat} + h_{dyn}$$

$$h_{stat}(t) = f_z \sin(\emptyset(t))$$

Vibration of tooth gathered in , $u = \begin{bmatrix} u_x & u_y \end{bmatrix}^T$

$$h_{dyn}(t) = \begin{bmatrix} \sin(\emptyset(t)) & \cos(\emptyset(t)) \end{bmatrix} (u(t) - u(t-\tau))$$

$$\tau = \frac{60}{z\Omega}$$

$$h_{stat} = f_z \sin \emptyset_j$$

$$\emptyset_j(t) = \emptyset_{j-1}(t-\tau)$$

$$h = h_{stat} + h_{dyn}$$

$$h_j\left(\emptyset_j(t)\right) = f_z \sin \emptyset_j(t) + \left(u_x(t) - u_x(t-\tau)\right) \sin \emptyset_j(t) + \left(u_y(t) - u_y(t-\tau)\right) \cos \emptyset_j(t)$$

$\emptyset_j(t) = \Omega t + j\vartheta$ j = 0,1,….,z-1

$$\vartheta = 2 \neq /z$$

To know if tooth is in cut or not, tooth is in cut if $\emptyset_s \leq \emptyset_j \leq \emptyset_e$

A function to describe the above,

$$g_j\left(\emptyset_j(t)\right) = \frac{1}{2}\left(1 + sign(\sin\left(\emptyset_j(t) - \Psi\right) - p)\right) = \begin{cases} 1, \emptyset_s \leq \emptyset_j \leq \emptyset_e \\ 0, else \end{cases}$$

where, $\tan\Psi = \frac{\sin\emptyset_s - \sin\emptyset_e}{\cos\emptyset_s - \cos\emptyset_e}$, $p = \sin(\emptyset_j - \Psi)$

$F_{t_j}(t) = \left(K_t a_p h_j(t)^{x_F}\right) + K_{te} a_p)\, g_j\left(\emptyset_j(t)\right)$

$$F_{r_j}(t) = \left(K_r a_p h_j(t)^{x_F}\right) + K_{re} a_p)\, g_j\left(\emptyset_j(t)\right)$$

where, $0 < x_F < 1$; $K_t, K_r > 0$ & $K_{te}, K_{re} \geq 0$

$$F(t) = \begin{bmatrix} F_x(t) \\ F_y(t) \end{bmatrix} = a_p \sum_{j=0}^{x-1} g_j\left(\emptyset_j(t)\right)\left(\begin{bmatrix} -K_{te}\cos\emptyset_j(t) - K_{re}\sin\emptyset_j(t) \\ +K_{te}\sin\emptyset_j(t) - K_{re}\cos\emptyset_j(t) \end{bmatrix}\right.$$
$$+ \left(\left(\mathrm{f_z}\sin\theta_j(t)\right) + u_x(t, t-\tau)\sin\emptyset_j(t) + u_y(t, t\right.$$
$$\left.\left. - \tau)\cos\emptyset_j(t)\right)^{x_F} \begin{bmatrix} -K_t\cos\emptyset_j(t) - K_r\sin\emptyset_j(t) \\ +K_t\sin\emptyset_j(t) - K_r\cos\emptyset_j(t) \end{bmatrix}\right)$$